Carbohydrate-based Polyurethanes and Polyamides: Synthesis, Characterization and Stereocomplex Formation

Ph.D. Thesis presented by Romina Marín Bernabé

Adviser: Prof. Sebastián Muñoz Guerra

Barcelona, March 2009

Departament d'Enginyeria Química

Escola Tècnica Superior d'Enginyeria Industrial de Barcelona

Universitat Politècnica de Catalunya

Table of Contents

Chapter 1. Aim and outline of this Thesis 1

Chapter 2. The chemistry of polyurethanes

2.1. Introduction 9
2.2. Basic raw materials for the production of linear polyurethanes 14
2.2.1. Diisocyanates 14
2.2.2. Polydiols 17
2.2.2.1. Polyethers 17
2.2.2.2. Polyesters 19
2.2.3. Difunctional *chain extenders* 21
2.2.4. Catalysts 21
2.2.5. Additives 22
2.3. Preparation methods for polyurethanes 23
2.3.1. Solvent-free reactions 23
2.3.1.1. One-shot process 23
2.3.1.2. Prepolymer process (Two-stage method) 24
2.3.2. Reactions in solution 25
2.3.3. Non-isocyanate methods 26
2.4. Structure of polyurethanes 27
2.4.1. Two-component polyurethanes without segmented structure 27
2.4.2. Segmented polyurethanes 28
2.4.3. Cross-linked polyurethanes 31
2.4.4. Ionomers 32
2.5. General applications of polyurethanes 33
2.6. Current applications for linear polyurethanes 34
2.6.1. Elastomers 35
2.6.2. Biomedical materials 36
2.6.3. Protective coatings, waterborne ecological lacquers, adhesives 38
2.7. Green polyurethanes 39
2.7.1. Polyurethanes from natural resources 39
2.7.2. Biodegradation of polyurethanes 43
2.8. References 44

Chapter 3. Linear polyurethanes made from methylated alditols and diisocyanates

3.1. Introduction 51
3.2. Experimental section 53
3.2.1. Materials and methods 53
3.2.2. Polyurethane synthesis 55
3.2.3. Hydrolytic degradation assays 58
3.3. Results and discussion 58
3.3.1. Synthesis and characterization 58
3.3.2. Thermal properties 60
3.3.3. Hydrolytic degradability 62
3.4. Conclusions 65
3.5. References 65

Chapter 4. Hydroxylated linear polyurethanes made from benzylated alditols and diisocyanates

4.1. Introduction 67
4.2. Experimental section 69
4.2.1. Materials and methods 69
4.2.2. Synthesis of monomers 70
4.2.3. Polyurethane synthesis 71
4.2.4. Hydrogenolysis of PUR-(LThBn-HDI) 75
4.2.5. Hydrolytic degradation assays 75
4.3. Results and discussion 76
4.3.1. Synthesis and characterization 76
4.3.2. Thermal and mechanical properties 78
4.3.3. Partially hydroxylated polyurethanes 80
4.3.4. Hydrolytic degradability 81
4.4. Conclusions 83
4.5. References 83

Chapter 5. Linear polyurethanes made from threitol: Acetalized and hydroxylated polymers

5.1. Introduction 85
5.2. Experimental section 87
5.2.1. Materials and methods 87

5.2.2. Synthesis of monomers 88
5.2.3. Polyurethane synthesis 89
5.2.4. Hydroxylated polyurethanes 91
5.2.5. Hydrolytic degradation assays 92
5.3. Results and discussion 92
5.3.1. Polyurethane synthesis 92
5.3.2. Thermal properties 95
5.3.3. Structure and crystallization study 99
5.3.4. Hydrolytic degradability 107
5.4. Conclusions 109
5.5. References 110

Chapter 6. Linear polyurethanes made from naturally-occurring tartaric acid
6.1. Introduction 113
6.2. Experimental section 115
6.2.1. Materials and methods 115
6.2.2. Polyurethane synthesis 117
6.2.3. Hydrogenolysis of PUR-(LTarBn-HDI) 120
6.2.4. Hydrolytic degradation assays 121
6.3. Results and discussion 122
6.3.1. Polyurethane synthesis 122
6.3.2. Structure and properties 125
6.3.3. Hydrolytic degradability 133
6.4. Conclusions 138
6.5. References 138

Chapter 7. Carbohydrate-based polyurethanes: A comparative study of polymers made from isosorbide and 1,4-butanediol
7.1. Introduction 141
7.2. Experimental section 143
7.2.1. Materials and methods 143
7.2.2. Synthesis of monomers and polymers 143
7.2.3. Hydrolytic degradation assays 146
7.3. Results and discussion 147
7.3.1. Polyurethane synthesis 147

7.3.2. Thermal properties and crystal structure 149
7.3.3. Hydrolytic degradability 153
7.4. Conclusions 155
7.5. References 155

Chapter 8. Carbohydrate-based poly(ester-urethane)s: Comparative study regarding cyclic alditol extenders and polymerization procedures
8.1. Introduction 157
8.2. Experimental section 159
8.2.1. Materials and methods 159
8.2.2. Synthesis of monomers 161
8.2.3. Synthesis of polymers 162
8.2.4. Hydrolytic degradation assays 165
8.3. Results and discussion 165
8.3.1. Polyurethane synthesis 165
8.3.2. Structure, thermal and mechanical properties 170
8.3.3. Hydrolytic degradability 179
8.4. Conclusions 182
8.5. References 182

Chapter 9. Polymer Stereocomplexes
9. 1. Introduction 185
9.2. Characterization of stereocomplexes 186
9.3. Polymeric stereocomplexes 187
9.3.1. Polylactones/polyesters 187
9.3.2. Polypeptides and polyamides 188
9.3.3. Polyketones 189
9.3.4. Polyethers and polysulfides 190
9.3.5. Poly(methyl methacrylate) 191
9.4. Biodegradable PLA stereocomplexes 193
9.5. Poly(hexamethylene di-*O*-methyl-tartaramide)s stereocomplex 196
9.6. Applications and perspectives of stereocomplexes 199
9.7. References 200

Chapter 10. Stereocomplex formation from enantiomeric polyamides derived from tartaric acid

10.1. Introduction 203
10.2. Experimental section 205
10.3. Results and discussion 206
10.3.1. Preparation of the stereocomplex 206
10.3.2. Crystallization kinetics 209
10.3.3. P*n*DMT with *n* other than 6 211
10.4. Conclusions 212
10.5. References 213

Chapter 11. Spectroscopic evidence for stereocomplex formation by enantiomeric polyamides derived from tartaric acid

11.1. Introduction 215
11.2. Experimental section 217
11.3. Results and discussion 218
11.3.1. Formation of the stereocomplex 218
11.3.2. ^{1}H NMR diffusion studies 219
11.3.3. FTIR analysis 223
11.4. Conclusions 226
11.5. References 226

Chapter 12. Exploration of stereocomplex formation in chiral carbohydrate-based polymers

12.1. Introduction 229
12.2. Experimental section. Polymer synthesis 231
12.3. Results and discussion 234
12.4. Conclusions 237
12.5. References 238

General conclusions 239

Agradecimientos 243

The author 245

Glossary

Acac	Acetylacetonate
ar	Aromatic
Ar	Arabinitol
Bn	Benzyl
BD	1,4-Butanediol
BOC	N-tertbutoxy-carbonyl
DCA	Dichloroacetic acid
DCCI	Dicyclohexyl carbodiimide
DMF	Dimethylformamide
DMSO	Dimethylsulfoxide
EG	Ethylene glycol
Gx	2,4:3,5-Di-O-methylidene-D-glucitol
HDI	1,6-Hexamethylene diisocyanate
HFIP	Hexafluoroisopropanol
Is	Isosorbide
MDI	4,4′-Methylenebis(phenyl isocyanate)
NMP	N-methyl-2-pyrrolidone
PCL	Polycaprolactone
PD	1,5-Pentanediol
Ph	Phenyl
PMMA	Poly(methyl methacrylate)
PUR	Polyurethane
Py	Pyridine
Tar	Tartrate
TFA	Trifluoroacetic acid
TFE	2,2,2-Trifluoroethanol
Th	Threitol
THF	Tetrahydrofuran
TMS	Trimethylsilyl
Xy	Xylitol

CHAPTER 1

AIM AND OUTLINE OF THIS THESIS

Introduction

Since the industrial revolution the XIX century, a major goal has been to bring technology and economy in line wherever is possible. After World War II, invention, production and application of plastics, and among them polyurethanes (PUR), have contributed highly to an extremely rapid growing of the standard of living. Such development has raised serious problems related with environment because air, water and soil have become severely polluted in many industrial areas. Society has taken consciousness of the significant damage made to the environment and has turn its eyes to biodegradable plastics as an ideal way to circumvent polluting effects.

On the other hand, limitations of petrochemical resources which were firstly evidenced in the 1970s have led to an increased awareness about sustainability of the materials that are used in both domestic and technological applications. Main commodity plastics as polyethylene, polypropylene, polystyrene, and polyvinyl chloride are all derived from petrochemical feedstocks. Most of engineering polymers as nylons, polyesters and polyurethanes are based on petroleum too. The utilization of fossil fuels in the manufacture of plastics accounts today for about 7% of worldwide oil and gas. It is commonly accepted that these resources will be depleted within the next one hundred years, and the peak in global oil production is estimated to occur within the next few decades. While the use of oil reserves and other fossil reserves for transportation and heating is certainly the most serious concern, the chemical industry will also be faced with the problematic issue associated to the use of an essentially non-renewable feedstock for the majority of their products. In fact, oil prices are rapidly increasing in last times and they are each time more subjected to unpredictable socio-political influences.

Therefore, there is today an urgent need to develop new synthetic polymeric materials using renewable resources. Naturally-occurring based polymers are attractive not only from a feedstock point of view but also because they will afford benefits from a waste

disposal perspective. Currently the disposal of petrochemically-derived plastics is a major concern, especially in high population density countries, since the majority of plastic residues end up in landfills. There is a considerable legislative drive and consumer pressure for the development of biodegradable and/or recyclable plastics. In fact, many of the products that derive from renewable resources can also be rendered biodegradable under the appropriate conditions. There is no question that polymers from natural resources will play an ever increasing role in the commodity plastics marketplace as well as continuing to be an important niche in medical markets. This will likely stand out not only for environmental benefits, but also for the new property profiles that renewable resource polymers can exhibit, such as biocompatibility and biodegradability, properties that are relevant to biomedicine applications.

Carbohydrates are naturally occurring products produced in huge amounts and most of them being very easily accessible. Nature generates $170 \cdot 10^9$ t of saccharides from carbon dioxide and water; however, only 3% of this immense potential is used as a foodstuff. They can be looked therefore as an extraordinary source of chemicals capable of providing a wide diversity of building blocks suitable for the synthesis of polycondensation polymers. However, there are only a few examples of carbohydrate-based plastics that have commercial development, which is mostly due to the relatively high cost of these materials compared to their petrochemical analogues. Another severe limitation in the use of carbohydrates as a source of monomers for the synthesis of linear polycondensates is their inherently high functionality. The large number of reactive groups usually present in carbohydrates leads to highly cross-linked products unless special precautions are taken. Protection of the exceeding hydroxyl groups as methoxy ethers has been the method more frequently applied to obtain linear polyamides, polyesters and polycarbonates from aldaric acids and alditols. A good amount of efforts are being made to achieve the synthesis of linear polycondensates from carbohydrate-derived monomers with the minimum of chemical modifications.

Aim of the Thesis

In this Thesis the potential use of carbohydrates resources to make polyurethanes is highlighted. More specifically, the Thesis is mainly addressed to the development of polyurethanes made from carbohydrate-derived diols. PUR are extremely versatile polymers that can be used in a wide variety of applications going from massive filling

foams to high-quality technical items. The preparation of polyurethanes from renewable feedstocks is currently receiving increasing attention in the polyurethane industry. Diols derived from naturally-occurring fats and oils as well as biotechnologically produced diols like 1,3-propanediol and hydroxyl end-caped poly(lactic acid) have been recently introduced in the synthesis of these polymers. A fair number of polyurethanes containing units derived from saccharides have been reported so far although none of them has reached industrialization; the selection embraces from polymers made from complex polyhydroxylated lignin fragments to cyclic diols such as isosorbide and gulonolactones.

The aim of this Thesis is to prepare, characterize and evaluate the basic properties of linear polyurethanes made from diols derived from carbohydrates, specifically alditols derived from threose, arabinose and xylose. Additionally, other diols with a cyclic structure and coming from glucose will be used. The final objective is to gain deeper insight in the structure-properties relationship of these polymers and to explore preliminary their potential as new materials. In this way, we expect to obtain new polyurethanes of interest in the biomedical field.

The diols used in this work are accessible via chemical synthesis or are commercially available, and therefore they stand for a good option to introduce natural products in the polyurethane chemistry (Scheme 1.1). The incorporation of these hydrophilic units will render polyurethanes more susceptible to hydrolysis. Two types of carbohydrate-derived diols have been used in this work:

- Acyclic diols derived from aldaric acids and alditols
- Cyclic diols derived from D-glucose

An aldaric acid is an aldose derivative that has both the hydroxyl function of the terminal carbon and the aldehyde function of the first carbon oxidized to carboxylic acid functions. Some aldaric acids such as tartaric acid are present in certain fermented fruits. The protection of the carboxylic groups of the aldaric acids makes aldaric acids usable as monomers for the production of linear polyurethanes by reaction of their secondary hydroxyl groups with diisocyanates. In this work the methyl, ethyl, isopropyl and benzyl tartrates have been polymerized with aliphatic and aromatic diisocyanates to produce linear polyurethanes bearing pendant alkyloxy- or benzyloxycarbonyl groups.

An alditol is an aldose derivative that has the aldehyde function reduced to hydroxyl. Alditols coming from reduction of aldoses or aldaric acids are useful to obtain linear polyurethanes by reaction with diisocyanates provided that all the secondary hydroxyl groups are duly protected. In this work, threitol, arabinitol and xylitol with the secondary OH groups protected as methyl ether, benzyl ether or acetal have been used for producing linear polyurethanes bearing pendant protected hydroxyl groups.

Deprotrection of the side protected carboxylic or hydroxylic groups is a convenient way to obtain functionalized polyurethanes. In this work, polyurethanes bearing isopropylidene, benzyloxy, and bezyloxycarbonyl side groups are hydrolyzed or hydrogenated to render polyurethanes bearing free hydroxyl or carboxylic side groups. This hydroxylated or carboxylated polyurethanes are highly hydrophilic materials that display enhanced hydrodegradability.

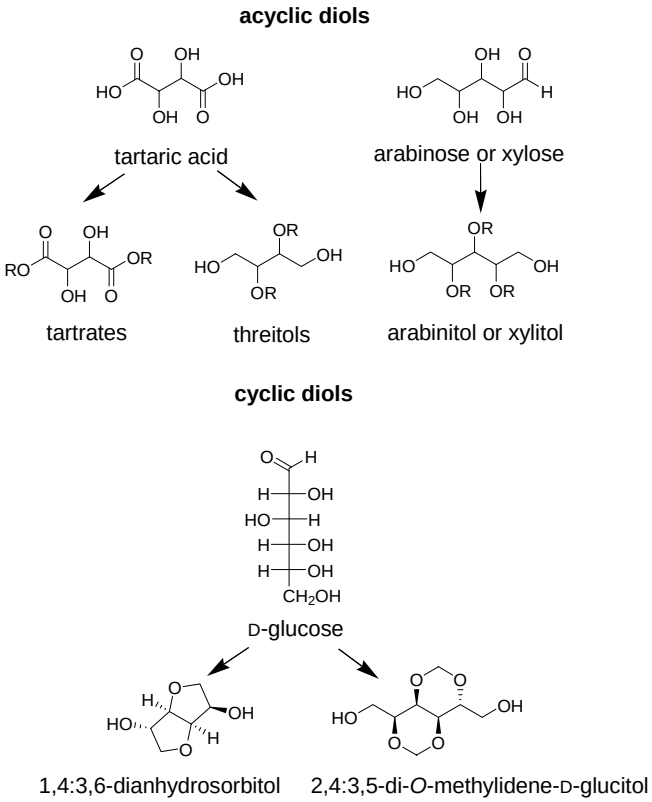

Scheme 1.1. Diols used in this Thesis.

Although the major part of this Thesis is focused on the synthesis of polyurethanes from acyclic diols, also cyclic diols derived from D-glucose were explored. They were chosen because a research agreement with the Spanish polyurethane producer Merquinsa S.L. was established. Since Merquinsa has recently launched a range of thermoplastic segmented-polyurethanes based on renewable polydiols, they were interested in the replacement of the conventional short chain diols used in the *hard segment* of these polyurethanes (known as *chain extenders*), such as 1,4-butanediol, by other diols based on naturally-occurring products of easy accessibility. In this work, two cyclic diols made from D-glucose are investigated as *chain extenders*. One of them, 1,4:3,6-dianhydrosorbitol, also known as isosorbide, is a well established compound that is produced at industrial level and that is being extensively explored for the synthesis of a wide variety of polycondensates. The second one is D-glucitol with the secondary hydroxyl groups protected as methylidene acetals; this compound is specifically synthesized for this Thesis and has been rarely used so far in polymer synthesis (Scheme 1.1).

Diisocyanates are the usual monomers complementary of diols for the formation of polyurethanes. A few diisocyanates are used in the industrial manufacture of polyurethanes, which can be grouped in aliphatic and aromatic families, the latter being the most frequently used. The aliphatic 1,6-hexamethylene diisocyanate (HDI) and the aromatic 4,4'-methylenebis(phenyl isocyanate) (MDI) are the only two diisocyanates used in this work (Scheme 1.2).

1,6-Hexamethylene diisocyanate 4,4'-methylenebis(phenyl isocyanate)

Scheme 1.2. Diisocyanates used in this Thesis.

The polymerizations of the different carbohydrate-based diols with the two selected diisocyanates have rendered a collection of polyurethanes covering a good diversity of structure and properties. The chemical structures of the polyurethanes studied in this Thesis are depicted in Scheme 1.3.

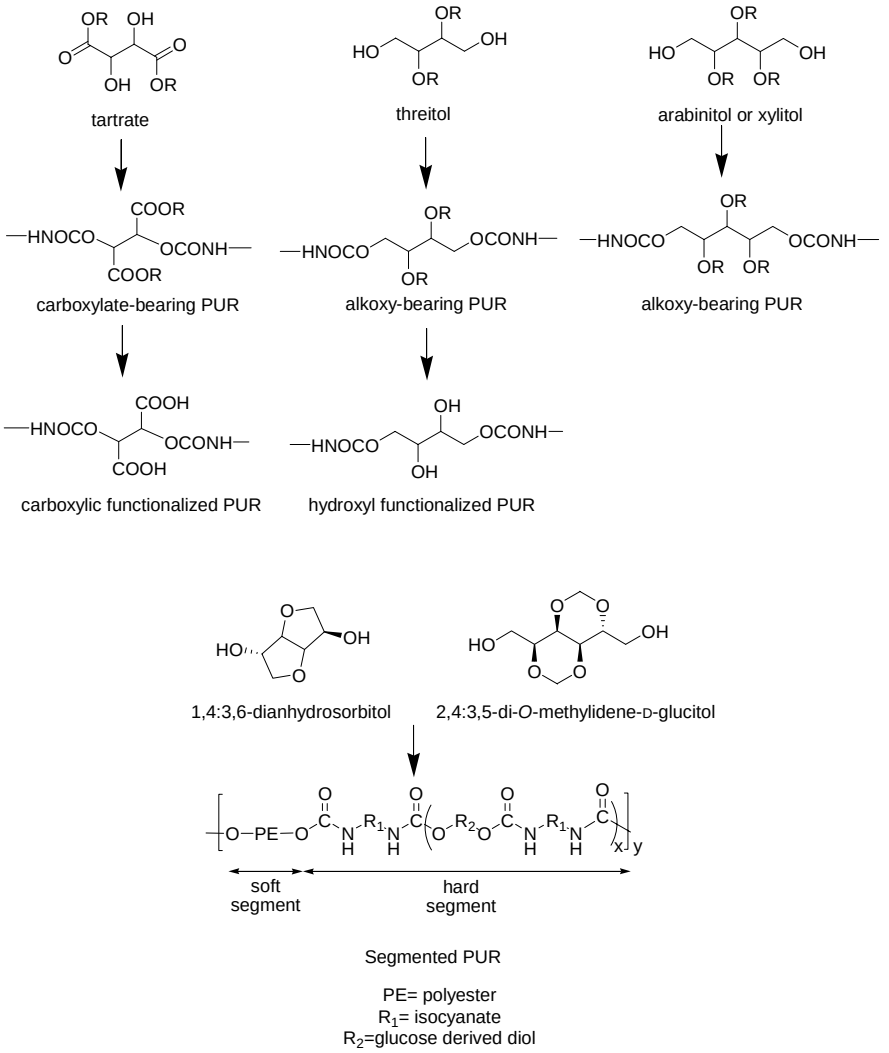

Scheme 1.3. Polyurethanes studied in this Thesis.

In addition to the work addressed to the study of polyurethanes, a parallel study on polymer stereocomplexation was performed as part of this Thesis. A polymer stereocomplex is defined as a stereoselective interaction between two complementing stereoregular polymers that interlock to form a new structure showing an altered physical pattern of behaviour in comparison to the parent polymers. Polymer stereocomplexes display singular properties of high interest for drug controlled-release applications. There are very few cases reported on stereocomplexation, one of them being that formed from

a pair of enantiomeric polytartaramides discovered some years ago in our research group (Scheme 1.4). This encouraged us to dedicate some efforts to continue these studies following two lines addressed to: a) Look for new evidences and evaluate properties of the polytartaramide stereocomplex, and b) Explore stereocomplex formation in other pairs of enantiomeric polyamides and polyurethanes closely related to the polytartaramide pair previously studied.

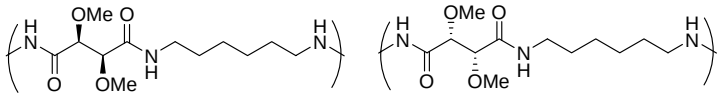

Scheme 1.4. Enantiomeric polyamides from tartaric acid.

Structure of the Thesis

This Thesis consists of twelve Chapters followed by a summary of the conclusions drawn from the whole work. Chapter 1 is a general introduction to the Thesis which includes its aims and organization. Chapter 2 is an introductory review to polyurethane synthesis, properties and applications, which is provided to assist the understanding of the basic principles of polyurethane chemistry and perspectives. Chapters 3-5 describe the synthesis, characterization and hydrodegradability of polyurethanes from alditols having all secondary hydroxyl groups protected as methyl ether, benzyl ether or acetal. Since total or partial splitting of the benzyl ethers or acetal groups after polymerization was feasible by hydrogenolysis or treatment by acids, respectively, these methods provided a suitable route to polyurethanes bearing pendant hydroxyl groups, which are highly hydrophilic and more susceptible to hydrolysis.

In Chapter 6, tartrate-derived polyurethanes are described. In this case, tartrates were directly reacted with diisocyanates, and polyurethanes with benzyl or different alkyl ester side groups were obtained. The hydrodegradability of these polyurethanes was enhanced by incubating them in acid or basic buffers to favour the hydrolysis of the side alkyl esters, or by hydrogenolysis of the benzyl esters; in both cases polyurethanes bearing carboxylic side groups, much more hydrolyzable than their parent polyurethanes, were prepared.

Chapter 7 and 8 are dedicated to the study of polyurethanes from carbohydrate-based cyclic diols. In Chapter 7 a set of polyurethanes containing isosorbide units were synthesized by polymerization in solution of 1,4-butanediol, isosorbide or diisosorbide diurethanes with diisocyanates. The thermal properties and crystal structure of the polyurethane homopolymers and copolymers containing isosorbide were evaluated and compared with those of the polyurethanes analogues entirely made of 1,4-butanediol. This work was a previous exploration to the study presented in Chapter 8.

Since there is a growing interest in introducing new *chain extenders* derived from renewable resources as an alternative to oil-based extenders, two carbohydrate-based cyclic diols were explored to obtain segmented polyurethanes. At the same time, an enhancement of the hydrophylicity and hydrodegradability could be expected from the use of such compounds. Chapter 8 includes the synthesis and characterization of poly(ester-urethane)s in which the *soft segment* is polycaprolactone and the hard block is built by the reaction of 1,6-hexamethylene diisocyanate (HDI) or 4,4'-methylenebis(phenyl isocyanate) (MDI) with the carbohydrate-derived diols. These studies are addressed to the evaluation of the thermal, mechanical and hydrodegradation properties of the new segmented polyurethanes in comparison to conventional segmented polyurethanes in which 1,4-butanediol is habitually used as *chain extender*.

Chapters 9 to 12 are dedicated to investigate the stereocomplexation phenomenon in a variety of polycondensates. The introduction to this issue is given in Chapter 9. The preparation method, formation evidences gathered by spectroscopic techniques and the crystallizability of the polytartaramide stereocomplex are described in Chapters 10 and 11. The results of searching for new stereocomplexes in related systems like other carbohydrate-derived polyamides and polyurethanes, are reported in Chapter 12; unfortunately, none of the other investigated systems showed signs on the occurrence of stereocomplexation.

CHAPTER 2

THE CHEMISTRY OF POLYURETHANES

Summary: *Polyurethane is the general name given to a family of synthetic polymers that contain the urethane group in their constitutional repeating unit. Since polyurethanes were first synthesized in 1937 by Otto Bayer, they have achieved use in a wide variety of applications including elastomers, foams, paints, and adhesives. Such diversity of applications originates from the tailorable chemistry of polyurethanes, i.e. the chemical constitution of polyurethanes can be dessigned at choice to satisfy a broad spectrum of specific requirements, by selecting adequate raw materials and processing conditions. Polyurethanes also can be used as biomaterials, most frequently synthesized as segmented block copolymers. This introductory chapter reviews some aspects of polyurethanes: basic chemical reactions and raw materials, synthesis and structure of segmented and non-segmented polyurethanes, and includes finally a review of the most common applications in daily life and biomedicine.*

2.1. Introduction

Linear polyurethanes (PUR) are polymers in which the main chain is composed of aliphatic or aromatic moieties, R_1 and R_2, linked together by urethane groups (Scheme 2.1),

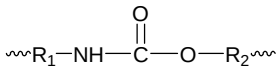

Scheme 2.1. General formula of polyurethanes.

wherein R_1 stands for an aliphatic, aromatic or alicyclic radical coming from the isocyanate monomer, and R_2 is a more or less complex group derived from the diol or polydiol component. The trivial name *urethane* which is used for the compound ethyl carbamate, is given to the whole polyurethane chemistry.

Polyurethanes are a versatile class of polymers that are used in a broad range of applications.[1] In most cases, the macromolecular structure of linear polyurethanes is based on the polyaddition reaction of dihydroxy compounds with diisocyanates, yielding AABB polymers or [*m,n*]-polyurethanes (Scheme 2.2). A comprehensive study of the parent aliphatic [*m,n*]-polyurethanes was reported by Otto Bayer in *Angewandte Chemie* in 1947.[2]

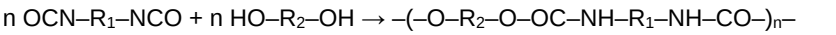

Scheme 2.2. Reaction leading to [*m,n*]-polyurethanes.

At that time, these novel polymers were structurally compared to aliphatic polyamides made from diamines and diacids, the [*m,n*]-nylons. However, polyurethanes of AB type, *i.e*. [*n*]-polyurethanes with a structure comparable to [*n*]-nylons made from aminoacids, were practically unknown despite its structural simplicity. These polyurethanes would be generated from isocyanatoalcohols, which are hardly accessible compounds. In 1999 Meijer *et al*. reported a general and convenient route to aliphatic α,ω-isocyanatoalcohols and their *in situ* polymerization into the corresponding [*n*]-polyurethanes[3] of respectable molecular weights (Scheme 2.3).

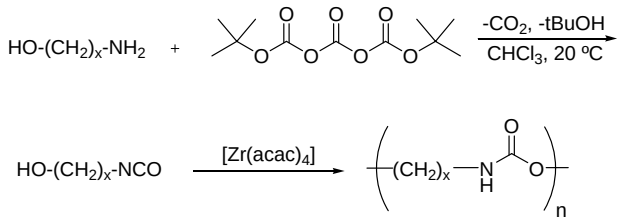

Scheme 2.3. Synthesis of [*n*]-polyurethanes (*x*= 4-12).[3]

Depending on the reagents used in the polyurethane synthesis, the obtained polyurethanes can have homogeneous or heterogeneous compositions. When a diisocyanate reacts with a diol, the resulting polyurethane has a homogeneous composition and the structure in the solid state can be that of an amorphous or semi-crystalline polymer (Figure 2.1a). When in this reaction a polydiol, normally a polyether or polyester with hydroxyl end groups, is also used, the polyurethane obtained has a segmented structure composed by two phases with different composition, which are called *soft segment* and *hard segment* (Figure 2.1b). As a general rule, the reaction of small size diols, called *chain extenders*, with diisocyanates generates the *hard segments* that impart rigidity to the polymer, whereas the polydiol gives rise to the so-called *soft segment*.

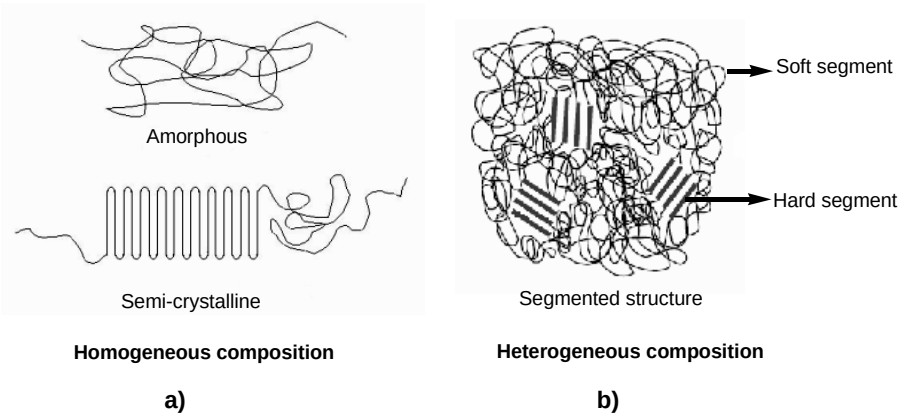

Figure 2.1. Structure of polyurethanes.

Segmented PUR chains usually contain therefore not only urethane groups but also ether and/or ester groups coming from the polydiols used in their synthesis. Depending on the specifications of feeds (*i.e.* purity), and on the method adopted for the polyaddition process, one can find also urea groups, biuret groups, allophanate groups, carbodiimide groups, aromatic hydrocarbon rings, azaheterocyclic (isocyanurate) structures or oxazolidone structures, and even ionic groups. The utilization of multi-functional components, *i.e.* triisocyanates obtained from the trimerization process of isocyanate monomers, or the use of branched hydroxyl polydiols, will yield polyurethanes with three-dimensional cross-linking.

The structure of segmented PUR chains can be additionally diversified by the polyaddition process regime, and in particular by the relative sequence of charging individual feeds. It is a frequent practice that a prepolymer is synthesized initially using an exceeding amount of one component, *i.e.* too much diisocyanate (I) in relation to polydiol (P); the molar ratio of polydiol to diisocyanate determines the size that is attained for the isocyanate prepolymer (Scheme 2.4).

$$2I + P \rightarrow IPI$$
$$3I + 2P \rightarrow IPIPI$$

Scheme 2.4. Prepolymer synthesis.

The synthesized urethane–isocyanate prepolymer IPI or IPIPI is then further extended at the next step by reaction with a low-molecular weight diol, *i.e.* 1,4-butanediol or any other compound which has active hydrogen atom(s). High-molecular weight polyurethanes are produced in this way, and the size of the final polymer is controlled by the molar ratio of the reacting functional groups (Scheme 2.5). It is also possible to synthesize segmented polyurethanes in a single-stage process. The molar ratios for diisocyanate, polydiol and *chain extender* should be carefully selected then and the chain microstructure will not be so precisely defined in this case.

$$n\ OCN–IPIPI–NCO + n\ HO–R–OH \rightarrow$$
$$–(O–CO–NH–IPIPI–NH–CO–O–R)–$$

Scheme 2.5. Reaction of the prepolymer with the *chain extender* leading to segmented polyurethanes.

Polyurethane plastics were initially synthesized by Otto Bayer (Figure 2.2), and they have been known for nearly 70 years now, predominantly as elastomers and foams. The first polyurethane, Perlon U, was obtained in 1937 by reaction of 1,6-hexamethylene diisocyanate with 1,4-butanediol.[4] Polyurethane products were introduced into the market in late 1940s and they quickly established a strong position there, mostly as elastomers and foamed materials. Polyurethane plastics belong now to the group of important materials applicable in numerous engineering fields.[5] The very wide applicability of PUR results from the fact that their performance properties can be widely modified by selecting appropriate raw materials, catalysts and auxiliary compounds, by employing various production methods and/or by employing various methods for further processing and/or for shaping the final products. Polyurethanes with segmented structure, formed by short rigid chain segments and long flexible chain segments, offer very good elasticity with reasonably high mechanical strength and high abrasion resistance at the same time, and also controllable hardness.

Figure 2.2. Otto Bayer (1902-1982) performs a foam experience during a lecture. The German chemist led development of polyurethanes.

Polyurethanes generally offer advantageous performance properties and ease of processing, good resistance to water, to atmospheric conditions, to oils, greases, organic solvents, diluted acids and alkalis, and in case of non-aromatic PUR also resistance to photo-oxidative aging. All that makes them applicable in numerous fields of technology and in everyday life. On the other hand, the exceptional combination of physical

properties, hydrolytic stability as well as low *in vitro* protein adsorption and platelet adhesion enables them for those medical applications where the contact with body fluids, *i.e.* plasma and blood, is required.[6,7] A recent trend in the development of PUR is the production of sustainable and biodegradable products. The use of vegetable raw materials: starch,[8] castor oil,[9] natural rubber,[10] lignin, wood flour, molasses, cellulose, glucose, fructose or saccharose, makes possible to obtain biodegradable PUR with relative easiness.

2.2. Basic raw materials for the production of linear polyurethanes

The basic materials applicable in the manufacture of polyurethanes are diisocyanates, polyether or polyester polydiols, low-molecular-weight diols and diamines, these two latter employed as *chain extenders*, catalysts, and auxiliary substances selected for specific processes, *i.e.* blowing agents for foamed polyurethanes, multi-functional amines or isocyanates as cross-linking agents, or organophosphorus antipyrene compounds which are widely used in foamed polyurethanes. The choice of those materials has been discussed in detail in numerous review papers intended to present production processes of polyurethane products.[11,12]

2.2.1. Diisocyanates

The only technically reasonable method today for the production of polyurethanes is the polyaddition process of diisocyanates and diols or/and polydiols. Isocyanates have their beginning in the synthesis of phenylisocyanate, developed by Hoffmann, and based on thermal dehydrogenation of di(*N*-phenyl)oxamide (Scheme 2.6).

$$C_6H_5–NH–CO–CO–NH–C_6H_5 \rightarrow 2\ C_6H_5–NCO + H_2$$

Scheme 2.6. Hoffmann synthesis of phenylisocyanate.

Diisocyanates can be obtained in the laboratory by rearrangement of compounds with electron deficiency at the nitrogen atom (nitrenes). The Curtius method can be used for that purpose (rearrangement of acyl azides) or alternatively amides can be subjected to Hoffmann rearrangement. Industrially, however, only the Hetschel method has been employed so far, *i.e.* phosgenation of amines with further modifications (Scheme 2.7).

The Hetschel method is pretty simple but is troublesome because of the extreme toxicity of phosgene, toxicity of amine feeds and toxicity of diisocyanate products themselves. In order to minimize the environmental impact of phosgene, extensive research has been directed toward the development of effective catalysts for oxidative carbonylation and reductive carbonylation.

$$2R–NH_2 + COCl_2 \rightarrow OCN\text{-}R–NCO + 2HCl$$

Scheme 2.7. Hetschel synthesis of diisocyanates.

Nevertheless, diisocyanates are today the compounds that are invariably used for the industrial production of polyurethanes. Both aliphatic and aromatic products with the chemical formula depicted in Scheme 2.8 are typically used diisocyanates.

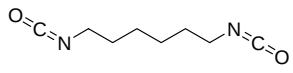

1,6-Hexamethylene diisocyanate

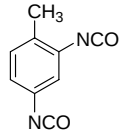

Toluene-2,4-diisocyanate

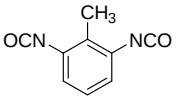

Toluene-2,6-diisocyanate

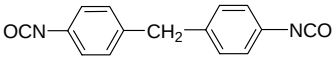

4,4'-Methylenebis(phenyl isocyanate)

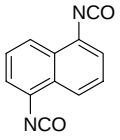

1,5-Naphthalene diisocyanate

Scheme 2.8. Diisocyanates commonly used in the production of polyurethanes.

Recently new alicyclic diisocyanates, which can afford polyurethane coatings more resistant to photo-degradation in direct sunlight service have been industrially introduced (Scheme 2.9).

Other diisocyanates, in particular 1,3-phenylene diisocyanate and 1,1-biphenylene diisocyanate, have much less importance and they are only employed in very specific applications. Table 2.1 lists some commercially available diisocyanates with some physical properties.[6]

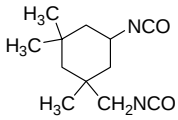

[5-Isocyanato-1-(isocyanatomethyl)-1,3,3-trimethylcyclo-hexane]

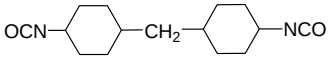

4,4'-Methylene-bis(cyclohexyl isocyanate)

Scheme 2.9. Alicyclic diisocyanates.

Aromatic, aliphatic and cycloaliphatic di-or poly-isocyanates are all suitable building blocks for polyurethane chemistry, the aromatic types being the more used due to its higher reactivity and economic availability. Aliphatic isocyanates are only used if special properties are required regarding the final product. For example, light stable coatings can only be obtained from aliphatic polyisocyanates.

Table 2.1. Some commercially available diisocyanates.

Designation	Acronymous	Formula	Molecular weight ($g \cdot mol^{-1}$)	Melting point (ºC)
2,4-Toluene diisocyanate	(TDI)	$C_9H_6O_2N_2$	174.2	21.8
4,4′-Methylenebis(phenyl isocyanate)	(MDI)	$C_{15}H_{10}O_2N_2$	250.3	39.5
1,6-Hexamethylene diisocyanate	(HDI)	$C_8H_{12}O_2N_2$	168.2	-67
Hydrogenated MDI	(H_{12}MDI)	$C_{15}H_{18}O_2N_2$	258.3	30
Isophorone diisocyanate	(IPDI)	$C_{12}H_{18}O_2N_2$	222.3	-60
Naphthalene diisocyanate	(NDI)	$C_{12}H_6O_2N_2$	210.2	127

The fundamental problem to be considered when using diisocyanates is the need to provide adequate reactivity of the isocyanate groups towards the compounds bearing active hydrogen atoms in their molecules. The isocyanate group is generally very reactive due to its two accumulated double bonds. However, depending on its location within the chain (location on primary or secondary carbon atoms), on possible steric hindrance, and on the so-called substitution effect, which is frequently the case in some

diisocyanates or urethane–isocyanates, considerable differences in reactivity can be observed. Such differences are critical for commercial processes and they should be compensated by the use of suitable catalysts. Table 2.2 presents the relative reaction rates of diisocyanates with some compounds typically used in polyurethane synthesis.[9]

Table 2.2. Relative reaction rates of diisocyanates.

Active hydrogen compound	Relative reaction rate
Primary amine	100,000
Secondary amine	20,000-50,000
Water	100
Primary alcohol	100
Secondary alcohol	30
Carboxylic acid	40

2.2.2. Polydiols

Compounds containing two hydroxyl functions in the molecule are, in addition to the diisocyanates, the essential components for the formation of linear polyurethanes. Lower molecular weight compounds usually act as *chain extenders*. Higher molecular weight diols, usually hydroxyl end-caped short chain polymers known as polydiols, are the actual basis for the formation of the commercial segmented polyurethanes. These higher molecular weight polydiols are usually polyethers or polyesters.

2.2.2.1. Polyethers

The basic polyether-polydiol applicable for the production of linear PUR can be obtained by the low conversion addition reaction of ethylene or propylene oxide to diols (Scheme 2.10).

Poly(ethylene glycol) Poly(propylene glycol)

Scheme 2.10. Polyethers commonly used in the production of polyurethanes.

Especially worthy of notice here is the block polyether which goes under the name of Pluronic, which is a polypropylene glycol ending in primary hydroxyl groups, more reactive towards isocyanates. Similar performance is provided by poly(tetramethylene glycol), which is a polydiol produced by cationic polymerization of tetrahydrofuran, and which is much more expensive (Scheme 2.11).

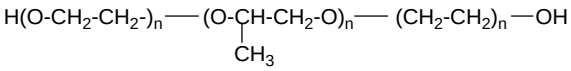

Pluronic glycol

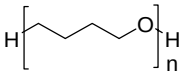

Poly(tetramethylene oxide) glycol

Scheme 2.11. Other polyethers used in the production of polyurethanes.

Within the group of aromatic polyethers which are important for the polyurethane processes, the family known as dianoles, is worthy of notice. Dianoles are obtained in the reaction of 2,2-bis(4-hydroxyphenyl)propane (bisphenol-A) with oxiranes (*i.e.* Dianol 24) or bisphenol-S polysulfone with oxiranes (Scheme 2.12). Dianoles can be additionally subjected to esterification with glycolic acid, phosphoric acid or acrylic acid, which yields linear polyester polydiols also applicable as *soft segments* in the production of polyurethanes.[13]

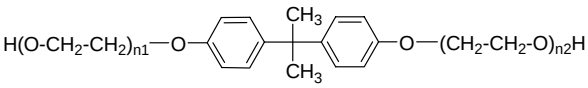

Dianol 24

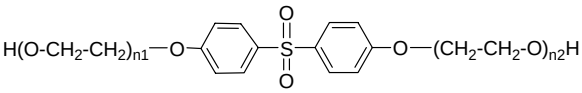

Dianol containing sulfone group

Scheme 2.12. Dianoles.

2.2.2.2. Polyesters

The polycondensation process of dicarboxylic acids with glycols is the most frequently method used for the synthesis of linear polyesters. Hydroxyl end-caped polyadipates of ethylene glycol, diethylene glycol or propylene glycol are typically used as linear polyesters in the polyurethane elastomers production processes (Scheme 2.13).

$$H[–O–CH_2–CH_2–O–CO–(CH_2)_4–CO–O–CH_2–CH_2]_n–OH$$

Scheme 2.13. Poly(ethylene adipate).

Since more and more attention is being paid to the development of biodegradable polyurethanes, polycaprolactone diol has gained popularity as a polydiol useful for the manufacture of such polymers. It is obtained by initiating the ring-opening polymerization of ε-caprolactone by a glycol such as di(2-hydroxyethyl) ether. The initial monomer is obtained by oxidation of cyclohexanone (Scheme 2.14).

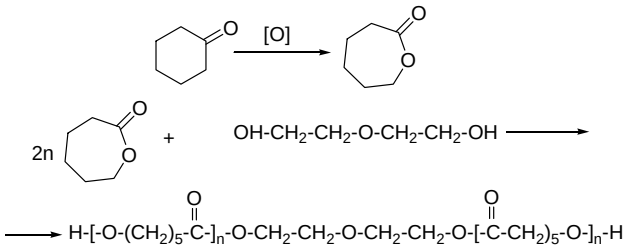

Scheme 2.14. Synthesis of polyester from ε-caprolactone.

Polycaprolactones offer lower viscosity than oligoesters derived from dicarboxylic acids and glycols. They are more expensive than traditional polyesters, but the derived polyurethanes have superior mechanical properties. Recently, general attention has been attracted by one new type of polyesterdiols for their application in the production of PUR elastomers, *i.e.* aliphatic polycarbonates obtained from cyclic alkylene carbonates (Scheme 2.15).[14]

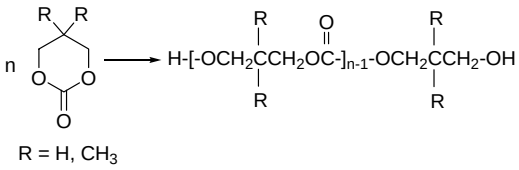

Scheme 2.15. Aliphatic polycarbonate glycol.

The chemical behaviour of the polyesters in the polyurethane chemistry is mainly determined by the hydroxyl end groups. Since they are generally primary, their reaction with the isocyanate groups occurs easily and quantitatively. The hydrolysis stability of the ester linkage in polyesters is clearly inferior to that of the ether linkage in polyethers. In addition, during polyester hydrolysis the carboxylic acids released have an auto-catalytic effect that hastens the hydrolysis rate. With increasing hydrophobicity and crystallinity, the resistance of the polyester to hydrolytic attack increases. Polyesters made from long chain monomers are more stable to hydrolysis than those made from short chain components. An example of this effect for two different poly(ester-urethane)s made of MDI, 1,4-butanediol, and various polydiols are compared in Table 2.3.[5]

Table 2.3. Effect of polyester structure on the hydrolytic stability of some poly(ester-urethane)s.[a]

Polydiol	Type	Initial tensile strength (MPa)	Tensile strength after incubation (MPa)
Poly(ethylene adipate) glycol	Polyester	42	17
Poly(hexylene-neopentyl adipate) glycol	Polyester	50	26

[a] Polyurethanes made from MDI, and 1,4-butanediol; mechanical properties retained after 7 days in H_2O at 80 ºC.

Linear polyesters made from adipic acid and aliphatic diols are wax-like crystalline.[15] This crystallinity is one factor for the high tensile strength displayed by poly(ester-urethane)s. However, the increase in stiffness due to crystallization induced by stretching at low temperature may be disadvantageous. By mixing diols, a fluid to hard-like polyester more suitable for some applications may be obtained.

2.2.3. Difunctional *chain extenders*

Polyurethanes lacking segmented structure are obtained by reaction of diisocyanates with short length diols. Additionally, these diols are used as *chain extenders* for urethane–isocyanate prepolymers in the production of segmented polyurethane elastomers. Common *extenders* are ethylene glycol, diethylene glycol, 1,4-butanediol and 1,6-hexanediol.[16-18] Diamines, like 1,2-ethylenediamine and 1,6-hexamethylenediamine, can also be used as *chain extenders*, but in this case the urethane chains are extended through urea groups.[19]

Chain extenders play a decisive role in the polymer morphology of polyurethane fibers, elastomers, and adhesives with segmented structure. The elastomeric properties of these materials are derived from the phase separation of the *hard* and *soft segments* of the polymer, such that the urethane *hard segment* domains serve as physical cross-links between the amorphous polyether or polyester *soft segment* domains. This phase separation occurs because the mainly non-polar, low melting *soft segments* are incompatible with the polar, high melting *hard segments*. The *soft segments*, which are formed from high molecular weight polydiols, are mobile and are normally present in coiled conformation, while the *hard segments*, which are formed from the isocyanate and *chain extenders,* are stiff and immobilized by extensive hydrogen-bonding. Since the *hard segments* are covalently coupled to the *soft segments*, plastic flow of the polymer chains is avoided and elastomeric resiliency is therefore generated. Upon mechanical deformation, a portion of the *soft segments* is stressed by uncoiling, and the *hard segments* become aligned in the stress direction. Such reorientation of the *hard segments*, which continue being tightened by a network of powerful hydrogen bonding, contributes to the high tensile strength, elongation, and tear resistance usually displayed by segmented polyurethanes. The choice of the *chain extender* also determines flexural, heat, and chemical resistance properties.

2.2.4. Catalysts

The catalytic activity in the reaction of isocyanates and compounds with unstable hydrogen atoms (*i.e.* alcohols, amines, water, carboxylic acids, malonates, etc.) is shown by tertiary amines and organometallic compounds, and among the latter the most important compounds are those of Sn, Pb and Fe. The most popular amine catalyst is

1,4-diazabicyclo-[2.2.2]-octane (DABCO), and the most widely used tin catalysts are dibutyltin dilaurate and dibutyltin dioctanate (Scheme 2.16). These tin compounds make the basis for very specific catalytic systems, which have been later developed and which offer a high selectivity with respect to polydiol components with different molecular weights and with primary, secondary or tertiary hydroxyl groups, and also with respect to small amounts of water eventually present in the reaction medium. These catalysts are used in the liquid form in most cases, or as solutions in glycols or polydiols, which constitute the so-called polydiol masterbatches. Catalytic salts of Bi, Ti, Co, Cd and Zn are also used but much less frequently.

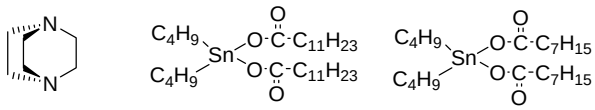

DABCO Dibutyltin dilaurate Dibutyltin dioctanate

Scheme 2.16. Commonly used catalysts in polyurethane production.

Alkyl tin carboxylates, oxides and mercaptides oxides are used in all types of polyurethane applications. For example, dibutyltin dilaurate is a standard catalyst for polyurethane adhesives and sealants, dioctyltin mercaptide is used in microcellular elastomer applications, and dibutyltin oxide is used in polyurethane paint and coating applications. Tin mercaptides are used to replace tin carboxylates in formulations that contain water, since the latter are susceptible to degradation by hydrolysis. The problems of catalysis in the polyurethane technology have been discussed in detail in many review papers that have been published dealing with that subject.[20,21]

2.2.5. Additives

In addition to the main components mentioned above, a large number of additives can be used for the successful manufacture of polyurethanes.[5] These additives are either useful or even necessary for the chemical process, or they contribute conveniently to the properties of the finished articles. Additives are, for example, stabilizers, blowing agents, flames retardants and compounds which protect the polyurethanes against hydrolytic, thermal and oxidative degradation as well as against degradation by light.

2.3. Preparation methods for polyurethanes

A significant impact on the properties of linear polyurethanes comes from the molecular weight and its distribution. These characteristics are in turn affected by a number of process parameters and by the issues associated to process equipment and timely organization of the process operations. The critical point of the polyurethane production processes, like in any step-growth polymerization, is the procedure followed to feed the isocyanate and the hydroxylic components. The volumes of feeds should be closely monitored to reach the required degree of polymerization. In order to obtain linear polyurethanes with high-molecular weights, it is advantageous to run the process with an equimolar ratio of functional groups. In case of two-stage processes, that recommendation concerns to the last stage of chain extension. The sequence and rate of adding components are also important for the production of polyurethane intermediates.

The polyaddition processes of diisocyanates and polydiols are carried out in solvents or directly in bulk, depending on the type of technology and performance properties expected for the final product. The bulk process is used predominantly to produce foamed materials, elastomers, and also coatings and adhesives which can be dissolved at the final stage of the process to be applied as solutions.

2.3.1. Solvent-free reactions

No solvents are used in the preparation of flexible and rigid foams, cast elastomers, and thermoplastic polyurethanes. No solvents are either necessary for the preparation of many of those products which are later processed in solution and eventually applied as solutions, such as textiles coatings and adhesives. Polyurethanes possess a significant technical and ecological advantage which is that they can be manufactured by solvent-free processes.

2.3.1.1. One-shot process

Processes which are carried out without solvents are generally very fast, especially, in the presence of catalysts.[22,23] This one-shot reaction requires that reactivities of the different components used for the synthesis are approximately the same and that they

are compatible for the applied process conditions. Di- or polyamines suitable for the preparation of poly(urea-urethane)s by one-shot processes in presence of diols usually have reduced reactivity, due to either severe steric hindrance or influence of electron withdrawing substituents.[24]

Polyurethane foams, can be produced specifically by the one-shot process through direct mixing of the coreactants and simultaneous addition of blowing agents, catalysts, foam stabilizers, flame retardants and other additives. The reaction is very exothermic and fast. The final properties, however, are often only achieved after 24 to 48 hours. This time can be reduced to a few hours by post curing at about 100 ºC. Table 2.4 and Figure 2.3 show the formulation and the picture of a conventional foam used for furniture cushions.

Table 2.4. One-shot formulation for the production of flexible foam.[8]

Components	**Parts**
TDI	51.6
Polydiol	100
Catalyst	0.5
Water	4
Surfactant	1

Figure 2.3. Image of a flexible foam.

2.3.1.2. Prepolymer process (Two-stage method)

In the nomenclature of polyurethane chemistry, prepolymers are intermediates of the isocyanate polyaddition reaction. Numerous polyurethane elastomers and almost all poly(urea-urethane)s are prepared via NCO prepolymers as intermediates. This method allows for the complete reaction even of polyether diols of low reactivity in the absence of catalysts and for the targeted formation of a segmented structure.

The prepolymer is obtained at the first stage with reactive isocyanate or hydroxyl end groups (Figure 2.4). Depending on both the type of prepolymer produced (isocyanate or hydroxyl ending type) and the assumed value of M_n, the required amounts of the convenient reacting substances are selected. The *chain extender* expands at the further

stage when the prepolymer reacts with the compounds containing two reactive groups at least. Depending on functional groups of the *extender* and its amount (*i.e.* ratio of groups r = NCO:OH), a linear polymer or a product cross-linked by urethane or allophanate bonds can be produced.

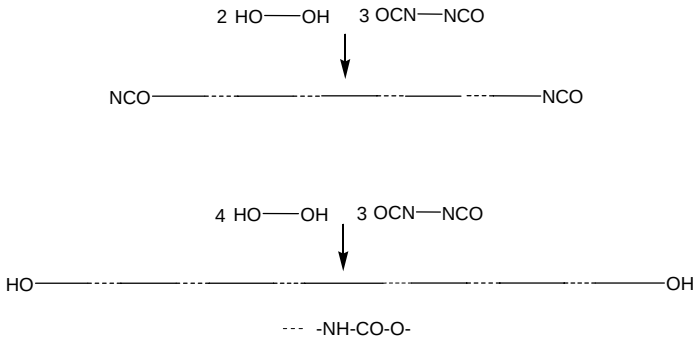

Figure 2.4. NCO and OH prepolymers.

The possibility of choosing the starting compounds among a variety of raw materials and at different ratios, and the ability to control the microstructure of the polymer chain, provide the chance of producing "tailored" PUR with a broad variety of properties.[25-27] Addition of other unusual compounds can be used to impart specific features to polyurethanes. For example, incorporation of mesogenic rigid segments makes possible to obtain PUR elastomers displaying liquid crystals properties.[28]

The two-stage method, depending on the relative amount of the monomers used, makes possible to obtain prepolymers with both isocyanate and hydroxyl terminal groups, and additionally to control their molecular weights. However, the use of large excess of one of the monomers will introduce considerable limitations to molecular weights and monodispersity of the prepolymers. Furthermore, unconverted significant amounts of diisocyanate are objectionable because of its toxicity and negative impact on other properties of the final products.

2.3.2. Reactions in solution

Polyurethanes of high molecular weight can be obtained by means of two methods: interfacial polycondensation or polycondensation in solution. In the interfacial

polycondensation, the reactives are dissolved in a couple of immiscible solvents, one of them water. The polymerization takes place nearby or on the liquid interface.

The polymerization in solution is made in a homogeneous system provided by an appropriate solvent.[29,30] The solvent can be only one compound or a mixture of organic solvents, at any case without reactive functional groups. The process begins with the previous dissolution of the reactives in the solvent, although it is not essential. The produced polyurethane can stay in solution or precipitate in some moment of the process.

2.3.3. Non-isocyanate methods

Is very interesting, although of no practical use so far, the production of polyurethanes by the cationic ring opening polymerization of cyclic urethanes. Polymerization of seven-membered rings takes place at the temperature which is only slightly above the monomer melting point. Six-membered rings would polymerize at 100 °C, while the five-membered structures do not polymerize at all; such a different behaviour comes from the positive contribution of the entropy component ΔS to the free enthalpy $\Delta G = \Delta H - T\Delta S$ of the polymerization reaction of six-membered cyclic compounds or larger. The value of the enthalpy component for such reactions is zero ($\Delta H \approx 0$) in practice. The dominant reaction at higher temperatures ($\Delta G > 0$) is polymer decomposition by cyclic depolymerization (Scheme 2.17).

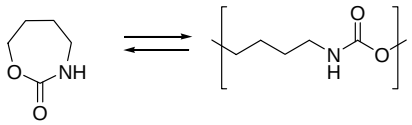

Scheme 2.17. Polymerization reaction of cyclic compounds and cyclodepolymerization.

This method is applicable to the production of multi-blocked urethane copolymers, *i.e.* with poly(tetrahydrofuran) as second block, by using initiators like methyl trifluoromethylsulfonate or trifluoromethylsulfonic anhydride.[31,32]

There are other methods for the production of linear polyurethanes, as the so-called isocyanate-free methods, which were developed pretty long ago. They are based on the

interphase condensation of diamines and bischloroformates (Scheme 2.18), or on the reaction of urea derivatives with carbonates. There is no commercial application for them[33] up to date although they are interesting because they provide a feasible way for the production of *N*-substituted polyurethanes.

$$n\ H_2N–R'–NH_2 + n\ Cl–CO–O–R–O–OC–Cl \rightarrow$$
$$–(NH–R'–NH–CO–O–R–O–CO)_n– + 2n\ HCl$$

Scheme 2.18. Condensation of diamines and bischloroformates.

Recently, Rokicki obtained aliphatic polyurethanes from diamines and diols or alternatively from α,ω-aminoalcohols using ethylene carbonate as a substitute for phosgene.[34] The five-membered cyclic ethylene carbonate is readily available from ethylene oxide and carbon dioxide. At difference to most carbonic acid derivatives, ethylene carbonate is an environmentally friendly compound since it is not prepared from phosgene. Based on Rokicki works, Ubaghs *et al*.[35,36] reported on the synthesis of a new AA' monomer derived from glycerol-phenoxycarbonyloxymethyl-ethylene carbonate, which upon reaction with diamines also yields polyurethanes bearing pendant primary or secondary hydroxyl groups in the repeating unit. As it was commented above, Meijer *et al.* also reported on the synthesis of [*n*]-polyurethanes from α,ω-isocyanatoalcohols, obtained in the reaction of α,ω–aminoalcohols with di-*tert*-butyltricarbonate.[3]

2.4. Structure of polyurethanes

Depending on their primary structure, polyurethanes can be divided into four groups: non-segmented, segmented, cross-linked and ionomeric. The primary structure largely determines the micromorphology adopted by polyurethanes in the solid state and this is which determines the final physical properties of the material.

2.4.1. Two-component polyurethanes without segmented structure

The properties of "pure" polyurethanes, prepared from a diisocyanate and a short diol, correspond to those of structurally similar polyamides.[37,38] Semicrystalline "pure" polyurethanes, *i.e*. 4,6-PUR prepared from 1,4-butanediol and 1,6-hexamethylene diisocyanate, usually display a high degree of crystallinity with extensive hydrogen

bonding between –NH– and –CO– groups, which results in high hardness and strength and a low solubility. Amorphous “pure” polyurethanes, *i.e.* those prepared from toluene diisocyanate and diethylene glycol, are hard and transparent but show only marginal dimensional stability at elevated temperatures. The other end of the “pure” polyurethane property range is represented by soft elastomeric products which are obtained by reaction of long chain, unbranched, OH– difunctional polyethers or polyesters with stoichiometric amounts of diisocyanates (Figure 2.5). They contain only about 4 to 6% urethane groups, as a result, hardness and strength are comparatively low.

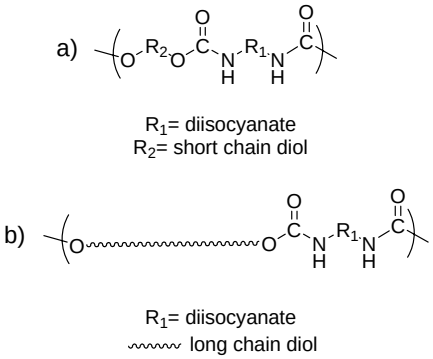

Figure 2.5. Structure of “pure” polyurethanes: **a)** hard and **b)** elastomeric products.

2.4.2. Segmented polyurethanes

Most segmented polyurethanes are composed of at least three basic components:

- Long chain polyether-polydiol or polyester-polydiol
- Diisocyanate
- Short chain diol, water or diamine (*chain extender*)

From a polymer physics point of view, segmented polyurethanes constitute a new class of elastomeric products which are characterized by a segmented structure (block copolymer structure) of the primary chain. The secondary and tertiary structure and, consequently, the morphology of these polyurethanes are dependent on the chemical composition and the length of the segments (blocks).[39-41] The distinguished property level of these products is due to their multiphase micromorphology.

Polyurethane prepared from one mole of long chain diol, one mol of short chain diol, and two moles of diisocyanate would have the following ideal structure (Figure 2.6).

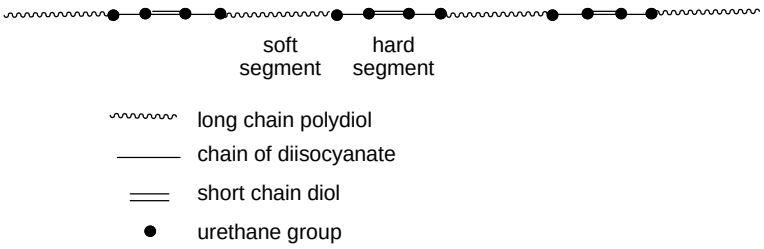

Figure 2.6. Ideal structure of segmented polyurethanes.

Soft segments, which are quite mobile and are normally present in coiled conformation, alternate with the so-called *hard segments* made of stiff oligourethane units. Under practical conditions, the microstructure of the *soft segments* as well as the urethane reaction, follow a statistical Flory distribution.[42] As a result, an amount of *hard segments* higher than one could theoretically predict is formed. Therefore, the average length of the segmented structure is in reality greater than predicted for the ideal case (Figure 2.7).

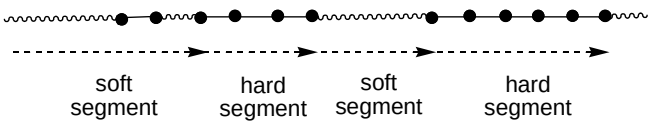

Figure 2.7. Structure of segmented polyurethanes.

The two-phase nature of the segmented polyurethanes is related to the fact that the low molecular weight diol has a relatively high polarity and, therefore, has only limited compatibility, *i.e.* with a polypropylene ether polydiol and toluene diisocyanate. In the first step, the oligomeric diol reacts with the diisocyanate, forming polar urethane groups which improve compatibility. As the reactions proceeds, the mainly non-polar, low melting *soft segments* are incompatible with the polar, high melting *hard segments*. As a result, phase separation (segregation) occurs and, simultaneously, covalently-linked microphases are formed.

The coherent matrix consisting of flexible *soft segments* is responsible of the high deformability of the resulting material. In contrast, the hard molecular segments are fixed by hydrogen bonding interaction. Since *hard segments* are covalently attached to the *soft segments*, they inhibit plastic flow of the chains, thus creating elastomeric resiliency.

The stress-strain curves of polyurethanes with different *soft segment* lengths (PCL with M_n from 750 to 2800 g·mol^{-1}), and *hard segment* of 1,4-butanediol and tetrabutylenen diisocyanate, are shown in Figure 2.8.[43] An increase in *soft segment* length leads to a decrease in *hard segment* content. In the curves, three different regimes are clearly visible. The behaviour at low deformations can be explained as the pure elastic deformation belonging to regular elastomers. With a decrease in *hard segment* content the Young's modulus also decreases.

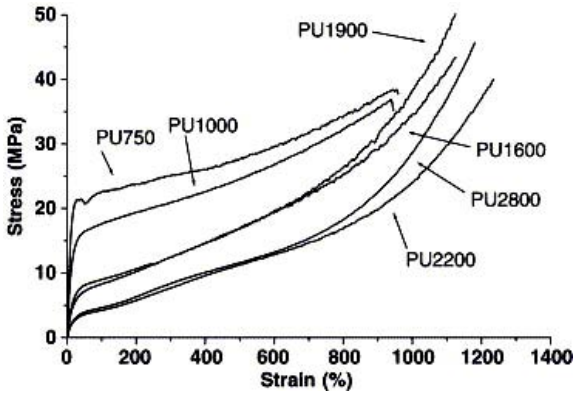

Figure 2.8. Effect of increasing the *soft segment* length in the stress-strain curves of segmented polyurethanes made from PCL.[43]

Hard segment domains can be looked at as multifunctional, spacious cross-linked areas. Temperature increase, and especial solvents, can reversibly eliminate the cross-linking allowing further deformation. The degree of deformation between *hard* and *soft segments* depends on the interaction (affinity) of *hard segments* with each other or with the *soft segments*, respectively. The segregation, therefore, is less pronounced in poly(ester-urethane)s than in poly(ether-urethane)s and it is the most pronounced in poly(butadiene-urethane)s.[44,45]

The affinity between the *hard* and *soft segments* depends largely on the symmetry of the diisocyanate and on the specific *chain extender* used (diol or diamine). The structure of these building blocks affects the symmetry of the *hard segments* and, hence, the formation of organized structures. *Chain extenders* having an even number of methylene groups in their backbone yield *hard segments* with higher melting ranges than those having an odd number of methylene groups. The diurethane connecting link formed by the reaction of long-chain polyether- or polyester-polydiols with diisocyanate does not possess *hard segment* features and remains dissolved in the *soft segment* phase.

2.4.3. Cross-linked polyurethanes

Flexible and semi-flexible foams, cast elastomers and most of the reactive systems are made of cross-linked polyurethanes.[46,47] Although these materials are no longer thermoplastic, melting of the *hard segment* domains is observed in the form of softening (decrease of shear modulus). Glass transition temperatures usually increase with greater cross-link density, but the tendency to crystallization decreases. Whereas the elongation decreases with increasing cross-link density, the tensile strength goes through a maximum.

Polyurethane adhesives mostly contain isocyanate polyurethane prepolymers which react with humidity and form highly cross-linked elastomers (Figure 2.9). By choosing appropriate additives, the adhesion characteristics can be adapted to various substrates like glass, metals, plastics and paints, leading to durable adhesion.

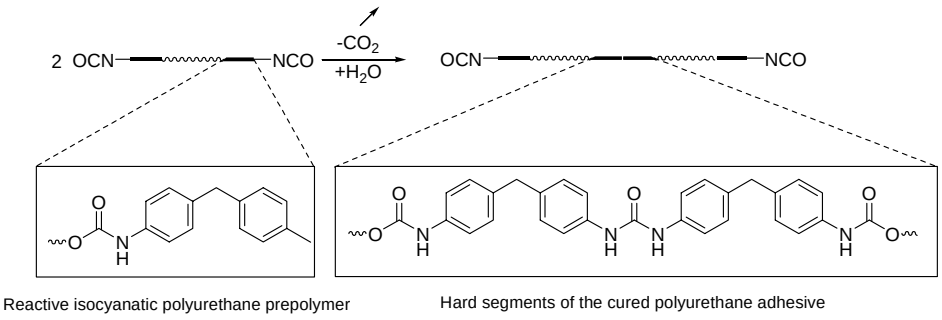

Figure 2.9. Prepolymer reaction to polyurethane adhesive.

2.4.4. Ionomers

Ionomers are polymers that contain numerous ionic centers more or less homogeneously distributed along the polymer chain and separated by a short chain apolar segment. The ionic centers can be hydrated with water to form stable dispersions. Typical ionomer properties are good dispersibility, high hydrophilicity, exceptional mechanical properties and adhesion. The reason for this outstanding behaviour lies in the fact that the ionically modified polyurethanes possess, compared to the neutral polymers, the possibility for intermolecular ionic interactions among the polymer chains. A multitude of preparation methods has been described for polyurethane ionomers.[48-50] Most of these are almost exclusively used for the preparation of self-emulsifying aqueous dispersions.

Polyurethane ionomers are suited for a wide variety of applications. They are compatible with chemically different ionomers (*i.e.* hydrocarbon-based products[51]), provide a changed gas permeability,[52] dispersibility, anti-fogging behaviour, amphiphilic properties, coagulability, and are comparable with biological substrates, *i.e.* especially with gelatine, for photographical applications. Blends of basic and acidic polymers are a special type of ionomer. Due to the principle of ionic interaction, otherwise incompatible polymers can be rendered compatible.[53]

Figure 2.10. Polyurethane ionomer cover of golf balls provides hardness, abrasion resistance and durability.

Also the ionomers, useful for golf ball covers, sealants, and adhesives, are manufactured by reaction of polydiols with polyisocyanates and ionic segment-containing *chain*

extenders in the absence of solvents. A golf ball cover made of ionomer polyurethanes shows excellent scratch resistance (Figure 2.10).

2.5. General applications of polyurethanes

Polyurethanes are one of the most versatile materials today. Their many uses range from flexible foam in upholstered furniture to rigid foam as insulation in walls and roofs to thermoplastic materials used in medical devices and footwear to coatings, adhesives, sealants and elastomers used on floors and automotive interiors. Depending on the application, a polyurethane chemist can vary density and stiffness to achieve acceptable product performance. Figure 2.11 classifies polyurethane usage by application.

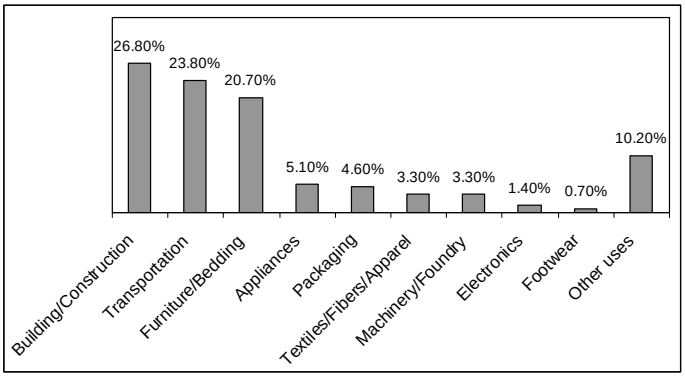

Figure 2.11. Polyurethane usage by application. Source: The Socio-Economic Impact of Polyurethanes in the United States (February 2004), prepared by the American Chemistry Council.

Polyurethanes can be classified in three groups depending on their properties and applications:

Foams

Flexible polyurethane foams can be seen in bedding, furniture, automotive interiors, carpet underlay and packaging. Rigid polyurethane and polyisocyanurate foams form one of the world's most popular, energy-efficient and versatile insulations. Foams can be created in almost any variety of shape and firmness. In addition, they are light, durable, supportive and comfortable.

Thermoplastics

Thermoplastic polyurethanes (TPU) are unique in offering a variety of physical property combinations and processing applications. They are highly elastic, flexible and resistant to abrasion, impact and weather. TPU can be coloured or fabricated in a wide variety of methods, and their use increases a product's overall durability.

Coatings, adhesives, sealants and elastomers

Polyurethane coatings make a product looking better and lasting longer. Polyurethane adhesives provide strong bonding advantages. Polyurethane sealants provide tighter seals. Polyurethane elastomers can be moulded into almost any shape, are lighter than metal, offer superior stress recovery and are resistant to many environmental factors.

Figure 2.12. Representative applications of polyurethanes.

2.6. Current applications of linear polyurethanes

This section is going to present a synthetic review of the current trends in applications of the materials based on linear polyurethanes.

2.6.1. Elastomers

Linear polyurethanes are important intermediate products for the manufacture of elastomeric structural materials and for a wide range of protective coatings. Applicability in these fields is usually controlled by numerous and different physico-chemical properties and by the specific performance resulting from the former, the static and dynamic mechanical properties playing the main role in this regard.

It is evident that the mechanical properties of the final goods will be decided by the structures of PUR chains and by the phase structures of PUR. That problem has been extensively described in literature since mechanical properties affect directly the fields of applicability for PUR foams, PUR elastomers and PUR coatings.[5] PUR behaviour under the effect of mechanical forces is determined by the polymer phase structure, and that in turn is controlled by the organization of its segments.[54,55] The presence of *soft segments* with negative T_g imparts elastomeric performance to the polymer, while *hard segments* contribute to its good strength. The quality of a PUR elastomer is defined not only by the negative value of its T_g but also by its mechanical properties, and in particular by its tensile strength, ultimate elongation, hardness, elasticity, abrasion resistance and impact resistance.

The most important contribution to mechanical properties comes from the chemical structure and from the size and structure of *hard* and *soft segment*. Higher elasticity is favourable for intermolecular interactions. In contrast to mechanical strength, which is controlled first of all by the structure of *hard segments*, elasticity is affected mainly by *soft segments*. Low energy of interactions in poly(ether-urethane)s makes them much more flexible than poly(ester-urethane)s.[56]

The highest mechanical strength is provided by PUR obtained from diisocyanates with symmetrical structures, like aromatic MDI or its alicyclic equivalent H_{12}MDI.[57,58] PUR produced from poly(propyleneglycol)s, known as Pluronics, with asymmetrical structures have lower mechanical strength than their analogues derived from poly(tetramethylene glycol), its hydrophobic nature enhances the phase separation potential and its regular structure favours crystallization.

The first high performance polyurethane elastomer applications were developed in the beginning of the 1950's, once people had realized that polyurethane elastomers could be

used in a variety of new designs besides simply replacing rubber in existing applications. Wheels and tires are the biggest application in terms of volume for polyurethane elastomers. The major reason for using them in place of rubber is their significantly higher *E*-modulus, outstanding abrasion resistance, and high elasticity. Polyurethane elastomers can be used virtually everywhere. Snowplow blades are made with polyurethane to reduce road damage caused by metal scraping the roads. Wheels for shopping carts, skateboards, roller coasters, and heavy trash containers are all produced from polyurethane, due to its high load-bearing capacity and abrasion resistance. And since polyurethane elastomers are so easily machined, they can be moulded and processed for custom uses such as valves, snowblower augers, balls, and factory fixtures.

2.6.2. Biomedical materials

Biomaterials must exhibit good mechanical, physical, or electrical properties depending on their application. Surface properties also taken in consideration are hydrophilicity, charge, polarity and energy, heterogeneous distribution of functional groups, wettability, water absorption and chain mobility. As well, morphological or topographical aspects including texture, smoothness and roughness should be accounted for. However, all these properties will be modified under a physiological environment because they will be subjected to the following effects: the duration of implantation, the temperature of the body and the pathological conditions at the implant site. Biomaterials must maintain their biostability and biofunctionality during implantation in order to avoid graft failure. Finally, any biomaterial and its degradation products, if biodegradable, should not induce any deleterious reactions or disturb the biological environment. Nowadays polymers, including polyurethanes, are extensively used for replacing or repairing a wide variety of organs and tissues (Figure 2.13).

The exceptional combination of good physical properties of PUR elastomers with their high hydrolytic stability and biological stability makes possible to use polyurethanes as highly specialized biomedical materials. Reasons for this are their high mechanical strength, flexibility, fatigue resistance, and tissue compatibility. Another advantage is their biodegradability through resorption. Many studies are aimed at the improvement of the blood compatibility of polyurethanes through surface modification, *i.e.* with heparin or

albumin.[59,60] Very important are the investigations of durability under physiological conditions, and of the biodegradability of polyurethanes.[61,62]

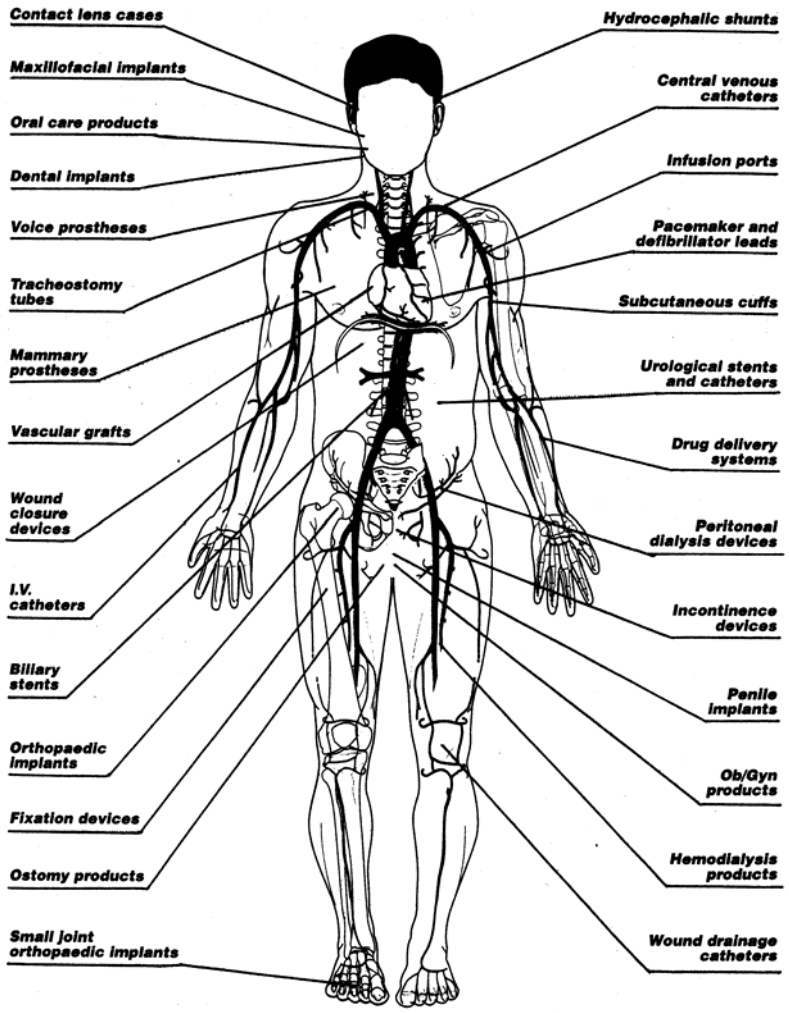

Figure 2.13. Biomaterials and biomedical devices are used throughout the human body.[68]

Polyurethanes are well known for their physiological inertness in relation to living organisms, hence making the interesting choice as materials for medical implants.[63-65] The advantageous reduction of adhesion, which prevents aggregation of blood cells, results from the level of phase separation and hydrophilic performance of surfaces of

such materials.[66] They do not induce any inflammatory condition of tissues or undergo destruction by body fluids, and no blood components are deposited on them.[7,57] Thus they will be suitable materials for intracorporeal applications, specifically for the manufacture of endoprostheses, cardiac valves or regenerative membranes for damaged internal organs. Also polyurethanes appear to be the most promising class of polymers for in-vivo applications.

The two most important biomedical applications of polyurethanes are external bandages and artificial organs. The plaster of Paris bandages which are normally applied to make plaster casts can be replaced by much lighter and easier to handle polyurethane bandages. These bandages are impregnated with a hydrophilic NCO- terminated prepolymer and after dipping in water and wrapping the cast, the product hardens in a few minutes. Polyurethanes are also used in the manufacturing of blood dialyzer (artificial kidneys) to bind together bundles of hollow fibers (generally from cellulose-hydrate). These are built into the blood cleaning unit in such a manner that the blood passes through the fibers and the dialysis fluid flows around them. The cast part containing the hollow fibers has to be elastic and cuttable at the same time and must not impede the free flow through the fibers. Two-component polyurethane cast systems have proven their specific usefulness for this application. Catheters are made from thermoplastic polyurethane elastomers. Polyurethanes are also materials extensively considered for orthopaedic applications.[67]

2.6.3. Protective coatings, waterborne ecological lacquers, adhesives and binders

One of the most recent trends in applications for polyurethanes is the production of ionomers from which aqueous dispersions can be obtained with no involvement of external emulsifiers. Such dispersions are then employed as environmentally friendly lacquers applicable to metal, ceramic, glass and wood substrates or as water-repellent glass finishes.[69] With a relatively high concentration of ionic groups which readily undergo solvation, polyurethanes (which are usually hydrophobic) become highly hydrophilic and soluble in typical organic solvents like methanol or acetone, and they form homogeneous solutions or stable emulsions and dispersions in water. The increasing content of ionic groups in a polyurethane chain is followed by the improved hydrophilic performance of the coatings obtained from polyurethane ionomers, better mechanical strength and elasticity of those coatings.

By combining emulsions of polyurethane ionomers with emulsions of other polymers, like poly(vinyl alcohol) or poly(vinyl acetate), one can produce interpenetrating polymer networks (IPN) with superior adhesion to metals and ceramic materials and with improved water resistance. An interesting field of application is the production of polymeric coatings with the use of polyurethane IPNs and other addition polymers like poly(methyl methacrylate)[70] and polystyrene,[71] or condensation polymers, *i.e.* unsaturated polyethers,[50] epoxides[72] and polysiloxanes.[73]

2.7. Green polyurethanes

The soaring prices of crude oil have sparked a debate about the benefits that increased use of renewable raw materials might bring to plastics production. Another aspect is the greater environmental compatibility attributed to products based on natural components. Industrial sugars and vegetable oils have been used in the production of polydiols, one of the two basic components in polyurethanes alongside isocyanates. Recently, Bayer MaterialScience and Dupont have developed polydiols based on 70-100% by weight on renewable raw materials to help cut down emissions.

However, the great majority of polyurethanes are produced today using petroleum resources such as feedstocks and are generally resistant to biodegradation in the environment. Moreover the efficient chemical recycling of conventional polyurethane has not been developed. To develop green and sustainable polyurethane, an adequate molecular design should be carried out by considering the starting materials, environmentally benign production and recycling processes, and the effect of the polymer in the environment. The production of recyclable and biodegradable polyurethanes based on renewable resources may be the best way to fulfill all these requirements.

2.7.1. Polyurethanes from natural resources

Today new materials have to fulfill ecological requirements with respect to the raw materials used, as far as both their manufacturing technology and their waste disposal are concerned. Therefore, renewable primary materials attract a great deal of attention (Figure 2.14). Compared with the raw materials from crude oil or coal, however, raw

materials from renewable resources are highly functional materials with a high content of oxygen and nitrogen, which often turns out to be impedimentary for an application.

Figure 2.14. Natural products as source of bioplastics.

Carbohydrates are carbon compounds that contain large amounts of hydroxyl groups. Therefore they are potential reagents in the preparation of polyurethanes. They can be divided into three categories: (1) monosaccharides, *i.e.* glucose, galactose, xylose, fructose, and others; (2) oligosaccharides (combination of two to ten monosaccharides, such as disaccharides and trisaccharides); (3) polysaccharides (long chains of monosaccharide units, such as cellulose, starch or hemicelluloses).

Because of their abundance, easy recovery from nature, and low cost, carbohydrates represent an interesting source for production of renewable resources-based products. Shiraishi *et al.* studied the preparation of polyurethanes from starch.[74,75] It was found that liquefied starch polydiols have suitable characteristics for making polyurethanes with comparable properties to conventional “petro-based” polyurethanes.[76] In addition to polysaccharides starch and cellulose, low cost monosaccharides, such as glucose, fructose, galactose, mannose, etc., are available on an industrial scale. Despite the high share of these materials on the total available biomass, the amount used for polymer synthesis is very low. A reason for this is the high functionality of these materials; a selective chemistry may be achieved however by using protective groups.

Polymers may be produced containing monosaccharides derivatives as building blocks in the main chain or in the side chains. Since the fifties, saccharose–phenol–formaldehyde resins have been known and prepared by polycondensation of saccharose with phenol and formaldehyde mixtures. To prepare linear polymers with monosaccharide units in the main chain the saccharide building block should have only two reactive functional groups.[77,78] As is shown for the polymerization of glucosamine with diisocyanates, in certain cases, two functional groups with higher reactivity can be used for selective reaction. In glucosamine, the amine group and the primary hydroxyl group are of higher reactivity than the secondary hydroxyl groups.[79]

Other saccharides with only two reactive functional groups are anhydroalditols of sorbitol or erythritol. These derivatives are suitable for production of homopolymers or copolymers with diamines, diisocyanates, phosgene or dicarboxylic acids.[80,81] Lactones based on glucaric and galactaric acid are monosaccharide based monomers; with respect to their functional groups they are diols and/or bislactones. These monomers react with diamines by ring-opening polymerization to give polyamides and with diisocyanates by polyaddition to give polyurethanes.[82]

In addition to carbohydrates, vegetable-oil-based polydiols can be used to produce polyurethanes (Figure 2.15) that compete in many ways with polyurethanes derived from petrochemical polydiols; their preparation for general polyurethane use has been the subject of many studies.[83-85] Vegetable oils are one of the cheapest and most abundant biological sources available in large quantities, and their use as starting materials has numerous advantages: for example, low toxicity, inherent biodegradability, and high purity.[86] They are considered to be one of the most important classes of renewable resources for the production of biobased thermosetting polyurethanes.[87] For natural oils to be used as raw materials for polydiol production, multiple hydroxyl functionality is required. Two different ways of preparing vegetable-oil-based polydiols have been successfully developed. In the first way, polydiols are formed by reaction at the double bond of the unsaturated fatty oil,[84] in the second, a combined reaction at the double bonds and subsequent reduction of the carboxyl group yields the hydroxyl moieties.[88]

In addition to carbohydrates and fatty acids, natural polyhydroxy alcohols such as 1,3-propanediol or glycerine have been used for polyurethane production. 1,3-Propanediol can be obtained from rape seed oil production in the presence of *Clostridium butyricum*[89]

or from corn.[90] Benefits of 1,3-propanediol include its purity, lack of irritation and sensitization, and environmentally-friendly nature. In polyurethane-based polymer systems, 1,3-propanediol can be used as a *chain extender*.[91,92] In thermoplastic polyurethanes its use leads to improve their thermal and hydrolytic properties as well as their thermal dimensional stability.

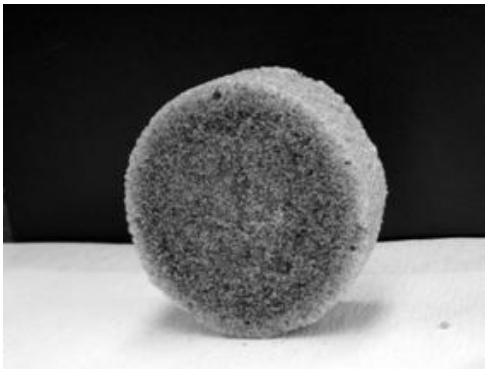

Figure 2.15. Liquefied wood can be used for synthesis of polyesters. These can react with isocyanates to give polyurethane foams comparable to commercial foams to be used in agriculture and horticulture.

Glycerine or glycerol is a sugar alcohol of low toxicity. Glycerol has three hydrophilic hydroxyl groups that are responsible for its solubility in water and its hygroscopic nature. Since glycerol forms the backbone of triglycerides, it is produced on saponification or transesterification. Current levels of glycerol production are about 350,000 tpa in USA and 600,000 tpa in Europe. Glycerol is one of the major raw materials for the manufacture of polydiols for flexible foams and also frequently used as *cross-linker*. Recently, some polyurethanes made of glycerol and natural polydiols such as soybean or castor oil have been reported.[93,94] In addition, glycerol is also useful for the production of biodegradable and biocompatible polyurethane delivery systems suitable for medical implants.[95,96]

Although several polyurethanes have been made and have reached industrial development using renewable resources, it is only the polydiol moiety which is biobased;[97] the polydiol component is easily extracted from natural resources such as plants or may be synthesized from naturally occurring precursors. Diisocyanates are not naturally accessible and they have to be fully synthesized from petrochemicals; these

syntheses are very challenging so that satisfactory results have not yet been reached. Therefore, 100% biobased polyurethanes with acceptable properties are not still available.

2.7.2. Biodegradation of polyurethanes

Conventional high molecular weight polyurethanes are generally resistant to biodegradation. However, low molecular weight urethane oligomers are not so stable. It has been reported that urethane oligomers can be hydrolyzed by some microorganisms and that the hydrolysis is catalyzed by an esterase.[98,99] However, it is still unclear whether the urethane bonds of high molecular weight polymers are directly hydrolyzed. The biodegradation of polyurethane containing some hydrolyzable groups other than the urethane bond has been reported. The microbial degradation of poly(ester-urethane)s (PEU) is thought to occur mainly by hydrolysis of ester bonds by esterases or lipases, leading to the molecular weight reduction. The oligomeric urethane fragments will then be further degraded.[100,101] The *in vitro* degradation of poly(ether-urethane-urea) was evaluated by exposure to enzymatic and aqueous environments. In this case, the mechanical properties deteriorated but a significant degradation of the polyurethane was not detected.[102,103]

In addition, Owen *et al.*[98] reported that the fungus *Exophila jeanselmei* REN-11A was able to metabolize low molecular weight *N*-tolylcarbamate model compounds, which has structures closely resembling the urethane linkages found in the polyurethane made from 2,4-toluene diisocyanate, to produce toluene diamine. This is a clear demonstration of that low molecular weight urethane could be hydrolyzed by microbes. The *Comamonas acidovorans* strain TB-35, isolated by Nakajima-Kambe *et al.*, is a gram-negative bacterium that has been reported to be capable of degrading solid PEU. These authors isolated this solid PEU-degrading enzyme, which has unique characteristics; it has a hydrophobic polyurethane surface-binding domain and a catalytic domain, the former being considered determinant for polyurethane degradation.[104-106] It is easy to understand that PEU are susceptible to hydrolysis by esterases. The PEU was hydrolyzed by *Rhizopus delemar* lipase at the polyester moiety.[107] Santerre *et al.*[108] and Wang *et al.*[109] reported that cholesterol esterase degraded the PEU synthesized from 2,4-toluene diisocyanate, polycaprolactonediol, and ethylene diamines, with releasing of the *hard-segment* components.

Polyurethane foams can be also biodegradable. Flexible PUR foams are usually obtained from the reaction between polyfunctional alcohol (polydiol), polyisocyanate, and water as a blowing agent. Natural polymers containing more than one hydroxyl group in the main chain (*i.e.* starch, cellulose, tannin, saccharides, etc.) can be used as biodegradable polydiols for PUR preparation rendering potential biodegradable materials (Figure 2.16).[110]

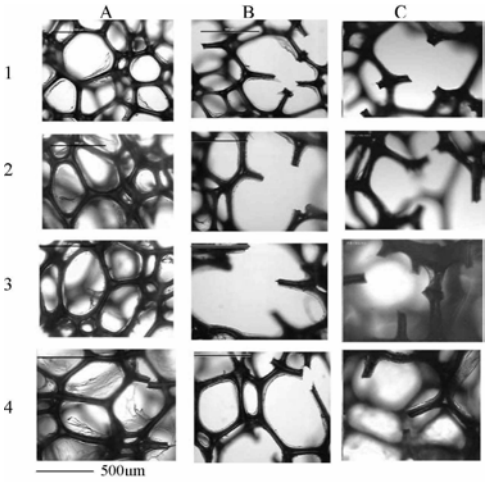

Figure 2.16. Light micrographs of BIO-PUR foams prepared by one-shot process using toluene diisocyanate (TDI), polyether polydiol (PEP), catalysts, water, and three types of cellulose. PEP reference polyurethane **(1)**, 2-hydroxyethylcellulose **(2)**, acetylated starch **(3)**, and acetylcellulose derived polyurethane **(4)**, Before biodegradation **(A)**, after biodegradation; by *Thermophillus sp*. **(B)**, and *Aureobasidium pullulans* **(C)**, bacteria producing large amounts of hydrolytic enzymes capable of degrading polymeric materials.[110]

2.8. References

1. Wirpsza, Z. *Polyurethanes: Chemistry, Technology and Applications*, Ellis Horwood, London **1993**.

2. Bayer, O. *Angew Chem* **1947**, 59, 257.

3. Versteegen, R.M.; Sijbesma, R.P.; Meijer, E.W. *Angew Chem, Int Ed* **1999**, 8, 2917.

4. Bayer, O. *Angew Chem* **1947**, 71, 26.

5. Oertel, G. *Polyurethane Handbook*, Hanser Publishers, Munich **1994**.

6. Thomson, T. *Polyurethanes as specialty chemicals: principles and applications*, CRC Press, Boca Raton **2005**.

7. Vermette, P.; Griesser, H.J.; Laroche, G.; Guidoin, R. *Biomedical applications of polyurethanes*, Eurekah-com Publishers, Georgetown **2001**.

8. Barikani, M.; Mohammadi, M. *Carbohyd Polym* **2007**, 68, 773.

9. Yeganeh, H.; Hojati-Talemi, P. *Polym Deg Stab* **2007**, 92, 480.

10. Paul, C.J.; Nair, M.R.G.; Neelakantan, N.R.; Koshy, P. *Polymer* **1998**, 39, 6861.

11. Król, P. *Prog Mater Sci* **2007**, 52, 915.

12. Chattopadhyay, D.K.; Raju, K.V.S. N. *Prog Polym Sci* **2007**, 32, 352.

13. Papava, G.S.; Maisuradze, N.A.; Zharkua, Z.L.; Dokhturishvili, N.S.; Sarishvili, Z.M.; Rozmadze, G.B.V. *Acta Polym* **1988**, 39, 445.

14. Kuran, W.; Sobczak, M.; Listoś, T.; Debek, C.; Florjańczyk, Z. *Polymer* **2000**, 41, 8531.

15. Wilfong, R.E. *J Polym Sci* **1961**, 54, 385.

16. Bajsic, E.G.; Rek, V. *J Elastomers Plast* **2000**, 32, 162.

17. Savelyev, Y.V.; Akhranovich, E.R.; Grekov, A.P.; Privalko, E.G.; Korskanov, V.V.; Shtompel, V.I.; Privalko, V.P.; Pissis, P.; Kanapitsas, A. *Polymer* **1998**, 39, 3425.

18. Zia, K.M.; Barikani, M.; Bhatti, I.A.; Zuber, M.; Bhatti, H.N. *J Appl Polym Sci* **2008**, 109, 1840.

19. Klinedinst, D.B.; Yilgoer, E.; Yilgoer, I.; Beyer, F.L.; Wilkes, G.L. *Polymer* **2005**, 46, 10191.

20. Ratier, M.; Khatmi, D.; Duboudin, J.G. *Appl Organomet Chem* **1992**, 6, 293.

21. Blank, W.J.; He, Z.A.; Hessel, E.T. *Progr Org Coat* **1999**, 35, 19.

22. Garçon, R.; Clerk, C.; Gesson, J.-P.; Bordado, J.; Nunes, T.; Caroco, S.; Gomes, P.T.; Da Piedade, M.E. Minas; Rauter, A.P. *Carbohydrate Polymers* **2001**, 45, 123.

23. Doseva, V.; Shenkov, S.; Vasilev, S.; Baranovsky, V.Y. *J Appl Polym Sci* **2004**, 91, 3651.

24. Blahak, J.; Meckel, W.; Müller, E. *Angew Makromol Chem* **1972**, 26, 29.

25. Du, H.; Zhao, Y.; Li, Q.; Wang, J.; Kang, M.; Wang, X.; Xiang, H. *J Appl Polym Sci* **2008**, 110, 1396.

26. Nanda, A.K.; Wicks, D.A.; Madbouly, S.A.; Otaigbe, J.U. *J Appl Polym Sci* **2005**, 98, 2514.

27. Oprea, S.; Vlad, S.; Stanciu, A. *Polymer* **2001**, 42, 7257.

28. Jeong, H.M.; Kim, B.K.; Choi, Y.J. *Polymer* **1999**, 41, 1849.

29. Abraham, G.A; Marcos-Fernández, A.; San-Roman, J. *J Biomed Mater Res A* **2006**, 76, 729.

30. Shelke, N.B.; Aminabhavi, T.M. *J Appl Polym Sci* **2007**, 105, 2155.

31. Kušan, J.; Keul, H.; Höcker, H. *e-Polymers* **2001**, 011, 1.

32. Neffgen, S.; Keul, H.; Höcker, H. *Macromol Rapid Commun* **1999**, 20, 194.

33. Morgan, P.W. *J Polym Sci* **1964**, 4, 1075.

34. Rokicki, G.; Piotrowska, A. *Polymer* **2002**, 43, 2927.

35. Ubaghs, L.; Fricke, N.; Keul, H.; Höcker, H. *Macromol Rapid Commun* **2004**, 25, 517.

36. Prompers, G.; Keul, H.; Höcker, H. *Green Chem* **2006**, 8, 467.

37. Nishio, A.; Mochizuki, A.; Sugiyama, J.–I.; Takeuchi, K.; Asai, M.; Ueda, M. *High Perform Polym* **2001**, 13, S233.

38. Versteegen, R.M.; Sijbesma, R.P.; Meijer, E.W. *Angew Chem Int Ed* **1999**, 38, 2917.

39. Rogulska, M.; Kultys, A.; Pikus, S. *J Appl Polym Sci* **2008**, 110, 1677.

40. Pukanszky, B.Jr.; Bagdi, K.; Tovolgyi, Z.; Varga, J.; Botz, L.; Hudak, S.; Doczi, T.; Pukanszky, B. *Eur Polym J* **2008**, 44, 2431.

41. Yoshihara, N.; Ishihara, H.; Yamada, T. *Polym Eng Sci* **2003**, 43, 1740.

42. (a) Tanaka, M. *Makromol Chem* **1986**, 187, 2345. (b) Tanaka, M.; Nakaya, T. *J Macromol Sci Chem* **1989**, 30, 291.

43. Heijkants, R.G.J.C.; Van Calck, R.V.; Van Tienen, T.G.; De Groot, J.H.; Buma, P.; Pennings, A.J.; Veth, R.P.H.; Schouten, A.J. *Biomaterials* **2005**, 26, 4219.

44. Schneider, N.S.; Sung, C.S. Paik. *Polym Eng Sci* **1977**, 17, 73.

45. Chee, K.K.; Farris, R. *J Appl Polym Sci* **1984**, 29, 2529.

46. Krol, P.; Pilch-Pitera, B. *J Appl Polym Sci* **2007**, 104, 1464.

47. Ciobanu, C.; Han, X.; Cascaval, C.N.; Guo, F.; Rosu, D.; Ignat, L.; Moroi, G. *J Appl Polym Sci* **2003**, 87, 1858.

48. Dietrich, D. *Angew Makromol Chem* **1981**, 98, 133.

49. Chen, H.; Chen, D.Z.; Fan, Q.L. *et al*. *J Appl Polym Sci* **2001**, 76, 2049.

50. Chen, K.Y.; Kuo, J.F.; Chen, C.Y. *Biomaterials* **2000**, 21, 161.

51. Hsieh, K.H.; Wu, M.L. *J Appl Polym Sci* **1989**, 37, 3471.

52. Chen, S.; Chan, W. *Polymer* **1991**, 32, 656.

53. Rutkowska, M.; Eisenberg, A. *J Appl Polym Sci* **1987**, 33, 2833.

54. Yoshihara, N.; Enomoto, M.; Doro, M.; Suzuki, Y.; Shibaya, M.; Ishihara, H. *J Polym Eng* **2007**, 27, 291.

55. Gruin, I. *Polymery* **1987**, 32, 441.

56. Liaw, D.J. *J Appl Polym Sci* **1997**, 66, 1251.

57. Ping, P.; Wang, W.; Chen, X.; Jing, X. *J Polym Sci Part B: Polym Phys* **2007**, 45, 557.

58. Das, S.; Cox, D.F.; Wilkes, G.L.; Klinedinst, D.B.; Yilgor, I.; Yilgor, E.; Beyer, F.L. *J Macromol Sci Part B: Phys* **2007**, 46, 853.

59. Wan, M.; Baek, D.K.; Cho, J.–H.; Kang, I.–K.; Kim, K. *J Mat Sci: Mat in Med* **2004**, 15, 1079.

60. Magoshi, T.; Matsuda, T. *Biomacromolecules* **2002**, 3, 976.

61. Bhowmick, A.K. *Current Topics in Elastomers Research*, CRC Press, Boca Raton **2008**.

62. Anderson, J.M.; Hiltner, A.; Collier, T.; Tan, J.; Shive, M.; Hasan, S.; Wiggins, M.; Schubert, M.; Mathur, A. *Polym Mater Sci Eng* **1998**, 79, 490.

63. Wang, W.; Guo, Y.; Otaigbe, J.U. *Polymer* **2008**, 49, 4393.

64. Karabanova, L.V.; Lloyd, A.W.; Mikhalovsky, S.V.; Helias, M.; Phillips, G.J.; Rose, S.F.; Mikhalovska, L.; Boiteux, G.; Sergeeva, L.M.; Lutsyk, E.D.; Svyatyna, A. *J Mat Sci: Mat in Med* **2006**, 17, 1283.

65. Park, J.H.; Park, K.D.; Bae, Y. H. *Biomaterials* **1999**, 20, 943.

66. Gorna, K.; Gogolewski, S. *Polym Degrad Stab* **2001**, 75, 113.

67. Adhikari, R.; Gunatillake, P.A.; Griffiths, I.; Tatai, L.; Wickramaratna, M.; Houshyar, S.; Moore, T.; Mayadunne, R.T.M.; Field, J.; McGee, M.; Carbone, T. *Biomaterials* **2008**, 29, 3762.

68. Hill, D. *Design Engineering of Biomaterials for Medical Devices*, John Wiley and Sons, Chichester **1998**.

69. Žagar, E.; Žigon, M. *Polymer* **1999**, 40, 2727.

70. a) Athawale, V.D.; Kolekar, S.L.; Raut, S.S. *J Macromol Sci, Polymer Rev* **2003**, C43, 1. b) Athawale, V.; Kolekar, S. *Eur Polym J* **1998**, 34, 1447.

71. Lepine, O.; Birot, M.; Deleuze, H. *Polymer* **2005**, 46, 9653.

72. Lin, M.S.; Lee, S.T. *Polymer* **1997**, 38, 53.

73. Vlad, S.; Vlad, A.; Oprea, S. *Eur Polym J* **2002**, 38, 829.

74. Madas, D.; Shiraishi, N. *Int J Polym Mater* **1996**, 33, 61.

75. Lin, L.; Yoshioka, M.; Yao, Y.; Shiraishi, N. *J Appl Polym Sci* **1995**, 55, 1563.

76. Yao, Y.; Yoshioka, M.; Shiraishi, N. *J Appl Polym Sci* **1996**, 60, 1939.

77. Bird, T.B.; Black, W.A.P.; Dewar, E.T.; Rutherford, D. *Chem Ind* **1960**, 1331.

78. Varela, O.; Orgueira, H. A. *Adv Carbohydr Chem Biochem* **2000**, 55, 137.

79. (a) Kurita, K.; Hirakawa, N.; Iwakura, Y. *Makromol Chem* **1977**, 178, 2939. (b) Kurita, K.; Hirakawa, N.; Iwakura, Y.; Morinaga, H. *Makromol Chem* **1979**, 180, 2769. (c) Kurita, K.; Murakami, K.; Masuda, N.; Aibe, S.; Ishii, S.; Nishimura, S.I. *Macromolecules* **1994**, 27, 7544.

80. (a) Thiem, J.; Lüders, H. *Starch/Stärke* **1984**, 36, 170. (b) Thiem, J.; Lüders, H. *Makromol Chem* **1986**, 187, 2775. (c) Thiem, J.; Bachmann, F. Makromol Chem **1991**, 192, 2163.

81. (a) Braun, D.; Bergmann, M. *J Prakt Chem* **1992**, 334, 298. (b) Braun, D.; Bergmann, M. *Angew Makromol Chem* **1992**, 199, 191.

82. (a) Hashimoto, K.; Wibullucksanakul, S.; Matsuura, M.; Okada, M. *J Polym Sci Part A: Polym Chem* **1993**, 31, 3141. (b) Hashimoto, K.; Wibullucksanakul, S.; Okada, M. *J Polym Sci Part A: Polym Chem* **1995**, 33, 1495.

83. Petrovic, Z.; Zhang, W.; Javni, I. *Biomacromolecules* **2005**, 6, 713.

84. Guo, A.; Cho, Y.-J.; Petrovic, Z.S. *J Polym Sci Part A: Polym Chem* **2000**, 38, 3900.

85. Lligadas, G.; Ronda, J.C.; Galia, M.; Cádiz, V. *Biomacromolecules* **2007**, 8, 1858.

86. (a) Baumann, H.; Bühler, M.; Fochem, H.; Hisrsinger, F.; Zoeblein, H.; Falbe, J. *Angew Chem Int Ed Engl* **1988**, 27, 41. (b) Biermann, U.; Friedt, W.; Lang, S.; Lühs, W.; Machmüller, G.; Metzger, J.O.; Klaas, M.R.; Schäfer, H.J.; Schneiderüsch, M.P. *Angew Chem Int Ed* **2000**, 39, 2206.

87. (a) Andjelkovic, D.D.; Larock, R.C. *Biomacromolecules* **2006**, 7, 927. (b) Tsujimoto, T.; Uyama, H.; Kobayashi, S. *Macromolecules* **2004**, 37, 177. (c) Eren, T.; Küsefoglu, S.H. *J Appl Polym Sci* **2004**, 91, 2700. (d) Khot, S.N.; LaScala, J.J.; Can, E.; Morye, S.S.; Williams, G.I.; Palmese, G.R.; Küsefoglu, S.H.; Wool, R.P. *J Appl Polym Sci* **2001**, 82, 703. (e) Güner, F.S.; Yagci, Y.; Erciyes, T. *Prog Polym Sci* **2006**, 31, 633.

88. Lligadas, G.; Ronda, J.C.; Galià, M.; Biermann, U.; Metzger, J.O. *J Polym Sci Part A: Polym Chem* **2006**, 44, 634.

89. Biebl, H.; Menzel, K.; Zeng, A.P. Deckwer, W.D. *Appl Microbiol Biotechnol* **1999**, 52, 289.

90. Kurian, J. *J Polym Environ* **2005**, 13, 159.

91. Zia, K.M.; Barikani, M.; Bhatti, I.A.; Zuber, M.; Bhatti, H.N. *J Appl Polym Sci* **2008**, 109, 1840.

92. Lligadas, G.; Ronda, J.C.; Galia, M.; Cádiz, V. *Biomacromolecules* **2007**, 8, 686.

93. Baser, S.A.; Khakhar, D.V. *Cellul Polym* **1993**, 12, 390.

94. Guo, A.; Zhang, W.; Petrovic, Z.S. *J Mater Sci* **2006**, 41, 4914.

95. (a) Sivak, W.N.; Pollack, I.F.; Petoud, S.; Zamboni, W.C.; Zhang, J.; Beckman, E.J. *Acta Biomater* **2008**, 4, 1263. (b) Sivak, W.N.; Pollack, I.F.; Petoud, S.; Zamboni, W.C.; Zhang, J.; Beckman, E.J. *Acta Biomater* **2008**, 4, 852.

96. Zang, J.Y.; Beckman, E.J.; Piesco, N.P.; Agrawal, S. *Biomaterials* **2000**, 21, 1247.

97. Dwan'Isa, J.–P.; Mohanty, A.K.; Misra, M.; Drzal, L.T. *Natural Fibers, Biopolymers, and Biocomposites*, CRC Press, Boca Raton **2005**.

98. Owen, S.; Otani, T.; Masaoka, S.; Ohe, T. *Biosci Biotechnol Biochem* **1996**, 60, 244.

99. Ohshiro, T.; Shinji, M.; Morita, Y.; Takayama, Y.; Izumi, Y. *Appl Microbiol Biotechnol* **1997**, 48, 546.

100. Nakajima-Kambe, T.; Shigeno-Akutsu, Y.; Nomura, N.; Onuma, F.; Nakahara, T. *Appl Microbiol Biotechnol* **1999**, 51, 134.

101. Dupret, I.; David, C.; Colpaert, M.; Loutz, J.-M.; Wauven, C. *Macromol Chem Phys* **1999**, 200, 2508.

102. Zhao, Q.; Marchant, R.E.; Anderson, J.M.; Hiltner, A. *Polymer* **1987**, 28, 2040.

103. Marchant, R.E.; Zhao, Q.; Anderson, J.M.; Hiltner, A. *Polymer* **1987**, 28, 2032.

104. Nakajima-Kambe, T.; Onuma, F.; Kimpara, N.; Nakahara, T. *Microbiol Lett* **1995**, 129, 39.

105. Nakajima-Kambe, T.; Onuma, F.; Akutsu, Y.; Nakahara, T. *J Ferment Bioeng* **1997**, 83, 456.

106. Nomura, N.; Shigeno-Akutsu, Y.; Nakajima-Kambe, T.; Nakahara, T. *J Ferment Bioeng* **1998**, 86, 339.

107. Tokiwa, Y.; Suzuki, T.; Takeda, K. *Agric Biol Chem* **1988**, 52, 1937.

108. Santerre, J.P.; Labow, R.S.; Duguay, D.G.; Erfle, D.; Adams, G.A. *J Biomed Mater Res* **1994**, 28, 1187.

109. Wang, G.B.; Santerre, J.P.; Labow, R.S. *J Chromatogr B* **1997**, 698, 69.

110. Vojtova, L.; Vavrova, M.; Bebnaik, K.; Sucman, E.; David, J.; Jana, J. *J Environ Sci Heal A* **2007**, 42:5, 67.

CHAPTER 3

LINEAR POLYURETHANES MADE FROM METHYLATED ALDITOLS AND DIISOCYANATES *

Purpose and specific aims: *The target of the work presented in this chapter was the synthesis of linear new polyurethanes from O-methylated alditols (threitol, L-arabinitol and xylitol), their characterization and the evaluation of their properties and hydrodegradability in comparison to unsubstituted analogues from 1,4-butanediol and 1,5-pentanediol.*

Summary: *A set of linear [m,n]-type polyurethanes was synthesized by polycondensation in solution from 1,6-hexamethylene diisocyanate and 4,4'-methylenebis(phenyl isocyanate) with alditols. Threitol, arabinitol, and xylitol bearing the secondary hydroxy groups blocked as methyl ethers were used. Either regioregular or non-regioregular polymers (depending on the configuration of the alditol) were obtained in high yields, and with number-average molecular weights within the 20–30 kDa range. All these polyurethanes were amorphous with T_g being highly dependent on the aliphatic or aromatic nature of the diisocyanate used, but scarcely depending on the chemical structure of the alditol moiety. They were found to be stable up to near 300 ºC, decomposing through a complex three-stage mechanism. PUR obtained from threitol did not show significant enhancement of hydrolytic degradability as compared with polyurethanes from 1,4-butanediol. Conversely, polyurethane from xylitol and 1,6-hexamethylene diisocyanate was found to be almost fully hydrolyzed in 1 month when incubated in water either at 80 ºC and pH 7.4 or at 37 ºC and pH 10. Alditol size seems to be of prime importance in determining the hydrodegradability of these sugar containing polyurethanes.*

* Publication derived from this work: De Paz, M.V.; Marín, R.; Zamora, F.; Hakkou, K.; Alla, A.; Galbis, J.A.; Muñoz-Guerra, S. *J Polym Sci Part A: Polym Chem* **2007**, 45, 4109.

3.1. Introduction

Polyurethanes (PUR) are a class of polycondensation polymers of wide industrial applicability that includes linear, branched, and cross-linked products.[1] The chemistry and physics of PUR are very well-known as well as the synthetic procedures that can be used for their fabrication.[2] The diversity of chemical structures in which PUR can be built, either as homopolymers or segmented copolymers, accounts for the extraordinary spreading that these materials have reached in both domestic and industrial applications.

PUR are chemically stable polymers being fairly resistant to hydrolysis.[3] Although the urethane group characteristic of these polymers can be envisaged as hybrid of ester and amide groups, its response to water attack is much closer to polyamides than to polyesters. Such a high hydrostability is certainly a drawback for those applications in which a self-destruction of the material would be desired while or after use. This affects particularly to their potential use in temporal applications in the biomedical field, a special attracting field for PUR given their extremely good biocompatibility.[4]

Methods used for rendering PUR more susceptible to hydrolysis are mainly based in the incorporation of easily degradable segments, such as aliphatic polyesters.[5] A second approach consists of introducing highly hydrophilic units with side groups which facilitate the water attack, diminish the crystallinity, and weaken the water-resistance of the urethane group by electronic effects. Carbohydrate-derived monomers bearing hydroxyl side groups are especially suitable for such end. A number of PUR containing units derived from saccharides have been reported so far[6] but most of these products were prepared from oligomeric diols or complex raw substance as lignin fragments.[7] Isosorbide has been also explored as a renewable source that could replace traditional diols of petrochemical origin.[8] More recently, a set of hydrolyzable PUR prepared from L-gulonic acid derived lactones have been described.[9]

In this chapter a report on novel PUR with a linear backbone structure that are obtained by polycondensation in solution from diisocyanates and alditols is presented. Partially methylated L- and D-threitol (LThMe and DThMe), L-arabinitol (LArMe) and xylitol (XyMe) were the alditols of choice. This selection allows evaluating comparatively the influence of configuration and size on properties. 1,6-Hexamethylene diisocyanate (HDI) and 4,4'-

methylenebis(phenyl isocyanate) (MDI) were used to compare the effect of the aliphatic and aromatic constitution of the diisocyanate on the behaviour of the resulting PUR.

Additionally, the non-substituted PUR derived from HDI and the aliphatic diols 1,4-butanediol (BD) and 1,5-pentanediol (PD) were synthesized for reference. The polymers were fully characterized, their thermal properties evaluated, and their susceptibility to hydrolysis explored for some selected cases. The chemical structures of all the PUR studied in this work are depicted in Scheme 3.1.

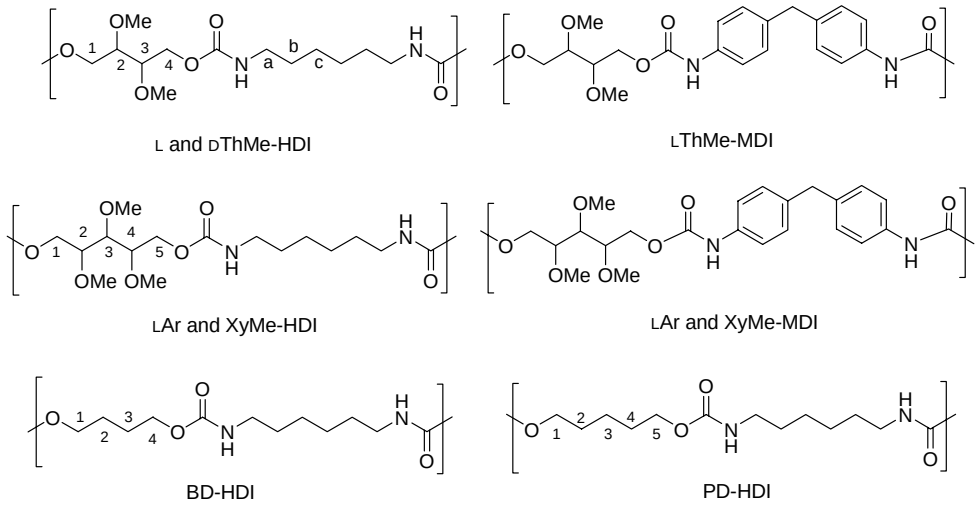

Scheme 3.1. Chemical structures of the polyurethanes described in this work. Labels refer to NMR peak assignments.

3.2. Experimental section

3.2.1. Materials and methods

Common reagents and solvents were purchased from Aldrich and used as received. Anhydrous tetrahydrofuran (THF) and *N,N*-dimethylformamide (DMF) polymerization solvents were further dried to eliminate residual water; THF was first refluxed in the presence of sodium, with benzophenone as indicator, and both THF and DMF were distilled under inert atmosphere prior to use. Diol monomers from L- and D-threitol, and from L-arabinitol and xylitol were synthesized as described elsewhere[10,11] and depicted in Scheme 3.2. All diols were purified by column chromatography or vacuum distillation.

The diols and reagents for the polymerizations were stored in a desiccator under vacuum until used. HDI was vacuum distilled prior use and 4,4'-methylenebis(phenyl isocyanate) (MDI) stored at 4 ºC. Both compounds were handled under inert atmosphere.

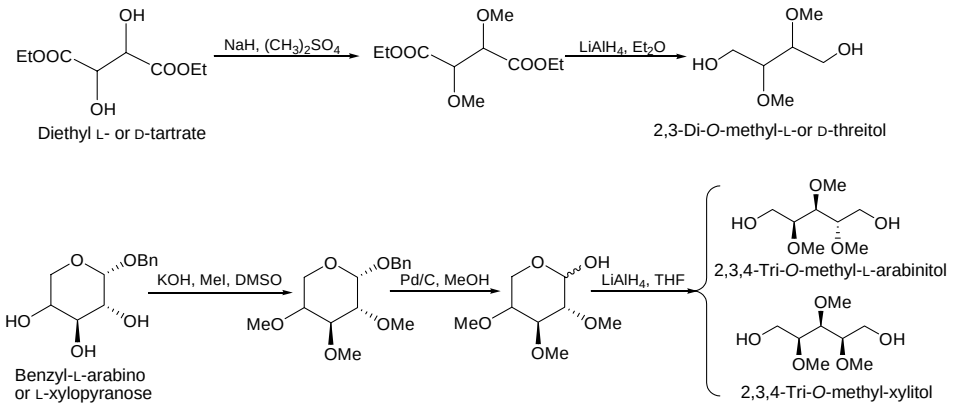

Scheme 3.2. Synthesis of carbohydrate-based diols.

Viscosities were measured in dichloroacetic acid at 25.0 ± 0.1 ºC using an Ubbelohde microviscometer. Elemental analyses were carried out by Centro de Investigación y Desarrollo (CIDCSIC, Barcelona) and CITIUS (University of Seville). Gel permeation chromatograms were acquired at 35 ºC with a Waters equipment provided with a refraction-index detector. The samples were chromatographed using 0.05 M sodium trifluoroacetate-hexafluoroisopropanol (NaTFA-HFIP) as eluent on a polystyrene-divinylbenzene packed linear column at a flow rate of 0.5 $mL \cdot min^{-1}$. Chromatograms were calibrated against poly(methyl methacrylate) (PMMA) monodisperse standards. IR spectra were recorded on a PerkinElmer 2000 spectrometer and NMR spectra on Bruker AMX-300 or AV-500 spectrometers. Differential scanning calorimetric (DSC) experiments were performed at heating/cooling rates of 10 $ºC \cdot min^{-1}$ on a Perkin Elmer Pyris 1 instrument calibrated with indium. Glass transition temperatures were determined on the heating traces recorded at 20 $ºC \cdot min^{-1}$ from samples that had been quickly cooled from the melt. All the experiments were carried under a nitrogen flow of 20 $mL \cdot min^{-1}$ to minimize possible oxidative degradations. Thermogravimetric analysis was carried out using a Mettler TA4000 thermobalance at a heating rate of 10 $ºC \cdot min^{-1}$ under inert atmosphere.

3.2.2. Polyurethane synthesis

General procedure. The carbohydrate-based diol was charged in a round bottom flask saturated with inert gas. The chosen dried-distilled solvent was added, and the mixture was stirred to homogenization. Finally, the diisocyanate (HDI or MDI) was added, followed by dibutyltin dilaurate (2% w/w) as catalyst. The mixture was stirred under inert atmosphere for 3 or 24 h at a temperature of 25 or 40 ºC depending on the diol used as monomer. The reaction mixture was added dropwise into cold diethyl ether where the polymer precipitated. The purification of the PUR was carried out by dissolving the polymer in the minimum volume of chloroform, or chloroform-trifluoroacetic acid (1:1), and reprecipitation into diethyl ether. The pure polymers were dried under vacuum and stored in a desiccator until needed.

PUR-(LThMe-HDI). It was prepared from 2,3-di-*O*-methyl-L-threitol (150 mg, 1mmol) and HDI (165 µl, 1 mmol) in dried-distilled DMF (2 mL). Yield 272 mg (85%). Intrinsic viscosity: 0.71 $dL \cdot g^{-1}$. IR: v (cm^{-1}) 3336 (N-H st), 1699 (C=O st), 1541 (N-H δ). ^{1}H NMR ($CDCl_3$/TFA, 300 MHz): δ (ppm) 4.48 (m, 2H, H1A/H4A), 4.29 (m, 2H, H1B/H4B), 3.82 (m, 2H, H2/H3), 3.60 (s, 6H, 2 OMe), 3.10 (m, 4H, 2 CH_2-a), 1.52 (m, 4H, 2 CH_2-b), and 1.33 (m, 4H, 2 CH_2-c). $^{13}C\{^{1}H\}$ NMR ($CDCl_3$/TFA, 65.5 MHz): δ (ppm) 158.33 (C=O), 79.35 (C2/C3), 63.39 (C1/C4), 58.46 (OMe), 41.33 (CH_2-a), 28.85 (CH_2-b), and 25.86 (CH_2-c). Anal. Calcd. for ($C_{14}H_{26}N_2O_6$): C, 52.82; H, 8.23; N, 8.80. Found: C, 52.88; H, 8.52; N, 8.97.

PUR-(DThMe-HDI). It was prepared from 2,3-di-*O*-methyl-D-threitol (150 mg, 1mmol) and HDI (165 µl, 1 mmol) in dried-distilled DMF (2 mL). Yield 270 mg (85%). Intrinsic viscosity: 0.68 $dL \cdot g^{-1}$. IR v (cm^{-1}): 3336 (N-H st), 1698 (C=O st), 1541 (N-H δ). ^{1}H NMR ($CDCl_3$/TFA, 300 MHz): δ (ppm) 4.50 (m, 2H, H1A/H4A), 4.31 (m, 2H, H1B/H4B), 3.83 (m, 2H, H2/H3), 3.62 (s, 6H, OMe), 3.10 (m, 4H, 2 CH_2-a), 1.53 (m, 4H, 2 CH_2-b), and 1.34 (m, 4H, 2 CH_2-c). $^{13}C\{^{1}H\}$ NMR ($CDCl_3$/TFA, 65.5 MHz): δ (ppm) 158.34 (C=O), 79.36 (C2/C3), 63.41 (C1/C4), 58.48 (OMe), 41.34 (CH_2-a), 28.85 (CH_2-b), and 25.88 (CH_2-c). Anal. Calcd. for ($C_{14}H_{26}N_2O_6$): C, 52.82; H, 8.23; N, 8.80. Found: C, 52.57; H, 8.44; N, 8.99.

PUR-(LArMe-HDI). It was prepared from 2,3,4-tri-*O*-methyl-L-arabinitol (194 mg, 1 mmol) and HDI (165 µl, 1 mmol) in dried-distilled DMF (2 mL). Yield 344 mg (95%). Intrinsic

viscosity: 0.67 dL·g^{-1}. IR: ν (cm^{-1}) 3332 (N-H st), 1703 (C=O st), 1536 (N-H δ). ^{1}H NMR ($CDCl_3$, 500 MHz): δ (ppm) 5.07 (bs, 2H, 2 NH), 4.55 (d, 1H, H5A, $J_{5A,5B}$ = 11.5 Hz), 4.30 (bs, 1H, H1A), 4.22 (bs, 1H, H1B), 4.11 (d, 1H, H5B), 3.63 (bs, 1H, H2), 3.50 (bs, 4H, OMe and H4), 3.47 (bs, 3H, OMe), 3.44 (bs, 3H, OMe), 3.36 (bs, 1H, H3), 3.19 (bs, 4H, 2 CH_2-a), 1.53 (bs, 4H, 2 CH_2-b), and 1.36 (bs, 4H, 2 CH_2-c). ^{13}C{^{1}H} NMR ($CDCl_3$, 125 MHz): δ (ppm) 156.38 (C=O), 79.76 (C3), 78.33 (C2/C4), 63.12 (C1), 62.08 (C5), 60.99, 59.21, 57.76 (OMe), 40.92 (CH_2-a), 29.86 (CH_2-b), and 26.29 (CH_2-c). Anal. Calcd. for $(C_{16}H_{30}N_2O_7)\cdot(DMF)_{0.1}$: C, 52.99; H, 8.37; N, 7.95. Found: C, 52.79; H, 8.39; N, 7.91.

PUR-(XyMe-HDI). It was prepared from 2,3,4-tri-*O*-methyl-xylitol (194 mg, 1 mmol) and HDI (165 µl, 1 mmol) in dried-distilled THF (2 mL). Yield 350 mg (quant.). Intrinsic viscosity: 1.03 dL·g^{-1}. IR: ν (cm^{-1}) 3333 (N-H st), 1703 (C=O st), 1532 (N-H δ). ^{1}H NMR ($CDCl_3$, 500 MHz): δ (ppm) 5.03 (bs, 2H, 2 NH), 4.36 (d, 2H, H1A/H5A, $J_{1A,IB}$ = $J_{5A,5B}$ = 9.2 Hz), 4.15 (bs, 2H, H1B/H5B), 3.61 (bs, 2H, H2/H4), 3.54 (bs, 3H, OMe-C3), 3.48 (bs, 6H, OMe-C2/OMe-C4), 3.38 (t, 1H, H3, $J_{3,2}$ = $J_{3.4}$ = 4.7 Hz), 3.18 (bs, 4H, 2 CH_2-a), 1.52 (bs, 4H, 2 CH_2-b), and 1.36 (bs, 4H, 2 CH_2-c). ^{13}C{^{1}H} NMR ($CDCl_3$, 125 MHz): δ (ppm) 156.41 (C=O), 80.72 (C3), 79.14 (C2/C4), 63.75 (C1/C5), 60.57 (OMe-C2/OMe-C4), 58.71 (OMe-C3), 40.90 (CH_2-a), 29.88 (CH_2-b), and 26.29 (CH_2-c). Anal. Calcd. for $(C_{16}H_{30}N_2O_7)\cdot(H_2O)_{0.25}$: C, 52.37; H, 8.38; N, 7.63. Found: C, 52.53; H, 8.11; N, 7.63.

PUR-(LThMe-MDI). It was prepared from 2,3-di-*O*-methyl-L-threitol (150 mg, 1mmol) and MDI (250 mg, 1 mmol) in dried-distilled DMF (2 mL). Yield 370 mg (92%). Intrinsic viscosity: 0.77 dL·g^{-1}. IR: ν (cm^{-1}) 3315 (N-H st), 1714 (C=O st), 1600 (C_{ar}-C_{ar} st), 1541 (N-H δ). ^{1}H NMR ($CDCl_3$/TFA, 300 MHz): δ (ppm) 7.13 (m, 8H, ar), 4.54 (m, 2H, H1A/H4A), 4.41 (m, 2H, H1B/H4B), 3.91 (s, 2H, Ph-C$\underline{H}_2$-Ph from MDI), 3.62 (m, 2H, H2/H3), and 3.60 (s, 6H, 2 OMe). ^{13}C{^{1}H} NMR ($CDCl_3$/TFA, 65.5 MHz): δ (ppm) 155.74 (C=O), 138.62, 133.51, 129.55, 121.32 (ar), 79.23 (C2/C3), 62.98 (C1/C4), 58.59 (OMe), and 40.39 (Ph-$\underline{C}H_2$-Ph from MDI). Anal. Calcd. for $(C_{21}H_{24}N_2O_6)\cdot(H_2O)_{0.5}$: C, 61.60; H, 6.15; N, 6.84. Found: C, 61.56; H, 6.03; N, 6.97.

PUR-(LArMe-MDI). It was prepared from 2,3,4-tri-*O*-methyl-L-arabinitol (194 mg, 1 mmol) and MDI (250 mg, 1 mmol) in dried-distilled THF (2 mL). Yield 422 mg (95%). Intrinsic viscosity: 0.75 dL·g^{-1}. IR: ν (cm^{-1}) 3324 (N-H st), 1715 (C=O st), 1596 (C_{ar}-C_{ar} st), 1525 (N-H δ). ^{1}H NMR ($CDCl_3$, 500 MHz): δ (ppm) 7.30 (bs, 6H, ar/NH), 7.06 (bs, 4H, ar), 4.67 (d, 1H, H5A, $J_{5A,5B}$ = 9.5 Hz), 4.35 (bs, 2H, H1), 4.21 (d, 1H, H5B), 3.85 (bs, 2H, Ph-C$\underline{H}_2$-

Ph from MDI), 3.68 (bs, 1H, H2), 3.59 (bs, 1H, H4), and 3.55-3.45 (m, 10H, OMe/H3). $^{13}C\{^1H\}$ NMR ($CDCl_3$, 125 MHz): δ (ppm) 153.69 (C=O), 136.48, 135.91, 129.37, 119.12 (ar), 80.14 (C3), 78.37 (C2/C4), 63.11 (C1), 62.30 (C5), 60.91, 59.12, 57.74 (OMe), and 40.53 (Ph-$\underline{C}H_2$-Ph from MDI). Anal. Calcd. for $(C_{23}H_{28}N_2O_7)\cdot(H_2O)_{0.5}$: C, 60.92; H, 6.45; N, 6.18. Found: C, 60.82; H, 6.47; N, 6.28.

PUR-(XyMe-MDI). It was prepared from 2,3,4-tri-*O*-methyl-xylitol (194 mg, 1 mmol) and MDI (250 mg, 1 mmol) in dried-distilled THF (2 mL). Yield 422 mg (95%). Intrinsic viscosity: 0.72 $dL\cdot g^{-1}$. IR: ν (cm^{-1}) 3305 (N-H st), 1706 (C=O st), 1599 (C_{ar}-C_{ar} st), 1530 (N-H δ). ^1H NMR ($CDCl_3$, 500 MHz): δ (ppm) 7.30 (d, 4H, ar, $J_{b,c}$ = 8.1 Hz), 7.22 (bs, 2H, 2 NH), 7.05 (d, 4H, ar), 4.54 (d, 2H, H1A/H5A, $J_{1A,1B}$ = $J_{5A,5B}$ = 11.7 Hz), 4.18 (dd, 2H, H1B/H5B, $J_{1B,2}$ = $J_{5B,2}$ = 5.3 Hz), 3.84 (bs, 2H, Ph-C$\underline{H}_2$-Ph from MDI), 3.66 (bs, 2H, H2/H4), 3.51 (bs, 3H, OMe-C3), and 3.47 (m, 7H, OMe-C2/OMe-C4 and H3). $^{13}C\{^1H\}$ NMR ($CDCl_3$, 125 MHz): δ (ppm) 153.62 (C=O), 136.4, 136.00, 129.36, 119.13 (ar), 81.08 (C3), 79.21 (C2/C4), 63.70 (C1/C5), and 40.54 (Ph-$\underline{C}H_2$-Ph from MDI). Anal. Calcd. for $(C_{23}H_{28}N_2O_7)\cdot(H_2O)_{0.6}$: C, 60.68; H, 6.46; N, 6.15. Found: C, 60.58; H, 6.36; N, 5.93.

PUR-(BD-HDI), and PUR-(PD-HDI). These unsubstituted linear polyurethanes were prepared from HDI, 1,4-butanediol and 1,5-pentanediol using the same procedure used for the preparation of methylated threitol derived polyurethanes described above.

PUR-(BD-HDI). Intrinsic viscosity: 0.63 $dL\cdot g^{-1}$. IR: ν (cm^{-1}) 3327 (N-H st), 1689 (C=O st), 1537 (N-H δ). ^1H NMR (DMSO, 300 MHz): δ (ppm) 6.56 (bs, 2H, 2 NH), 3.91 (m, 4H, H1/H4), 2.93 (m, 4H, 2 CH_2-a), 1.54 (m, 4H, H2/H3), 1.36 (m, 4H, 2 CH_2-b), and 1.21 (m, 4H, 2 CH_2-c). $^{13}C\{^1H\}$ NMR (DMSO, 75.5 MHz): δ (ppm) 161.47 (C=O), 68.49 (C1/C4), 45.59 (CH_2-a), 34.59 (CH_2-b), 31.14 (CH_2-c), and 30.72 (C2/C3). Anal. Calcd. for ($C_{12}H_{22}N_2O_4$): C, 55.80; H, 8.58; N, 10.84. Found: C, 55.69; H, 8.53; N, 10.78.

PUR-(PD-HDI). Intrinsic viscosity: 0.56 $dL\cdot g^{-1}$. IR: ν (cm^{-1}) 3324 (N-H st), 1687 (C=O st), 1538 (N-H δ). ^1H NMR (DMSO, 300 MHz): δ (ppm) 7.00 (bs, 2H, 2 NH), 3.90 (m, 4H, H1/H5), 2.94 (m, 4H, 2 CH_2-a), 1.53 (m, 4H, H2/H4), 1.35 (m, 6H, 2 CH_2-b and H3), and 1.21 (m, 4H, 2 CH_2-c). $^{13}C\{^1H\}$ NMR (DMSO, 75.5 MHz): δ (ppm) 161.52 (C=O), 68.62 (C1/C5), 45.28 (CH_2-a), 34.59 (C2/C4), 33.62 (CH_2-b), 31.14 (CH_2-c), and 27.16 (C3).

Anal. Calcd. for ($C_{13}H_{24}N_2O_4$): C, 57.33; H, 8.88; N, 10.29. Found: C, 57.19; H, 8.78; N, 10.23.

3.2.3. Hydrolytic degradation assays

Films of selected polyurethanes with a thickness of ~250 μm, were prepared by casting at room temperature from a 10% (w/v) solution in $CHCl_3$ or $CHCl_3$/TFA (1:1 v/v) on a silanized Petri dish. The films were cut into 8-mm diameter, 20 to 30-mg weight disks, which were dried in vacuo at 60 °C to constant weight. Samples were immersed in sodium phosphate buffer (pH 7.4), sodium carbonate buffer (pH 10) and citric acid buffer (pH 2); in parallel experiments at 37 and 80 °C. After immersion for the fixed period of time, the samples were rinsed thoroughly in water and dried to constant weight. Sample weighing and GPC measurements were used to follow the evolution of the hydrodegradation.

3.3. Results and discussion

3.3.1. Synthesis and characterization

The polycondensation in solution under mild conditions was found to be an effective procedure for the preparation of these polyurethanes. Different solvents were assayed, the best results being attained with freshly dried DMF or THF. The reaction was carried out in one step using dibutyltin dilaurate as catalyst. Isolation and purification of the polymers were carried out by precipitation with diethyl ether and subsequent drying under vacuum. High yields were attained in all cases (85-100%) and the appearance of the samples ranged from sticky to powdery materials, depending on the used monomer.

Although especial attention was paid to eliminate residual solvents and humidity, which appeared firmly retained to the polymer, some samples showed to contain small amounts of them, which could not be removed by usual methods. In fact, elemental analyses were in good agreement with those calculated for the expected compositions of the polymers, but in some cases the correspondence is improved if a small amount of water or DMF (less than 3% w/w) is assumed to be present in the polymer. Some polycondensation data and polymer characteristics are collected in Table 3.1.

Table 3.1. Polycondensation results and some properties of polyurethanes.

PUR	Reaction[a]			Molecular size[b]			
	T (ºC)	*t* (h)	Yield (%)	[*η*] (dL·g^{-1})	M_w (g·mol^{-1})	M_n (g·mol^{-1})	PD
LThMe-HDI	40	24	85	0.71	58,000	25,200	2.3
DThMe-HDI	40	24	85	0.68	56,400	23,700	2.4
LArMe-HDI	25	3	95	0.67	56,800	22,000	2.6
XyMe-HDI	25	3	Quant.	1.03	84,200	29,700	2.8
BD-HDI	40	2[c]	88	0.63	30,000	13,600	2.2
PD-HDI	40	2[c]	90	0.56	25,700	12,200	2.1
LThMe-MDI	40	24	92	0.77	62,300	22,700	2.7
LArMe-MDI	25	3	95	0.75	62,100	23,800	2.6
XyMe-MDI	25	3	95	0.72	58,200	22,200	2.6

[a] Polycondensation carried out in DMF or THF with 2M monomer concentration.
[b] Intrinsic viscosity measured in DCA and molecular weights determined by GPC.
[c] Precipitates after 2 hours of reaction.

The chemical structures of polyurethanes were assessed by FTIR and NMR spectroscopy. Characteristic IR absorption bands of the urethane group and the sugar moieties were observed at the predicted positions and with the expected intensities. Some differences worth of mentioning were detected however between aromatic and aliphatic products. Thus, the N-H, C-N and C-O-C stretching bands, that appeared at 3340, 1250 and 1100-1140 cm^{-1} in PUR-HDI respectively, moved down about 20-50 cm^{-1} in PUR-MDI. On the contrary, the carbonyl stretching band appearing around 1700 cm^{-1} for the aliphatic compounds, changed to around 1715 cm^{-1} for the aromatic ones, indicating that variations should not be attributed to differences in hydrogen bond association.

^{1}H and ^{13}C{^{1}H} NMR spectra were in full concordance with the expected chemical structures. Spectra recorded from PUR-(LThMe-HDI) with the corresponding assignment of the signals are shown in Figure 3.1 for illustration. No splitting of CH peaks arising from the alditol units was detected in any case, which allows excluding the occurrence of racemization along the synthesis. It should be noted that, although polymers made from L-arabinitol and xylitol should be *aregic*, no splitting indicative of such microstructure was

observed either. This is a highly expected result given the length of the diisocyanate units spacing the sugar units along the polymer chain.

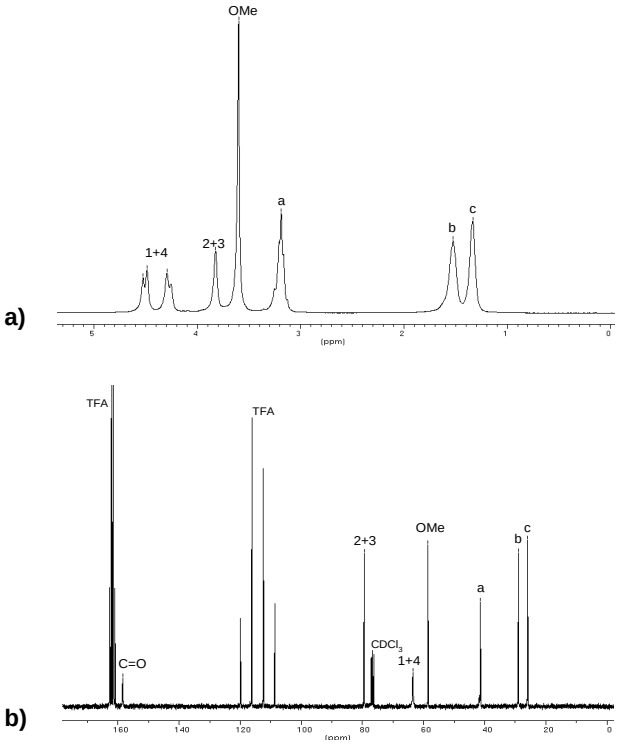

Figure 3.1. ^{1}H **(a)** and $^{13}C\{^{1}H\}$ **(b)** spectra of PUR-(LThMe-HDI) with peak assignments.

3.3.2. Thermal properties

The DSC traces of all the sugar-based polyurethanes reported in this paper did not show either endothermic peak indicative of melting or exothermic peak indicative of cold crystallization. Isothermal heating treatments did not produce changes in such behaviour either. It can be concluded therefore that we are dealing with amorphous polymers, or at least, polymers that are unable to crystallize under usual conditions. This is not a surprising result since side substituents are known to distort severely the packing of polyurethane chains lowering crystallinity dramatically.

It should be noticed that both stereoregular (ThMe based compounds) and non-stereoregular (LArMe and XyMe based compounds) polyurethanes are unable to crystallize, which indicates that microstructural heterogeneity must not be responsible for such behaviour. In fact, polyamides prepared from sugar units lacking C2 symmetry axis, *i.e.* leading to non-regioregular polymers, are known to crystallize displaying high cristallinity.[11]

Glass transition in these polyurethanes takes places at well definite temperatures with values that are highly depending on the constitution of the polymers. The heating DSC traces recorded from quenched samples with the same thermal history are compared in Figure 3.2a and T_g measured from these traces are collected in Table 3.2. It can be said that the replacement of the alkanediol by alditol in the polyurethane chain increases the T_g, and that such increasing is more noticeable when threitol or L-arabinitol are the alditols of choice. On the other hand, a great increase in T_g is observed when the aliphatic diisocyanate unit is replaced by the aromatic one. This is a largely expected result attributable to the chain stiffness caused by the presence of the biphenyl unit.

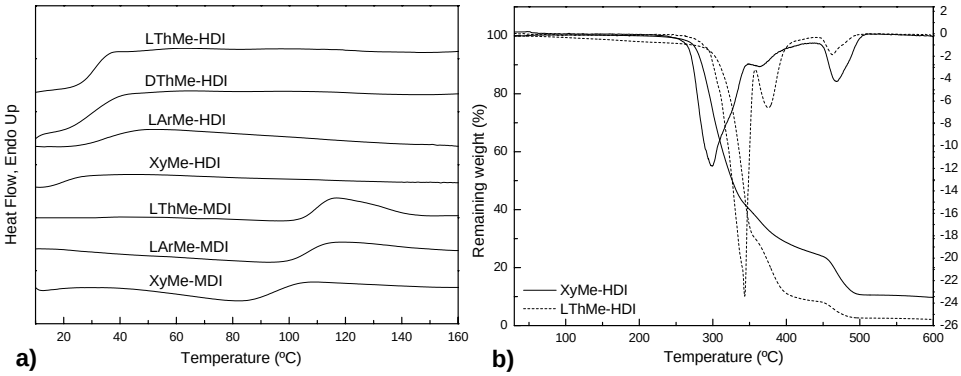

Figure 3.2. a) DSC traces of polyurethanes. **b)** Weight loss traces and derivative curves for polyurethanes LThMe-HDI and XyMe-HDI.

The thermal stability of the polyurethanes was evaluated by thermogravimetry under inert atmosphere. Representative TGA traces along with their corresponding derivative curves are shown in Figure 3.2b, where it can be seen that decomposition takes place through a three-stage process leaving a maximum final residue of about 10% of the initial weight. Detailed temperature and weight loss data are given in Table 3.2.

Table 3.2. Thermal properties of polyurethanes.

PUR	T_g[a] (ºC)	^0T_d[b] (ºC)	T_{d1}[c] (ºC)	W_{d1}[c] (%)	T_{d2}[c] (ºC)	W_{d2}[c] (%)	T_{d3}[c] (ºC)	W_{d3}[c] (%)
LThMe-HDI	31	310	341	69	379	23	464	6
DThMe-HDI	30	309	342	69	380	23	463	6
LArMe-HDI	30	282	304	53	370	23	468	12
XyMe-HDI	22	283	301	56	366	20	468	13
BD-HDI	15	300	340	57	371	31	464	11
PD-HDI	10	310	360	58	378	24	470	7
LThMe-MDI	110	294	315	49	360	22	546	6
LArMe-MDI	106	290	312	48	371	21	528	9
XyMe-MDI	95	294	310	47	362	21	533	8

[a] Glass transition temperatures measured by DSC on quenched samples.
[b] Onset decomposition temperature.
[c] Maximum rate weight loss temperatures and weight losses in every stage.

Several conclusions can be drawn from comparison of such data. a) The insertion of the sugar unit in the polyurethane chain entails a slight reduction in thermal stability compared to their unsubstituted analogues, such reduction being greater for the aldopentitol derivatives. b) The influence of the aromatic nature of the diisocyanate unit on thermal stability is opposite for pentitols and threitol derivatives, increasing it for the former but strikingly decreasing it for the later. c) Intermediate decomposition temperatures and weight losses for the first and second steps follow the same tendency for all the polyurethanes suggesting that a common decomposition mechanism must be operating in such stages. Conversely, much higher decomposition temperatures are observed for MDI-derived polyurethanes in the third step reflecting the heating resistance that usually confers the presence of the aromatic units.

3.3.3. Hydrolytic degradability

To evaluate the hydrolytic degradability of these polyurethanes as a function of the constitution of the alditol unit, PUR-(LThMe-HDI) and PUR-(XyMe-HDI) were incubated in parallel in aqueous buffer under different conditions and the evolution of the

degradation was followed by sample weighing and GPC analysis. Polyurethanes PUR-(BD-HDI) and PUR-(PD-HDI) were also subjected to the same treatment to estimate the influence of the replacement of the unsubstituted diol by the aldotetrol and aldopentitol.

Changes in weight sample and weight-average molecular weight of PUR-(XyMe-HDI) with incubation time at different pHs are plotted in Figures 3.3 and 3.4 for 80 and 37 ºC, respectively. Data collected from PUR-(LThMe-HDI) and PUR-(XyMe-HDI) are compared in Table 3.3. Also comparative changes in weight of all the polyurethanes studied, at pH 10 and 80 ºC, are plotted in Figure 3.5.

Table 3.3. Compared hydrolytic degradation data.

		LThMe-HDI					
		pH 2		pH 7.4		pH 10	
Days		37 ºC	80 ºC	37 ºC	80 ºC	37 ºC	80 ºC
0	*W* (%)	100	100	100	100	100	100
	M_w (g·mol^{-1})	58,200	58,200	58,200	58,200	58,200	58,200
13	*W* (%)	97.7	97.4	97.9	98.2	97.5	98.3
	M_w (g·mol^{-1})	57,400	54,300	58,900	58,000	59,000	55,200
39	*W* (%)	98.1	98.2	97.1	97.2	97.2	97.2
	M_w (g·mol^{-1})	57,500	53,900	58,800	58,200	58,800	54,300
		XyMe-HDI					
		pH 2		pH 7.4		pH 10	
Days		37 ºC	80 ºC	37 ºC	80 ºC	37 ºC	80 ºC
0	*W* (%)	-	100	100	100	100	100
	M_w (g·mol^{-1})	-	84,800	84,800	84,800	84,800	84,800
13	*W* (%)	-	83.4	98.2	78.9	80.9	70.0
	M_w (g·mol^{-1})	-	51,100	84,200	37,000	48,200	28,100
39	*W* (%)	-	73.3	98.1	67.8	77.0	60.1
	M_w (g·mol^{-1})	-	28,700	84,100	15,300	34,300	8,500

W: Remaining weight.
M_w: Weight-average molecular weight determined by GPC in HFIP against PMMA standards.

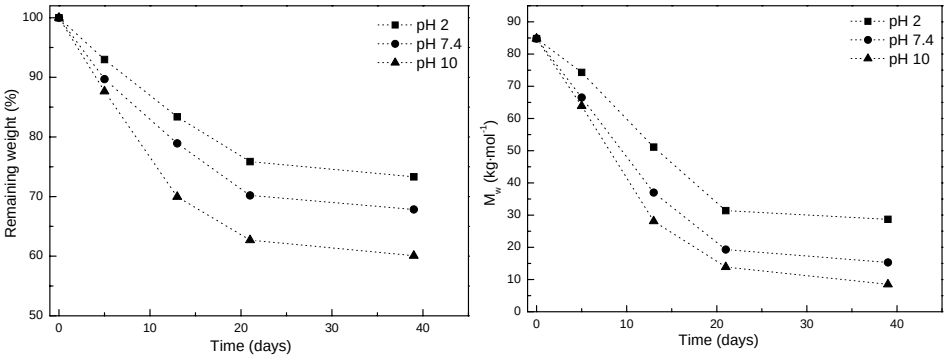

Figure 3.3. Changes in weight **(a)**, and weight-average molecular weight **(b)** of PUR-(XyMe-HDI) with time at 80 ºC.

Main conclusions derived from these experiments are the following: a) No perceivable degradation was observed for PUR-(BD-HDI) and PUR-(PD-HDI) according to well-known antecedents on the high resistant to hydrodegradability displayed by polyurethanes. b) Substitution of BD by LThMe does not alter significantly the resistance of the polyurethane to water attack; on the contrary, replacement of PD by Xy renders a polyurethane much more susceptible to hydrolysis. c) Hydrolysis rate of PUR-(XyMe-HDI) is critically affected by both pH and temperature; no changes either in weight or weight-average molecular weight were perceivable upon incubation of the polymer at 37 ºC and pH 7.4 whereas an extensive degradation was observed at 80 ºC whichever was the pH used.

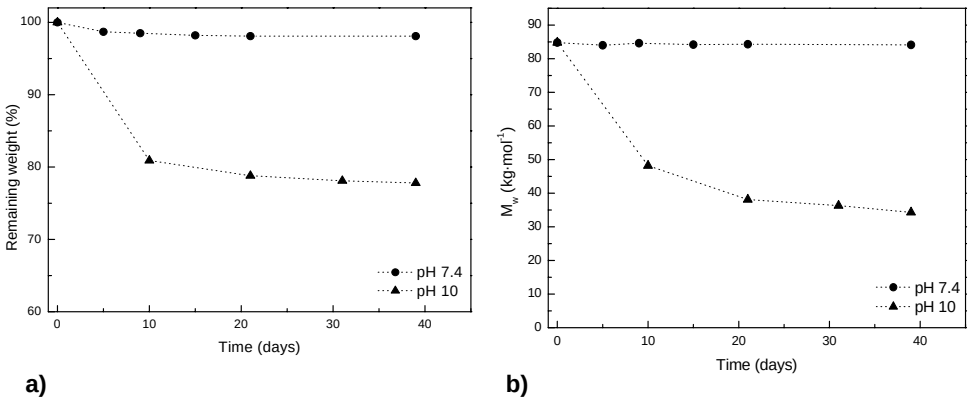

Figure 3.4. Changes in weight **(a)** and weight-average molecular weight **(b)** of PUR-(XyMe-HDI) with time at 37 ºC.

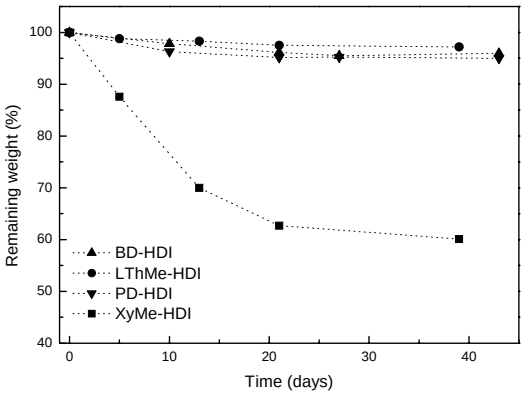

Figure 3.5. Comparative changes in weight of polyurethanes BD-HDI, LThMe-HDI, PD-HDI and XyMe-HDI with time at pH 10 and 80 ºC.

3.4. Conclusions

Linear polyurethanes made of methylated alditols and either aliphatic or aromatic diisocyanates could be prepared in high yields and with fair molecular weights by polycondensation in solution under mild conditions. These polyurethanes continue showing a thermal stability comparable to that polyurethanes made from non-sugar-based alkanediols.

The presence of the methoxy side groups in the polyurethane chain represses polymer crystallization, so that all these products are amorphous displaying a more or less rubbery behaviour according to their T_g. A second effect produced by the presence of the alditol unit is the increase of the T_g. Polyurethanes containing alditol units are more hydrophilic than their unsubstituted analogues but their hydrodegradability appears to be only enhanced for the aldopentitol-based ones. It seem that the alditol size, *i.e.* the number of methoxy side groups present in the repeating unit, is of prime importance for exerting a perceivable influence on the hydrolysis rate of these polyurethanes.

3.5. References

1. Howarth, G.A. *Surf Coat Int Part B Coat Trans* **2003**, 86, 111.

2. a) Bayer, O. *Angew Chem* **1947**, 59, 257. b) Oertel, G. *Polyurethane Handbook*, Hanser Publishers, Munich **1994**.

3. Chapman, T.M. *J Polym Sci Part A: Polym Chem* **1989**, 27, 1993.

4. Jayabalan, M.; Lizymol, P.P.; Thomas, V. *Polym Int* **2000**, 49, 88.

5. Furukawa, M. *Angew Makrom Chem* **1997**, 252, 33.

6. Donnelly, M.J.; Stanford, J.L.; Still, R.H. *Carbohydr Polym* **1990**, 14, 221.

7. Bonini, C.; D'Auria, M.; Ernanuele, L. *J Appl Polym Sci* **2005**, 98, 1451.

8. Braun, D.; Bergmann, M. *J Prakt Chem Chem Ztg* **1992**, 334, 298.

9. Yamanaka, C.; Hashimoto, K. *J Polym Sci Part A: Polym Chem* **2002**, 40, 4158.

10. Bou, J.J.; Rodríguez-Galán, A.; Muñoz-Guerra, S. *Macromolecules* **1993**, 26, 566.

11. García-Martín, M.G.; Ruiz-Pérez, R.; Benito-Hernández, E.; Galbis, J.A. *Carbohydr Res* **2001**, 333, 95.

CHAPTER 4

HYDROXYLATED LINEAR POLYURETHANES MADE FROM BENZYLATED ALDITOLS AND DIISOCYANATES *

Purpose and specific aims: *Due to the low hydrodegradable character of polyurethanes derived from methylated alditols in aqueous buffer at 37 ºC, a new way of increasing hydrodegradability of polyurethanes was studied. The target was the synthesis of new polyurethanes from alditols with the secondary hydroxyl groups protected as benzyl ether. Removal of the benzyl groups in the polymer by hydrogenolysis provided a suitable route to polyurethanes bearing pendant hydroxyl groups. By this method new partially hydroxylated polyurethanes with enhanced hydrodegradability could be produced.*

Summary: *A set of linear [m,n]-type polyurethanes was synthesized by reaction in solution of 1,6-hexamethylene diisocyanate (HDI) or 4,4'-methylenebis(phenyl isocyanate) (MDI) with conveniently protected sugar alditols.* L*-Threitol (*L*Th),* L*-arabinitol (*L*Ar) and xylitol (Xy) bearing the secondary hydroxyl groups protected as benzyl ethers were used. Number-average molecular weights of the resulting polyurethanes ranged between 10-60 kDa with polydispersities around 2. They were thermally stable showing no decomposition up to temperatures near 300 ºC. All of them were amorphous polymers with T_g highly dependent on the constitution of the diisocyanate but scarcely dependent on the structure of the alditol. Hydrogenolysis of* L*ThBn-HDI polyurethane afforded partially debenzylated products that were amorphous with T_g values ranging between 20 and 30 ºC. Fully benzylated polyurethanes showed high resistance to hydrolytic degradation, whereas polyurethane bearing free hydroxyl groups degraded significantly in saline buffer at pH 10 and 37 ºC.*

* Publication derived from this work: Marín, R.; De Paz, M.V.; Ittobanne, N.; Galbis, J.A.; Muñoz-Guerra, S. *Macromol Chem Phys* (accepted **2009**).

4.1. Introduction

PUR are chemically stable polymers with an outstanding resistance to hydrolysis. Such a high hydrolytic stability however prevents them to be used in temporary applications, as can be, for instance, biomaterials for biodegradable endoprosthesis, a highly potential niche for this family of polymers given their extremely good biocompatibility.[1] One method for rendering polyurethanes more susceptible to hydrolysis is the use of carbohydrate derived monomers. A number of PUR containing units derived from carbohydrates have been reported so far; the selection embraces compounds such as anhydrohexitols[2,3] and gulonolactones[4]. As seen in previous chapter, methylated alditols were used in an attempt to obtain highly hydrodegradable polyurethanes.[5] However, results showed low or inexistent enhancement of hydrolytic degradability.

In this chapter a report on novel linear PUR obtained by reaction of 1,6-hexamethylene diisocyanate (HDI) or 4,4′-methylenebis(phenyl isocyanate) (MDI) with benzylated alditols, specifically, 2,3-di-*O*-benzyl-L-threitol (LThBn), 2,3,4-tri-*O*-benzyl-L-arabinitol (LArBn) and 2,3,4-tri-*O*-benzyl-xylitol (XyBn), is presented. Unsubstituted PUR were also synthesized using the aliphatic diols 1,4-butanediol (BD) and 1,5-pentanediol (PD) and used for reference. The chemical structures of the PUR included in this study are depicted in Scheme 4.1.

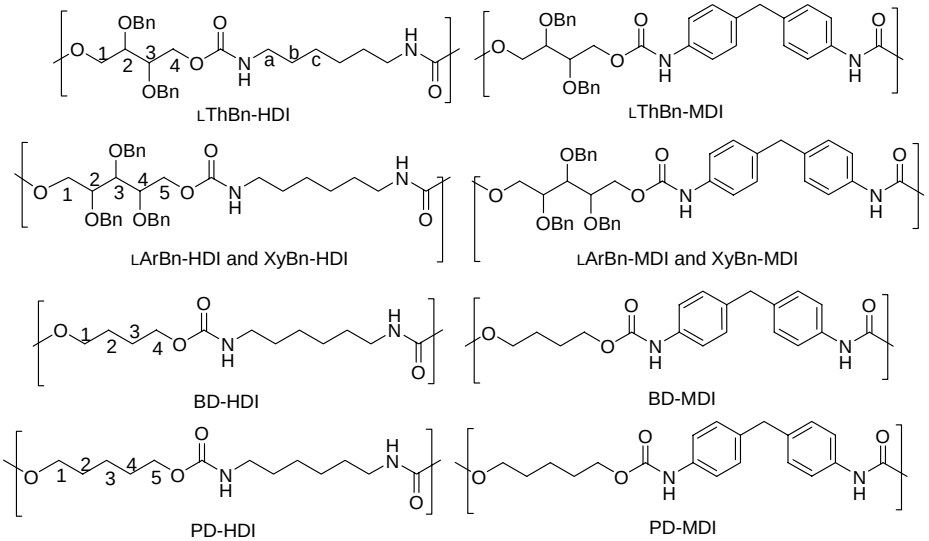

Scheme 4.1. Chemical structures of polyurethanes. Labels refer to NMR peak assignments.

The use of benzyl ether as protecting group provides a convenient route for the preparation of PUR bearing pendant free hydroxyl groups by hydrogenolysis of the precursor benzylated polymers. It must be remarked that such polyurethanes are not accessible by direct reaction of unprotected polydiols with diisocyanates, since the high reactivity and low selectivity of the addition reaction of the hydroxyl to the isocyanate group inevitably lead to generation of cross-linked products. Nevertheless, Höcker *et al.*[6] have recently described the preparation of polyurethanes bearing free hydroxyl side groups by polycondensation of 1,6-di-*O*-phenoxycarbonylalditols with diamines.

4.2. Experimental section

4.2.1. Materials and methods

Common reagents and solvents were purchased from Aldrich and used as received. Anhydrous tetrahydrofuran (THF) and *N,N*-dimethylformamide (DMF) polymerization solvents were further dried in order to eliminate residual water; THF was first refluxed in the presence of sodium with benzophenone as indicator, and both THF and DMF were distilled under inert atmosphere prior to use. HDI was vacuum distilled and both HDI and MDI were stored at 4 ºC and handled under inert atmosphere.

Viscosities were measured in dichloroacetic acid at 25.0 ± 0.1 °C and concentrations ranging from 5 to 10 $mg \cdot mL^{-1}$. Elemental analyses were carried out by Centro de Investigación y Desarrollo (CID-CSIC, Barcelona) and CITIUS (University of Seville). Gel permeation chromatograms were acquired at 35 ºC with a Waters instrument equipped with a styragel column. Chloroform was used as eluent and calibration was made against poly(methyl methacrylate) standards. IR spectra were recorded on a Perkin–Elmer 2000 spectrometer and NMR spectra on Bruker AMX-300 or AMX-500 spectrometers. Optical rotations were measured in dichloromethane solutions in a Krüss Electronic Polarimeter P3001 at 25 ºC (1 dm-cell).

Differential scanning calorimetric (DSC) experiments were performed at heating/cooling rates of 10 $ºC \cdot min^{-1}$ on a Perkin-Elmer Pyris 1 instrument calibrated with indium. Glass transition temperatures were determined on the heating traces recorded at 20 $ºC \cdot min^{-1}$ from samples that had been quickly cooled from the melt. All the experiments were carried out under a nitrogen flow of 20 $mL \cdot min^{-1}$ to minimize possible oxidative

degradations. Thermogravimetric analyses were carried at a heating rate of 10 °C·min^{-1} under a nitrogen atmosphere using a Mettler TA4000 thermobalance. Specimens for measuring mechanical properties were cut in rectangular shape (3x10 mm) from films with a thickness of ~250 µm. Films of alditol derived PUR were prepared by casting from chloroform at room temperature on a silanized Petri dish and those of PUR made from 1,4-butanediol were obtained by hot-press molding at 20 ºC above their melting temperatures. The tensile strength (σ_{break}), elongation at break (ε_{break}), and Young's modulus (E) were measured at a stretching rate of 20 mm·min^{-1} using a Zwick 2.5/TN1S testing machine coupled with a compressor Dalbe DR 150. All measurements were made in triplicates.

4.2.2. Synthesis of monomers

2,3,4-Tri-*O*-benzyl-L-arabinitol and 2,3,4-tri-*O*-benzyl-xylitol compounds were synthesized as described elsewhere,[7] and 2,3-di-*O*-benzyl-L-threitol was synthesized specifically for this work following the procedure described below. A scheme of the chemical synthetic routes leading to the alditol monomers used in this work is depicted in Scheme 4.2.

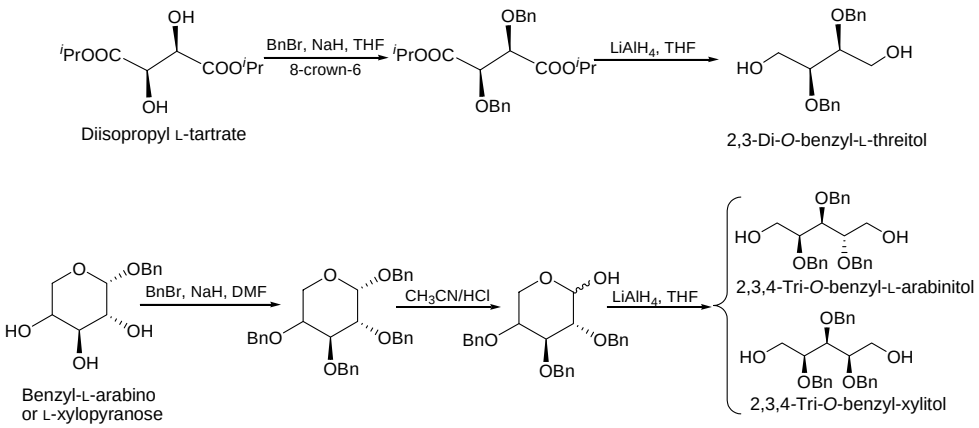

Scheme 4.2. Synthesis of carbohydrate-based diols.

Diisopropyl 2,3-di-O-benzyl-L-tartrate. To a cold suspension of 60% NaH (6.83 g, 170 mmol) in THF (100 mL), a cold solution of diisopropyl-L-tartrate (20 g, 85 mmol) in THF

(200 mL) was added dropwise under stirring, and the mixture left at room temperature for 1 hour. Then, benzyl bromide (21 mL, 170 mmol), tetrabutylammonium iodide (6.44 g, 17 mmol) and 18-crown-6 (60 mg, 0.23 mmol) were added and the mixture stirred for 12 hours. After cooling to 0 ºC, 4M HCl (100 mL) was added and the mixture extracted with ethyl acetate (3x100 mL). The combined extracts were washed successively with saturated aqueous $NaHCO_3$ and brine, and then dried and concentrated to a solid residue that was recrystallized from methanol (30 g, 85%). ^{1}H NMR ($CDCl_3$, 300 MHz): δ (ppm) 7.30 (m, 10H, 2 Ph), 5.05 (m, 2H, 2 CH), 4.86-4.45 (dd, 4H, 2 O$\underline{C}H_2$Ph), 4.39 (bs, 2H, $C\underline{H}$-CH_3), 1.26-1.24 (d, 6H, 2 CH_3), and 1.18-1.15 (d, 6H, 2 CH_3). $^{13}C\{^1H\}$ NMR ($CDCl_3$, 75.5 MHz): δ (ppm) 170.91 (C=O), 137.65, 128.72, 127.94, 127.52 (Ph), 80.53 (CH), 72.24 (O$\underline{C}H_2$Ph), 69.78 ($\underline{C}H$-CH_3) and 23.91 (CH_3).

2,3-Di-O-benzyl-L-threitol. To a cooled solution of diisopropyl 2,3-di-*O*-benzyl-L-tartrate (13 g, 31.4 mmol) in dried THF (80 mL), a suspension of $LiAlH_4$ (97%) (3.1 g, 78.5 mmol) in dried THF (70 mL) was added and the mixture stirred for 12 hours under nitrogen atmosphere. After cooling to 0 ºC, H_2O (6 mL), NaOH (15% w/v) (10 mL) and H_2O (15 mL) were sequentially and slowly added. The mixture was then filtered and the solid extracted with hot acetone. The combined extracts were evaporated to dryness and the residue recrystallized from methanol (white powder, 7.6 g, 80%). ^{1}H NMR (DMSO, 300 MHz): δ (ppm) 7.33 (m, 10H, 2 Ph), 4.64 (s, 4H, 2 O$\underline{C}H_2$Ph), and 3.83-3.69 (m, 4H, 2 CH_2, and m, 2H, 2 CH). $^{13}C\{^1H\}$ NMR (DMSO, 75.5 MHz): δ (ppm) 144.57, 133.26, 132.70, 132.37 (Ph), 85.70 (CH), 77.20 (O$\underline{C}H_2$Ph), and 66.65 (CH_2).

4.2.3. Polyurethane synthesis

General procedure. The selected diol (0.5 mmol) was charged in a round bottom flask provided with a nitrogen flow. Dry DMF or THF (for Th and Ar/Xy, respectively) (2 mL) was added and the mixture was homogenized by vigorous stirring. Then, the diisocyanate (0.5 mmol), either HDI or MDI, and one drop of dibutyltin dilaurate catalyst were added. The polymerization solution was stirred for 24 or 3 hours (for Th and Ar/Xy, respectively) under nitrogen atmosphere at room temperature. Finally, the solution was poured dropwise into cold diethyl ether (150 mL), to precipitate the polymer. Purification was accomplished by redissolution of the polyurethane in a small volume of chloroform and reprecipitation into diethyl ether. The pure polymer was dried under vacuum at room temperature for 2 days and stored in a desiccator.

PUR-(LThBn-HDI). It was prepared from 2,3-di-*O*-benzyl-L-threitol (151 mg, 0.5 mmol) and HDI (82.5 µl, 0.5 mmol) in dried-distilled DMF (2 mL). Yield= 83%. $[\alpha]_D$ +2.50º (25 ºC, *c* 1.0, dichloromethane). IR: v (cm^{-1}) 3333 (N-H st), 3058, 3030 (C_{ar}-H), 1698 (C=O st), 1540 (N-H δ), 1098 (C-O-CH_2Ph st), 738, 699 (ar). ^{1}H NMR ($CDCl_3$, 300 MHz): δ (ppm) 7.30 (m, 10H, 2 Ph), 4.75 (bs, 2H, 2 NH), 4.66-4.58 (m, 4H, 2 OC$\underline{H}_2$Ph), 4.21 (m, 4H, H1/H4), 3.72 (bs, 2 H, H2/H3), 3.11 (m, 4H, 2 CH_2-a), 1.44 (m, 4H, 2 CH_2-b), and 1.28 (m, 4H, 2 CH_2-c). ^{13}C{^{1}H} NMR ($CDCl_3$, 75.5 MHz): δ (ppm) 156.80 (C=O), 138.65, 128.90, 128.65, 128.29 (Ph), 77.38 (C2/C3), 73.56 (O$\underline{C}H_2$Ph), 63.98 (C1/C4), 41.43 (CH_2-a), 30.39 (CH_2-b), and 26.85 (CH_2-c). Anal. Calcd. for $(C_{26}H_{34}N_2O_6)\cdot(H_2O)_{0.4}$: C, 65.36; H, 7.34; N, 5.86. Found: C, 65.33; H, 7.34; N, 5.98.

PUR-(LArBn-HDI). It was prepared from 2,3,4-tri-*O*-benzyl-L-arabinitol (211 mg, 0.5 mmol) and HDI (82.5 µl, 0.5 mmol) in dried-distilled THF (2 mL). Yield= 95%. $[\alpha]_D$ -0.03º (25 ºC, *c* 1.0, dichloromethane). IR: v (cm^{-1}) 3334 (N-H st), 3056, 3031 (C_{ar}-H st), 1703 (C=O st), 1536 (N-H δ), 1097 (C-O-CH_2Ph st), 739, 699 (ar). ^{1}H NMR ($CDCl_3$, 500 MHz): δ (ppm) 7.31 (m, 15H, 3 Ph), 4.86 (bs, 2H, 2 NH), 4.79-4.17 (m, 10H, H1/H5, and 3 OC$\underline{H}_2$Ph), 3.88 (bs, 2H, H2/H4), 3.79 (m, 1 H, H3), 3.13 (bs, 4H, 2 CH_2-a), 1.47 (bs, 4H, 2 CH_2-b), and 1.31 (bs, 4H, 2 CH_2-c). ^{13}C{^{1}H} NMR ($CDCl_3$, 125 MHz): δ (ppm) 156.37, 156.20 (C=O), 138.38, 138.14, 138.07, 128.34, 128.17, 127.96, 127.89, 127.74, 127.66 (Ph), 79.06 (C3), 77.28, 77.03 (C2/C4), 74.65, 73.13, 72.06 (O$\underline{C}H_2$Ph), 63.52, 62.98 (C1/C5), 40.91 (CH_2-a), 29.85 (CH_2-b), and 26.34 (CH_2-c). Anal. Calcd. for $(C_{34}H_{42}N_2O_7)\cdot(H_2O)_{0.5}$: C, 68.09; H, 7.23; N, 4.67. Found: C, 68.05; H, 7.34; N, 4.95.

PUR-(XyBn-HDI). It was prepared from 2,3,4-tri-*O*-benzyl-xylitol (211 mg, 0.5 mmol) and HDI (82.5 µl, 0.5 mmol) in dried-distilled THF (2 mL). Yield= 91%. IR: v (cm^{-1}) 3336 (N-H st), 3064, 3031 (C_{ar}-H st), 1704 (C=O st), 1523 (N-H δ), 1092 (C-O-CH_2Ph st), 735, 698 (ar). ^{1}H NMR ($CDCl_3$, 500 MHz): δ (ppm) 7.30 (m, 15H, 3 Ph), 4.91 (bs, 2H, 2 NH), 4.73-4.59 (m, 6H, 3 OC$\underline{H}_2$Ph), 4.41 (bs, 2H, H1A/H5A), 4.16 (bs, 2H, H1B/H5B), 3.88 (bs, 2H, H2/H4), 3.67 (m, 1 H, H3), 3.13 (bs, 4H, 2 CH_2-a), 1.48 (bs, 4H, 2 CH_2-b), and 1.30 (bs, 4H, 2 CH_2-c). ^{13}C{^{1}H} NMR ($CDCl_3$, 125 MHz): δ (ppm) 156.36 (C=O), 138.30, 138.13, 128.46, 128.41, 128.34, 128.30, 128.15, 128.00, 127.84, 127.74, 127.67 (Ph), 79.10 (C3), 77.54 (C2/C4), 74.46, 73.12 (O$\underline{C}H_2$Ph), 63.88 (C1/C5), 40.91 (CH_2-a), 29.87 (CH_2-b), and 26.37 (CH_2-c). Anal. Calcd. for $(C_{34}H_{42}N_2O_7)\cdot(H_2O)_{1.0}$: C, 67.09; H, 7.29; N, 4.60. Found: C, 66.74; H, 7.00; N, 4.31.

PUR-(LThBn-MDI). It was prepared from 2,3-di-*O*-methyl-L-threitol (151 mg, 0.5 mmol) and MDI (125 mg, 0.5 mmol) in dried-distilled DMF (2 mL). Yield= 85%. $[\alpha]_D$ +6.00º (25 ºC, *c* 1.0, dichloromethane). IR: ν (cm^{-1}) 3321 (N-H st), 3060, 3030 (C_{ar}-H st), 1712 (C=O st), 1526 (N-H δ), 1065 (C-O-CH_2Ph st), 740, 698 (ar). ^{1}H NMR ($CDCl_3$, 300 MHz): δ (ppm) 7.26-7.02 (m, 18H, ar-MDI, and 2 Ph), 6.77 (bs, 2H, 2 NH), 4.60 (m, 4H, 2 OC$\underline{H}_2$Ph), 4.32 (bs, 4H, H1/H4), 3.81 (bs, 2H, Ph-C$\underline{H}_2$-Ph from MDI), and 3.76 (m, 2H, H2/H3). ^{13}C{^{1}H} NMR ($CDCl_3$, 75.5 MHz): δ (ppm) 153.47 (C=O), 137.74, 136.63, 136.56, 129.40, 128.41, 128.25, 127.92, 119.14 (ar), 76.34 (C2/C3), 73.08 (O$\underline{C}H_2$Ph), 63.43 (C1/C4), and 40.53 (Ph-$\underline{C}H_2$-Ph from MDI). Anal. Calcd. for ($C_{33}H_{32}N_2O_6$): C, 71.72; H, 5.84; N, 5.07. Found: C, 71.66; H, 5.75; N, 5.09.

PUR-(LArBn-MDI). It was prepared from 2,3,4-tri-*O*-methyl-L-arabinitol (211 mg, 0.5 mmol) and MDI (125 mg, 0.5 mmol) in dried-distilled THF (2 mL). Yield= 98%. $[\alpha]_D$ -0.05º (25 ºC, *c* 0.9, dichloromethane). IR: ν (cm^{-1}) 3315 (N-H st), 3051, 3030 (C_{ar}-H st), 1709 (C=O st), 1524 (N-H δ), 1067 (C-O-CH_2Ph st), 737, 698 (ar). ^{1}H NMR ($CDCl_3$, 500 MHz): δ (ppm) 7.42-6.91 (m, 25H, 3 Ph, ar-MDI, and 2 NH), 4.75-4.42 (m, 10H, H1/H5, and 3 OC$\underline{H}_2$Ph), 4.37-4.30 (m, 2H, H2/H4), 3.94 (bs, 1H, H3), and 3.87 (bs, 2H, Ph-C$\underline{H}_2$-Ph from MDI). ^{13}C{^{1}H} NMR ($CDCl_3$, 125 MHz): δ (ppm) 153.51, 153.27 (C=O), 138.20, 138.00, 137.90, 136.50, 135.90, 129.40, 128.50, 128.40, 128.20, 128.10, 128.00, 127.80, 118.97 (ar), 79.56 (C3), 77.24, 77.12 (C2/C4), 74.71, 73.23, 71.81 (O$\underline{C}H_2$Ph), 63.36 (C1/C5), and 40.57 (Ph-$\underline{C}H_2$-Ph from MDI). Anal. Calcd. for ($C_{41}H_{40}N_2O_7$): C, 73.20; H, 5.99; N, 4.16. Found: C, 72.79; H, 6.38; N, 4.20.

PUR-(XyBn-MDI). It was prepared from 2,3,4-tri-*O*-methyl-xylitol (211 mg, 0.5 mmol) and MDI (125 mg, 0.5 mmol) in dried-distilled DMF (2 mL). Yield= 89%. IR: ν (cm^{-1}) 3309 (N-H st), 3050, 3030 (C_{ar}-H st), 1708 (C=O st), 1526 (N-H δ), 1059 (C-O-CH_2Ph st), 740, 699 (ar). ^{1}H NMR ($CDCl_3$, 500 MHz): δ (ppm) 7.33-7.03 (m, 25H, 3 Ph, ar-MDI, and 2 NH), 4.69-4.62 (m, 8H, H1A/H5A, and 3 OC$\underline{H}_2$Ph), 4.20-4.16 (m, 2H, H1B/H5B), 3.92-3.88 (m, 4H, H2/H4, and Ph-C$\underline{H}_2$-Ph from MDI), and 3.70 (bs, 1H, H3). ^{13}C{^{1}H} NMR ($CDCl_3$, 125 MHz): δ (ppm) 153.53 (C=O), 138.10, 138.00, 136.30, 136.00, 129.40, 128.40, 128.30, 128.00, 127.90, 127.80, 119.10 (ar), 79.02 (C3), 77.31 (C2/C4), 74.54, 74.40, 73.31 (O$\underline{C}H_2$Ph), 63.74 (C1/C5), and 40.52 (Ph-$\underline{C}H_2$-Ph from MDI). Anal. Calcd. for ($C_{41}H_{40}N_2O_7$): C, 73.20; H, 5.99; N, 4.16. Found: C, 72.66; H, 6.08; N, 4.16.

PUR-(BD-HDI), PUR(PD-HDI), PUR(BD-MDI) and PUR-(PD-MDI). These unsubstituted linear polyurethanes were prepared from diisocyantes HDI and MDI, and diols BD and PD in DMF using the same procedure described above.

PUR-(BD-HDI). Yield= 88%. IR: v (cm^{-1}) 3327 (N-H st), 1689 (C=O st), 1537 (N-H δ). ^{1}H NMR (DMSO, 300 MHz): δ (ppm) 6.56 (bs, 2H, 2 NH), 3.91 (m, 4H, H1/H4), 2.93 (m, 4H, 2 CH_2-a), 1.54 (m, 4H, H2/H3), 1.36 (m, 4H, 2 CH_2-b), and 1.21 (m, 4H, 2 CH_2-c). $^{13}C\{^{1}H\}$ NMR (DMSO, 75.5 MHz): δ (ppm) 161.47 (C=O), 68.49 (C1/C4), 45.59 (CH_2-a), 34.59 (CH_2-b), 31.14 (CH_2-c), and 30.72 (C2/C3). Anal. Calcd. for ($C_{12}H_{22}N_2O_4$): C, 55.80; H, 8.58; N, 10.84. Found: C, 55.69; H, 8.53; N, 10.78.

PUR-(PD-HDI). Yield= 90%. IR: v (cm^{-1}) 3324 (N-H st), 1687 (C=O st), 1538 (N-H δ). ^{1}H NMR (DMSO, 300 MHz): δ (ppm) 7.00 (bs, 2H, 2 NH), 3.90 (m, 4H, H1/H5), 2.94 (m, 4H, 2 CH_2-a), 1.53 (m, 4H, H2/H4), 1.35 (m, 6H, 2 CH_2-b and H3), and 1.21 (m, 4H, 2 CH_2-c). $^{13}C\{^{1}H\}$ NMR (DMSO, 75.5 MHz): δ (ppm) 161.52 (C=O), 68.62 (C1/C5), 45.28 (CH_2-a), 34.59 (C2/C4), 33.62 (CH_2-b), 31.14 (CH_2-c), and 27.16 (C3). Anal. Calcd. for ($C_{13}H_{24}N_2O_4$): C, 57.33; H, 8.88; N, 10.29. Found: C, 57.19; H, 8.78; N, 10.23.

PUR-(BD-MDI). Yield= 90%. IR: v (cm^{-1}) 3322 (N-H st), 1605 (C_{ar}-C_{ar} st), 1701 (C=O st), 1535 (N-H δ). ^{1}H NMR (DMSO, 300 MHz): δ (ppm) 9.45 (bs, 2H, 2 NH), 7.31-7.02 (dd, 8H, ar), 4.05 (m, 4H, H1/H4), 3.72 (bs, 2H, Ph-C$\underline{H_2}$-Ph from MDI) and 1.65 (m, 4H, H2/H3). $^{13}C\{^{1}H\}$ NMR (DMSO, 75.5 MHz): δ (ppm) 158.81 (C=O), 142.30, 140.67, 134.04, 123.59 (ar), 68.90 (C1/C4), 44.99 (Ph-$\underline{C}H_2$-Ph from MDI), and 30.46 (C2/C3). Anal. Calcd. for ($C_{19}H_{20}N_2O_4$): C, 67.05; H, 5.92; N, 8.23. Found: C, 66.92; H, 5.88; N, 8.17.

PUR-(PD-MDI). Yield= 85%. IR: v (cm^{-1}) 3328 (N-H st), 1605 (C_{ar}-C_{ar} st), 1698 (C=O st), 1536 (N-H δ). ^{1}H NMR (DMSO, 300 MHz): δ (ppm) 9.49 (bs, 2H, 2 NH), 7.34-7.09 (dd, 8H, ar), 4.06 (m, 4H, H1/H5), 3.77 (bs, 2H, Ph-C$\underline{H_2}$-Ph from MDI), 1.64 (m, 4H, H2/H4) and 1.43 (m, 2H, H3). $^{13}C\{^{1}H\}$ NMR (DMSO, 75.5 MHz): δ (ppm) 158.84 (C=O), 142.33, 140.64, 134.03, 123.57 (ar), 69.15 (C1/C5), 44.99 (Ph-$\underline{C}H_2$-Ph from MDI), 33.45 (C2/C4) and 27.19 (C3). Anal. Calcd. for ($C_{20}H_{22}N_2O_4$): C, 67.78; H, 6.26; N, 7.90. Found: C, 67.63; H, 6.21; N, 7.86.

4.2.4. Hydrogenolysis of PUR-(LThBn-HDI)

In a stainless steel reactor provided with a 150 mL Teflon flask, a solution of PUR-(LThBn-HDI) (250 mg) in a mixture of chloroform/trifluoroacetic acid (1:1 v/v, 50 mL) and Pd/C (10%) in the amount of 10 mol-% of the benzyloxy groups were put together. The reactor was purged with nitrogen, filled with hydrogen to a pressure of 50 bar and the mixture left under stirred at room temperature for a scheduled time. Then, the catalyst was removed by filtration and the clean filtrate evaporated to give the partially deprotected polyurethanes. The products were dried under vacuum at 30 ºC for 24 h. Different degrees of debenzylation were attained according to the applied hydrogenation time, which ranged between 24 and 120 hours; PUR-(LTh($Bn_{30}OH_{70}$)-HDI) (70% of OH) was the hydrogenated PUR containing the maximum amount of free hydroxyl groups.

PUR-(LTh($Bn_{30}OH_{70}$)-HDI): Yield= 78%. ^{1}H NMR (DMSO, 300 MHz): δ (ppm) 7.28 (bs, 3H instead of 10H, Ph), 6.65 (bs, 2H, 2 NH), 4.65-4.49 (m, 1.2H instead of 4H, 2 O$C\underline{H}_2$Ph), 4.22-3.86 (m, 4H, H1/H4 of ThBn; and H1/H4 of ThOH), 3.75 (m, 0.6 H, H2/H3 of ThBn), 3.59 (m, 1.4H, H2/H3 of ThOH), 2.93 (bs, 4H, 2 CH_2-a), 1.36 (bs, 4H, 2 CH_2-b), and 1.21 (bs, 4H, 2 CH_2-c). The NMR spectra of PUR-(LTh($Bn_{80}OH_{20}$)-HDI) (Yield= 80%) and PUR-(LTh($Bn_{60}OH_{40}$)-HDI) (Yield= 80%) are very similar to those of PUR-(LTh($Bn_{30}OH_{70}$)-HDI) with differences concerning only peak intensities**.**

4.2.5. Hydrolytic degradation assays

Films of selected polyurethanes with a thickness of ~250 µm, were prepared by casting from chloroform at room temperature on a silanized Petri dish. The films were cut into 0.8-mm diameter, 20 to 30-mg weight disks, which were then dried under vacuum to constant weight. Samples were incubated in sodium carbonate buffer (pH 10) in parallel at 37 and 60 °C, and after the scheduled period of time, they were rinsed thoroughly with water and dried to constant weight. Sample weighing and GPC measurements were used to follow the evolution of the hydrolytic degradation.

4.3. Results and discussion

4.3.1. Synthesis and characterization

The polymerization reaction of diisocyanates with alditols bearing their secondary hydroxyls protected as benzyl ethers was proved to be effective for the preparation of polyurethanes containing carbohydrate-derived units. Reactions were carried out in DMF or THF solution under mild conditions and in the presence of dibutyltin dilaurate as catalyst. This procedure had been used previously for the preparation of methylated sugar-derived polyurethanes.[5] The reaction proceeded in one step and isolation and purification of the polymers were carried out by solution-precipitation cycles and subsequent drying under vacuum. In some cases the resulting polymer precipitated from the reaction medium which prevented reaching high molecular weights. High yields were attained with values varying from 83 to 98%, such differences caused by fractionation effects of the precipitation procedure used for purification; presumably, low molecular weight species of more soluble PUR remained dissolved upon precipitation leading to purified products with higher average molecular weight but in lower yields.

Although especial care was taken to eliminate humidity, some samples still contained small amounts of adsorbed water that could not be removed by drying under vacuum. In fact, although elemental analyses were in good agreement with those calculated for the expected compositions, in some cases they fit better by assuming that a small amount of water (less than 3% w/w) was still present in the polymer. Polymerization data and polymer characteristics are collected in Table 4.1.

The chemical structures of polyurethanes were assessed by FTIR and NMR spectroscopy; these data are detailed in the experimental section. Characteristic IR absorption bands of the urethane group and the sugar moieties were observed as the predicted positions and with the expected intensities. Some significant differences were detected between aromatic and aliphatic products. Thus, the N-H and C-O-C stretching bands appearing at around 3335 cm^{-1} and 1090 cm^{-1} in PUR-HDI respectively, moved down about 15-30 cm^{-1} in PUR-MDI. On the contrary, the carbonyl stretching band appears at around 1700-1710 cm^{-1} for both aliphatic and aromatic compounds. ^{1}H and $^{13}C\{^{1}H\}$ NMR spectra were in full concordance with the expected chemical structures of synthesized PUR. Spectra recorded from PUR-(LThBn-MDI) with the corresponding assignment of the signals are shown in Figure 4.1 for illustration.

Table 4.1. Characteristics of polyurethanes.

PUR	Molecular size[a]		DSC[c]	TGA[d]			Mechanical properties		
	$[\eta]$ (dL·g^{-1})	M_w/M_n (g·mol^{-1})	T_g (ºC)	$^{o}T_d$ (ºC)	$^{max}T_d$ (ºC)	W (%)	E (MPa)	σ_{break} (MPa)	ε_{break} (%)
LThBn-HDI	1.31	119,700/58,400	32	327	**350**/375/459	1	169	15	304
LArBn-HDI	0.39	52,100/29,200	36	318	**360/**456	1	--	--	--
XyBn-HDI	0.19	15,100/10,200	50	280	**326/**431	2	--	--	--
LThBn-MDI	0.75	48,600/24,300	79	322	337	14	1424	66	8
LArBn-MDI	0.20	19,500/11,800	58	315	349	5	--	--	--
XyBn-MDI	0.23	34,500/13,800	67	303	340	8	--	--	--
L$Th(Bn_{80}OH_{20})$-HDI[b]	1.26	110,400/55,200	30	267	**311**/346/448	1	--	--	--
L$Th(Bn_{60}OH_{40})$-HDI[b]	1.12	93,600/46,100	27	253	**297**/336/445	1	--	--	--
L$Th(Bn_{30}OH_{70})$-HDI[b]	0.92	71,000/35,500	21	240	**258**/318/440	1	--	--	--
BD-HDI	0.63	30,000/13,600	15	300	**340**/371/464	1	1081	45	10
PD-HDI	0.56	25,700/12,200	10	310	**360**/378/470	1	--	--	--
BD-MDI	0.60	28,600/13,200	93	282	**315**/366	24		Brittle	

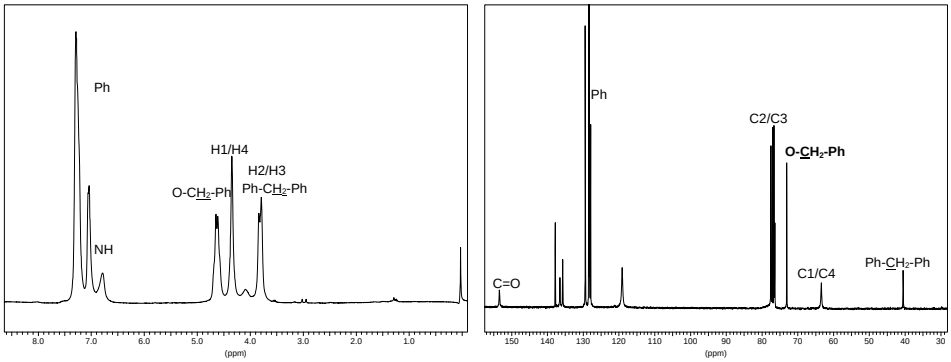

Figure 4.1. ^{1}H **(a)** and $^{13}C\{^{1}H\}$ **(b)** spectra of PUR-(LThBn-MDI) with peak assignments.

No splitting of CH peaks arising from the alditol units was detected in any case, which allows excluding the occurrence of racemization along the synthesis. Although polymers made from L-arabinitol and xylitol should be *aregic*, no peak splitting indicative of such microstructure was detected; this would result from the diluting effect played by the diisocyanate segment that separates the neighbouring alditol units along the polymer chain.

4.3.2. Thermal and mechanical properties

The thermal stability of the polyurethanes was evaluated by thermogravimetry under inert atmosphere. Representative TGA traces along with their corresponding derivative curves are shown in Figure 4.2a, where it is seen that decomposition takes place through a two or three-stages process leaving a final residue of 1-2% of the initial weight in the case of aliphatic polyurethanes and through a single step leaving between 5 and 15% of weight in the case of the aromatic ones. Detailed temperature and weight loss data for all the studied compounds are given in Table 4.1.

These data allow us to conclude that the insertion of the sugar unit in the polyurethane chain increases slightly the thermal stability compared to their unsubstituted analogues and that this effect is more pronounced in the case of the threitol derivatives. The DSC analysis of the sugar-based polyurethanes studied in this work revealed that they are essentially amorphous polymers displaying DSC traces absent of any heat exchange.

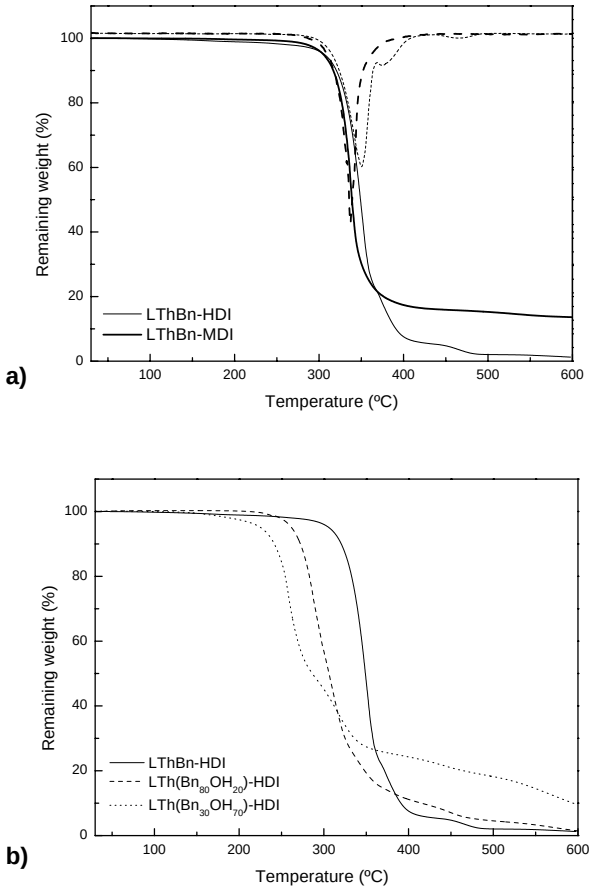

Figure 4.2. **(a)** Weight loss traces and their corresponding derivative curves for PUR-(LThBn-HDI) and PUR-(LThBn-MDI). **(b)** Comparative TGA of PUR-(LThBn-HDI) and their hydrogenated derivatives.

This is not an unexpected result at all since polyurethanes similar to those studied in this work but containing methylated alditol units have been reported to be amorphous without exception.[5] It should be noticed however that PUR containing benzylated arabinitol units showed weak broad endotherms in the temperature range of 70-90 ºC, which could be interpreted as arising from some crystalline fraction present in very minor amount. As it is seen in Table 4.1, the glass transition of these PUR takes places at well defined temperatures with values that are highly dependent on the constitution of the polymers. The DSC traces recorded at heating from samples quenched from the melt revealed that

the replacement of alkanediol by either the threitol or the pentitol increases in a similar extent the T_g of the aliphatic polyurethanes. On the contrary, a decrease in T_g was observed when the replacement was made on the aromatic polyurethanes. This behaviour clearly differs from that observed for methylated sugar-derived polyurethanes[5] where T_g invariably increased with the introduction of the sugar units in the polymer chain.

Linear unsubstituted PUR derived from BD and PD used as references are crystalline powders that formed consistent films by either casting or hot-press molding; the aliphatic products displayed typical stress-strain profiles whereas the aromatic ones, with much higher T_g, appeared to be brittle materials. The physical behaviour displayed by the sugar derived PUR depended largely also on the constitution of the diisocyanate counterpart; aliphatic PUR are gummy materials at room temperature whereas aromatic ones are powders able to form mechanically resistant films. Tensile parameters for polyurethanes LThBn-HDI and LThBn-MDI are compared in Table 4.1 illustrating vividly such differences. It is also remarkable the influence exerted by the incorporation of the sugar unit on mechanical properties compared to unsubstituted PUR, which is doubtlessly a consequence of the amorphous nature of these polymers. In general, the sugar derived PUR display lower elastic module and larger elongation than their homologous unsubstituted polymers.

4.3.3. Partially hydroxylated polyurethanes

Hydrogenolysis of the benzyl ethers, which is a common reaction extensively used for removing the benzyl group, required severe reaction conditions to proceed in this case. Rather high amounts of catalyst and application of fairly high pressures were needed to obtain significant conversion degrees. Best results were obtained with PUR-(LThBn-HDI) which became debenzylated in near 70% after five days of reaction. Intermediate debenzylated products containing 20 and 40% of hydroxyl side groups were obtained limiting the reaction time to two and three days, respectively. The evolution of the debenzylation reaction was followed by ^{1}H NMR, and spectra of the initial and final products are compared in Figure 4.3.

The peaks arising from the benzyl side group diminished and most of other peaks arising from backbone protons became more complex and shifted according to what should be

expected for the mixed constitution of PUR-(LTh($Bn_{30}OH_{70}$)-HDI). A slight reduction in the molecular weight of the polyurethane, which increased with the degree of debenzylation, took place upon hydrogenation whereas no appreciable change in polydispersity was detected. This result is in agreement with what should be expected from the removal of the benzyl group and discards the occurrence of main chain cleavage by uncontrolled hydrolysis. The partially hydroxylated polyurethanes were amorphous, displayed T_g values decreasing from 30 to 20 ºC with the conversion degree, and decomposed by heating at lower temperatures than the fully benzylated compound (Figure 4.2b).

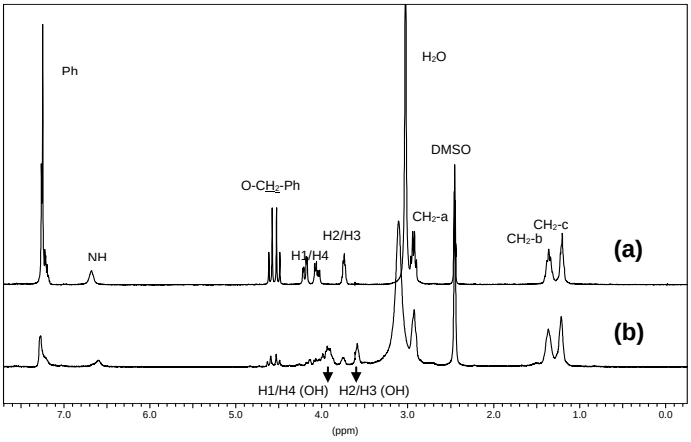

Figure 4.3. ^{1}H NMR spectra of polyurethanes LThBn-HDI **(a)** and LTh($Bn_{30}OH_{70}$)-HDI.

4.3.4. Hydrolytic degradability

The hydrolytic degradability of these polyurethanes was evaluated for both fully and partially benzylated PUR, and results were compared to those obtained for unsubstituted analogues. Given the resistance to hydrolysis usually displayed by polyurethanes, this study was confined to the aliphatic series with lower *T*g and therefore more accessible to the water attack than their aromatic analogues.

Polyurethanes LThBn-HDI, LArBn-HDI and LTh($Bn_{30}OH_{70}$)-HDI were incubated in parallel in aqueous buffer under a variety of conditions and the evolution of the degradation was followed by sample weighing and GPC analysis. Polyurethanes BD-HDI and PD-HDI were also subjected to the same treatment to estimate the influence of the replacement

of the alkanediol by alditols, threitol or pentitol, respectively. Changes in weight sample and weight-average molecular weight taking place upon incubation at pH 10 and 37 or 60 ºC are comparatively plotted in Figure 4.4.

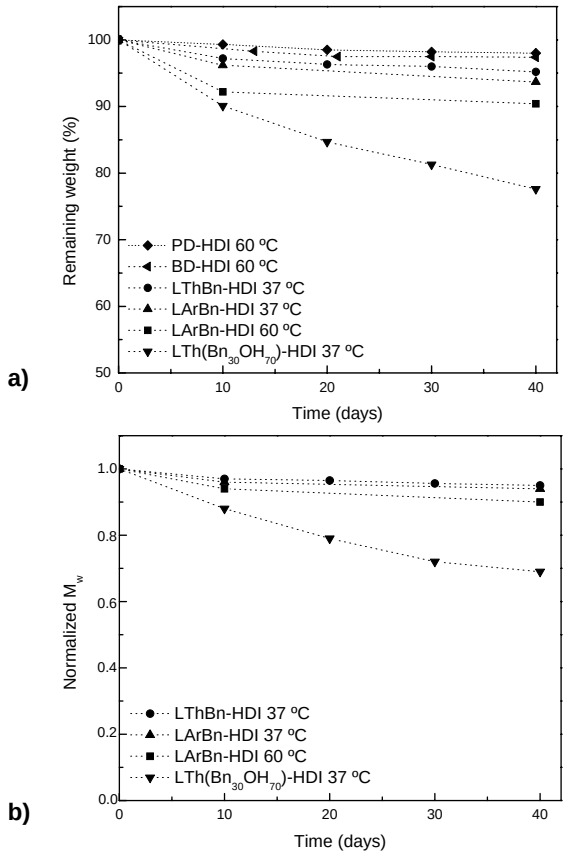

Figure 4.4. Changes in sample weight **(a)** and weight-average molecular weight **(b)** of the indicated polyurethanes incubated at pH 10 and 37 ºC or 60 ºC.

Main conclusions derived from these experiments are the following: a) No degradation was perceived for BD-HDI and PD-HDI, which is in full agreement with antecedents on the high resistance to hydrodegradability displayed by polyurethanes. b) Substitution of BD or PD by benzylated threitol or pentitols, respectively, did not alter significantly the hydrolytic behaviour of the polyurethanes. c) A significant increase of the hydrolysis rate was observed for PUR-(LTh($Bn_{30}OH_{70}$)-HDI); this polymer lost more than 25% of its initial

weight and decreased significantly in molecular size upon incubation for 40 days at 37 ºC and pH 10. The enhancement observed in degradability upon debenzylation is a result of notable interest. Nevertheless, further degradation studies, including experiments under simulated physiological conditions for longer incubation times, will be required for a proper evaluation of the potential of hydroxylated polyurethanes.

4.4. Conclusions

Linear polyurethanes made of benzylated alditols and either aliphatic or aromatic diisocyanates could be prepared in high yields and with fair molecular weights by polymerization in solution under mild conditions. These polyurethanes continue displaying a thermal stability comparable to that of polyurethanes made from non-sugar-based alkanediols. The presence of the benzyloxy side groups in the polyurethane chain repressed polymer crystallization, an effect similar to that previously observed for alditol derived PUR bearing methoxy side groups. The effect of the presence of the benzylated alditol unit on T_g was of opposite sign depending on the aliphatic or aromatic nature of the polyurethane.

Polyurethanes bearing free hydroxyl side groups could be prepared by hydrogenation under pressure of the fully benzylated LThBn-HDI polyurethane. These hydroxylated polyurethanes were amorphous and less thermally stable than their parent polymer but showed higher hydrophilicity and hydrodegradability. The final conclusion of this work is that insertion of benzylated alditols in polyurethanes produces significant changes in both thermal and mechanical properties. These polymers are suitable intermediates towards the preparation of hydroxyl containing polyurethanes that distinguish by displaying significant hydrodegradability.

4.5. References

1. Król, P. *Prog Mater Sci* **2007**, 52, 915.

2. Braun, D.; Bergmann, M. *J Prakt Chem Chemiker* **1992**, 334, 298.

3. a) Bachmann, F.; Reimer, J.; Ruppenstein, M.; Thiem, J. *Macromol Rapid Commun* **1998**, 19, 21. b) Bachmann, F.; Reimer, J.; Ruppenstein, M.; Thiem, J. *J Macromol Chem Phys* **2001**, 202, 3410.

4. Yamanaka, C.; Hashimoto, K. *Polym Sci Part A: Polym Chem* **2002**, 40, 4158.

5. de Paz, M.V.; Marín, R.; Zamora, F.; Hakkou, K.; Alla, A.; Galbis, J.A.; Muñoz-Guerra, S. *J Polym Sci Part A: Polym Chem* **2007**, 45, 4109.

6. a) Prömpers, G.; Keul, H.; Höcke, H. *Green Chem* **2006**, 8, 467. b) Ubaghs, L.; Fricke, N.; Keul, H.; Höcker, H. *Macromol Rapid Commun* **2004**, 25, 517.

7. Paz Báñez, M.V.; Aznar-Moreno, J.A.; Galbis, J.A. *J Carbohydr Chem* **2008**, 27, 120.

8. a) Mancera, M.; Zamora, F.; Roffé, I.; Bermúdez, M.; Alla, A.; Muñoz-Guerra, S.; Galbis, J.A. *Macromolecules* **2004**, 37, 2779. b) García-Martín, M.G.; Benito, E.; Ruiz, R.; Alla, A.; Muñoz-Guerra, S.; Galbis, J.A. *Macromolecules* **2004**, 37, 5550.

CHAPTER 5

LINEAR POLYURETHANES MADE FROM THREITOL: ACETALIZED AND HYDROXYLATED POLYMERS *

Purpose and specific aims: *In the previous chapter only partially hydroxylated polyurethanes could be produced, although the objective was the production of totally hydroxylated polyurethanes. In this work new polyurethanes from threitol with side groups protected as acetal are presented. Removal of the acetal group by treatment with acid provided a suitable route to polyurethanes bearing all hydroxyl side groups in the free state. This method succeeded in produced highly hydrophilic and hydrodegradable polyurethanes.*

Summary: *A set of novel linear polyurethanes was synthesized by reaction in solution of 1,6-hexamethylene diisocyanate (HDI) or 4,4'-methylenebis(phenyl isocyanate) (MDI) with 2,3-acetalized threitols, specifically, 2,3-O-methylidene-L-threitol and 2,3-O-isopropylidene-D-threitol. The polyurethanes containing acetalized threitols had weight-average molecular weights between 40-65 kDa. Most of them were amorphous and they displayed T_g higher than their unsubstituted analogues. Deprotection of acetalized polyurethanes by treatment with acid allowed preparing semicrystalline polyurethanes bearing two free hydroxyl groups in the repeating unit. The crystalline structure and crystallizability of the hydroxylated polyurethane made from HDI were investigated taken as reference the polyurethane made of 1,4-butanediol and HDI. The hydrolytic degradability of threitol-derived polyurethanes was comparatively evaluated under a variety of conditions. Highest degradation rates were obtained upon incubation at pH 10 at temperatures above T_g, the aliphatic hydroxylated polyurethane being the fastest degraded compound.*

* Publication derived from this work: Marín, R.; Muñoz-Guerra, S. *J Polym Sci Part A: Polym Chem* **2008**, 46, 7996.

5.1. Introduction

Difunctional monomers are usually required for the synthesis of linear polycondensates, which is incompatible with the high functionality generally displayed by carbohydrate derivatives. Protection of exceeding hydroxyl groups as methyl ethers has been a convenient method to obtain linear polyamides,[1] polyesters,[2] and polycarbonates[3] from aldaric acids and alditols. And in previous works a number of linear polyurethanes were obtained from partially methylated or benzylated alditols.[4,5] In this chapter a report on the synthesis and characterization of new polyurethanes with a linear backbone structure which are obtained by reaction of 1,6-hexamethylene diisocyanate (HDI) or 4,4′-methylenebis(phenyl isocyanate) (MDI) with 2,3-acetalized threitols, specifically, 2,3-*O*-methylidene-L-threitol (LThMed) and 2,3-*O*-isopropylidene-D-threitol (DTh^{i}Prd), is presented.

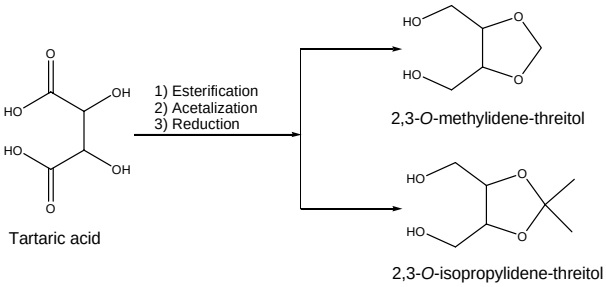

Scheme 5.1. Synthesis of tartaric acid based diols.

Threitol is the alditol derived from tartaric acid, a dihydroxy dicarboxylic acid occurring in many plants and fermented grape juice.[6] As indicated in Scheme 5.1, the acetalized threitols used in this work are produced from tartaric acid by a synthetic route that involves esterification, acetal formation and reduction of the carboxylate groups to hydroxyl groups. Since removal of the acetal group after polymerization is feasible by treatment with acids, this method provides a suitable route to polyurethanes bearing only pendant hydroxyl groups. The utilization of HDI and MDI diisocyanates allows evaluating comparatively the influence of the incorporation of the acetalized threitol unit on the properties of aliphatic and aromatic polyurethanes. For reference, two non-substituted linear PUR from BD and HDI or MDI, were studied in parallel. The chemical structures of all the polyurethanes studied in this work are depicted in Scheme 5.2.

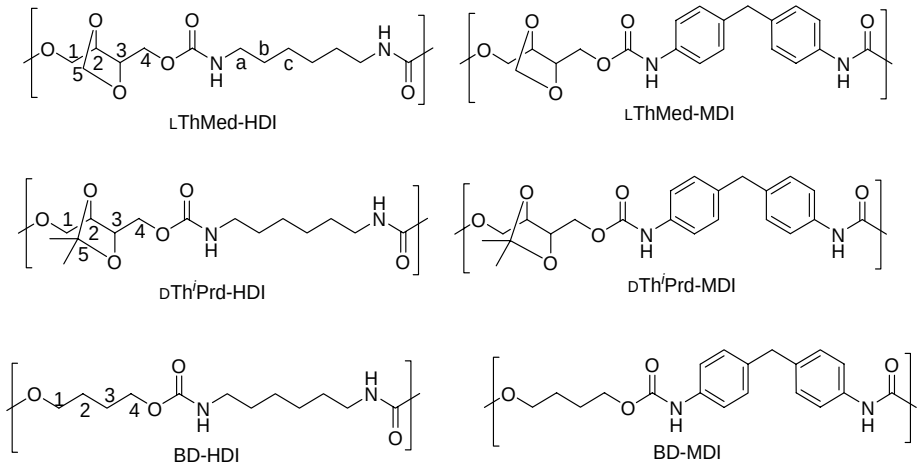

Scheme 5.2. Chemical structures of polyurethanes. Labels refer to NMR peak assignments.

5.2. Experimental section

5.2.1. Materials and methods

Common reagents and solvents, as well as dimethyl L-tartrate and 2,3-*O*-isopropylidene-D-threitol were purchased from Aldrich and used as received. All polymerization reagents were stored in a desiccator under vacuum until used. HDI was vacuum distilled and together with MDI stored at 4 ºC until needed. Both diisocyanates were handled under inert atmosphere.

Viscosities were measured in dichloroacetic acid at 25.0 ± 0.1 °C using an Ubbelohde microviscometer. Elemental analyses were carried out by Centro de Investigación y Desarrollo (CID-CSIC, Barcelona). Gel permeation chromatograms were acquired at 35 ºC with a Waters equipment provided with a refraction-index detector. The samples were chromatographed using 0.05 M sodium trifluoroacetate-hexafluoroisopropanol (NaTFA-HFIP) as eluent on a polystyrene-divinylbenzene packed linear column at a flow rate of 0.5 $mL \cdot min^{-1}$. Chromatograms were calibrated against poly(methyl methacrylate) (PMMA) monodisperse standards. IR spectra were obtained from KBr discs with a Perkin–Elmer 2000 spectrometer. For the measurement of IR spectra at variable temperatures, the discs were mounted into a sample holder equipped with a heating device. The temperature was adjusted with an accuracy of ± 1 °C by using a P/N 20120

automatic temperature controller (Graseby Specac) provided with a copper–constantan thermocouple connected to the cell. Usually 10 min were allowed for reaching the thermal equilibrium after the temperature was raised to the preset value. ^{1}H and $^{13}C\{^{1}H\}$ NMR spectra were recorded on a Bruker AMX-300 spectrometer operating at 300.1 and 75.5 MHz for ^{1}H and $^{13}C\{^{1}H\}$, respectively, and using TMS as internal reference. Sample concentrations of about 1-5% (w/v) were used for these analyses. The spectra were acquired with 64 scans and 1000-10000 scans, and relaxation delays of 1 and 2 s, for ^{1}H and $^{13}C\{^{1}H\}$ respectively. Optical rotations were measured in DMSO solutions in a Krüss Electronic Polarimeter P3001 at 20 ± 5 ºC (1 dm-cell).

Differential scanning calorimetric (DSC) experiments were performed at heating/cooling rates of 10 ºC·min^{-1} on a Perkin-Elmer Pyris 1 instrument calibrated with indium. All the experiments were carried with 3-4 mg samples, at temperatures ranging from 0 ºC to 200 or 250 ºC, and under a nitrogen flow of 20 mL·min^{-1} to minimize possible oxidative degradations. Glass transition temperatures were determined on the heating traces obtained at 20 ºC·min^{-1} from samples that were quickly cooled from the melt. Isothermal crystallizations were carried out from samples molten at 200 ºC and cooled to different crystallization temperatures. Thermogravimetric analysis was carried out using a Mettler TA4000 thermobalance at a heating rate of 10 °C·min^{-1} under inert atmosphere and within a temperature range of 30 to 600 ºC. Sample weights of about 15 mg were used in these experiments. Wide angle X-ray scattering were performed on a Philips automatic horizontal axis diffractometer using Cu K_{α}-Ni filtered radiation. Spectra were taken at room temperature with the scattering angle 2θ varying from 3 to 50º. Contact angles between water and the solid polymer surface were measured by means of an OCA 15+ contact angle measuring system supported by an SCA20 software (Dataphysics, Germany). Angle values were registered at room temperature after 30 seconds of dropping the water onto the polymer surface and at least 5 measurements were made for each determination.

5.2.2. Synthesis of monomers

Dimethyl 2,3-O-methylidene-L-tartrate. It was prepared according to previous work.[7] To 15 g of 95% aqueous solution of paraformaldehyde in 20 mL of sulphuric acid 98% was added dropwise dimethyl L-tartrate (15 g, 84.3 mmol) and the mixture stirred for 30 minutes at 60 ºC. The reaction solution was then repeatedly extracted with chloroform.

The combined organic layers were washed with ammonia (25% w/w) and water, and dried over anhydrous sodium sulphate. The solution was evaporated to dryness and purified by vacuum distillation (0.1 bar, 100 ºC) to obtain an oily product (9.6 g, 60% yield). ^{1}H NMR ($CDCl_3$, 300 MHz): δ (ppm) 5.26 (s, 2H, 2 CH), 4.77 (s, 2H, CH_2), and 3.83 (s, 6H, 2 CH_3). $^{13}C\{^{1}H\}$ NMR ($CDCl_3$, 75.5 MHz): δ (ppm) 170.91 (C=O), 96.00 (CH_2), 78.92 (CH), and 52.24 (CH_3).

2,3-O-methylidene-L-threitol. To a cooled solution of dimethyl 2,3-*O*-methylidene-L-tartrate (5 g, 26.3 mmol) in dried diethyl ether (40 mL), was added $LiAlH_4$ (97%) (2.67 g, 68.1 mmol) in dried diethyl ether (40 mL) under nitrogen atmosphere. The mixture was stirred for 12 hours, then cooled to 0 ºC, and sequentially and slowly added H_2O (7 mL), NaOH (15% w/v, 8 mL) and H_2O (25 mL). Then, the mixture was filtrated and the solid extracted with hot acetone. The combined extracts were evaporated to dryness and purified by vacuum distillation (0.1 bar, 105 ºC) to obtain an oily product (2.6 g, 75% yield). ^{1}H NMR ($CDCl_3$, 300 MHz): δ (ppm) 5.05 (s, 2H, O-CH_2-O), 3.96 (m, 2H, 2 CH), and 3.84-3.71 (m, 4H, 2 CH_2). $^{13}C\{^{1}H\}$ NMR ($CDCl_3$, 75.5 MHz): δ (ppm) 97.17 (O-CH_2-O), 82.26 (CH), and 61.70 (CH_2).

5.2.3. Polyurethane synthesis

Acetal-protected L- and D-threitol derived polyurethanes. In a typical procedure, 2,3-*O*-methylidene-L-threitol or 2,3-*O*-isopropylidene-D-threitol (1 mmol) was charged in a round bottom flask saturated with inert gas, *N,N*-dimethylformamide (4 mL) was added under stirring, and the mixture stirred up to homogenization at room temperature. 1 mmol of diisocyanate HDI or MDI followed by dibutyltin dilaurate (2% w/w) catalyst were then added and the mixture was stirred for 24 hours at 40 ºC under inert atmosphere. The reaction mixture was added dropwise into cold diethyl ether (50 mL) to precipitate the polymer. Purification of the polyurethane was carried out by dissolving the polymer in the minimum volume of chloroform or tetrahydrofuran, and reprecipitation into diethyl ether. The pure polymers (white solids) were dried under vacuum and stored in a desiccator until needed.

PUR-(LThMed-HDI). It was prepared from 2,3-*O*-methylidene-L-threitol (134 mg, 1 mmol) and diisocyanate HDI (164 µL, 1 mmol). Yield 266 mg (88%). IR: ν (cm^{-1}) 3335 (N-H st), 1693 (C=O st), 1547 (N-H δ). ^{1}H NMR (DMSO, 300 MHz): δ (ppm) 7.16 (bs, 2H, 2 NH),

4.91 (bs, 2H, H5), 4.08 (m, 4H, H1/H4), 3.91 (bs, 2H, H2/H3), 2.96 (m, 4H, 2 CH_2-a), 1.37 (m, 4H, 2 CH_2-b), and 1.22 (m, 4H, 2 CH_2-c). $^{13}C\{^1H\}$ NMR (DMSO, 75.5 MHz): δ (ppm) 155.87 (C=O), 94.15 (C5), 75.43 (C2/C3), 63.14 (C1/C4), 40.21 (CH_2-a), 29.32 (CH_2-b), and 25.94 (CH_2-c). Anal. Calcd. for ($C_{13}H_{22}N_2O_6$): C, 51.65; H, 7.33; N, 9.27. Found: C, 51.65; H, 7.30; N, 9.37.

PUR-(DTh^{i}Prd-HDI). It was prepared from 2,3-*O*-isopropylidene-D-threitol (162 mg, 1 mmol) and HDI (164 µL, 1 mmol). Yield 267 mg (81%). IR: ν (cm^{-1}) 3342 (N-H st), 1702 (C=O st), 1541 (N-H δ). ^1H NMR (DMSO, 300 MHz): δ (ppm) 7.16 (bs, 2H, 2 NH), 4.13-3.90 (m, 4H, H1/H4, and; s, 2H, H2/H3), 2.89 (m, 4H, 2 CH_2-a), 1.32 (m, 4H, 2 CH_2-b), 1.26 (s, 6H, 2 CH_3), and 1.17 (m, 4H, 2 CH_2-c). $^{13}C\{^1H\}$ NMR (DMSO, 75.5 MHz): δ (ppm) 155.81 (C=O), 108.97 (C5), 75.64 (C2/C3), 63.48 (C1/C4), 38.83 (CH_2-a), 29.31 (CH_2-b), 26.81 (CH_3), and 25.92 (CH_2-c). Anal. Calcd. for ($C_{15}H_{26}N_2O_6$): C, 54.53; H, 7.93; N, 8.48. Found: C, 54.46; H, 7.92; N, 8.46.

PUR-(LThMed-MDI). It was prepared from 2,3-*O*-methylidene-L-threitol (134 mg, 1 mmol) and MDI (250 mg, 1 mmol) in dried-distilled DMF (4 mL). Yield 326 mg (85%). IR: ν (cm^{-1}) 3302 (N-H st), 1724 (C=O st), 1598 (C_{ar}-C_{ar} st), 1546 (N-H δ). ^1H NMR (DMSO, 300 MHz): δ (ppm) 9.60 (bs, 2H, 2 NH), 7.31-7.03 (dd, 8H, ar), 4.93 (s, 2H, H5), 4.25-4.13 (m, 4H, H1/H4), 4.00 (bs, 2H, H2/H3), and 3.73 (s, 2H, Ph-C<u>H</u>$_2$-Ph from MDI). $^{13}C\{^1H\}$ NMR (DMSO, 75.5 MHz): δ (ppm) 153.22 (C=O), 136.86, 135.63, 128.85, 118.47 (ar), 94.22 (C5), 75.23 (C2/C3), 40.05 (Ph-<u>C</u>H$_2$-Ph from MDI), 63.45 (C1/C4). Anal. Calcd. for ($C_{20}H_{20}N_2O_6$): C, 62.49; H, 5.24; N, 7.29. Found: C, 62.42; H, 5.25; N, 7.25.

PUR-(DTh^{i}Prd-MDI). It was prepared from 2,3-*O*-isopropylidene-D-threitol (162 mg, 1 mmol) and MDI (250 mg, 1 mmol). Yield 371 mg (90%). IR: ν (cm^{-1}) 3310 (N-H st), 1728 (C=O st), 1600 (C_{ar}-C_{ar} st), 1540 (N-H δ). ^1H NMR (DMSO, 300 MHz): δ (ppm) 9.62 (bs, 2H, 2 NH), 7.32-7.02 (dd, 8H, ar), 4.33-4.05 (m, 4H, H1/H4, and; s, 2H, H2/H3), 3.74 (s, 2H, Ph-C<u>H</u>$_2$-Ph from MDI), and 1.29 (s, 6H, 2 CH_3). $^{13}C\{^1H\}$ NMR (DMSO, 75.5 MHz): δ (ppm) 153.22 (C=O), 136.88, 135.64, 128.87, 118.50 (ar), 109.23 (C5), 75.48 (C2/C3), 63.86 (C1/C4), 40.80 (Ph-<u>C</u>H$_2$-Ph from MDI), and 26.83 (CH_3). Anal. Calcd. for ($C_{22}H_{24}N_2O_6$): C, 64.07; H, 5.87; N, 6.79. Found: C, 64.12; H, 5.88; N, 6.74.

Unsubstituted polyurethanes PUR-(BD-HDI) and PUR-(BD-MDI). These two polyurethanes were prepared by reaction of 1,4-butanediol with HDI and MDI

respectively, by following the same procedure described above for threitol derived polyurethanes.

PUR-(BD-HDI). It was prepared from 1,4-butanediol (90 mg, 1 mmol) and HDI (164 µL, 1 mmol) in dried-distilled DMF (4 mL). Yield 227 mg (88%). IR: ν (cm^{-1}) 3327 (N-H st), 1689 (C=O st), 1537 (N-H δ). ^{1}H NMR (DMSO, 300 MHz): δ (ppm) 6.56 (bs, 2H, 2 NH), 3.91 (m, 4H, H1/H4), 2.93 (m, 4H, 2 CH_2-a), 1.54 (m, 4H, H2/H3), 1.36 (m, 4H, 2 CH_2-b), and 1.21 (m, 4H, 2 CH_2-c). $^{13}C\{^{1}H\}$ NMR (DMSO, 75.5 MHz): δ (ppm) 161.47 (C=O), 68.49 (C1/C4), 45.59 (CH_2-a), 34.59 (CH_2-b), 31.14 (CH_2-c), and 30.72 (C2/C3). Anal. Calcd. for ($C_{12}H_{22}N_2O_4$): C, 55.69; H, 8.53; N, 10.78. Found: C, 55.80; H, 8.58; N, 10.84.

PUR-(BD-MDI). It was prepared from 1,4-butanediol (90 mg, 1 mmol) and MDI (250 mg, 1 mmol) in dried-distilled DMF (4 mL). Yield 306 mg (90%). IR: ν (cm^{-1}) 3322 (N-H st), 1701 (C=O st), 1605 (C_{ar}-C_{ar} st), 1535 (N-H δ). ^{1}H NMR (DMSO, 300 MHz): δ (ppm) 9.45 (bs, 2H, 2 NH), 7.31-7.02 (dd, 8H, ar), 4.05 (m, 4H, H1/H4), 3.72 (bs, 2H, Ph-C$\underline{H}_2$-Ph from MDI), and 1.65 (m, 4H, H2/H3). $^{13}C\{^{1}H\}$ NMR (DMSO, 75.5 MHz): δ (ppm) 158.81 (C=O), 142.30, 140.67, 134.04, 123.59 (ar), 68.90 (C1/C4), 44.99 (Ph-$\underline{C}H_2$-Ph from MDI), and 30.46 (C2/C3). Anal. Calcd. for ($C_{19}H_{20}N_2O_4$): C, 66.92; H, 5.88; N, 8.17. Found: C, 67.05; H, 5.92; N, 8.23.

5.2.4. Hydroxylated polyurethanes

Removal of the acetal group was accomplished by treatment with trifluoroacetic acid (TFA). 1 g of the selected polyurethane from 2,3-*O*-isopropylidene-D-threitol was stirred in 15 mL of aqueous TFA (4:1 v/v) at 25 ºC for 30 min until complete solution. The mixture was poured into diethyl ether to precipitate the polyurethane containing free hydroxyl groups. The polymer was dried under vacuum and stored in a desiccator until needed.

PUR-(DThOH-HDI). IR: ν (cm^{-1}) 3339 (N-H st), 1697 (C=O st), 1536 (N-H δ). ^{1}H NMR (DMSO, 300 MHz): δ (ppm) 6.62 (bs, 2H, 2 NH), 3.92 (m, 4H, H1/H4), 3.58 (m, 2H, H2/H3), 2.92 (m, 4H, 2 CH_2-a), 1.35 (m, 4H, 2 CH_2-b), and 1.20 (m, 4H, 2 CH_2-c). $^{13}C\{^{1}H\}$ NMR (DMSO, 75.5 MHz): δ (ppm) 150.89 (C=O), 63.84 (C2/C3), 59.75 (C1/C4), 34.61 (CH_2-a), 23.87 (CH_2-b), and 20.47 (CH_2-c). Anal. Calcd. for ($C_{12}H_{22}N_2O_6$)·(H_2O)$_{0.5}$: C, 48.16; H, 7.69; N, 9.36. Found: C, 48.75; H, 7.63; N, 9.46.

PUR-(DThOH-MDI). IR: ν (cm^{-1}) 3326 (N-H st), 1601 (C_{ar}-C_{ar} st), 1718 (C=O st), 1528 (N-H δ). ^{1}H NMR (DMSO, 300 MHz): δ (ppm) 9.15 (bs, 2H, 2 NH), 7.31-7.00 (dd, 8H, ar), 4.09 (m, 4H, H1/H4), and 3.74 (m, 2H, H2/H3, and s, 2H, Ph-C$\underline{H}_2$-Ph from MDI). $^{13}C\{^{1}H\}$ NMR (DMSO, 75.5 MHz): δ (ppm) 153.48 (C=O), 136.77, 135.34, 128.50, 118.62 (ar), 68.88 (C2/C3), 65.29 (C1/C4) and 40.16 (Ph-$\underline{C}H_2$-Ph from MDI). Anal. Calcd. for $(C_{19}H_{20}N_2O_6)\cdot(H_2O)_{0.5}$: C, 59.84; H, 5.51; N, 7.35. Found: C, 59.86; H, 5.48; N, 7.33.

5.2.5. Hydrolytic degradation assays

Films of polyurethanes with a thickness of ~250 μm, were prepared by casting at room temperature from THF for PUR-(DTh^{i}Pr-HDI) and PUR-(DTh^{i}Pr-MDI), or by hot-press molding for PUR-(BD-HDI) and PUR-(DThOH-HDI). The films were cut into 8-mm diameter, 20 to 30-mg weight disks, which were dried in vacuum at 30 °C to constant weight. The degradation study was performed by placing the disks in sealed vials containing 10 mL of the buffered solution at the selected pH (sodium phosphate buffer, pH 7.4; sodium carbonate buffer, pH 10.0; citric acid buffer, pH 2.0) and experiments were carried out at temperatures within the 37-60 °C range. After incubation for the scheduled period of time, samples were removed, rinsed thoroughly with water and dried to constant weight. Sample weighing and GPC measurements were used to follow the evolution of the hydrodegradation.

5.3. Results and discussion

5.3.1. Polyurethane synthesis

Results obtained in the synthesis of polyurethanes studied in this work as well as some of their characterization data are given in Table 5.1. According to our results, the polymerization reaction of diisocyanates with 2,3-*O*-alkyliden-threitols carried out in DMF solution under mild conditions (40 ºC, 24 h) and using dibutyltin dilaurate as catalyst appears to be an effective method for the preparation of acetalized sugar-derived PUR. This procedure had been used previously by us for the preparation of methylated and benzylated sugar-derived polyurethanes.[4,5] The reactions proceeded in one step and isolation and purification of the polymers were carried out by solution-precipitation cycles and subsequent drying under vacuum. Yields were in the 80-90% range and weight-average molecular weights were in the 40,000-65,000 $g\cdot mol^{-1}$ range with polydispersities

around two in all cases. Both viscosity and molecular weight data for the whole set of PUR are compared in Table 5.1 showing a fully satisfactory correlation between the two series of data. Elemental analyses were in full agreement with those calculated for the expected compositions.

The chemical structures of polyurethanes were assessed by FTIR and NMR spectroscopy; these data are fully detailed in the experimental section. Characteristic IR absorption bands of the urethane group and the acetalized threitol moieties were observed at the predicted positions and with the expected intensities. Some significant differences were detected between the spectra of aromatic and aliphatic products in addition to those arising directly from the presence of the biphenyl structure. Thus, the N-H stretching band appearing at around 3335-3340 cm^{-1} in HDI derived PUR moved down to 3300-3310 cm^{-1} in their aromatic anaogues. On the contrary, the C=O stretching band appears in aliphatic PUR about 20-30 cm^{-1} lower than in the aromatic compounds. In all cases, ^{1}H and $^{13}C\{^{1}H\}$ NMR spectra were in full concordance with the expected chemical structures of PUR. The complex signal observed for the CH-C$\underline{H}_2$ of the threitol unit may be interpreted as due to an ABX system caused by the asymmetric CH carbon. On the other hand, no splitting of the CH signals unit was detected in any case, which allows excluding the occurrence of racemization reaction along the synthesis work.

As it is seen in Table 5.1, the polyurethanes containing acetalized threitol display solubility similar to their corresponding unsubstituted analogues; they are non-soluble in water but soluble in a variety of organic solvents including $CHCl_3$ and THF. Solubility appears reduced in the case of the aromatic compounds whereas it is not affected by the constitution of the alkylidene counterpart. Hydrophilicity was slightly enhanced as compared to unsubstituted PUR; the contact angle decreased with the insertion of the threitol units, the observed changes being larger in the case of the aliphatic compounds.

Acetalization is a well known method for protecting hydroxyl groups in neutral or basic media. The free hydroxyl groups can be recovered by cleaving the acetal by hydrolysis catalyzed by strong acids. Whereas the methylidene acetal prepared from formaldehyde is largely resistant to cleavage, acetals derived from higher carbonyl compounds, as it is the case of isopropylidene acetal, can be easily decomposed.

Table 5.1. Polycondensation and deprotection results of polyurethanes.

PUR	Reaction[a]				Molecular size[c]			Solubility[d]					Contact angle
	T (ºC)	*t* (h)	Yield (%)	$[\alpha]_D$[b] (º)	$[\eta]$ (dL·g^{-1})	M_w (g·mol^{-1})	PD	H_2O	DMSO	HFIP	$CHCl_3$	THF	(degrees)
LThMed-HDI	40	24	88	-15	0.67	41,400	2.0	-	+	+	+	+	58.6
LThMed-MDI	40	24	85	-30	0.75	47,200	2.0	-	+	+	-	+	76.2
DTh^{i}Prd-HDI	40	24	81	+17	0.83	62,400	2.0	-	+	+	+	+	59.1
DTh^{i}Prd-MDI	40	24	90	+36	0.85	65,600	2.1	-	+	+	-	+	78.4
DThOH-HDI[e]	25	0.5	90	+6	0.80	58,500	2.1	-	+	+	-	-	51.3
DThOH-MDI[e]	25	0.5	90	+19	nd	nd	nd	-	+	-	-	-	64.2
BD-HDI	40	2	88	--	0.63	30,000	2.2	-	+	+	+/-	+/-	72.5
BD-MDI	40	2	90	--	0.60	28,600	2.2	-	+	+	-	+/-	81.9

[a] Polycondensation reaction carried out in DMF.
[b] Measured in DMSO at 20 ± 5 ºC, *c*= 1 g·dL^{-1}.
[c] Intrinsic viscosity measured in DCA and average molecular weights determined by GPC in HFIP against PMMA standards.
[d] Solubility at 25 ºC (sample conc: 1 g·L^{-1}): + soluble, +/- partially soluble, - insoluble.
[e] Fully hydroxylated PUR from *O*-isopropylidene derived polyurethanes by treatment with TFA; nd: not determined.

As it is depicted in Scheme 5.3, deacetalization of both HDI and MDI derived PUR containing 2,3-*O*-isopropylidene threitol units was attained in 90% yield by treatment with aqueous TFA at room temperature for 30 minutes. The deacetalization reaction could be followed by ^{1}H NMR.

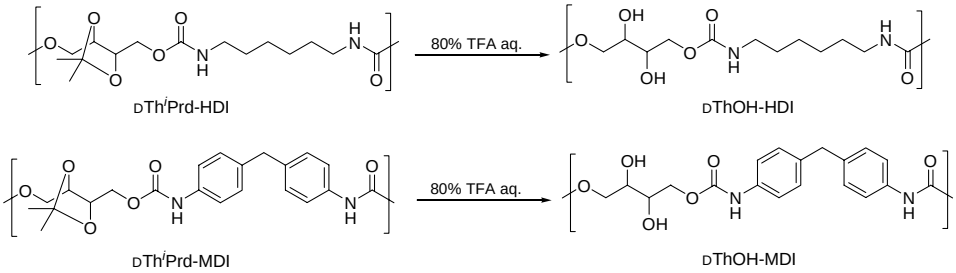

Scheme 5.3. Deprotection reactions leading to hydroxylated PUR derived from D-threitol.

The ^{1}H NMR spectra of PUR-(DTh^{i}Prd-HDI) and its corresponding hydroxyl-free derivative PUR-(DThOH-HDI) are compared in Figure 5.1; in addition to the shift to higher field observed for the signals arising from C<u>H</u> and C<u>H$_2$</u> of the threitol unit, the disappearance of the singlet arising from the pair of isopropylidene methyls provides a quantitative indication of the deacetalization degree that is attained. The deprotection reaction was found to take place without apparent breaking of the main backbone; the light decrease observed in the molecular weight (less than 10%) can be fully accounted by the mass loss that is subsequent to the removal of the isopropylidene group.

PUR bearing free hydroxyls display much lower solubility than the acetal protected polymers they come from; they are non-soluble in $CHCl_3$ and THF and the aromatic one is only soluble in DMSO, a fact that prevented analyzing this compound by GPC. Although they all continue to be non-soluble in water their hydrophilicity becomes greatly enhanced, as it is reflected in their contact angles with water, which are about 20º smaller than those measured for the unsubstituted PUR.

5.3.2. Thermal properties

The thermal stability of these polyurethanes was comparatively evaluated by thermogravimetry under inert atmosphere. Representative TGA traces are compared in

Figure 5.2 for protected and unprotected PUR, and main thermal decomposition parameters are given in Table 5.2. TGA results indicate that the thermal stability of PUR invariably increased when the acetalized threitol unit was incorporated in the polymer chain; both the onset and the maximum rate decomposition temperatures increased significantly, the change being more remarkable in the case of the aromatic based PUR.

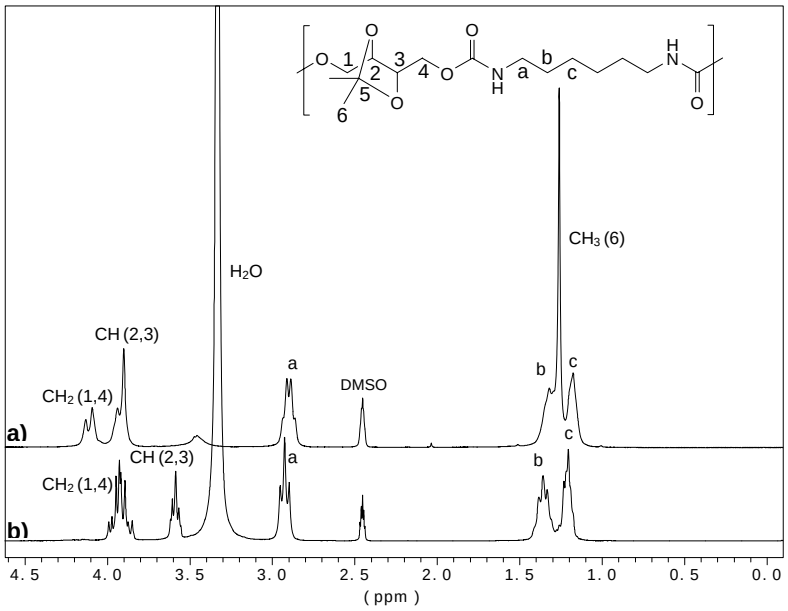

Figure 5.1. Compared ^{1}H NMR spectra of PUR-(DTh-HDI): acetal protected **(a)** and deprotected **(b)**.

On the contrary, the PUR bearing free hydroxyl groups appeared to be much less stable than the unsubstituted ones displaying onset temperatures near 50 ºC lower. Regarding the residue left upon decomposition at high temperature, no apparent influence seems to be exerted by the modifications; 1% and 20-30% of the original sample weights were the residual weights left by aliphatic and aromatic PUR, respectively, after heating at 600 ºC. It should be stressed that similar beneficial effects on thermal stability were observed for PUR containing *O*-methylated and *O*-benzylated alditols made from threitol, xylitol and arabinitol, the largest increment in decomposition temperatures being observed for the threitol derivatives.[4,5]

The effect on thermal transitions, T_g and T_m arising from the insertion of the threitol units in the PUR chain was investigated by DSC. It was found that the presence of the acetalized threitol unit in the PUR increased the T_g as compared to the unsubstituted analogues, the changes being more pronounced for the PUR made of HDI and for the isopropylidene acetal derivatives. On the other hand, no significant changes in T_g were observed among protected and deprotected compounds indicating that the T_g enhancing effect due to the stiff dioxolane cycle is replaced in the deacetalized PUR by the anchoring effect of the hydrogen-bonding hydroxyl groups.

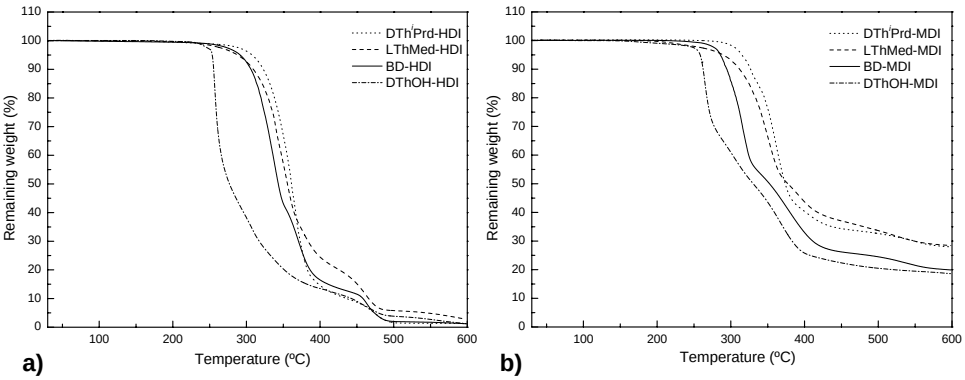

Figure 5.2. Comparative TGA for protected and deprotected PUR from HDI **(a)**, and from MDI **(b)**.

The DSC analyses of acetalized PUR revealed that only PUR-(LThMed-HDI) displayed crystallinity and only if samples are coming from precipitation in solution. The heating traces recorded from the synthesis powder of this compound before and after annealing are depicted in Figure 5.3a; upon the heating treatment, the complex endotherm observed at 135-145 ºC moved to 150 ºC and became a sharp peak characteristic of well crystallized material. Conversely, the two PUR bearing free hydroxyl groups are crystalline and the aliphatic one is able to crystallize from the melt. They display melting temperatures higher than the acetalized PUR-(LThMed-HDI), as it should be expected from their ability to form intermolecular hydrogen-bonds. Characteristic DSC traces recorded from PUR-(DThOH-HDI) and PUR-(DThOH-MDI) are depicted in Figure 5.3b and detailed DSC data are given in Table 5.2 for the whole set of compounds studied in this work.

Table 5.2. Thermal properties and WAXS data of polyurethanes.

PUR	DSC[a]			TGA[b]			X-ray diffraction						
	T_g (ºC)	T_m (ºC)	ΔH_m (J·g^{-1})	$^{o}T_d$ (ºC)	$^{max}T_d$ (ºC)	W (%)	d_{hkl}[c] (nm)						
LThMed-HDI	35	137, 146 / 150[d]	40 / 48[d]	315	**348**/385/462	1		1.75m	0.88w		0.43s	0.41s	0.37m
LThMed-MDI	93	no	no	313	**346**/401	28	--	--	--	--	--	--	--
DTh^{i}Prd-HDI	45	no	no	324	**362**/408/475	1	--	--	--	--	--	--	--
DTh^{i}Prd-MDI	126	no	no	320	**360**/410	28	--	--	--	--	--	--	--
DThOH-HDI[e]	38	166, 174, 180 / 180[f]	50 / 65[f]	254	**257**/328/462	1	2.89w	1.76s		0.46s		0.42s	0.39s
DThOH-MDI	111	229	30	257	**264**/307/373	19		1.67s		0.49s	0.44s		0.39s
BD-HDI[g]	15	184	77	300	**340**/371/464	1	3.07m				0.44s	0.41s	0.37s
BD-MDI	93	212, **232**	50	282	**315**/366	20			0.77w		0.43s		

[a] Glass transition temperature (T_g) of quenched samples. Melting temperature (T_m) and enthalpy (ΔH_m) of samples coming from synthesis and measured by DSC during first heating; no: not observed.
[b] Onset decomposition temperature ($^{o}T_d$), maximum rate decomposition temperatures ($^{max}T_d$) and remaining weight (W) measured by thermogravimetry.
[c] Visually estimated intensities as: s, strong; m, medium; w, weak. Data of annealed samples for PUR-(LThMed-HDI), PUR-(DThOH-HDI) and PUR-(DThOH-MDI).
[d] Sample annealed at 135 ºC for 12 hours.
[e] This compound crystallized from the melt at 119 ºC and remelted showing peaks at 157 and 169 ºC with a total enthalpy of 38 J·g^{-1}. The annealing at 160 ºC for 12 hours of a non-isothermally crystallized sample from the melt, shows one melting peak at 169 ºC with an enthalpy of 39 J·g^{-1}.

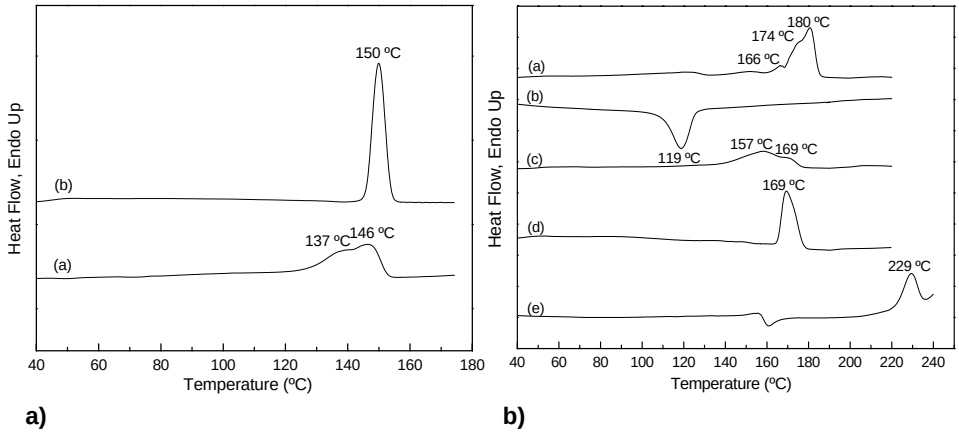

Figure 5.3. **a)** DSC traces of PUR-(LThMed-HDI); from synthesis **(a)**, and after annealing at 135 ºC for 12 hours **(b)**. **b)** DSC traces of PUR-(DThOH-HDI); first heating **(a)**, cooling **(b)**, second heating **(c)**, sample crystallized non-isothermally from the melt and annealed at 160 ºC for 2 hours **(d)**; and DSC trace of PUR-(DThOH-MDI) first heating **(e)**.

5.3.3. Structure and crystallization study

The interesting thermal properties displayed by PUR-(DThOH-HDI) (T_g=38 ºC, T_m=180 ºC, ΔH >60 J·g^{-1}) together with its ability to crystallize from the melt encouraged us to study the structural and crystallization behaviour of this compound to see how it compares to its unsubstituted analogue PUR-(BD-HDI), which can be taken as representative of conventional hard polyurethanes.

Typical aliphatic *m,n*-polyurethanes (where *m* and *n* stand for the number of carbons contained in the diol and diisocyanate counterparts, respectively) have crystal structures similar to the corresponding aliphatic polyamides. They usually crystallize with chains in *all-trans* conformation arranged in hydrogen-bonded sheets. The distance between neighbouring chains along the sheet is about 0.48 nm and the stacking distance of the sheets is about 0.37 nm. The crystal structure may be triclinic or monoclinic depending on the values of *m* and *n* and it is usually mixed with a varying amount of pseudohexagonal phase in which the interchain distance is about 0.48 nm. Accordingly, Bragg spacings characteristic of PUR are ~0.44 nm, ~0.37 nm and ~0.42 nm corresponding to the d_{100} and d_{010} spacings of the oblique lattices and the d_{100} spacing of the hexagonal lattice.[8-10]

The powder X-ray diffraction profiles of the crystalline aliphatic PUR studied in this work are depicted in Figure 5.4 and the main spacing values measured for all crystalline PUR are given in Table 5.2. The profile registered from PUR-(BD-HDI) consists of two main peaks at 0.44 nm and 0.37 nm along with a shoulder at 0.41 nm. These are the expected values for the triclinic structure of this polyurethane accompanied of a minor amount of a hexagonal phase. The profile obtained from PUR-(DThOH-HDI) coming from synthesis consists of a broad peak characteristic of defective crystallized material with hydrogen bonds disorderly established. After annealing, this broad peak split in two sharp peaks at 0.46 nm and 0.39 nm with some discrete scattering at 0.42 nm remaining between of them. This profile is essentially the same as that obtained for PUR-(BD-HDI) indicating that a similar crystal structure must be adopted in both cases; the slight variation observed in the spacing values may be the logical consequence of the expansive effect of the side hydroxyl groups on the packing of the structure.

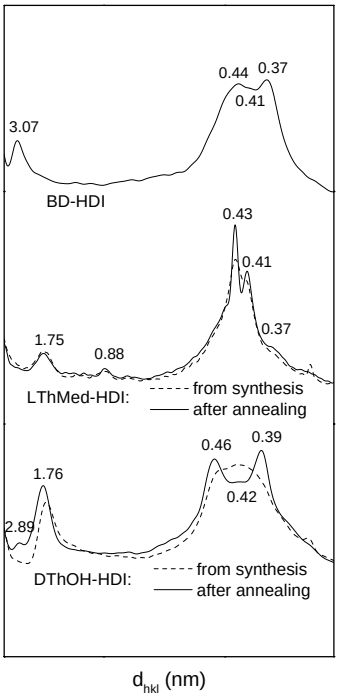

Figure 5.4. X-ray diffraction patterns of PUR-(BD-HDI), PUR-(LThMed-HDI) (before and after annealing for 12 hours at 135 ºC), and PUR-(DThOH-HDI) (before and after annealing for 1 hour at 170 ºC).

The X-ray diffraction data obtained from the acetalized PUR-(LThMed-HDI) were more difficult to interpret. In this case, the profile contains two sharp peaks at 0.43 nm and 0.41 nm, and the 0.37 nm spacing appearing as a hardly seen weak shoulder. A possible explanation would be that the intersheet repeating period of the structure disappeared as a consequence of the large disturbing effect that the bulky dioxolane group has on the side-by-side packing of the sheets, which would provoke the missing of the 010 reflection. A second interpretation would assume the occurrence of a triclinic structure of the same characteristics as that described for PUR-(BD-HDI) but with the interplanar distances changed due to the presence of the side group. In this case, the hexagonal phase should be assumed to be absent and the 0.41 nm spacing would arise therefore from an expanded intersheet distance of the triclinic structure.

To evaluate the crystallizability of PUR-(DThOH-HDI), a comparative isothermal crystallization study of this compound and PUR-(BD-HDI) was carried out by DSC. In Figure 5.5, the isothermal crystallization plots giving the evolution of the relative crystallinity with time are depicted for these two polymers at different temperatures. The Avrami treatment[11] of these data using equation 1 within the time range in which secondary crystallization is excluded, led to evaluate the isothermal crystallization parameters, *i.e.* the Avrami's constant *K* and exponent *n*, as well as the half-crystallization times $t_{1/2}$.

(Eq. 1) $$1\text{-}V_c(t\text{-}t_0) = e^{-k(t\text{-}t0)n}$$

V_c= relative volume fraction of crystallized material normalized by the maximum crystallization enthalpy; t= crystallization time; t_0= induction time, *i.e*. time elapsed before crystallization was detected.

The values obtained for these parameters are given in Table 5.3 indicating that crystallization was heterogeneously nucleated and that the process was speeded at lower temperatures. Since crystallization could not be carried out at the same temperatures for PUR-(BD-HDI) and PUR-(DThOH-HDI), a straight comparison of the crystallizability of these two polymers is not feasible. Nevertheless, a relative evaluation of their crystallizabilities could be obtained by plotting the crystallization half-time $t_{1/2}$ against the crystallization supercooling, which is defined as T_m^0-T_c, T_m^0 being the equilibrium melting temperature and T_c the crystallization temperature. T_m^0 was previously determined according to the procedure of Hoffman and Weeks.[12]

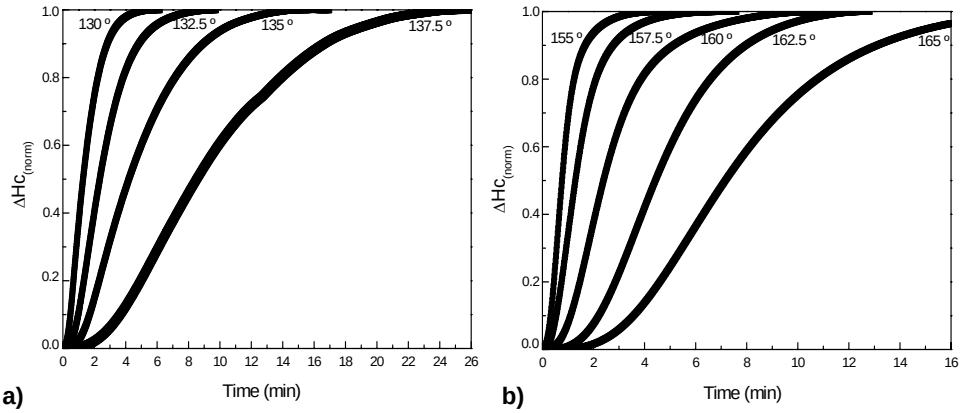

Figure 5.5. Crystallinity evolution with time of PUR-(DThOH-HDI) **(a)**, and PUR-(BD-HDI) **(b)**, at different crystallization temperatures (ºC).

Table 5.3. Crystallization parameters for the isothermal crystallization of PUR-(DThOH-HDI) and PUR-(BD-HDI).

PUR	Temperature (ºC)	*n*	*K* (min^{-n})	$t_{½}$ (min)
DThOH-HDI	130	2.29	0.563	1.30
	132.5	2.52	0.110	2.35
	135	2.65	0.025	4.22
	137.5	2.55	0.004	8.53
BD-HDI	155	2.29	1.407	0.78
	157.5	2.34	0.444	1.30
	160	2.72	0.080	2.40
	162.5	2.99	0.010	4.43
	165	3.08	0.002	7.17

As it is seen in Figure 5.6a, the plot of T_m *vs* T_c for a set of isothermal crystallizations results in a straight line that upon extrapolation intersects with the T_m=T_c line at the equilibrium temperature. The $t_{1/2}^{-1}$ *vs*. T_m^0-T_c plots depicted in Figure 5.6b reveal that to attain the same crystallization half-time, a larger supercooling should be required in the

case of the hydroxylated PUR. The result may be interpreted as due to the hindering effect that side hydroxyl groups must have on the mobility of the chains in the molten state that precedes crystallization, presumably as consequence of additional hydrogen-bonding formation.

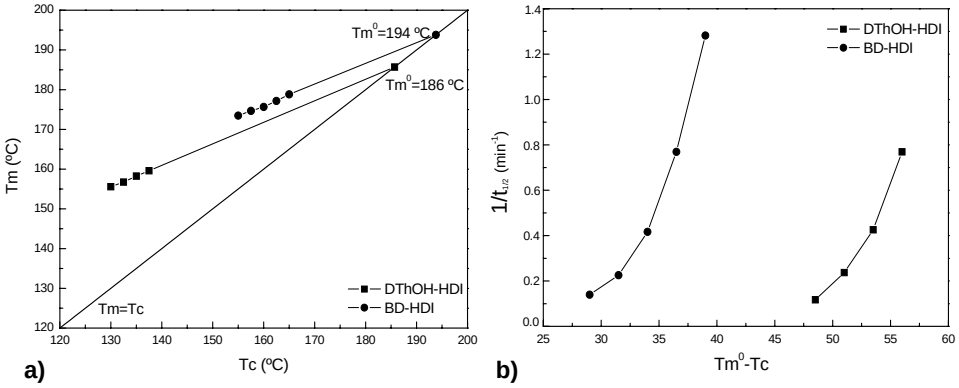

Figure 5.6. Determination of the equilibrium temperatures **(a)**, and crystallization half time *vs. ΔT= Tm⁰-Tc* **(b)**; of PUR-(DThOH-HDI) and PUR-(BD-HDI).

In order to get insight into the role played by hydrogen-bonding in the crystallization rate of these PUR, a FTIR analysis under heating was carried out in a range of temperatures in which melting takes place. Although there is a good number of published infrared studies of hydrogen bonding in polyurethanes,[13-15] most of them deal with segmented polymers. Much less information is available on the IR analysis of semicrystalline simple polyurethanes.

Fortunately, IR changes taking place in PUR-(BD-HDI) by effect of heating were studied in detail by Coleman and Painter[16] who made a fine interpretation of the different components contributing to the characteristic absorption bands of this compound. According to this study, the N-H stretching band envelopes two separate bands appearing at 3440 and 3320 cm^{-1} attributed to "free" and hydrogen bonded N-H respectively, as well as two phonon bands at 3362 and 3260 cm^{-1}, which complicate the spectrum in this region. The carbonyl absorption band is composed of three bands at 1684, 1699 and 1721 cm^{-1}, which are attributed to ordered and disordered hydrogen bonded carbonyl groups and non-hydrogen bonded carbonyl groups, respectively.

The IR spectral regions of particular interest, *i.e*. the N-H stretching from 3600-3100 cm^{-1} and the C=O stretching from 1600-1800 cm^{-1} of the aliphatic PUR-(LThMed-HDI) and PUR-(DThOH-HDI) recorded at increasing temperatures are shown in Figures 5.7 and 5.8. In both cases, a noticeable shift of the N-H and C=O absorption bands towards lower wavenumbers, which is indicative that hydrogen-bonded groups were transformed in free groups upon the heating treatment, was observed. The shift occurred abruptly at well defined temperatures, which are about 160 ºC and 180 ºC for PUR-(LThMed-HDI) and PUR-(DThOH-HDI), respectively. Such temperatures correspond approximately to their respective melting temperatures determined by DSC.

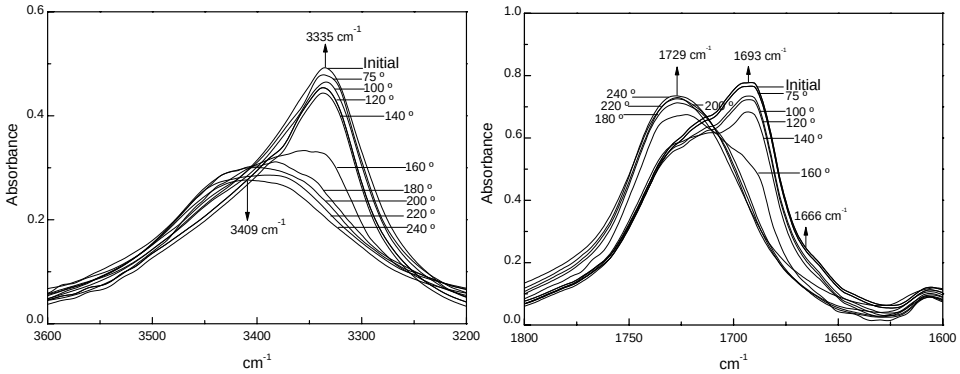

Figure 5.7. FTIR spectra of PUR-(LThMed-HDI) **(a** and **b)** at the indicated temperatures (ºC).

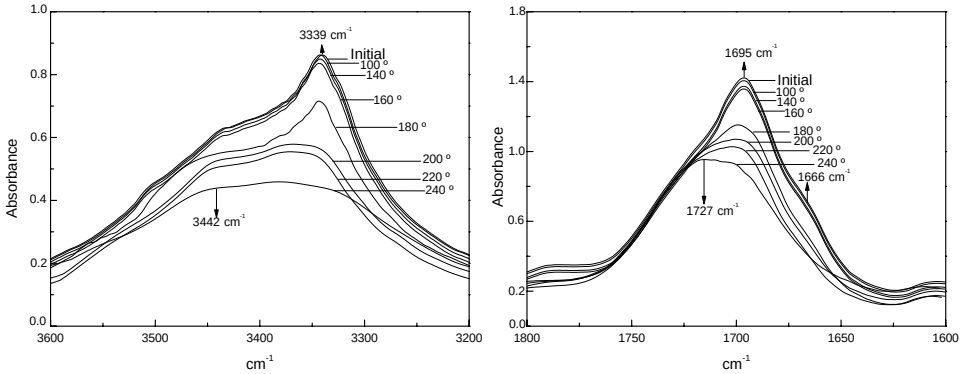

Figure 5.8. FTIR spectra of PUR-(DThOH-HDI) **(a** and **b)** at the indicated temperatures (ºC).

It is apparent therefore that hydrogen bonds are destroyed by heating and that this effect is particularly much more noticeable at melting. However, some significant differences between the two polymers are appreciated in the evolution of the N-H and C=O absorption bands with temperature. In the case of PUR-(DThOH-HDI), the absorption observed in the 3600-3200 cm^{-1} region is more complex, as it should be expected from the contribution of the present hydroxyl groups. Furthermore, at temperatures above melting, the band continues being broad although the contribution of the peak at 3339 cm^{-1} is almost vanished.

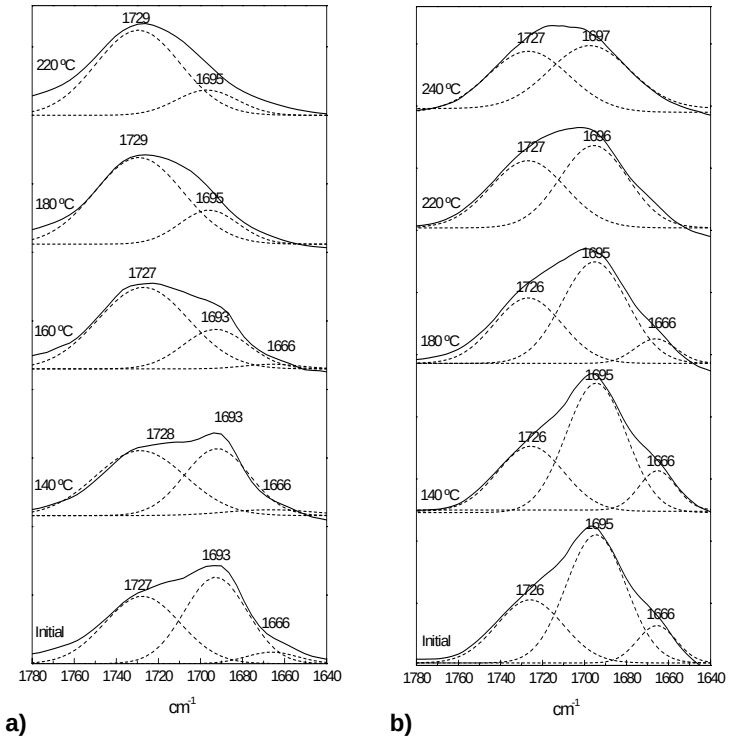

Figure 5.9. Curve fitting results in the carbonyl stretching region of polyurethanes LThMed-HDI **(a)**, and DThOH-HDI **(b)**, recorded at different temperatures.

The behaviour observed for the C=O stretching band is that it moved from 1695 to 1727 cm^{-1} but broadened and retained an important contribution of the absorption arising from associated C=O groups. In order to quantify the contribution of associated and free carbonyl groups, curve-fitting of this stretching band was made using two or three

components corresponding to free, and hydrogen bonded disordered and ordered carbonyl groups. The graphical results are shown in Figure 5.9 and relative values of the areas for each component are compared in Table 5.4. The conclusion is that although hydrogen bonds are weakened with temperature in both PUR, the amount of association remaining after melting is much more important in the case of PUR-(DThOH-HDI) (around 50%) than in PUR-(DThMed-HDI) (less than 20%), most likely due to the contribution of the free hydroxyl groups present in this compound; this fact would explain convincingly the relative low crystallizability displayed by PUR-(DThOH-HDI).

Table 5.4. Curve fitting of the C=O stretching region of PUR-(LThMed-HDI) and PUR-(DThOH-HDI).

LThMed-HDI					
	hydrogen bonded C=O		"free" C=O		
Temp (ºC)	ν (cm^{-1})	A_{HB} [a]	ν (cm^{-1})	A_F	A_{HB}/A_F
Initial	1666, 1693	26.2	1727	22.0	1.19
140	1666, 1693	21.1	1728	25.4	0.83
160	1666, 1693	12.3	1727	32.1	0.38
180	1695	8.6	1729	33.2	0.26
220	1695	6.7	1729	31.2	0.21
DThOH-HDI					
	hydrogen bonded C=O		"free" C=O		
Temp (ºC)	ν (cm^{-1})	A_{HB} [a]	ν (cm^{-1})	A_F	A_{HB}/A_F
Initial	1666, 1695	43.8	1726	20.1	2.18
140	1666, 1695	44.3	1726	20.7	2.14
180	1666, 1695	36.5	1726	21.2	1.72
220	1696	26.9	1727	24.1	1.12
240	1697	24.5	1727	23.7	1.03

[a] $A_{HB} = A_{HB,\ ordered} + A_{HB,\ disordered}$

5.3.4. Hydrolytic degradability

Polyurethanes are difficult to degrade by hydrolysis. Our previous degradation studies on PUR containing methylated and benzylated carbohydrate derived units revealed that significant hydrolysis was only attainable at basic pH and high temperatures.[4,5] In this work we have undertaken a degradation study focused to evaluate the hydrodegradability of PUR containing threitol units with the hydroxyl side groups in the free form. The evolution of the degradation with time was followed by measuring changes taking place in the weight and weight-average molecular weight of the residual polymer. Results from this study are presented in Figures 5.10 and 5.11 and Table 5.5.

Firstly a comparative study of a representative selection of the PUR studied in this work was carried out under favourable degrading conditions, *i.e* pH = 10 and T = 60 ºC. The changes in the remaining weight as a function of incubation time are represented in Figure 5.10a.

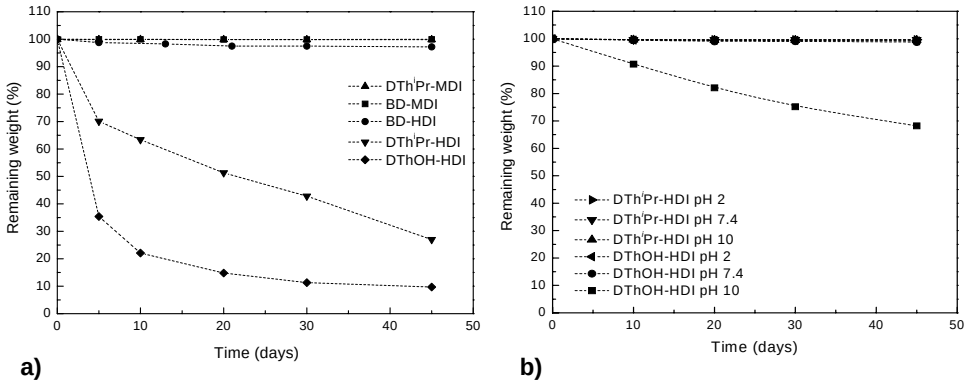

Figure 5.10. Changes in sample weight of some polyurethanes studied at pH 10 and 60 ºC **(a)**. Compared changes in sample weight of PUR-(DThiPrd-HDI) and PUR-(DThOH-HDI) at 37 ºC and different pH **(b)**.

The main conclusions drawn from these exploratory assays are that aliphatic PUR bearing free hydroxyl side groups is the most degradable of the series and that the isopropylidene acetalized PUR displays a considerable hydrodegradability too. On the contrary, aromatic PUR-(DThiPrd-MDI) and the unsubstituted PUR-(BD-HDI) and PUR-(BD-MDI) remained essentially unaltered under the assayed conditions.

As it is seen in the last column of Table 5.5, the GPC analysis of the residual polymer afforded molecular weight data consistent with weight loss measurements. The average-weight molecular weight of PUR-(DTh^{i}Prd-HDI) and PUR-(DThOH-HDI) decreased from the initial value of about 60,000 to about 5,000 g·mol^{-1} in forty-five days at 60 ºC. When these two PUR were incubated at 37 ºC, only PUR-(DThOH-HDI) at pH 10 was perceivably degraded (Figure 5.10b).

Table 5.5. Compared hydrolytic degradation data of selected threitol derived polyurethanes.

		DTh^{i}Prd-HDI					
		pH 2		pH 7.4		pH 10	
Days		37 ºC	60 ºC	37 ºC	60 ºC	37 ºC	60 ºC
0	*W* (%)	100	100	100	100	100	100
	M_w (g·mol^{-1})	62,400	62,400	62,400	62,400	62,400	62,400
10	*W* (%)	99.7	91.7	99.6	75.4	99.6	63.4
	M_w (g·mol^{-1})	62,400	57,900	62,200	43,600	62,200	30,400
45	*W* (%)	99.6	71.6	99.6	46.8	99.5	27.0
	M_w (g·mol^{-1})	62,200	50,800	62,200	13,200	62,100	6,300
		DThOH-HDI					
0	*W* (%)	100	100	100	100	100	100
	M_w (g·mol^{-1})	58,500	58,500	58,500	58,500	58,500	58,500
10	*W* (%)	99.5	86.0	99.5	54.1	90.7	22.1
	M_w (g·mol^{-1})	58,400	50,300	58,400	26,800	51,400	8,500
45	*W* (%)	99.2	62.4	98.8	13.1	68.2	9.7
	M_w (g·mol^{-1})	58,200	39,200	58,100	5,700	21,900	4,200
		DTh^{i}Prd-MDI		BD-HDI		BD-MDI	
		pH 10, 60 ºC		pH 10, 60 ºC		pH 10, 60 ºC	
0	*W* (%)	100		100		100	
	M_w (g·mol^{-1})	65,600		30,000		28,600	
10	*W* (%)	99.9		98.3		99.9	
	M_w (g·mol^{-1})	65,600		30,000		28,600	
45	*W* (%)	99.8		97.2		99.9	
	M_w (g·mol^{-1})	65,600		29,900		28,600	

W: Remaining weight.
M_w: Weight-average molecular weight determined by GPC in HFIP against PMMA standards.

The influence of temperature on the hydrolytic degradability rate was then investigated. In Figure 5.11a and 5.11b, the respective changes in remaining weight and weight-average molecular weight with temperature are plotted for PUR-(DTh^{i}Prd-HDI) and PUR-(DThOH-HDI) incubated at pH 7.4 for 10 days.

The behaviour displayed by the two polymers is very similar in the two plots revealing that the loss in remaining weight is a consequence of the removal of the chain fragments originated by hydrolysis. As much expected, degradation rate increased with incubation temperature, this effect being similar for the two polymers above 45 ºC. Below this temperature the acetalized PUR remained practically unaltered whereas the deprotected PUR became significantly degraded. This rather striking behaviour could be explained taking into account the T_g of the polymers, which are 35 and 45 ºC respectively; apparently, hydrolysis is severely hindered below T_g, most probably due to the impediment to water diffusion caused by the immobility of the polymer chain under such conditions.

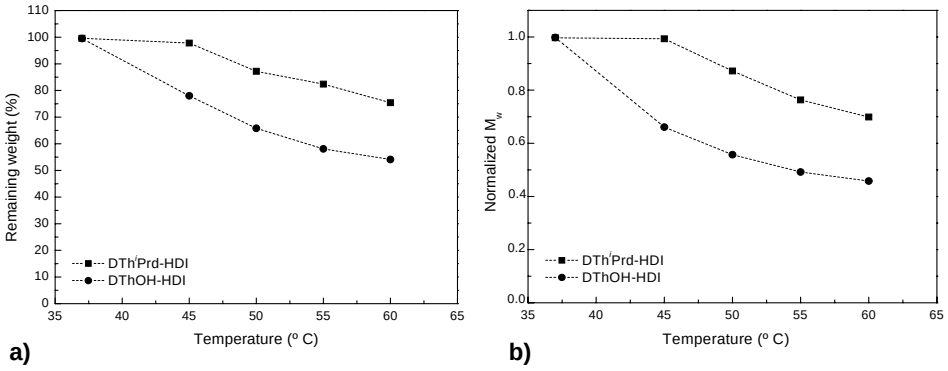

Figure 5.11. Compared hydrolytic degradation data of PUR-(DTh^{i}Prd-HDI) and PUR-(DThOH-HDI) for 10 days of incubation at pH 7.4 and at different temperatures. Changes in sample weight **(a)**, and changes in weight-average molecular weight **(b)**.

5.4. Conclusions

Moderate molecular weight PUR containing acetalized-threitol units could be prepared in high yields by polymerization in solution of the 2,3-*O*-methylidene and 2,3-*O*-isopropylidene with diisocyanates. Most of these acetalized threitol containing PUR are

amorphous compounds with T_g higher than their unsubstituted analogues. The treatment of the isopropylidene derivatives with TFA led to the corresponding free-hydroxyl threitol derived PUR.

The hydroxylated PUR made from HDI, PUR-(DThOH-HDI), is a semicrystalline compound with highly interesting thermal properties, *i.e.* T_g = 38 ºC, T_m = 180 ºC, it is stable up to 250 ºC and its crystal structure is made of hydrogen-bonded sheets typical of linear unsubstituted PUR. This compound was able to crystallize from the melt but at lower rate than its unsubstituted analogue made from 1,4-butanediol and HDI because of the extensive occurrence of hydrogen bonds in the melt, which is attributed to the presence of the free hydroxyl side groups. The hydrolytic degradability of threitol containing PUR was highly dependent on pH and temperature and appeared greatly enhanced in polymers made of HDI; PUR-(DThOH-HDI) was almost fully degraded at pH 7.4 and 60 ºC whereas it remained essentially unaltered upon incubation at room temperature.

5.5. References

1. Bou, J.J.; Rodríguez-Galán, A.; Muñoz-Guerra, S. *Macromolecules* **1993**, 26, 5664.

2. Kint, D.; Wigstrom, E.; Martinez de Ilarduya, A.; Alla, A.; Muñoz-Guerra, S. *J Polym Sci Part A: Polym Chem* **2001**, 39, 3250.

3. García-Martín, M.G.; Ruíz, R.; Benito E.; Espartero, J.L.; Muñoz-Guerra, S.; Galbis, J.A. *Macromolecules* **2005**, 38, 8664.

4. de Paz, M.V.; Marín, R.; Zamora, F.; Hakkou, K.; Alla, A.; Galbis, J.A.; Muñoz-Guerra, S. *J Polym Sci Part A: Polym Chem* **2007**, 45, 4109.

5. Marín, R.; de Paz, M.V.; Ittobane, N.; Galbis, J.A.; Muñoz-Guerra, S. *Macromol Chem Phys* (accepted **2009**).

6. Kluba, R.M.; Mattick, L.R. *J Food Sci* **1978**, 43, 717.

7. Rodríguez-Galán, A.; Bou, J.J.; Muñoz-Guerra, S. *J Polym Sci: Polym Chem Ed* **1992**, 30, 713.

8. Saito, Y.; Nansai, S.; Kinoshita, S. *Polym J (Tokyo)* **1972**, 3, 113.

9. Borchert, W.Z. *Angew Chem* **1951**, 63, 31.

10. McKiernan, R.L.; Heintz, A.M.; Hsu, S.L.; Atkins, D.T.; Penelle, J.; Gido, S.P. *Macromolecules* **2002**, 35, 6970.

11. a) Avrami, M.J. *J Chem Phys* **1939**, 7, 1103. b) *ibid J Chem Phys* **1940**, 8, 212. c) *ibid J Chem Phys* **1941**, 9, 177.

12. Hoffman, J.D.; Weeks, J.J. *J Research Natl Bur Standards* **1962**, 66A(1), 13.

13. Seymour, R.W.; Allegrezza, A.E.; Cooper, S.L. *Macromolecules* **1973**, 6, 896.

14. Sung, C.S.P.; Schneider, N.S. *Macromolecules* **1977**, 10, 452.

15. Brunette, C.M.; Hsu, S.L.; MacKnight, W.J. *Macromolecules* **1982**, 15, 71.

16. Coleman, M.M.; Lee, K.H.; Skrovanek, D.J.; Painter, P.C. *Macromolecules* **1986**, 19, 2149.

CHAPTER 6

LINEAR POLYURETHANES MADE FROM NATURALLY-OCCURRING TARTARIC ACID *

Purpose and specific aims: *The target of this work was the synthesis of new polyurethanes by direct reaction of tartaric acid esters with diisocyanates. Ester side groups in the polyurethane could be converted to acid groups by hydrogenolysis of benzyl esters, or by hydrolysis of alkyl esters. By these methods, polyurethanes with carboxyl side groups and enhanced hydrodegradability could be obtained.*

Summary: *Naturally-occurring tartaric acid was used as raw material for the synthesis of novel linear polyurethanes (PUR) bearing two carboxylate side groups in the repeating unit. Aliphatic and aromatic PUR were obtained by reaction in solution of alkyl and benzyl tartrates with 1,6-hexamethylene diisocyanate and 4,4'-methylenebis(phenyl isocyanate), respectively. All the novel PUR were thermally stable and optically active. The aliphatic carboxylate-containing PUR had M_w in the 40-70 kDa range, and all they were semicrystalline polymers with melting temperatures between 100 and 150 ºC and T_g comprised in the 50-80 ºC interval. The aromatic PUR were amorphous materials with molecular weights between 18 and 25 kDa and T_g above 130 ºC. Hydrogenolysis of the PUR made from 1,6-hexamethylene diisocyanate and benzyl tartrate yielded PUR containing up to 40% of free carboxylic groups. The tartrate derived PUR displayed enhanced sensitivity to hydrolysis compared to their unsubstituted analogue PUR-(EG-HDI) (from ethylene glycol). The PUR bearing free carboxylic groups were unique in being degraded by water upon incubation under physiological conditions.*

* Publication derived from this work: Marín, R.; Martínez de Ilarduya, A.; Muñoz-Guerra, S. *J Polym Sci Part A: Polym Chem* (accepted **2009**).

6.1. Introduction

PUR are chemically stable polymers that display a high resistance to hydrolysis, a highly acknowledged property of prime importance for a good number of applications. However, degradability in an aqueous medium under physiological conditions is indispensable if PUR are intended to be used for temporal applications in the biomedical field. Segmented linear polyurethanes made of soft and rigid chain blocks are extensively used in this regards due to their satisfactory physical and mechanical properties and good biocompatibility.[1,2] Biodegradability of segmented polyurethanes is generally achieved by using hydroxyl terminated polyesters or polyethers of recognized degradability (PCL, PEO, etc) as *soft segment*.[3,4] On the other hand, homogeneous linear PUR entirely made of urethane links, *i.e*. lacking *soft segment*, are monophasic materials still scarcely developed for technical applications. The extreme resistance to hydrolysis of these PUR may be weakened by replacing the conventional alkanediols typically used as hydroxyl supplying monomers by highly hydrophilic diols more susceptible to water attack.

The preparation of polymers from renewable feedstocks is currently receiving increasing attention because of economic and environmental concerns.[5,6] This has renewed the interest for PUR made from carbohydrate compounds or their derivatives. A severe limitation in the use of carbohydrates as a source of diol-monomers for the synthesis of linear polycondensates is their inherently high functionality.[7,8] Polyamides prepared by direct polycondensation reaction of aldaric acid diesters with diamines usually have low molecular weights.[9,10] In previous chapters, the preparation of linear polyurethanes from partially methylated or benzylated alditols has been reported,[11,12] and selective deprotection reactions were carried out to render PUR bearing free hydroxyl side groups.[13]

In this chapter a report on the synthesis, characterization, and properties of a series of PUR made from 1,6-hexamethylene diisocyanate (HDI) and 4,4′-methylenebis(phenyl isocyanate) (MDI) and naturally-occurring tartaric acid, is presented. In the recent literature, there are some antecedents on the use of tartaric acid for the preparation of polyurethanes.[14,15] Tartaric acid (2,3-dihydroxy butanedioic acid) is an aldaric acid bearing two secondary hydroxyl groups that can be added to the two isocyanate groups of a diisocyanate to generate a linear polyurethane chain. In order to avoid undesirable

reactions of the carboxylic groups, alkyl or benzyl tartrates instead of tartaric acid itself are used for polymerization; by this means linear polyurethanes bearing two carboxylate side groups per repeating unit are obtained. The optically active forms of tartaric acid are used in this work; since these forms are dissymmetric, *i.e.* they have C_2 symmetry, the resulting PUR will be stereoregular polymers. In previous chapters, aliphatic and aromatic linear polyurethanes derived from threitol, an aldotetritol that is obtained by reduction of the carboxylate groups of tartrates to hydroxymethyl groups, were described. 2,3-Di-*O*-protected threitols were used to produce polyurethanes bearing protected hydroxyl side groups, which in certain cases could be deprotected to render polyurethanes bearing free hydroxyl groups (Scheme 6.1).[12,13]

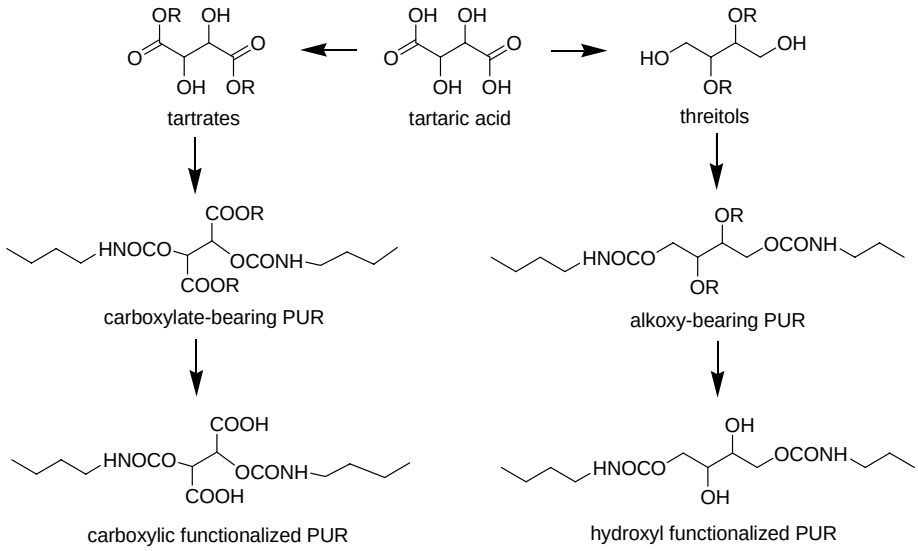

Scheme 6.1. Tartaric acid as source of functionalized polyurethanes.

6.2. Experimental section

6.2.1. Materials and methods

Common reagents, solvents and tartrates were purchased from Aldrich and used as received. *N,N*-dimethylformamide (DMF) used as polymerization solvent was distilled prior to use to eliminate residual water. HDI was distilled under vacuum and MDI was used as received. Both compounds were stored at 4 ºC and handled under inert

atmosphere. Diols and other reagents for polymerization were stored in a desiccator under vacuum until used. Viscosities were measured in dichloroacetic acid at 25.0 °C using an Ubbelohde microviscometer. Elemental analyses were carried out by Centro de Investigación y Desarrollo (CID-CSIC, Barcelona). Optical rotations were measured in DMSO solutions in a Krüss Electronic Polarimeter P3001 at 20 ± 5 ºC (1-dm cell). Gel permeation chromatograms were acquired at 35 ºC with a Waters equipment provided with a refraction-index detector. The samples were chromatographed with 0.05 M sodium trifluoroacetate-hexafluoroisopropanol (NaTFA-HFIP) at a flow rate of 0.5 $mL \cdot min^{-1}$ using a polystyrene-divinylbenzene packed linear column. Chromatograms were calibrated against poly(methyl methacrylate) (PMMA) monodisperse standards. IR spectra were obtained from KBr discs using a Perkin–Elmer 2000 spectrometer. ^{1}H and $^{13}C\{^{1}H\}$ NMR spectra were recorded on a Bruker AMX-300 spectrometer operating at 300.1 and 75.5 MHz for ^{1}H and $^{13}C\{^{1}H\}$, respectively, and using TMS as internal reference. Sample concentrations of about 1-5% (w/v) were used for these analyses. The spectra were acquired with 64 scans and 1000-10000 scans, and relaxation delays of 1 and 2 s, for ^{1}H and $^{13}C\{^{1}H\}$ respectively.

Differential scanning calorimetric (DSC) experiments were performed at heating/cooling rates of 10 $ºC \cdot min^{-1}$ on a Perkin-Elmer Pyris 1 instrument calibrated with indium. All the experiments were carried out with 3-4 mg samples within a temperature range from 0 to 275 ºC, and under a nitrogen flow of 20 $mL \cdot min^{-1}$ to minimize possible oxidative degradations. Melting temperatures were obtained from the first heating run since no crystallization from the melt was observed for any sample except for the reference ethylene glycol derived polyurethanes. Glass transition temperatures were determined on the heating traces obtained at 20 $ºC \cdot min^{-1}$ from samples that were quickly cooled from the melt. Thermogravimetric analysis was carried out using a Mettler TA4000 thermobalance at a heating rate of 10 $°C \cdot min^{-1}$ under inert atmosphere and within a temperature range of 30 to 600 ºC. Sample weights of about 15 mg were used in these experiments. Powder X-ray diffraction patterns were recorded on flat films in a modified Statton-type Wharus camera using nickel-filtered Cu-K_α radiation of wavelength 0.1541 nm, and they were calibrated with molybdenum sulphide (d_{002} = 0.6147 nm). Polarized optical micrographs were taken with a Olympus BX51 polarizing microscope from films prepared by casting from 5% w/v formic acid solutions at room temperature. For mechanical properties, films with a thickness of ~250 µm were prepared by casting from tetrahydrofuran at room temperature on a silanized Petri dish. In the case of

polyurethanes made from ethylene glycol, films were obtained by hot-press molding at 10-20 ºC above their melting temperature. Test specimens of 3-mm width and a distance between testing marks of 10 mm were prepared from these films by cutting. The tensile strength (σ_{break}), elongation at break (ε_{break}), and Young's modulus (E) were measured in triplicates on a Zwick 2.5/TN1S testing machine coupled with a compressor Dalbe DR 150, at a strain rate of 20 mm·min^{-1}.

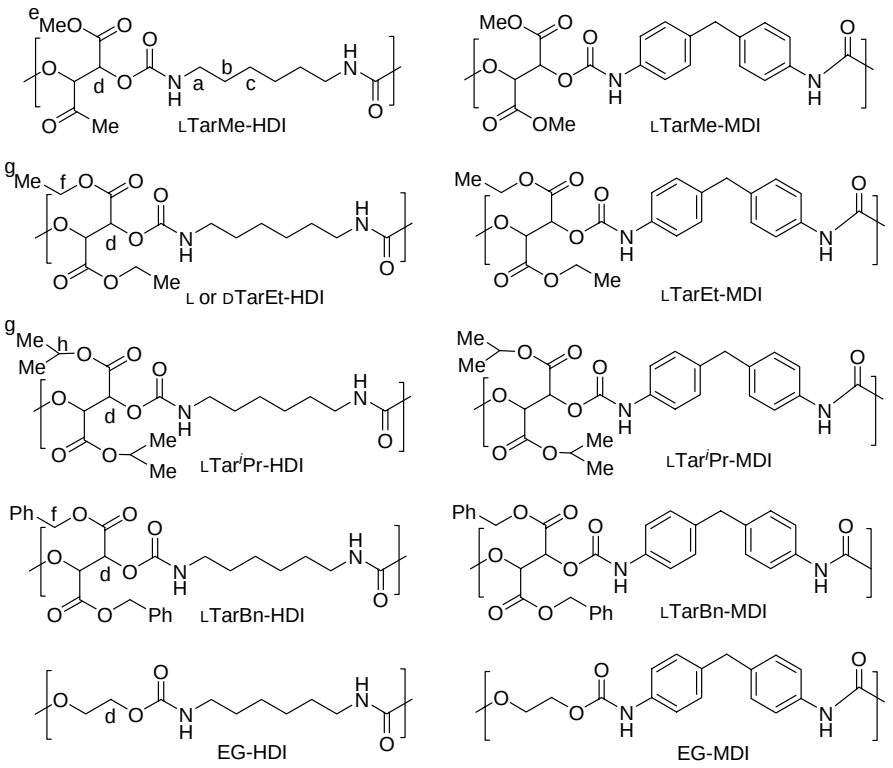

Scheme 6.2. Chemical structures of polyurethanes. Labels refer to NMR peak assignments.

6.2.2. Polyurethane synthesis

Tartrate derived polyurethanes. In a typical procedure, a round bottom flask saturated with inert gas was charged with the selected tartrate (1 mmol) and *N,N*-dimethylformamide (4 mL), and the mixture was stirred up at room temperature until homogenization. 1 mmol of HDI or MDI followed by dibutyltin dilaurate (2% w/w) catalyst

were then added and the mixture stirred for 24 hours further at 50 ºC. The reaction mixture was then added dropwise into cold diethyl ether (50 mL) to precipitate the polymer. Purification of the polyurethane was carried out by dissolving the polymer in the minimum volume of chloroform or tetrahydrofuran, and reprecipitation into diethyl ether. The pure polymers (all them white solids) were dried under vacuum and stored in a desiccator until needed.

PUR-(LTarMe-HDI). It was prepared from dimethyl L-tartrate (178 mg, 1 mmol) and diisocyanate HDI (164 µL, 1 mmol). Yield 294 mg (85%). IR: ν (cm^{-1}) 3375 (N-H st), 1733 (C=O st), 1526 (N-H δ). ^{1}H NMR ($CDCl_3$, 300 MHz): δ (ppm) 6.38 (bs, 2H, 2 NH), 5.64 (s, 2H, 2 CH-d), 3.71 (s, 6H, 2 CH_3-e), 3.05 (m, 4H, 2 CH_2-a), 1.41 (m, 4H, 2 CH_2-b), and 1.24 (m, 4H, 2 CH_2-c). $^{13}C\{^{1}H\}$ NMR ($CDCl_3$, 75.5 MHz): δ (ppm) 169.03 (C=O ester), 155.43 (C=O urethane), 71.48 (CH-d), 53.54 (CH_3-e), 41.75 (CH_2-a), 29.37 (CH_2-b), and 26.82 (CH_2-c). Anal. Calcd. for ($C_{14}H_{22}N_2O_8$): C, 48.55; H, 6.40; N, 8.09. Found: C, 47.96; H, 6.37; N, 8.02.

PUR-(L or DTarEt-HDI). They were prepared from diethyl L or D-tartrate (206 mg, 1 mmol) and HDI (164 µL, 1 mmol). Yield 329 mg (L) and 303 mg (D) (88% and 81%, respectively). IR: ν (cm^{-1}) 3375 (N-H st), 1733 (C=O st), 1524 (N-H δ). ^{1}H NMR ($CDCl_3$, 300 MHz): δ (ppm) 6.42 (bs, 2H, 2 NH), 5.65 (s, 2H, 2 CH-d), 4.16 (m, 4H, 2 CH_2-f), 3.04 (m, 4H, 2 CH_2-a), 1.39 (m, 4H, 2 CH_2-b), and 1.19 (m, 4H, 2 CH_2-c; and, m, 6H, 2 CH_3-g). $^{13}C\{^{1}H\}$ NMR ($CDCl_3$, 75.5 MHz): δ (ppm) 168.55 (C=O ester), 155.53 (C=O urethane), 71.55 (CH-d), 62.74 (CH_2-f), 41.69 (CH_2-a), 29.48 (CH_2-b), 26.89 (CH_2-c) and 14.54 (CH_3-g). Anal. Calcd. for ($C_{16}H_{26}N_2O_8$): C, 51.33; H, 7.00; N, 7.48. Found: C, 50.79; H, 7.03; N, 7.46 for (L); and C, 51.49; H, 7.09; N, 7.50 for (D).

PUR-(LTar^{i}Pr-HDI). It was prepared from diisopropyl L-tartrate (234 mg, 1 mmol) and HDI (164 µL, 1 mmol). Yield 326 mg (81%). IR: ν (cm^{-1}) 3372 (N-H st), 1735 (C=O st), 1524 (N-H δ). ^{1}H NMR ($CDCl_3$/TFA, 300 MHz): δ (ppm) 6.40 (bs, 2H, 2 NH), 5.68 (s, 2H, 2 CH-d), 5.19 (m, 2H, 2 CH-h), 3.20 (m, 4H, 2 CH_2-a), 1.52 (m, 4H, 2 CH_2-b), 1.34 (m, 4H, 2 CH_2-c) and 1.32-1.24 (dd, 12H, 4 CH_3-g). $^{13}C\{^{1}H\}$ NMR ($CDCl_3$/TFA, 75.5 MHz): δ (ppm) 169.51 (C=O ester), 156.84 (C=O urethane), 74.47 (CH-d), 72.86 (CH-h), 42.16 (CH_2-a), 29.61 (CH_2-b), 26.68 (CH_2-c) and 21.45 (CH_3-g). Anal. Calcd. for ($C_{18}H_{30}N_2O_8$): C, 53.72; H, 7.51; N, 6.96. Found: C, 53.67; H, 7.50; N, 6.98.

PUR-(L-TarBn-HDI). It was prepared from dibenzyl L-tartrate (330 mg, 1 mmol) and HDI (164 µL, 1 mmol). Yield 388 mg (78%). IR: ν (cm-1) 3382 (N-H st), 1733 (C=O st), 1592 (C_{ar}-C_{ar} st), 1522 (N-H δ). ^{1}H NMR ($CDCl_3$/TFA, 300 MHz): δ (ppm) 7.32 (m, 10H, 2 Ph), 6.25 (bs, 2H, 2 NH), 5.77 (s, 2H, 2 CH-d), 5.15 (m, 4H, 2 CH_2-f), 3.05 (m, 4H, 2 CH_2-a), 1.43 (m, 4H, 2 CH_2-b), and 1.28 (m, 4H, 2 CH_2-c). $^{13}C\{^{1}H\}$ NMR ($CDCl_3$/TFA, 75.5 MHz): δ (ppm) 168.44 (C=O ester), 155.70 (C=O urethane), 133.75, 129.12, 128.90, 128.75 (Ph), 71.83 (CH-d), 62.49 (CH_2-f), 41.41 (CH_2-a), 28.84 (CH_2-b), and 26.00 (CH_2-c). Anal. Calcd. for ($C_{26}H_{30}N_2O_8$): C, 62.64; H, 6.07; N, 5.62. Found: C, 62.48; H, 6.09; N, 5.63.

PUR-(L-TarMe-MDI). It was prepared from dimethyl L-tartrate (178 mg, 1 mmol) and diisocyanate MDI (250 mg, 1 mmol). Yield 342 mg (80%). IR: ν (cm^{-1}) 3334 (N-H st), 1747 (C=O st), 1602 (C_{ar}-C_{ar} st), and 1532 (N-H δ). ^{1}H NMR ($CDCl_3$/TFA, 300 MHz): δ (ppm) 7.81 (bs, 2H, 2 NH), 7.22-7.18 (m, 8H, ar), 5.82 (s, 2H, 2 CH-d), and 3.93 (m, 2H, Ph-C<u>H</u>$_2$-Ph from MDI; and m, 6H, 2 CH_3-e). $^{13}C\{^{1}H\}$ NMR ($CDCl_3$/TFA, 75.5 MHz): δ (ppm) 165.89 (C=O ester), 150.20 (C=O urethane), 135.34, 130.04, 126.32, 117.67 (ar), 68.47 (CH-d), 51.00 (CH_3-e), and 37.02 (Ph-<u>C</u>H$_2$-Ph from MDI). Anal. Calcd. for ($C_{21}H_{20}N_2O_8$): C, 58.88; H, 4.71; N, 6.54. Found: C, 58.86; H, 4.70; N, 6.50.

PUR-(L-TarEt-MDI). It was prepared from diethyl L-tartrate (206 mg, 1 mmol) and MDI (250 mg, 1 mmol). Yield 401 mg (88%). IR: ν (cm^{-1}) 3326 (N-H st), 1744 (C=O st), 1601 (C_{ar}-C_{ar} st), and 1533 (N-H δ). ^{1}H NMR ($CDCl_3$/TFA, 300 MHz): δ (ppm) 7.91 (bs, 2H, 2 NH), 7.20-7.14 (m, 8H, ar), 5.84 (s, 2H, 2 CH-d), 4.39 (m, 4H, 2 CH_2-f), 3.93 (s, 2H, Ph-C<u>H</u>$_2$-Ph from MDI), and 1.32 (m, 6H, 2 CH_3-g). $^{13}C\{^{1}H\}$ NMR ($CDCl_3$/TFA, 75.5 MHz): δ (ppm) 168.97 (C=O ester), 153.79 (C=O urethane), 138.82, 133.28, 129.61, 121.04 (ar), 72.01 (CH-d), 64.76 (CH_2-f), 40.28 (Ph-<u>C</u>H$_2$-Ph from MDI) and 12.91 (CH_3-g). Anal. Calcd. for ($C_{23}H_{24}N_2O_8$): C, 60.52; H, 5.30; N, 6.14. Found: C, 60.65; H, 5.22; N, 6.08.

PUR-(L-Tar^{i}Pr-MDI). It was prepared from diisopropyl L-tartrate (234 mg, 1 mmol) and MDI (250 mg, 1 mmol). Yield 363 mg (75%). IR: ν (cm^{-1}) 3324 (N-H st), 1747 (C=O st), 1602 (C_{ar}-C_{ar} st), and 1532 (N-H δ). ^{1}H NMR ($CDCl_3$/TFA, 300 MHz): δ (ppm) 7.96 (bs, 2H, 2 NH), 7.22-7.16 (m, 8H, ar), 5.89 (s, 2H, 2 CH-d), 5.25 (m, 2H, 2 CH-h), 3.96 (s, 2H, Ph-C<u>H</u>$_2$-Ph from MDI), and 1.37-1.30 (dd, 12H, 4 CH_3-g). $^{13}C\{^{1}H\}$ NMR ($CDCl_3$/TFA, 75.5 MHz): δ (ppm) 168.45 (C=O ester), 153.77 (C=O urethane), 138.68, 133.38, 129.60, 120.99 (ar), 73.83 (CH-d), 72.14 (CH-h), 40.29 (Ph-<u>C</u>H$_2$-Ph from MDI) and 20.65 (CH_3-

g). Anal. Calcd. for ($C_{25}H_{28}N_2O_8$): C, 61.97; H, 5.83; N, 5.78. Found: C, 61.91; H, 5.81; N, 5.73.

PUR-(LTarBn-MDI). It was prepared from dibenzyl L-tartrate (330 mg, 1 mmol) and MDI (250 mg, 1 mmol). Yield 481 mg (83%). IR: ν (cm^{-1}) 3326 (N-H st), 1743 (C=O st), 1598 (C_{ar}-C_{ar} st), and 1528 (N-H δ). ^{1}H NMR ($CDCl_3$/TFA, 300 MHz): δ (ppm) 8.00 (bs, 2H, 2 NH), 7.30-7.15 (m, 18H, 2 Ph and ar-MDI), 5.86 (s, 2H, 2 CH-d), 5.20 (m, 4H, 2 CH_2-f), and 3.96 (s, 2H, Ph-C$\underline{H}_2$-Ph from MDI). ^{13}C{^{1}H} NMR ($CDCl_3$/TFA, 75.5 MHz): δ (ppm) 164.79 (C=O ester), 149.60 (C=O urethane), 139.00, 135.00, 133.48, 130.25, 126.16, 126.00, 125.84, 116.95 (Ph and ar-MDI), 68.45 (CH-d), 66.32 (CH_2-f), and 38.00 (Ph-$\underline{C}H_2$-Ph from MDI). Anal. Calcd. for ($C_{33}H_{28}N_2O_8$): C, 68.27; H, 4.86; N, 4.83. Found: C, 68.38; H, 4.82; N, 4.79.

Unsubstituted polyurethanes PUR-(EG-HDI) and PUR-(EG-MDI). These two polyurethanes were prepared following the same procedure described above for tartrate-derived polyurethanes. In these cases purification was carried out by dissolving the polymer in $CHCl_3$/trifluoroacetic acid and reprecipitation into diethyl ether.

PUR-(EG-HDI). It was prepared from ethylene glycol (62 mg, 1 mmol) and HDI (164 µL, 1 mmol). After two hours of reaction the polymer precipitates. Yield 207 mg (90%). IR: ν (cm^{-1}) 3330 (N-H st), 1695 (C=O st), 1540 (N-H δ). ^{1}H NMR ($CDCl_3$/TFA, 300 MHz): δ (ppm) 6.52 (bs, 2H, 2 NH), 4.42 (s, 4H, 2 CH_2-d), 3.23 (m, 4H, 2 CH_2-a), 1.57 (m, 4H, 2 CH_2-b), and 1.37 (m, 4H, 2 CH_2-c). ^{13}C{^{1}H} NMR ($CDCl_3$/TFA, 75.5 MHz): δ (ppm) 158.77 (C=O), 64.20 (CH_2-d), 41.29 (CH_2-a), 28.94 (CH_2-b), and 25.86 (CH_2-c).

PUR-(EG-MDI). It was prepared from ethylene glycol (62 mg, 1 mmol) and MDI (250 mg, 1 mmol). Yield 274 mg (88%). IR: ν (cm^{-1}) 3314 (N-H st), 1708 (C=O st), 1600 (C_{ar}-C_{ar} st), 1534 (N-H δ). ^{1}H NMR ($CDCl_3$/TFA, 300 MHz): δ (ppm) 8.13 (bs, 2H, 2 NH), 7.20-7.15 (m, 8H, ar), 4.52 (s, 4H, 2 CH_2-d), and 3.92 (s, 2H, Ph-C$\underline{H}_2$-Ph from MDI). ^{13}C{^{1}H} NMR ($CDCl_3$/TFA, 75.5 MHz): δ (ppm) 156.08 (C=O), 138.33, 133.79, 129.53, 121.29 (ar), 63.90 (CH_2-d), and 40 39 (Ph-$\underline{C}H_2$-Ph from MDI).

6.2.3. Hydrogenolysis of PUR-(LTarBn-HDI)

In a stainless steel reactor provided with a 150 mL Teflon flask, a solution of 250 mg of PUR-(LTarBn-HDI) in 50 mL of chloroform/trifluoroacetic acid (1:1 v/v) containing Pd/C

(10%) in the amount of 0.1 mol-% of the benzyl groups was placed. The reactor was purged with nitrogen, filled with hydrogen to a pressure of 50 bars and stirred at room temperature for the scheduled time. Once the reaction was finished the catalyst was removed by filtration and the clean filtrate was evaporated to give the partially debenzylated polyurethanes. The products were dried under vacuum at 30 ºC for 24 h. Different degrees of debenzylation were attained according to the hydrogenation time; PUR-(LTar($Bn_{60}OH_{40}$)-HDI) was the hydrogenated PUR containing the maximum amount of free hydroxyl groups (40%).

PUR-(LTar($Bn_{60}OH_{40}$)-HDI): ^{1}H NMR (DMSO, 300 MHz): δ (ppm) 7.25 (bs, 6H instead of 10H, Ph), 6.90 (bs, 2H, 2 NH), 5.50 (s, 1H, CH-d from TarBn), 5.46-5.36 (dd, 0.4H, CH-d from TarBnOH), 5.32 (s, 0.6H, CH-d from TarOH), 5.12 (m, 2.4H instead of 4H, 2 CH_2-f), 2.88 (m, 4H, 2 CH_2-a), 1.28 (m, 4H, 2 CH_2-b), and 1.13 (m, 4H, 2 CH_2-c). The NMR spectra of PUR-(LTar($Bn_{80}OH_{20}$)-HDI) is very similar to those of PUR-(LTar($Bn_{60}OH_{40}$)-HDI) with differences concerning only peak intensities**.**

6.2.4. Hydrolytic degradation assays

Films of aliphatic polyurethanes with a thickness of ~200 µm, were prepared by casting at room temperature from a solution in tetrahydrofuran. A film of PUR-(EG-HDI) was prepared by hot-press molding at 20 ºC above the melting temperature of the polymer. The films were cut into 10-mm diameter, 20 to 30-mg weight disks, which were dried in vacuum at 30 °C to constant weight. For incubation, samples were immersed in vials containing 10 mL of sodium phosphate buffer (pH 7.4), sodium carbonate buffer (pH 10) or citric acid buffer (pH 2); parallel experiments were carried out at 37, 60 and 80 °C in each buffer. The sample vials were sealed to avoid partial evaporation of the fluids in the heated chamber. After incubation for the scheduled period of time, the samples were rinsed thoroughly with water and dried to constant weight. Sample weighing and viscosity of the residual polymer were used to follow the evolution of the hydrodegradation. NMR analysis of the products released to the incubation medium was performed directly from the NMR tubes used for sampling; spectra were registered at scheduled period of times without removing the residual polymer which stayed at the bottom of the tube.

6.3. Results and discussion

6.3.1. Polyurethane synthesis

Results obtained in the synthesis of polyurethanes studied in this work as well as some characterization data are given in Table 6.1. Several alkyl tartrates (Me, Et and ^{i}Pr) and benzyl tartrate were polymerized with HDI and MDI diisocyanates in DMF solution at 50 ºC for 24 h using dibutyltin dilaurate as catalyst. Under these conditions, the secondary hydroxyl groups of tartaric acid were able to react with the isocyanate groups to generate the polyurethane chain whereas the carboxylate groups remained unaffected. Such reaction conditions had been previously used by us with success for the preparation of different protected sugar-derived polyurethanes.[11-13] The reaction proceeded in one step and isolation and purification of the polymers were carried out by solution-precipitation cycles and subsequent drying under vacuum; yields were in the 75-90% range. Weight-average molecular weights of polyurethanes made from HDI were in the 40-70 kDa range whereas those made from MDI were in the 18-25 kDa range. Such differences could be the result of the steric effect exerted by the phenyl groups of MDI on the addition of the secondary hydroxyl to the N=C bond. On the other hand, polydispersity degrees oscillated between 2.1 and 2.5 for the whole series without perceivable differences between aliphatic and aromatic products. Intrinsic viscosity and molecular weight data for the whole set of PUR are compared in Table 6.1 showing a fully satisfactory correlation between the two series of data. Elemental analysis results were in full agreement with values calculated for the expected compositions. The chemical structures of polyurethanes were assessed by FTIR and NMR spectroscopy; these spectroscopic data are precisely detailed in the experimental section.

Characteristic IR absorption bands of main chain urethane and side chain carboxylate groups were observed at the predicted positions with the expected relative intensities. Some significant differences were detected between the spectra of aromatic and aliphatic products in addition to those arising directly from the presence of the MDI structure. Thus, the NH stretching band appearing at around 3370-3375 cm^{-1} in PUR made from HDI moved down to 3325-3335 cm^{-1} in their aromatic analogues. On the contrary, the complex C=O stretching band arising from both carboxylate and urethane groups appeared in aliphatic PUR about 10 cm^{-1} lower than in the aromatic compounds.

Table 6.1. Polycondensation results and some properties of polyurethanes.

PUR	Reaction[a]				Molecular size[c]			Solubility[f]						
	T (ºC)	*T* (h)	Yield (%)	$[\alpha]_D$[b] (º)	$[\eta]$ (dL·g^{-1})	M_w (g·mol^{-1})	PD	H_2O	DMSO	$CHCl_3$	THF	EtOH	AcOH	Acetone
LTarMe-HDI	50	24	85	-58	0.71	68,200	2.5	-	+	+	+	-	+	+
LTarEt-HDI	50	24	88	-47	0.68	60,400	2.1	-	+	+	+	-	+	+
DTarEt-HDI	50	24	81	+49	0.66	58,200	2.2	-	+	+	+	-	+	+
LTar^{i}Pr HDI	50	24	81	-40	0.74	70,200	2.3	-	+	-	+	-	+	+
LTarBn-HDI	50	24	78	-21	0.58	41,000	2.4	-	+	-	+	-	-	-
LTarMe-MDI	50	24	80	-66	0.55	25,300	2.3	-	+	-	+	-	-	+
LTarEt-MDI	50	24	88	-54	0.54	24,300	2.3	-	+	-	+	-	-	+
LTar^{i}Pr-MDI	50	24	75	-48	0.55	26,200	2.4	-	+	-	+	-	-	+/-
LTarBn-MDI	50	24	83	-26	0.38	18,700	2.1	-	+	-	+	-	-	+
EG-HDI	50	2[d]	90	--	0.43	28,800	2.1	-	+	-	-	-	-	-
EG-MDI	50	24	88	--	0.56	ns	ns	-	+	-	-	-	-	-
LTar($Bn_{80}OH_{20}$)-HDI[e]	30	24	90	--	0.55	38,600	2.2	-	+	-	+	-	-	-
LTar($Bn_{60}OH_{40}$)-HDI[e]	30	72	88	--	0.53	35,100	2.2	-	+	-	+	-	-	-

[a] Polycondensation carried out in DMF.
[b] Measured in DMSO at 20 ± 5 ºC, *c*= 1 g·dL^{-1}.

^{1}H and $^{13}C\{^{1}H\}$ NMR spectra were in all cases in full concordance with the expected chemical structures of PUR. In particular, no splitting of the CH-d signals arising from the tartrate unit was detected in any case, which allows excluding the occurrence of racemization reaction along the synthesis work.

As it is seen in Table 6.1, all the PUR containing tartrate units displayed fair optical rotations with positive and negative values for the D and L series, respectively. It is worthy to note that polyurethanes made from alditols (arabinitol and threitol) protected as methyl or benzyl ethers, are reported to rotate weakly the polarized light and they all showed low or very low specific optical activities. The results found here for PUR made from tartrates evidence the remarkable effect exerted by the carboxylate side group on the polymer backbone conformation compared to the methoxy or benzyloxy side groups.

The solubility of the tartrate-derived PUR are compared in Table 6.1 for a set of representative solvents evidencing that these compounds are more soluble than their unsubstituted analogues PUR-(EG-HDI) and PUR-(EG-MDI). All they are soluble in DMSO, THF and acetone and some of those made from HDI are even soluble in acetic acid and chloroform. The lower solubility of aromatic polyurethanes compared to aliphatic ones is a general feature of this family of polymers.[11-13]

As it is depicted in Scheme 6.3, hydrogenolysis of benzyl tartrate-derived polyurethanes allowed preparing polyurethanes bearing free carboxylic side groups. The evolution of the reaction could be followed by ^{1}H NMR; the spectra of initial PUR-(LTarBn-HDI) and the polymer resulting from its hydrogenation for 72 h are compared in Figure 6.1.

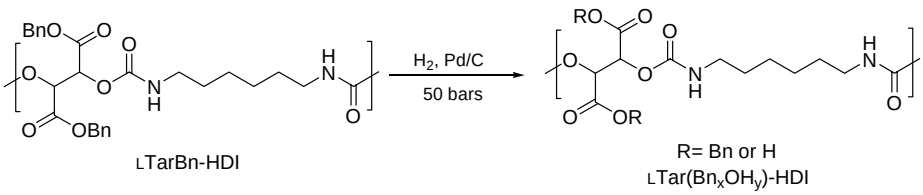

LTarBn-HDI

R= Bn or H

LTar(Bn_xOH_y)-HDI

Scheme 6.3. Hydrogenolysis of dibenzyl L-tartrate derived polyurethane.

The reduction in intensity observed for the peaks arising from the methylene and the aromatic protons of the benzyl group was used to estimate the degree of debenzylation; the maximum content of free carboxylic groups attainable by this method was 40%.

Other changes in the spectra include the splitting of the signals arising from the tartrate CH-d units due to the random occurrence of carboxyl and benzyloxycarbonyl groups on the same tartrate moiety. Apparently, the hydrogenation reaction took place without significant breaking of the main backbone; the slight decrease observed in the molecular weight (between 10 and 15%) can be accounted by the mass loss subsequent to the removal of the benzyl group. The solubility of PUR bearing free carboxyl groups does not differ significantly from that displayed by the fully esterified polymers they come from, and they continue being non-water soluble polymers.

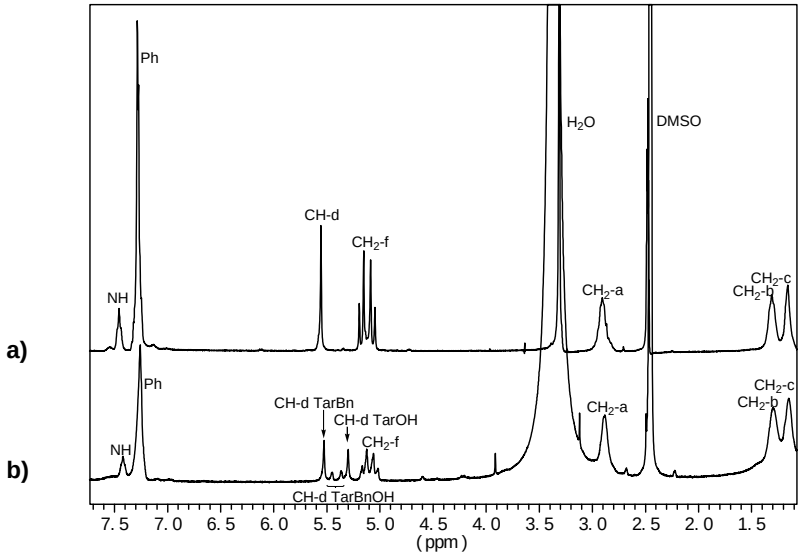

Figure 6.1. Compared ^{1}H NMR spectra of PUR: LTarBn-HDI **(a)**, and LTar($Bn_{60}OH_{40}$)-HDI **(b)**.

6.3.2. Structure and properties

The thermal stability of polyurethanes containing tartrate units was evaluated by thermogravimetry under inert atmosphere and compared to that of unsubstituted analogues. Their TGA traces are shown in Figure 6.2 and their main thermal decomposition parameters are given in Table 6.2. TGA results indicated that the thermal stability of PUR invariably increased when the tartrate unit was incorporated in the polymer chain; both the onset and the maximum rate decomposition temperatures increased significantly when compared to the unsubstituted PUR. On the contrary, those PUR bearing free carboxyl groups appeared to be much less stable than the

unsubstituted ones displaying onset temperatures around 70 ºC lower and also much lower maximum rate decomposition temperatures.

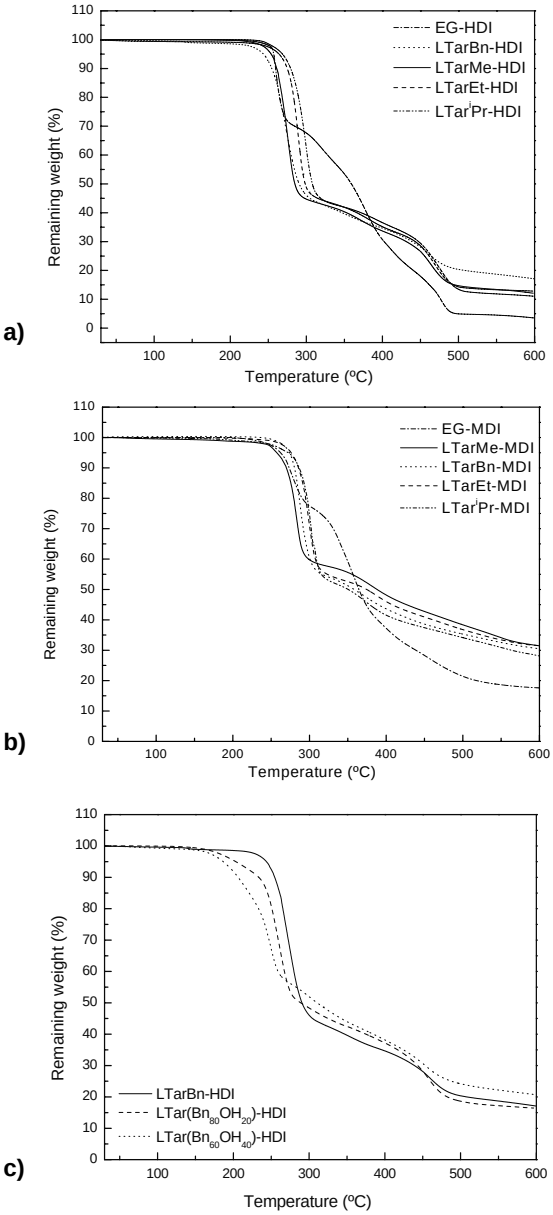

Figure 6.2. TGA traces of HDI **(a)**, MDI **(b)**, and hydrogenated **(c)** polyurethanes.

Table 6.2. Thermal properties of polyurethanes.

PUR	DSC[a]			TGA[b]		
	T_g (ºC)	T_m (ºC)	ΔH_m (J·g^{-1})	$^{o}T_d$ (ºC)	$^{max}T_d$ (ºC)	W (%)
LTarMe-HDI	55	119 / 128[c]	18 / 16[c]	256	**276**/369/463	12
LTarEt-HDI	62	117	26	270	**291**/381/469	13
DTarEt-HDI	61	118	26	269	**288**/376/467	13
LTar^{i}Pr-HDI	82	104	26	276	**299**/387/477	11
LTarBn-HDI	53	124,145 / 145[d]	38 / 30[d]	251	**273**/359/460	17
LTarMe-MDI	145	--	--	267	**284**/378/552	32
LTarEt-MDI	166	--	--	282	**293**/382/552	31
LTar^{i}Pr-MDI	185	249 / 249[e]	23 / 26[e]	283	**300**/372/551	28
LTarBn-MDI	130	--	--	273	**287**/368/550	30
EG-HDI	45	166,**178**	60	254	**259**/379/477	3
EG-MDI	126	250	57	261	**276**/357/466	18
LTar(Bn$_{80}$OH$_{20}$)-HDI	56	--	--	178	215/**260**/309/456	17
LTar(Bn$_{60}$OH$_{40}$)-HDI	61	--	--	176	207/**249**/300/458	21

[a] Glass transition temperature (T_g) of quenched samples. Melting temperature (T_m) and enthalpy (ΔH_m) measured by DSC in the first heating.
[b] Onset decomposition temperature ($^{o}T_d$), maximum rate decomposition temperatures ($^{max}T_d$) and remaining weight (W) measured by thermogravimetry.
[c] Melting temperature and enthalpy for a 12 h annealed sample at 110 ºC.
[d] Melting temperature and enthalpy for a 12 h annealed sample at 128 ºC.
[e] Melting temperature and enthalpy for a 1 h annealed sample at 210 ºC.

Regarding the residue left upon decomposition after heating, PUR containing tartrate units left much higher residual material than the unsubstituted ones. The beneficial effect that the presence of tartrate units exerts on the thermal stability of the polyurethane chain is remarkable; a similar effect was observed for the alditol units in PUR made from hydroxyl-protected alditols, the largest effect being noticed for the threitol derivatives.

The effect on thermal transitions, T_g and T_m arising from the insertion of the tartrate units in the PUR chain was investigated by DSC. The heating traces registered from PUR samples that were quenched from the melt to make clear the observation of the glass transition, are compared in Figure 6.3a, and T_g values measured on such traces are given in Table 6.2.

These results revealed that the presence of alkyl tartrate units in PUR invariably increased the T_g as compared to the unsubstituted analogue, the increment being more pronounced as the size of the alkyl side group increases. On the contrary, the PUR derived from benzyl tartrate showed the smallest increase in T_g in spite of the bulkiness of this group. The heating DSC traces recorded from PUR samples coming directly from synthesis are shown in Figure 6.3b, and T_m values measured on such traces are given in Table 6.2.

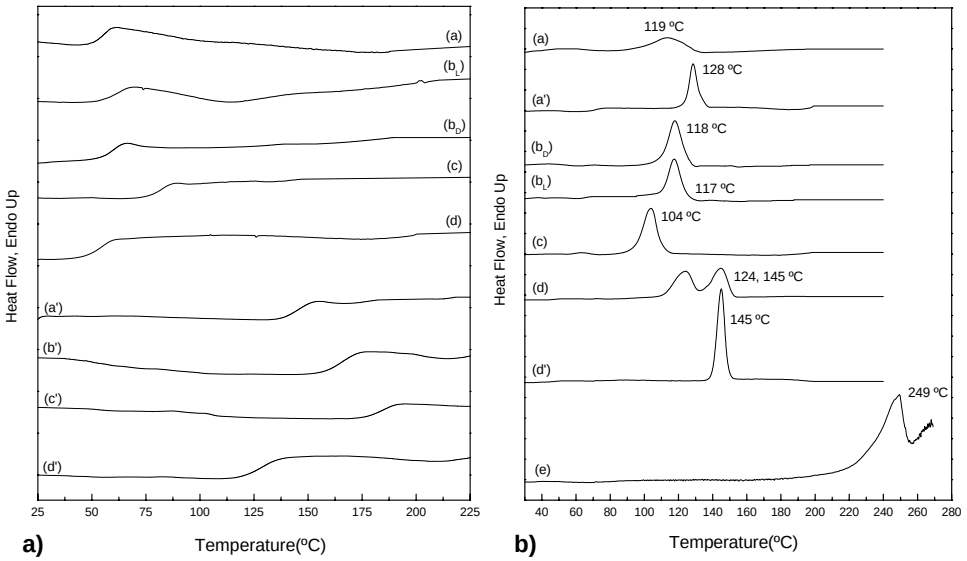

Figure 6.3. DSC of tartrate-derived PUR. **a)** Heating traces of samples quickly cooled from the melt of PUR-(TarR-HDI), R=LMe (a), R=LEt (b_L), R=DEt (b_D), R=L^{i}Pr (c), R=LBn (d); and PUR-(TarR-MDI), R=LMe (a'), R=LEt (b'), R=L^{i}Pr (c'), R=LBn (d'). **b)** Heating traces of crystallized samples of PUR-(TarR-HDI): R=LMe (a), R=LMe (annealed at 110 ºC for 12 h) (a'), R=DEt (b_D), R=LEt (b_L), R=L^{i}Pr (c), R=LBn (d), R=LBn (annealed at 128 ºC for 12 h) (d'); and polyurethane PUR-(LTar^{i}Pr-MDI) (e).

All tartrate-derived PUR made from HDI displayed endothermal peaks characteristic of crystalline material. In some cases, *i.e.* methyl and benzyl tartrates, broad or double melting peaks were observed, which were converted in sharp single peaks by annealing. The T_m of these PUR were limited in the 100-150 ºC interval with enthalpies ranging between 15 and 30 J·g^{-1}. Comparison of these values with those obtained for PUR-(EG-HDI) (T_m = 178 ºC, ΔH = 60 J·g^{-1}), reveals that the insertion of the tartrate units must hamper crystal formation and depress the crystallinity of PUR. On the other hand, all

PUR made from MDI except PUR-(L-Tar^{i}Pr-MDI), produced DSC traces characteristic of amorphous material without detectable heat exchange peaks. As much expected, partially debenzylated PUR appeared to be also amorphous whereas the parent PUR-(L-TarBn-HDI) displayed significant crystallinity.

As it is shown in Figure 6.4, the crystalline nature of PUR was vividly illustrated by polarizing optical microscopy. Films of aliphatic PUR prepared by casting from formic acid displayed well developed non-banded spherulites with sizes up to near 0.2 mm in diameter.

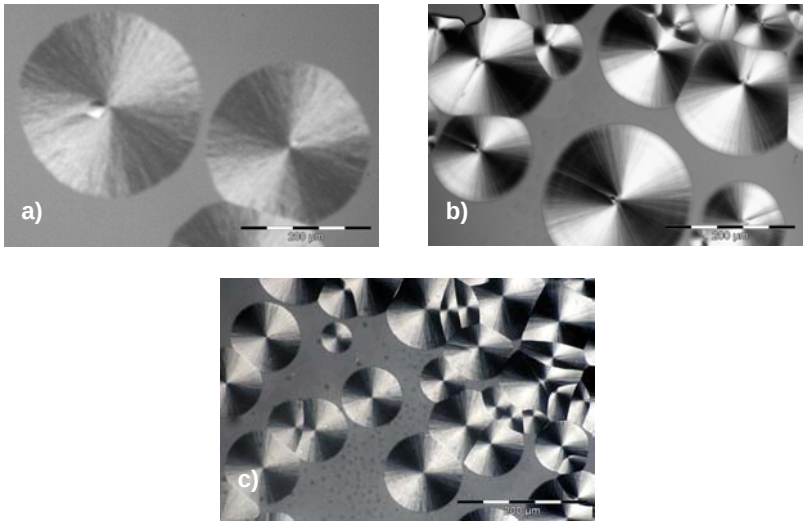

Figure 6.4. Polarized optical micrographs of films of PUR-(L-TarR-HDI) prepared by casting from formic acid at room temperature: **a)** R=Me, **b)** R=Et, and **c)** R=^{i}Pr. The scale bar corresponds to 200 μm.

The analysis by X-ray diffraction assessed the crystalline nature of PUR firstly revealed by DSC. The WAXS powder patterns recorded from aliphatic tartrate-derived PUR are shown in Figure 6.5, and Bragg spacings measured in these patterns are listed in Table 6.3 together with those measured for PUR-(L-Tar^{i}Pr-MDI) and the reference PUR-(EG-HDI) and (EG-MDI). Linear aliphatic *m,n*-polyurethanes (where *m* and *n* stand for the number of carbons contained in the diol and diisocyanate counterparts, respectively) usually crystallize with chains in extended or almost extended conformation arranged in hydrogen-bonded sheets.[16]

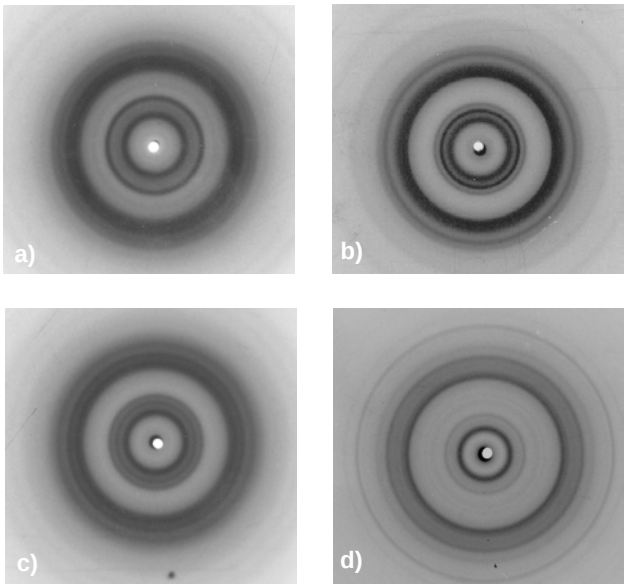

Figure 6.5. Powder X-ray diffraction patterns of PUR-(LTarR-HDI): R=Me (annealed at 110 ºC for 12 h) **(a)**, R=Et **(b)**, R=^{i}Pr **(c)**, and R=Bn (annealed at 128 ºC for 12 h) **(d)**.

The distance between neighbouring chains in the sheet is about 0.48 nm and the stacking distance of sheets is about 0.37 nm. Several crystal structures have been described differing in the model in which sheets are packed in the lattice. Bragg spacings characteristic of this family of PUR usually appear in the 0.40-0.45 nm and 0.36-0.39 nm ranges. In fact, PUR-(EG-HDI), named 2,6-PUR according to the conventional nomenclature, displays three strong reflections at 0.45, 0.42 and 0.39 nm and two crystal forms, one fully extended and the other with the urethane groups tilted approximately 30º with respect to the chain axis.[17]

The WAXS patterns of all aliphatic tartrate-derived PUR contain strong reflections in the 0.40-0.45 nm range, which could be taken as indicative of a crystal structure of the same type as that adopted by 2,6-PUR. However, a group of three strong reflections in the 1.0-0.7 nm range without parallelism in the unsubstituted PUR is invariably observed in such patterns. The presence of these reflections cannot be satisfactorily accounted by a crystal structure made of hydrogen-bonded sheets but rather it suggests a different one made of helical chains with hydrogen bonds intramolecularly set. In such structure, the strong ~1.15 nm reflection could be assigned to the *hk0* interplanar distance of the lattice

made of packed helices, the distance varying according to the size of the alkyl ester side group. This proposal is not absent at all of close precedents. Helical conformations for polyurethanes were described firstly by Green, although in that case the hydrogen bonding capability of the urethane group was blocked by attaching an alkyl group to the nitrogen atom.[18]

Table 6.3. Structural and mechanical data of polyurethanes.

PUR	X-ray diffraction[a]								Mechanical properties		
	d_{hkl}[a] (nm)								E (MPa)	σ_{max} (MPa)	ε_{break} (%)
LTarMe-HDI	1.15s/df		0.75s	0.59w	0.46s		0.42s	0.39w 0.37w	220	8	310
LTarEt-HDI	1.15s/df	0.88s	0.75m		0.45s	0.44s	0.41df	0.38s 0.35w	588	21	222
DTarEt-HDI	1.15s/df	0.88s	0.75m		0.45s	0.44s	0.41df	0.38s 0.36w	--	--	--
LTar^{i}Pr-HDI	1.17s/df	0.89m	0.77m		0.46s		0.42s	0.38df 0.35df	1167	33	167
LTarBn-HDI	1.44s/df	0.92m	0.70w	0.61w	0.48s	0.45w	0.42w	0.39m 0.35w	1311	54	34
LTarMe-MDI					--				430	16	91
LTarEt-MDI					--				819	60	56
LTar^{i}Pr-MDI	1.09s/df	0.88w	0.76w	0.51df	0.47df			0.40df 0.34df	1701	84	40
LTarBn-MDI					--				1836	95	22
EG-HDI	1.22w					0.45s	0.42s	0.39s 0.37m	1334	59	9
EG-MDI	1.53m		0.78m	0.51s	0.48s		0.43s	0.40df 0.35s	brittle		

[a] Visually estimated intensities denoted as: s, strong; m, medium; w, weak; df, diffuse. Data of annealed samples for LTarMe-HDI, LTarBn-HDI and LTar^{i}Pr-MDI.

The strong helicogenic effect of carboxylate groups is a well known fact in polypeptides where polyaspartates and polyglutamates distinguish by their great facility to adopt helical conformations following a diversity of intramolecular hydrogen-bonded arrangements.[19] On the other hand, optically active nylons bearing alkoxycarbonyl side

groups have been extensively described as helices of α-type that are side-by-side effectively packed generating well stable crystal structures.[20,21]

The mechanical parameters of PUR measured in tensile assays are compared in Table 6.3 and typical stress-strain traces are compared in Figure 6.6. Linear unsubstituted PUR made from EG used as references are crystalline powders that formed consistent films by either casting or hot-press molding; the aliphatic PUR-(EG-HDI) displays a typical stress-strain profile whereas the aromatic PUR-(EG-MDI), with a much higher T_g, is brittle and could not be tested.

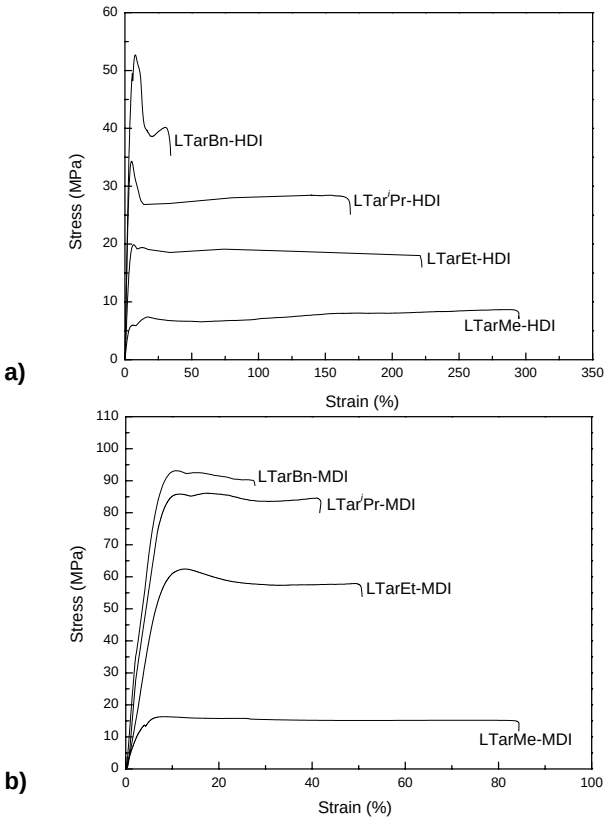

Figure 6.6. Stress-strain curves of tartrate-derived polyurethanes: made from HDI **(a)**, and MDI **(b)**.

Similarly, the physical behaviour displayed by the tartrate-derived PUR was found to depend largely on the constitution of the diisocyanate counterpart. Aliphatic PUR bearing alcoxycarbonyl side groups showed a flexible-soft behaviour with a rather low stress and could be stretched two or three folds their original lengths before breaking. Aromatic PUR displayed much lower elongations to break but higher elastic moduli and maximum stresses. The behaviour of the aliphatic PUR with benzyloxycarbonyl side groups, PUR-(LTarBn-HDI) was closer to the aromatic than to the aliphatic series. It seems therefore that T_g is the parameter that mainly determines the mechanical behaviour of these polyurethanes. It is also remarkable the influence exerted by the incorporation of the tartrate unit on the mechanical properties compared to unsubstituted PUR; in general the aliphatic tartrate-derived PUR displayed lower elastic module and larger elongation than their homologous unsubstituted polymer PUR-(EG-HDI). On the contrary, the presence of the carboxylate side group in aromatic PUR, confers flexibility to the polymer compared to PUR-(EG-MDI), presumably as a consequence of the amorphous nature of such polymers. In this case however the mechanical parameters could not be compared since measuring of PUR-(EG-MDI) was not feasible.

6.3.3. Hydrolytic degradability

The hydrolytic degradability of aliphatic tartrate-derived polyurethanes was evaluated in incubation assays and results were compared to those obtained for the unsubstituted PUR-(EG-HDI). The evolution of degradation was followed by both weighing and viscosimetry of the residual polymer. In some selected cases, the products released to the incubation medium upon degradation were analyzed by NMR. Weight loss and intrinsic viscosity data measured in the degradation of the fully esterified polymers upon incubation at 80 ºC and pH 2, 7.4 and 10 are shown in Figure 6.7, which indicate that all these PUR were significantly hydrolyzed at such temperature and that hydrolysis was faster as the pH increased.

Furthermore, at a given pH, the degradation rate was dependent on the size of the alkyl side group. On the contrary, the reference PUR-(EG-HDI) appeared to be fully resistant to degradation under the assayed conditions. These results evidenced that the attachment of the carboxylate groups to the ethylenic unit of unsubstituted 2,6-polyurethane enhanced significantly its propensity to hydrolysis.

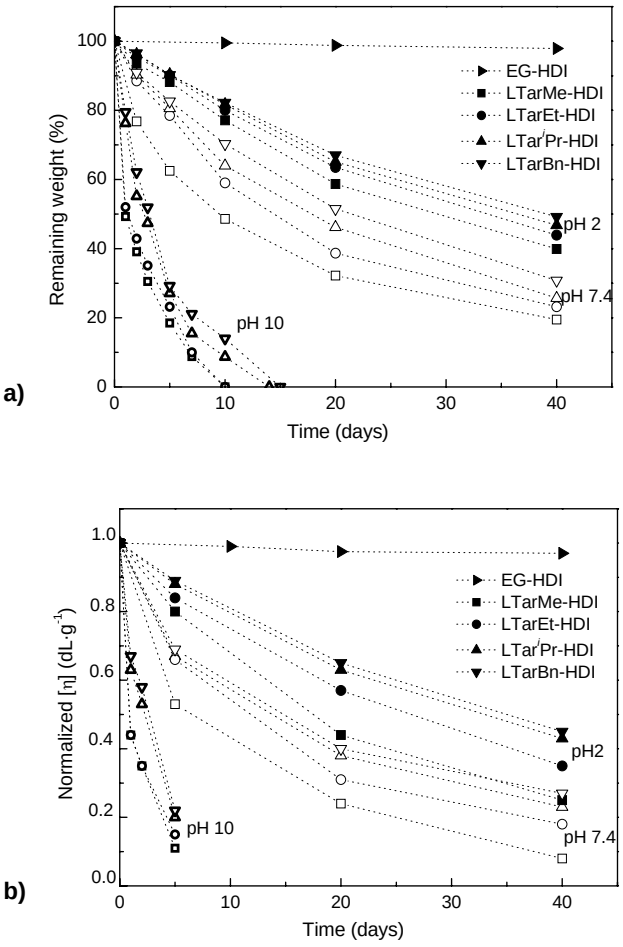

Figure 6.7. Changes in weight **(a)**, and intrinsic viscosity **(b)** of aliphatic polyurethanes at 80 ºC.

A further point deserving attention concerns the influence of temperature on degradability. The effect of temperature on the degradation rate of PUR-(LTarEt-HDI) is illustrated in Figure 6.8, where the decay in weight and viscosity of the residual sample are plotted against time of incubation at pH 10 and at 37, 60 and 80 ºC. As it could be largely anticipated, an increase in temperature favours the hydrolysis process and the polymer degrades faster. It is striking however that such effect is so noticeable, particularly at 80 ºC, where the full degradation of the polymer took place in ten days whereas it remained undegraded after 3 months of incubation at 37 ºC. Since the T_g of this polyurethane is 61 ºC, these results reveal clearly the decisive role played by such

transition in the hydrolysis process; since degradation takes place under heterogeneous conditions, the accessibility of the urethane group to water is critical and the process is indeed highly dependent on polymer chain mobility.

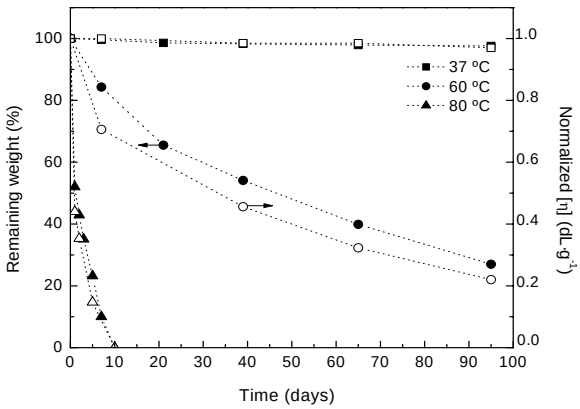

Figure 6.8. Changes in weight (solid symbols) and intrinsic viscosity (empty symbols) of PUR-(LTarEt-HDI) incubated in aqueous buffer at pH 10, at the indicated temperatures.

The comparative degradation study of the pair PUR-(LTarBn-HDI) and PUR-(LTar($Bn_{60}OH_{40}$)-HDI), provided useful information on how the degradability of tartrate-derived polyurethanes may be altered by the presence of free carboxylic groups. The plots representing weight loss and intrinsic viscosity against time for the degradation assays carried out at pH 7.4 and 10, and at a temperature of 37 ºC, are depicted in Figure 6.9. Such data reveal that carboxylic groups are extremely effective in enhancing the hydrodegradability of these polyurethanes; they become significantly degraded upon incubation under physiological conditions whereas the fully esterified polymer remains unaffected even at pH 10.

A preliminary approach to the understanding of the mechanism through which degradation of these tartrate-derived PUR takes place was made by the NMR analysis of the degradation products released to the aqueous medium in the degradation of PUR-(LTarEt-HDI) incubated at pH 7.4 and 80 ºC. The ^{1}H and $^{13}C\{^{1}H\}$ NMR spectra registered after 30 days of incubation are shown in Figure 6.10. After such period of time, the polymer had lost approximately 50% of its initial mass and its intrinsic viscosity decreased to about the half of its initial value. Such spectra may be interpreted as arising

from a mixture of ethanol, 1,6-hexamethylenediamine and tartaric acid, the amount of alcohol being four times the sum of the other two compounds.

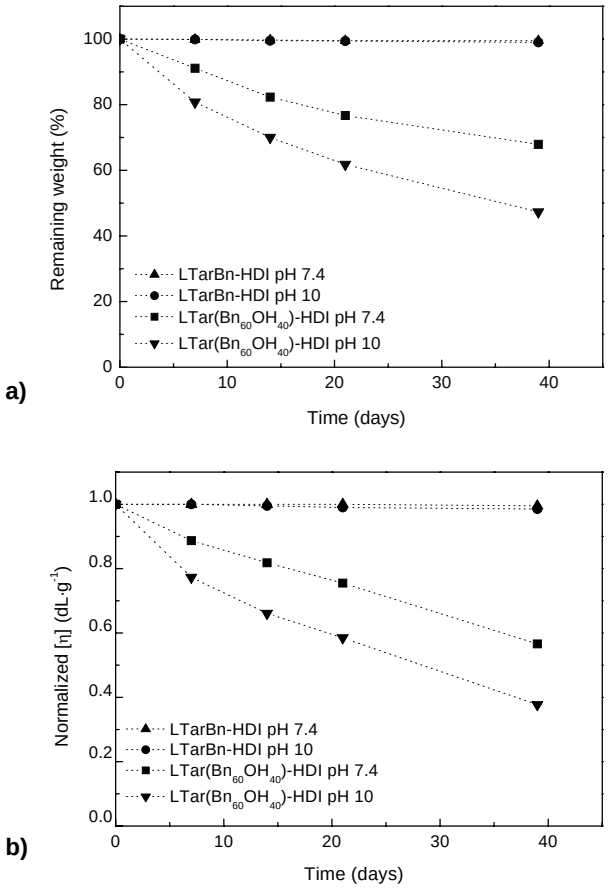

Figure 6.9. Changes in the residual weight **(a)** and intrinsic viscosity **(b)** of PUR-(LTarBn-HDI) and PUR(LTar($Bn_{60}OH_{40}$)-HDI) incubated at 37 ºC and different ps.

The spectra taken after shorter periods of incubation (not shown) contained mainly ethanol and small amounts of the other two compounds. Unfortunately, the residual polymer could not be analyzed in the same way due to its insolubility in the common solvents used for the spectroscopic analysis. Nevertheless, results are clear enough to conclude that degradation of PUR (LTarEt-HDI) proceeds by hydrolysis of the

carboxylate side group with release of ethanol and subsequent breaking of the polyurethane backbone.

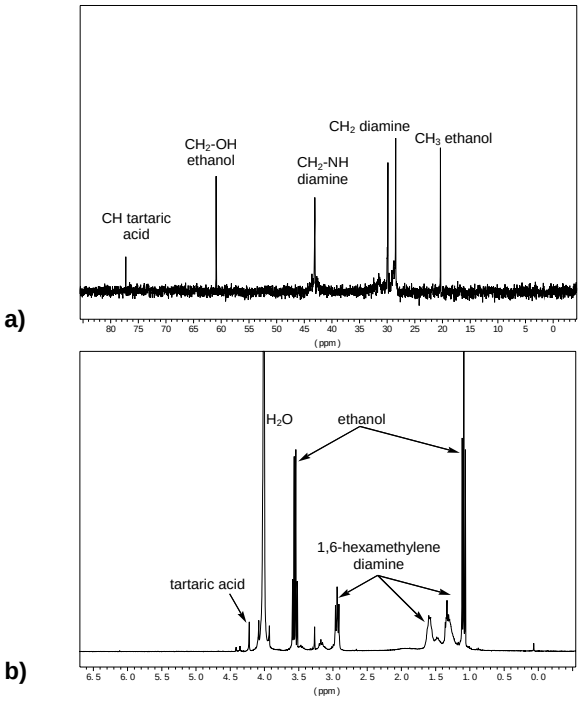

Figure 6.10. $^{13}C\{^{1}H\}$ NMR **(a)** and ^{1}H NMR **(b)** spectra registered from the mother solution of PUR-(LTarEt-HDI) after 30 days of incubation at pH 7.4.

It should be remarked that PUR containing threitol units were reluctant to hydrolysis when treated under similar conditions. In fact, the 4,6-polyurethane made from HDI and 2,3-di-*O*-methyl-L-threitol remained essentially unaltered after incubation at 80 ºC and pH 10 for six weeks. On the contrary, the polyurethane made from 2,3,4-tri-*O*-methyl-xylitol, and HDI bearing the three secondary hydroxyl groups protected as methyl ether, displayed a degradability in water comparable to that observed in this work for the tartrate-derived polyurethane. The whole collected information indicates that the sensitivity of carbohydrate-derived polyurethanes to water depends not only on the size of the sugar unit but also on the nature of the side groups attached to it; the carboxylate groups, and more specifically the free carboxylic groups appear much more effective than the alkoxy groups in enhancing the hydrodegradability of the polyurethane chain.

6.4. Conclusions

Optically active alkyl (Me, Et and ^{i}Pr) and benzyl tartrates have been successfully used for the synthesis of polyurethanes. These compounds derive from naturally-occurring tartaric acid and all they are commercially accessible. The polymerization reaction with both aliphatic and aromatic diisocyanates was conducted under mild conditions so that the carboxylate groups of tartrates did not participate in the reaction. Thus, linear polyurethanes bearing two carboxylate groups attached to the repeating unit could be obtained. All the novel PUR were thermally stable and optically active; the aliphatic polymers were semicrystalline polymers with melting temperatures between 100 and 150 ºC and T_g comprised in the 50-80 ºC interval, whereas the aromatic ones were amorphous materials with T_g above 130 ºC. PUR made from 1,6-hexamethylene diisocyanate and benzyl tartrate was hydrogenated to yield PUR containing up to 40% of free carboxylic groups.

The tartrate derived PUR displayed enhanced sensitivity to hydrolysis compared to 2,6-PUR without substituents. The PUR bearing free carboxylic groups were unique in being degraded by water upon incubation under physiological conditions. We have reported previously on linear polyurethanes bearing free hydroxyl side groups, which were prepared from threitol, the aldotetritol deriving from tartaric acid. These exploratory works on the potential of tartaric acid for the synthesis of linear polyurethanes reveal that this aldaric acid is a suitable feedstock for the preparation of stereoregular polyurethanes functionalized with either hydroxyl or carboxylic groups.

6.5. References

1. Hasirci, N.; Aksoy, E.A. *High Perform Polym* **2007**, 19, 621.

2. Hsu, S.H.; Tseng, H.J. *J Biomater Appl* **2004**, 19, 135.

3. Wang, W.; Guo, Y.; Otaigbe, J.U. *Polymer* **2008**, 49, 4393.

4. Jiang, X.; Li, J.; Ding, M.; Tan, H.; Ling, Q.; Zhong, Y.; Fu, Q. *Eur Polym J* **2007**, 43, 1838.

5. Petrovic, Z.S. *Polym Rev* **2008**, 48, 109.

6. a) Lligadas, G.; Ronda, J.C.; Galia, M.; Cádiz, V. *Biomacromolecules* **2007**, 8, 686. b) Lligadas, G.; Ronda, J.C.; Galia, M.; Cadiz, V. *Biomacromolecules* **2006**, 7, 2420. c) Lligadas, G.; Ronda, J.C.; Galia, M.; Cadiz, V. *Biomacromolecules* **2007**,

8, 686. d) Lligadas, G.; Ronda, J.C.; Galia, M.; Cadiz, V. *Biomacromolecules* **2007**, 8, 1858. e) Lligadas, G.; Ronda, J.C.; Galia, M.; Cadiz, V. *J Polym Sci Part A: Polym Chem* **2006**, 44, 6717.

7. Hatakeyama, T.; Izuta, Y.; Hirose, S.; Hatakeyama, H. *Polymer* **2002**, 43, 1177.

8. Varela, O.; Orgueira, H.A. *Adv Carbohydr Chem Biochem* **1999**, 55, 135.

9. Kiely, D.E.; Chen, L.; Lin, T.-H. *J Am Chem Soc* **1994**, 116, 571.

10. Kiely, D.E.; Chen, L.; Lin, T.-H. *J Polym Sc Part A: Polym Chem* **2000**, 38, 594.

11. De Paz, M.V.; Marín, R.; Zamora, F.; Hakkou, K.; Alla, A.; Galbis, J.A.; Muñoz-Guerra, S. *J Polym Sci Part A: Polym Chem* **2007**, 45, 4109.

12. Marín, R.; De Paz, M.V.; Ittobanne, N.; Galbis, J.A.; Muñoz-Guerra, S. M*acromol Chem Phys* (accepted **2009**).

13. Marín, R.; Muñoz-Guerra, S. *J Polym Sc Part A: Polym Chem* **2008**, 46, 7996.

14. Kuramoto, N.; Sakamoto, M.; Teshirogi, T.; Komiyama, J.; Iijima, T. *J Appl Polymer Sci* **1984**, 29, 977.

15. Chen, C.-F.; Su, Q.; Chen, Y.-M.; Xi, F. *Chinese J Polym Sci* **1999**, 17, 371.

16. Borchert, W.Z. *Angew Chem* **1951**, 63, 31.

17. Saito, Y.; Nansai, S.; Kinoshita, S. *Polym J (Tokyo)* **1972**, 3, 113.

18. Lifson, S.; Green, M.M.; Andreola, C.; Peterson, N.C. *J Am Chem Soc* **1989**, 111, 8850.

19. Walton, A.G. *Polypeptides and Protein Structure*, Elsevier Publishers, New York **1981**.

20. Fernández Santín, J.M.; Aymamí, J.; Rodríguez-Galán, A.; Muñoz-Guerra, S.; Subirana, J.A. *Nature* **1984**, 311, 53.

21. Melis, J.; Zanuy, D.; Alemán, C.; García-Alvárez, M.; Muñoz-Guerra, S. *Macromolecules* **2002**, 35, 8774.

CHAPTER 7

CARBOHYDRATE-BASED POLYURETHANES: A COMPARATIVE STUDY OF POLYMERS MADE FROM ISOSORBIDE AND 1,4-BUTANEDIOL*

Purpose and specific aims: *The main purpose of this work was to make an explorative comparative study of linear polyurethanes containing isosorbide with their analogues made from 1,4-butanediol. The results of this exploration will be useful to understand the effect of the substitution of 1,4-butanediol for isosorbide as chain extender in segmented polyurethanes.*

Summary: *A set of polyurethanes containing isosorbide units were synthesized by polymerization in solution from HDI and MDI diisocyanates and 1,4-butanediol (BD), isosorbide (Is) or diisosorbide diurethanes (Is_2HDI and Is_2MDI) as diols. The thermal properties and stability, and crystal structure of the polyurethane homopolymers and copolymers containing isosorbide were evaluated and compared with those of the polyurethanes analogues entirely made of BD. Incorporation of isosorbide produced significant changes in T_g, T_m and T_d but no noteworthy differences were found between copolymers made from Is or Is_2 monomers. Degradation assays revealed that incorporation of Is units increased slightly the hydrolysis rate.*

* Publication derived from this work: Marín, R.; Alla, A.; Martínez de Ilarduya, A.; Muñoz-Guerra, S. e-*Polymer* (submitted **2009**).

7.1. Introduction

A growing interest is currently devoted to chemicals deriving from renewable resources as an alternative to oil-based monomers for the production of well-established industrial polymers. Specifically, utilization of carbohydrate derivatives for polymer synthesis has attracted much attention not only because of the huge abundance of these resources but also because of the promising degradability and biocompatibility of the polymers that can be produced from them.[1,2] Carbohydrates stand out as very highly convenient raw materials because they are inexpensive, readily available, and provide great functional diversity.[3,4] In recent years, several notable examples of carbohydrate-based polymers have been reported in the literature.[5-7]

One of the most promising carbohydrate derivatives for the synthesis of polymeric materials is the cyclic diol 1,4:3,6-dianhydro-D-glucitol, also known as isosorbide. This carbohydrate-based diol is a suitable monomer for the synthesis of a variety of polycondensates such as polyesters, polyamides and polycarbonates.[8] The reactivity of isosorbide as monomer is somewhat limited by the secondary nature of their hydroxyl groups. Furthermore, the two hydroxyl groups have different spatial position relative to the puckered bicycle and they display therefore different reactivity.[9,10] The influence of isosorbide on physical properties of polymers is well-known: *i.e*. T_g increases and crystallinity decreases with the content in Is units.[10-12] On the other side, it has been proved that polyesters, poly(esteramide)s, poly(estercarbonate)s, and polycarbonates derived from isosorbide are more or less biodegradable depending on the structures, as judged from degradation tests carried out in activated sludge, in soil, and in the presence of hydrolytic enzymes.[13]

Some polyurethanes containing isosorbide were described in the nineties[14,15] but the knowledge on these carbohydrate-based polyurethanes is very limited. The main purpose of this work was to make an explorative comparative study of polyurethanes containing isosorbide (Is) with their analogues made from 1,4-butanediol (BD). 1,6-Hexamethylene diisocyanate (HDI) and 4,4'-methylenebis(phenyl isocyanate) (MDI) are the diisocyanates chosen for their synthesis. Incorporation of the Is units was accomplished by using either isosorbide directly or a diol-diurethane compound made from diisocyanate and isosorbide. The chemical structure of the PUR homopolymers and copolymers studied in this work are depicted in Scheme 7.1. Thermal properties

including stability to heating and some data of the crystalline structure are compared. The influence of the presence of the isosorbide units on the susceptibility to hydrolysis of the polyurethane chain was also assessed.

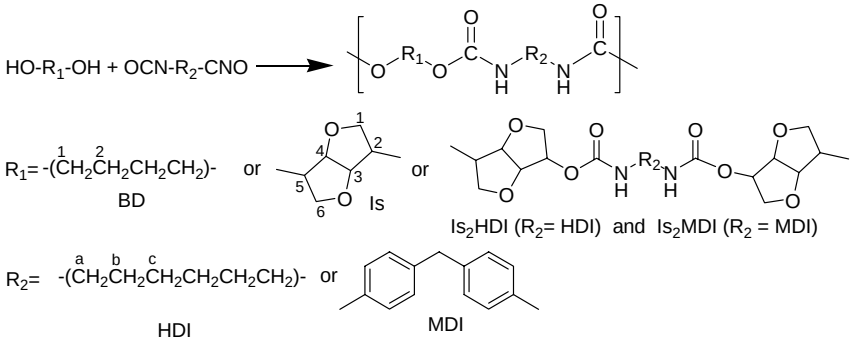

Scheme 7.1. Chemical structures of polyurethanes studied in this work.

7.2. Experimental section

7.2.1. Materials and methods

Isosorbide was a gift from Roquette Freres S.A. This cyclic dianhydride is prepared from corn starch following a well-established procedure of the proprietary company. Common reagents and solvents, and 1,4-butanediol (BD) were purchased from Aldrich and used as received. N,N-Dimethylformamide (DMF) and tetrahydrofuran (THF) solvents were dried prior to use by distillation under inert atmosphere. Diols and reagents for polymerization were stored in a desiccator under vacuum until used. Hexamethylene diisocyanate (HDI) was vacuum distilled prior to use, and 4,4'-methylenebis(phenyl isocyanate) (MDI) stored at 4 ºC. Both compounds were handled under inert atmosphere.

Gel permeation chromatograms (GPC) were acquired at 35 ºC with a Waters equipment provided with a refraction-index detector. The samples were chromatographed with 0.05 M sodium trifluoroacetate-hexafluoroisopropanol (NaTFA-HFIP) at a flow rate of 0.5 $mL \cdot min^{-1}$ using a polystyrene-divinylbenzene packed linear column. Chromatograms were calibrated against poly(methyl methacrylate) (PMMA) monodisperse standards. ^{1}H and $^{13}C\{^{1}H\}$ NMR spectra were recorded on a Bruker AMX-300 spectrometer operating

at 300.1 and 75.5 MHz for ^{1}H and $^{13}C\{^{1}H\}$, respectively, in deuterated DMSO and using TMS as internal reference. Sample concentrations of about 1-5% (w/v) were used for these analyses, and spectra were recorded either at 298.1 and 343.1 K. The spectra were acquired with 64 scans and 1000-10,000 scans for ^{1}H and $^{13}C\{^{1}H\}$, respectively, and relaxation delays of 1 and 2 s. Differential scanning calorimetric (DSC) experiments were performed at heating/cooling rates of 10 ºC·min^{-1} on a Perkin-Elmer Pyris 1 instrument calibrated with indium. All the experiments were carried with samples of 3-4 mg within a range of temperatures from 0 ºC to 200 or 250 ºC, and under a nitrogen flow of 20 mL·min^{-1} to minimize possible oxidative degradations. Thermogravimetric analysis (TGA) was carried out under inert atmosphere at a heating rate of 10 °C·min^{-1} and within a temperature range of 30 to 600 ºC using a Mettler TA4000 thermobalance. Sample weights of about 15 mg were used in these experiments. Wide angle X-ray scattering were performed on a Philips automatic horizontal axis diffractometer using Cu Kα-Ni filtered radiation. Spectra were taken at room temperature with the scattering angle 2θ varying from 3 to 50º. In addition, wide-angle X-ray scattering (WAXS) experiments using synchrotron radiation were performed at the A2 beamline of the HASYLAB synchrotron facility (DESY, Hamburg). The experiments were performed with monochromatic X-rays of 0.154 nm wavelength. The scattering was detected with linear detectors and calibrated with semicrystalline PET standard.

7.2.2. Synthesis of monomers and polymers

Urethane-diols Is$_2$HDI and Is$_2$MDI. To a solution of 4 mmol of isosorbide in 10 mL of dry tetrahydrofuran, 1 mmol of either HDI or MDI was added dropwise. Dibutyltin dilaurate (2% w/w) catalyst was added and the mixture stirred for 3 h at room temperature under inert atmosphere and then concentrated to oil from which a white solid precipitated. The two diols were dried under vacuum and stored in a desiccator until needed. Is$_2$HDI: Yield 85%. Is$_2$MDI: Yield 83%.

Is$_2$HDI: ^{1}H NMR (DMSO, 300 MHz at 298.1 K): δ (ppm) 7.23, 7.18, (2 m, N-H), 5.08, 4.20 (2 m, 1H, H-5(Is)), 5.00, 4.15 (2 m, H-2(Is)), 4.82, 4.55 (2 m, H-4(Is)), 4.55, 4.30 (2 m, H-3(Is)), 3.91–3.30 (m, H-1(Is), H-6(Is)), 2.88 (m, H-a), 1.31 (m, H-b), and 1.18 (m, H-c). $^{13}C\{^{1}H\}$ NMR (DMSO, 75.5 MHz at 298.1 K): δ (ppm) 155.54, 155.22, (C=O), 87.97, 85.31 (C-3(Is)), 81.59, 80.27 (C-4(Is)), 78.11, 75.15 (C-2(Is)), 73.66, 72.00 (C-5(Is)), 72.87, 75.26 (C-1(Is)), 71.31, 69.30 (C-6(Is)), 40.17 (C-a), 29.26 (C-b), and 25.89 (C-c).

Is_2MDI: ^{1}H NMR (DMSO, 300 MHz at 343.1 K): δ (ppm) 9.44, 9.39, (2 bs, N-H), 7.31-7.00 (2 d, ar), 5.02, 4.10 (m, 1H, H-5(Is)), 5.00, 4.02 (m, H-2(Is)), 4.66, 4.38 (t, H-4(Is)), 4.45, 4.25 (s, d, H-3(Is)), 3.91–3.30 (m, H-1(Is), H-6(Is)). ^{13}C{^{1}H} NMR (DMSO, 75.5 MHz at 343.1 ºK): δ (ppm) 152.57, 152.33, (C=O), 136.66, 135.22, 128.42, 118.34 (a), 87.96, 85.04 (C-3(Is)), 81.37, 79.93 (C-4(Is)), 78.35, 74.93 (C-2(Is)), 73.83, 71.62 (C-5(Is)), 72.42, 74.97 (C-1(Is)), 71.36, 69.04 (C-6(Is)).

Synthesis of polymers. The selected diol or combination of diols (1 mmol) (1,4-butanediol, isosorbide, Is_2HDI or Is_2MDI) and N,N-dimethylformamide (4 mL) were placed in a round bottom flask saturated with inert gas. The mixture was stirred at room temperature up to homogenization and then 1 mmol of diisocyanate, HDI or MDI, followed by dibutyltin dilaurate (20 ppm) catalyst were added, and the mixture maintained under stirring for 24 h. The reaction mixture was then added dropwise into cold diethyl ether (25 mL) to precipitate the polymer. Purification of the polyurethane was carried out by redissolution in the minimum volume of chloroform or chloroform/trifluoroacetic acid and reprecipitation into diethyl ether.

PUR-(BD-HDI): ^{1}H NMR (DMSO, 300 MHz at 298.1 K): δ (ppm) 6.56 (bs, 2H, N-H), 3.91 (m, 4H, H-1), 2.93 (m, 4H, H-a), 1.54 (m, 4H, H-2), 1.36 (m, 4H, H-b), and 1.21 (m, 4H, H-c). ^{13}C{^{1}H} NMR (DMSO, 75.5 MHz at 298.1 ºK): δ (ppm) 161.47 (C=O), 68.40 (C-1), 45.59 (C-a), 34.59 (C-b), 31.14 (C-c), and 30.72 (C-2).

PUR-(Is-HDI): ^{1}H NMR (DMSO, 300 MHz, at 298.1 K): δ (ppm) 7.25, 7.20 (2 t N-H), 4.90 (m, 1H, H-5), 4.85 (m, 1H, H-2), 4.60 (t, 1H, H-4), 4.30 (d, 1H, H-3), 3.85-3.45 (m, 4H, H-1, H-6), 2.94 (m, 4H, H-a), 1.36 (m, 4H, H-b), and 1.22 (m, 4H, H-c). ^{13}C{^{1}H} NMR (DMSO, 75.5 MHz at 298.1 ºK): δ (ppm) 155.15 (C=O), 85.57 (C-3), 80.71 (C-4), 77.44 (C-2), 73.93 (C-5), 73.26 (C-1), 69.92 (C-6), 40.59 (C-a), 29.21 (C-b), and 25.81 (C-c).

PUR-(BDIs-HDI) and *PUR-(BDIs_2-HDI):* ^{1}H NMR (DMSO, 300 MHz at 343.1 K): δ (ppm) 6.95, 6.68 (2 bs , 2H, N-H), 4.92 (m, 1H, H-5(Is)), 4.89 (m, 1H, H-2(Is)), 4.61 (t, 1H, H-4(Is)), 4.34 (d, 1H, H-3(Is)), 3.90 (m, 4H, H-1(BD)), 3.86-3.20 (m, 4H, H-1(Is) and H-6(Is)), 2.91 (m, 4H, H-a), 1.53 (m, 4H, H-2(BD)), 1.34 (m, 4H, H-b), and 1.22 (m, 4H, H-c). ^{13}C{^{1}H} NMR (DMSO, 75.5 MHz at 343.1 ºK): δ (ppm) 155.85, 155.04, 154.82 (C=O) , 85.40 (C-3(Is)), 80.31 (C-4(Is)), 77.40 (C-2(Is)), 73.06 (C-5(Is)), 72.54 (C-1(Is)), 69.56 (C-6(Is)), 62.86 (C 1(BD)), 39.96 (C-a), 29.03 (C-b), 25.60 (C-c), and 25.11 (C 2(BD)).

PUR-(BD-MDI): ^{1}H NMR (DMSO, 300 MHz at 298.1 K): δ (ppm) 9.45 (bs, 2H, N-H), 7.31-7.02 (2d, 8H, ar), 4.05 (m, 4H, H-1), 3.72 (bs, 2H, Ph- CH_2-Ph from MDI), and 1.65 (m, 4H, H-2). ^{13}C{^{1}H} NMR (DMSO, 75.5 MHz at 298.1 ºK): δ (ppm) 153.6 (C=O), 137.1, 135.47, 128.84, 118.39 (ar), 63.70 (C-1), 39.79 (Ph-CH_2-Ph from MDI), and 25.26 (C-2).

PUR-(Is-MDI): ^{1}H NMR (DMSO, 300 MHz at 298.1 K): δ (ppm) 9.76 (2 s, 2H, N-H), 7.38-7.11 (2d, 8H, ar), 5.10 (m, 1H, H-5), 5.04 (m, 1H, H-2), 4.76 (m, 1H, H-4), 4.45 (m, 1H, H-3), and 3.91–3.73 (m, 4 H, H-1, H-6), 3.74 (bs, 2H, Ph-CH_2-Ph from MDI). ^{13}C{^{1}H} NMR (DMSO, 75.5 MHz at 298.1 ºK): δ (ppm) 152.68, 152.45 (C=O), 136.93, 135.55, 128.83, 118.25 (ar), 85.65 (C-3), 80.90 (C-4), 77.66 (C-2), 73.40 (C-5), 72.65 (C-1), 70.20 (C-6), and 39.5 (Ph-CH_2-Ph from MDI).

PUR-(BDIs-MDI) and *PUR-(BDIs$_2$-MDI):* ^{1}H NMR (DMSO, 300 MHz at 343.1 K): δ (ppm) 9.48, 9.45, 9.43 (3 bs, 2H, N-H), 7.31-7.00 (2 d, 8H, ar), 5.10 (m, 1H, H-5(Is)), 5.0 (m, 1H, H-2(Is)), 4.76 (t, 1H, H-4(Is)), 4.48 (d, 1H, H-3(Is)), 4.07 (m, 4H, H-1(BD)), and 3.91–3.50 (m, 6 H, H-1(Is), H-6(Is)), 3.74 (bs, 2H, Ph- CH_2-Ph from MDI), and 1.64 (m, 4H, H-2(BD)). ^{13}C{^{1}H} NMR (DMSO, 75.5 MHz at 343.1 ºK): δ (ppm) 153.3, 152.60, 152.53 (C=O), 137.38, 135.13, 128.40, 118.35 (ar), 85.44 (C-3(Is)), 80.49 (C-4(Is)) , 78.35 (C-2(Is)), 75.50 (C-5(Is)), 72.42 (C-1(Is)), 69.75 (C-6(Is)), 63.39 (C 1(BD)), 39.54 (Ph- CH_2-Ph from MDI), and 25.00 (C 2(BD)).

7.2.3. Hydrolytic degradation assays

For hydrolytic degradation studies, films of selected polyurethanes with a thickness of ~300 µm were prepared by hot-press molding. The films were cut into 10-mm diameter, 20 to 30-mg weight disks, which were dried in vacuum at 30 °C to constant weight. The degradation study was performed by placing the discs into vials and 10 mL of buffered solutions were added at the selected pH. Parallel experiments were carried out with samples immersed in sodium phosphate buffer (pH 7.4), sodium carbonate buffer (pH 10) and citric acid buffer (pH 2) at temperatures of 37 and 60 °C. Vials were sealed to avoid partial evaporation of the fluids in the heated chamber. After immersion for the fixed period of time, the samples were rinsed thoroughly with water and dried to constant weight. Sample weighing and GPC measurements were used to follow the evolution of the hydrodegradation.

7.3. Results and discussion

7.3.1. Polyurethane synthesis

Polyurethanes were prepared by polymerization reaction in DMF solution at room temperature with dibutyltin dilaurate as catalyst and using HDI and MDI as diisocyanates. 1,4-Butanediol, isosorbide, and compounds Is_2HDI or Is_2MDI were the diols of choice for this study. The use of these diol-urethane compounds as monomers ensured the incorporation of the Is units as dyads in the forming PUR chain and contributed to minimize decomposition of isosorbide during polymerization. Results from polymerizations and copolymerizations are compared in Table 7.1; copolymers were made from a 1,4-butanediol to isosorbide or urethane-diol molar ratios of 4:1 or 8:1 respectively, so that the BD to Is units ratio in the resulting copolymers were expected to be 4:1 in both cases.

Polymerization yields were of 85-90% and the resulting Is-containing PUR displayed molecular weights significantly lower than the reference polyurethanes BD-HDI and BD-MDI, according to what should be expected from the lower reactivity of secondary hydroxyl groups of Is compared to primary ones of BD. The chemical structure of PUR was ascertained by ^{1}H and ^{13}C{^{1}H} NMR spectroscopy, all peak data and assignments being listed in the Experimental section. The ^{1}H NMR spectra showed that copolyurethanes were enriched in BD units and all them show predominance of isosorbide end groups, most of them with the unreacted hydroxyl in *exo* position. This result can be explained again by the lower reactivity of secondary hydroxyl groups of isosorbide, and more specifically by the hydroxyl in *exo* position. This result is in agreement with the work of Lemieux *et al.* on tosilation of isosorbide[9] but contrary to the relative reactivity of the two isosorbide hydroxyl groups observed in the reaction with carboxylic diacids to give polyesters.[10]

The low solubility characteristic of PUR is not only essentially maintained but even slightly more restricted in the Is-containing PUR; specifically, the partial solubility in $CHCl_3$ and THF displayed by PUR-(BD-HDI) and PUR-(BD-MDI) disappears upon insertion of Is units.

Table 7.1. Polymerization results and some properties of polyurethanes.

PUR	Reaction			Molecular size[b]			Solubility[c]					
	%[a]	%[a]	Yield (%)	$[\eta]$ ($dL \cdot g^{-1}$)	M_w ($g \cdot mol^{-1}$)	M_w/M_n	H_2O	DMSO	$CHCl_3$	THF	EtOH	AcOH
BD-HDI[d]	-	-	88	0.63	30,000	2.2	-	+	+/-	+/-	-	-
Is-HDI	-	-	85	0.32	18,000	2.0	-	+	-	-	-	-
BDIs-HDI	20	18.5	85	0.29	17,200	1.8	-	+	-	-	-	-
$BDIs_2$-HDI	20	12.2	86	0.30	17,600	1.9	-	+	-	-	-	-
BD-MDI	-	-	90	0.60	28,600	2.2	-	+	-	+/-	-	-
Is-MDI	-	-.	86	0.38	18,500	2.1	-	+	-	-	-	-
BDIs-MDI	20	8.9	84	0.33	19,900	2.0	-	+	-	-	-	-
$BDIs_2$-MDI	20	15.9	85	0.35	21,000	2.1	-	+	-	-	-	-

[a] Molar percentage of Is or Is_2HDI/Is_2MDI in the total of diols in the feed and in the resulting polymer.
[b] Intrinsic viscosity measured in DCA and average molecular weights determined by GPC.
[c] Solubility at 20 ± 5 ºC at a sample concentration of 1 $g \cdot L^{-1}$: + soluble; +/- partially soluble; - insoluble.
[d] Precipitated from solution after 2 hours of reaction.

7.3.2. Thermal properties and crystalline structure

The effect of Is units on the thermal properties of PUR was assessed by DSC and data collected from this study are compared in Table 7.2. Firstly T_g were measured at heating from samples rapidly quenched at -70 ºC from the melt. As it could be anticipated, the insertion of the rigid isosorbide ring hampered the molecular mobility of the polymer chain with the subsequent increase in T_g. In fact T_g values of PUR increased with the content in Is, the highest values being displayed by PUR entirely made of isosorbide. The same trend was observed for both aliphatic and aromatic series and, as it should be expected, much higher T_g were observed for the latter (93-183 ºC) than for the former (15-77 ºC).

Table 7.2. Thermal properties of polyurethanes studied in this work.

PUR	T_g[a] (ºC)	T_m[b] (ºC)	ΔH_m[b] (J·g^{-1})	T_c[c] (ºC)	ΔH_c[c] (J·g^{-1})	T_m[d] (ºC)	ΔH_m[d] (J·g^{-1})	T_m[e] (ºC)	ΔH_m[e] (J·g^{-1})
BD-HDI	15	184	77	157	76	--	--	177, **182**	73
Is-HDI	77	169,189,208/224[e]	27/50[e]	147	9	149	8	169,189,**210**	19
BDIs-HDI	30	162	48	129	44	--	--	153,**161**	44
$BDIs_2$-HDI	24	167	61	136	50	--	--	159,**165**	49
BD-MDI	93	186,212,232	50	119	9	182	11	215,**231**	21
Is-MDI	183	216/235[e]	20/20[e]	--	--	--	--	--	--
BDIs-MDI	120	186,210	18	180	9	--	--	204	11
$BDIs_2$-MDI	115	190,212	18	182	10	--	--	206	13

[a] Glass transition temperatures measured by DSC at heating on samples quickly cooled from the melt.
[b] Melting temperature and enthalpy measured at the first heating (main peaks in bold).
[c] Crystallization during cooling.
[d] Melting temperature and enthalpy measured at the second heating (main peaks in bold).
[e] Annealed samples: Is-HDI at 190 ºC for 12 h, Is-MDI at 200 ºC for 12 h.

All the studied polyurethanes were semicrystalline polymers and able to crystallize from the melt. The heating DSC traces of samples of PUR coming directly from synthesis are compared in Figure 7.1. They all contain more or less pronounced endothermic peaks characteristic of melting. DSC traces recorded from Is-containing PUR homopolymers showed multiple broad melting peaks, presumably arising from crystallite size heterogeneities; such multiple peaks could be merged in only one sharper peak shifted upwards by annealing for 12 h at temperatures close to the highest temperature melting

peak. For both aliphatic and aromatic PUR, the Is homopolymer displayed higher T_m than the BD homopolymer, and copolymers with intermediate compositions had T_m lower than the homopolymers. Furthermore no remarkable differences in melting behaviour were observed between copolymers with the Is units distributed in either monads or dyads.

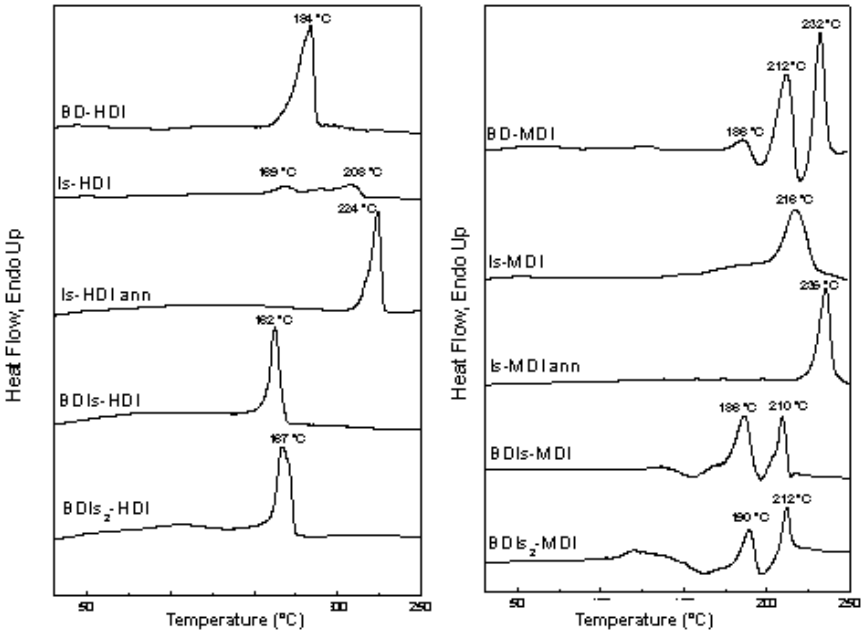

Figure 7.1. Comparative heating DSC traces of aliphatic **(a)** and aromatic **(b)** polyurethanes.

The thermal stability of PUR under inert atmosphere was comparatively evaluated by TGA. The TGA traces of aliphatic an aromatic PUR are compared in Figures 7.2a and 7.2b, respectively, and the decomposition parameters determined on such traces are listed in Table 7.3. As it is well known results indicated that major differences are those between aliphatic and aromatic PUR whereas no significant changes in thermal stability were produced by replacing BD by Is. In all cases, polyurethanes made of HDI appeared to be more stable than the aromatic ones showing higher onset and maximum rate decomposition temperatures and leaving much lower amounts of residue after heating at 600 ºC.

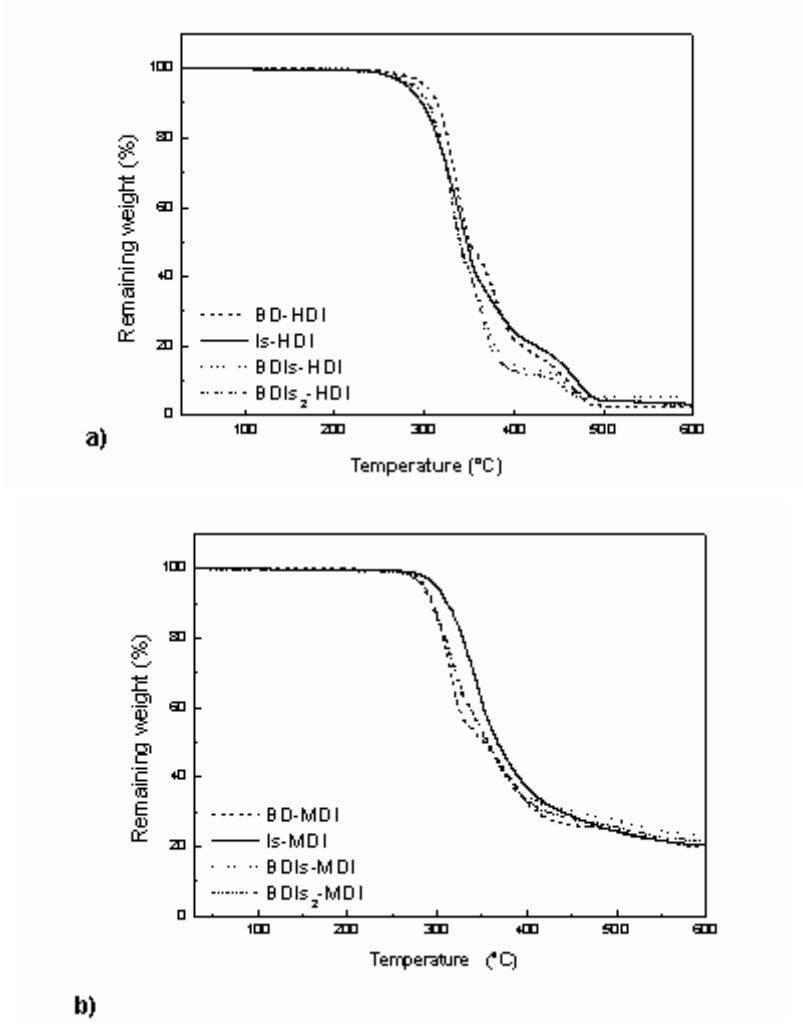

Figure 7.2. TGA traces of aliphatic **(a)**, and aromatic **(b)** polyurethanes.

The X-ray diffraction profiles of PUR are compared in Figure 7.3a and 7.3b, and the Bragg's spacings measured on them are listed in Table 7.3. The profile recorded from PUR-(BD-HDI) displays the three characteristic spacing of PUR made of HDI at 0.44, 0.37 y 0.40 nm, which have been reported for linear aliphatic polyurethanes as indexed as 100 and 010 of a triclinic structure, and as 100 of a second hexagonal form.[16] It is observed in general therefore that the insertion of the Is units in the PUR chain depress crystal formation and decrease the crystallinity, a result which is in full agreement with DSC observations above described.

Table 7.3. Thermal degradation and observed Bragg spacings of polyurethanes studied.

PUR	TGA[a]			X-ray diffraction[b]			
	$^{o}T_d$ (ºC)	$^{max}T_d$ (ºC)	W (%)	d_{hkl} (nm)			
BD-HDI	300	340, 371, 464	1		0.44s	0.40s	0.37s
Is-HDI	296	342, 384, 471	3	0.47s	0.43s		
BDIs-HDI	300	331, 365, 453	5	0.45s	0.43s	0.41s	0.37s
$BDIs_2$-HDI	302	330, 363, 452	3			nd	
BD-MDI	282	315, 366	20	0.49s	0.45s		0.38s
Is-MDI	297	346, 375	20	0.47s			
BDIs-MDI	281	318, 355	23	0.47s	0.44s		
$BDIs_2$-MDI	283	320, 353	21			nd	

[a] Onset decomposition temperature ($^{o}T_d$), maximum rate decomposition temperatures ($^{max}T_d$) and remaining weight at 600 ºC (W).
[b] Powder X-ray diffraction. Visually estimated intensities denoted as: s, strong; m, medium; w, weak. nd = not determined.

The copolymer PUR-(BDIs-HDI) gave a profile containing again the characteristic peaks at 0.43, 0.37 and 0.41 nm with a broad shoulder at ~0.45 nm. It seems therefore that the crystalline structure of the parent homopolymer PUR-(BD-HDI) is essentially retained in the copolymer although some disorder is introduced by the presence of the Is units. It is a plausible explanation given the low content in Is and the preferred location of these units at the end chains, i.e. the amount of inner Is units in the PUR chains is low enough as to allow the polymer to adopt the same crystal structure, most probably by excluding them from the crystal lattice. On the other hand, all the aromatic PUR gave profiles consisting of broad peaks centred at 0.44-0.47 nm which evidence the presence of defective crystallized material. PUR entirely made of Is display a different behaviour.

The profile obtained from PUR-(Is-HDI) displays a broad peak at ~0.43 nm which is indicative of a structure made of poorer formed crystallites. The evolution of the X-ray profiles with time of PUR-(Is-HDI) annealed at 190 ºC is depicted in Figure 7.3c. Upon heating, the peak at 0.43 nm indicative of a hexagonal or pseudohexagonal crystal structure split in the two peaks at 0.43 and 0.47 nm indicating that a new crystal structure is adopted in this case.

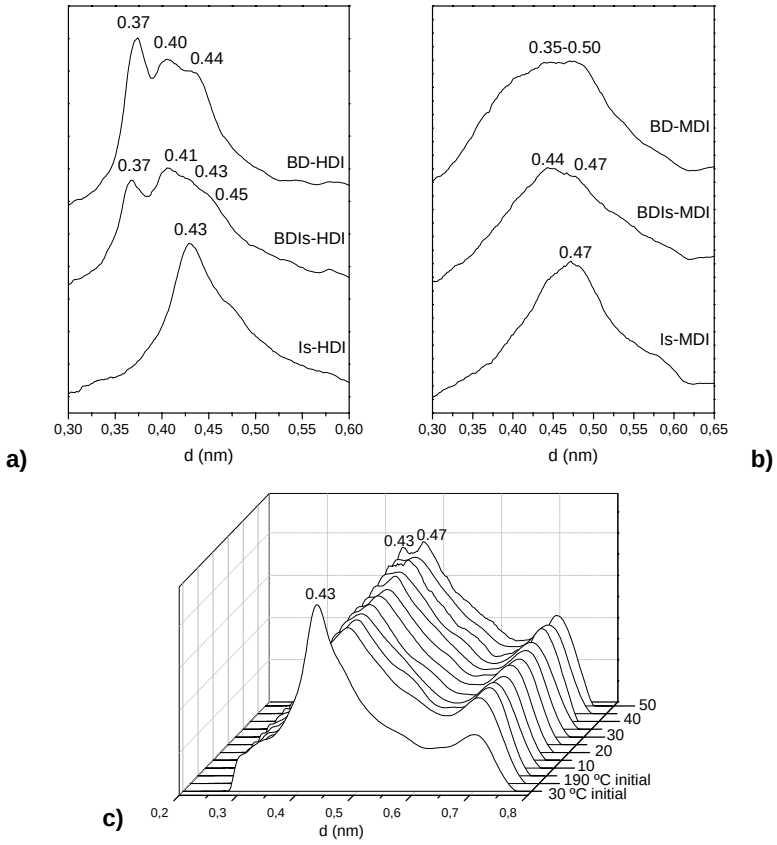

Figure 7.3. X-ray diffraction profiles of the HDI (**a**) and MDI (**b**) polyurethanes and evolution of the X-ray diffraction profile of PUR-(Is-HDI) with time (in min) under annealing at a temperature of 190 ºC (**c**).

7.3.3. Hydrolytic degradability

The reluctance of PUR entirely consisting of hard segments made of alkanediols is a well known fact. It was interesting to explore the effect of the insertion of a carbohydrate-based diol such as isosorbide in a polyurethane chain. With this aim, the hydrolytic degradation of the pair PUR-(BD-HDI) and PUR-(Is-HDI) was comparatively evaluated by incubation in aqueous buffers at pH 2, 7.4 and 10, and at temperatures of 37 and 60 ºC for a period of 40 days. The evolution of the process was followed by weighing and GPC running of the samples after regular periods of time and results are given in Table 7.4.

Table 7.4. Hydrolytic degradation of PUR-(BD-HDI) and PUR-(Is-HDI).[a]

		BD-HDI					
		pH 2		pH 7.4		pH 10	
Days		37 ºC	60 ºC	37 ºC	60 ºC	37 ºC	60 ºC
0	*W* (%)	--	100	--	100	--	100
	M_w (g·mol^{-1})	--	30,000	--	30,000	--	30,000
20	*W* (%)	--	99.5	--	99.0	--	97.8
	M_w (g·mol^{-1})	--	30,000	--	30,000	--	29,700
40	*W* (%)	--	99.0	--	98.3	--	97.0
	M_w (g·mol^{-1})	--	30,000	--	29,900	--	29,700
		Is-HDI					
0	*W* (%)	100	100	100	100	100	100
	M_w (g·mol^{-1})	18,000	18,000	18,000	18,000	18,000	18,000
20	*W* (%)	98.7	94.0	98.8	94.6	98.7	94.2
	M_w (g·mol^{-1})	18,000	17,200	18,000	17,300	17,900	17,200
40	*W* (%)	97.3	93.4	98.5	94.2	97.4	93.5
	M_w (g·mol^{-1})	17,500	17,100	17,900	17,300	17,400	17,000

[a] Percentage of remaining weight (*W*) and weight-average molecular weight (M_w).

The general observation is that PUR containing isosorbide show a slightly greater weight loss than PUR made of 1,4-butanediol, the weight loss being more perceivable at neutral or basic pH. The fact that the decay in molecular weight is so meagre could be due to the rapid solubilisation of the generated PUR fragments. These data indicate that the replacement of BD by isosorbide slightly weaken the resistance of the polyurethane to be attacked by water. This result is in agreement to previously reported work on polycondensates as polyamides, and polyesters in which the hydrodegradability of these polymers was enhanced by the presence of carbohydrate-based units in the polymer chain.[17-20]

7.4. Conclusions

A set of polyurethanes containing isosorbide units were synthesized by polymerization in solution from HDI and MDI diisocyanates and 1,4-butanediol (BD), isosorbide (Is) or diisosorbide diurethanes as diols. Results showed that copolyurethanes were enriched in BD units and show predominance of isosorbide end groups, most of them with the unreacted hydroxyl in *exo* position. The insertion of the rigid isosorbide ring hampered the molecular mobility of the polymer chain with the subsequent increase in T_g, but do not show significant changes in thermal stability. Degradation assays revealed that incorporation of Is units increased slightly the hydrolysis rate.

7.5. References

1. Bayer, O. Angew Chem **1947**, A59, 257.

2. Oertel, G. "Polyurethane Handbook", Hanser, Munich **1994**.

3. Thiem, J.; Bachmann, F. Trend Polym Sci **1994**, 2, 425.

4. Okada, M. Prog Polym Sci **2002**, 27, 87.

5. a) Bachmann, F.; Reimer, J.; Ruppenstein, M.; Thiem, J. Macromol Rapid Commun **1998**, 19, 21. b) Bachmann, F.; Reimer, J.; Ruppenstein, M.; Thiem, J. J Macromol Chem Phys **2001**, 202, 3410.

6. García-Martín, M.G.; Pérez, R.R.; Hernández, E.B.; Alla, A.; Muñoz-Guerra, S.; Galbis, J.A. Macromolecules **2004**, 37, 5550.

7. Yamanaka, C.; Hashimoto, K. J Polym Sci Part A: Polym Chem **2002**, 40, 4158.

8. Yokoe, M.; Aoi, K.; Okada, M. J Polym Sci Part A: Polym Chem **2005**, 43, 3909.

9. Lemieux, R.U.; McInnes, A.G. Can. J. **1960,** 38,136.

10. Noordover, B.A.J.; van Staalduinen, V.G.; Duchateau, R.; Koning, C.E.; van Benthem, R.A.T.M.; Mak, M.; Heise, A.; Frisen, A.E.; van Haveren, J. Biomacromolecules **2006**, 7, 3406.

11. Kricheldorf, H.R. J.M.S. Rev. Macromol Chem Phys, **1997**, C37, 599.

12. Gomurashvili, Z.; Kricheldorf, H.R.; Katsarava, R. J.M.S. Pure Appl Chem **2000** A37(3), 215.

13. Yokoe, M.; Okada, M.; Aoi, K. J Polym Sci Part A: Polym Chem **2003**, 41, 2312.

14. Braun B., Bergmann, M. J Prakt Chem **1992,** 334, 298.

15. Cognet-Georjon, E.; Mechin, F.; Pascault, J.P. Makromol Chem **1995**, 196, 3733.

16. Saito, Y.; Nansai, S.; Kinoshita, S. Polym J **1972**, 3, 113.

CHAPTER 8

CARBOHYDRATE-BASED POLY(ESTER-URETHANE)S: COMPARATIVE STUDY REGARDING CYCLIC ALDITOLS EXTENDERS AND POLYMERIZATION PROCEDURES *

Purpose and specific aims: *The main purpose of this work is to study comparatively the effect of the preparation method and composition on the structure and some properties of new thermoplastic segmented poly(ester-urethane)s in which the hard segment is made of D-glucose-derived extenders. The influence of the extender on the properties and structure of the segmented PUR is evaluated.*

Summary: *A set of segmented poly(ester-urethane)s were prepared from diisocyanates HDI or MDI and using 1,4-butanediol and D-glucose derived cyclic diols (1,4:3,6-dianhydro-D-glucitol (isosorbide) or 2,4;3,5-di-O-methylidene-D-glucitol (gludioxol) or mixtures of them) as extenders. Hydroxyl end-capped polycaprolactone with molecular weight of 3,000 g·mol^{-1} was used as soft segment. Two polymerization methods, in solution and in bulk, were applied for synthesis. The influence of the preparation procedure and composition in cyclic extender on synthesis results, structure and properties of the novel poly(ester-urethane)s was comparatively evaluated and discussed. The effect of replacement of 1,4-butanediol by isosorbide or gludioxol on hydrodegradability was also assessed; although the rate of hydrolysis increased noticeably with the presence of glucitol derived units, degradation of the polymers took place essentially by hydrolysis of the polyester soft segment.*

* Publication derived from this work: Marín, R.; Muñoz-Guerra, S. *J Appl Polym Sci Part A: Polym Chem* (submitted **2009**).

8.1. Introduction

Segmented polyurethanes constitute a large family of high performance materials with a wide variety of properties that are tunable by an appropriate molecular design.[1] These linear thermoplastics usually exhibit elastomeric behaviour at room temperature. Segmented polyurethanes are usually obtained by reaction of two diols, a macroglycol (precursor of the soft segment) and a short diol (which leads to the hard segment), with a diisocyanate. Different macroglycols are suitable for this synthesis, the most frequently used being hydroxyl end capped polyesters of low molecular weight.[2] Although the poly(ester-urethane)s resulting from these synthesis display an excellent thermal and environmental stability, they are vulnerable to hydrolysis, their hydrodegradability being mainly decided by the chemical structure of the polyester segment.[3] Polycaprolactone, polylactides and aliphatic polyesters derived from alkanediols and dicarboxilic acids as succinic and adipic acids, are polyesters commonly found as soft segments of industrial thermoplastic polyurethanes. The use of these materials range from adhesives and coatings to high performance engineering parts; they also offer a great potential for applications in biomedicine as biocompatible biodegradable materials.[4]

A growing interest currently exists for chemicals deriving from renewable resources as an alternative to oil-based monomers for the production of well-established industrial polymers. Specifically, utilization of carbohydrate derivatives for polymer synthesis has attracted much attention not only because of the huge abundance of these resources but also because of the degradable and biocompatible behaviour that can be expected for such polymers.[5,6] Moreover, carbohydrates stand out as very convenient raw materials because they are inexpensive, readily available, and provide great functional diversity. In recent years, several notable examples of carbohydrate-based polymers have been reported in the literature.[7-9]

A highly promising carbohydrate derivative for the development of sustainable polymeric materials is the cyclic compound 1,4:3,6-dianhydro-D-glucitol, also known as isosorbide. This carbohydrate-based diol is a potentially useful monomer for the synthesis of polyesters, polyamides and polycarbonates.[10] It has been proved that polyesters, poly(esteramide)s, poly(estercarbonate)s, and polycarbonates derived from isosorbide are more or less biodegradable depending on the structures, as judged from degradation tests carried out in activated sludge, in soil, and in the presence of hydrolytic enzymes.[11]

The use of other cyclic diols derived from sugars as monomers for the synthesis of polycondensation has been scarcely explored. Nevertheless several optically polyamides derived from 2,3-*O*-methylene-L-tartaric acid have been described in the old and more recent literature.[12-14]

The main purpose of this work was to study comparatively the effect of the preparation method and composition on the structure and some properties of new thermoplastic segmented poly(ester-urethane)s in which the hard segment is made of D-glucitol-derived extenders. These PUR are prepared from 1,6-hexamethylene diisocyanate (HDI) or 4,4'-methylenebis(phenyl isocyanate) (MDI) and polycaprolactone diol (PCL) with molecular weight of 3,000 $g \cdot mol^{-1}$ as soft segment. The diols chosen to be used as extenders are the habitual 1,4-butanediol (BD), and the cyclic glucitols, isosorbide and gludioxol (2,4;3,5-di-*O*-methylidene-D-glucitol). Two polymerization methods, in solution and in bulk, are used for the preparation of these poly(ester-urethane)s and results obtained from each method are compared The influence of the selected extender, isosorbide or gludioxol, on the properties of the resulting segmented PUR is also evaluated and discussed.

8.2. Experimental section

8.2.1. Materials and methods

Common reagents and solvents were purchased from Aldrich and used as received. *N,N*-dimethylformamide (DMF) and tetrahydrofuran (THF) solvents were dried under inert atmosphere prior to use by distillation. 1,4-Butanediol and polycaprolactone with a number-average molecular weight of 3,000 $g \cdot mol^{-1}$ were donated by Merquinsa (Mercados Químicos S.L.), and 1,4:3,6-dianhydro-D-glucitol (isosorbide, Is) was a gift from Roquette Freres S.A. This cyclic dianhydride was prepared from corn starch following the route depicted in Scheme 8.1. Diols and reagents for polymerization were stored in a desiccator under vacuum until used. 1,6-Hexamethylene diisocyanate was vacuum distilled prior to use, and together with 4,4'-methylenebis(phenyl isocyanate), stored at 4 ºC. Both compounds were invariably handled under inert atmosphere.

Gel permeation chromatograms (GPC) were acquired at 35 ºC on a Waters equipment provided with a refraction-index detector. The samples were chromatographed with 0.05 M sodium trifluoroacetate-hexafluoroisopropanol (NaTFA-HFIP) at a flow rate of 0.5

mL·min^{-1} using a polystyrene-divinylbenzene packed linear column. Chromatograms were calibrated against poly(methyl methacrylate) (PMMA) monodisperse standards. ^{1}H and ^{13}C{^{1}H} NMR spectra were recorded on a Bruker AMX-300 spectrometer operating at 300.1 and 75.5 MHz for ^{1}H and ^{13}C{^{1}H}, respectively, and using TMS as internal reference. Sample concentrations within the 1-5% (w/v) range were used for these analyses. The spectra were acquired with 64 scans and 1000-10,000 scans for ^{1}H and ^{13}C{^{1}H}, respectively, and relaxation delays of 1 and 2 s.

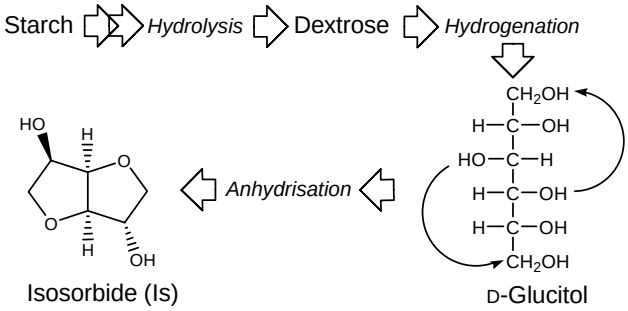

Scheme 8.1. Synthetic route to isosorbide from corn starch.

Differential scanning calorimetry (DSC) experiments were performed at heating/cooling rates of 10 ºC·min^{-1} on a Perkin-Elmer Pyris 1 instrument calibrated with indium. All the experiments were carried out with sample amounts of 3-4 mg within a range of temperatures from 0 ºC to 200 or 250 ºC, and under a 20 mL·min^{-1} nitrogen flow in order to minimize possible oxidative degradations. Glass transition data were obtained by DSC with a Thermal Analysis instrument TA-Q100 equipped with a refrigerated cooling system. These experiments were conducted under a flow of dry nitrogen (50 mL·min^{-1}) with sample weights of around 5 mg, and calibration was performed with indium and sapphire. Determinations were made at a heating rate of 20 ºC·min^{-1} on samples quenched to -70ºC from samples melt at temperatures between 200 and 250 ºC. Thermogravimetric analysis (TGA) was carried out under inert atmosphere at a heating rate of 10 °C·min^{-1} and within a temperature range of 30 to 600 ºC using a Mettler TA4000 thermobalance. Sample weights of about 15 mg were used in these experiments.

Wide angle X-ray scattering were performed on a Philips automatic horizontal axis diffractometer using Cu-K_α Ni-filtered radiation. Spectra were taken at room temperature with the scattering angle 2θ varying from 3 to 50º. Films for mechanical properties of selected polyurethanes with a thickness of ~300 µm were prepared by hot-press molding at 10-20 ºC above the melting temperature. The tensile strength (σ), elongation at break (ε), and Young's modulus (E) were measured at a stretching rate of 20 mm·min^{-1} on a Zwick 2.5/TN1S testing machine coupled with a compressor Dalbe DR 150. The tested samples were cut into rectangular strips with a width of 3 mm and a distance between testing marks of 10 mm. Measurements were made in triplicates.

8.2.2. Synthesis of monomers

The cyclic diol 2,4:3,5-di-*O*-methylidene-D-glucitol (gludioxol, Gx) was prepared following the chemical synthetic route depicted in Scheme 8.2. Compounds 2,4:3,5-di-*O*-methylidene-D-gluconic acid and methyl 2,4:3,5-di-*O*-methylidene-D-gluconate were synthesized from commercial 1,5-D-gluconolactone as described elsewhere.[16]

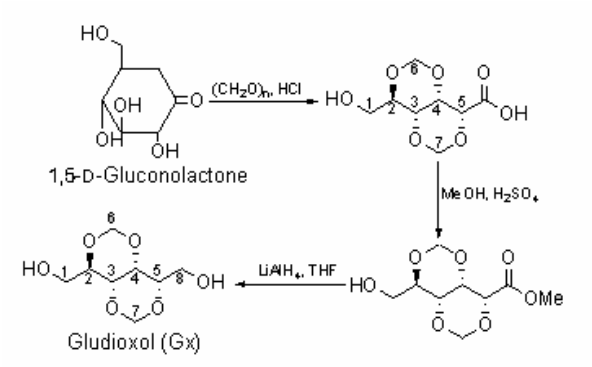

Scheme 8.2. Synthetic route to gludioxol from gluconolactone.

2,4:3,5-di-O-methylidene-D-gluconic acid. A mixture of 30 g (0.168 mol) of 1,5-D-gluconolactone, 30 g of paraformaldehyde, and 42 mL of concentrated hydrochloric acid was refluxed at 110 ºC for 1 h. The product precipitated from the solution upon cooling. Yield: 80%. ^{1}H NMR (DMSO, 300 MHz): δ (ppm) 4.99-4.69 (2 dd, 4H, CH_2-6 and CH_2-7), 4.34 (m, 1H, CH-5), 4.04 (m, 1H, CH-4), and 3.73-3.61 (m, 4H, CH-3, CH-2 and CH_2-1).

$^{13}C\{^{1}H\}$ NMR (DMSO, 75.5 MHz): δ (ppm) 170.02 (C=O), 92.42 (C-7), 88.72 (C-6), 77.31 (C-5), 76.65 (C-1), 71.29 (C-3), 69.11 (C-4), and 59.72 (C-2).

Methyl 2,4:3,5-di-O-methylidene-D-gluconate. A mixture of 30 g (0.136 mol) of di-*O*-methylidene-D-gluconic acid, 250 mL of methanol and 0.75 mL of concentrated sulfuric acid was refluxed until complete dissolution. The product precipitated from the solution upon cooling; additional crops were obtained upon concentrating the mother liquors. Yield: 70%. ^{1}H NMR (DMSO, 300 MHz): δ (ppm) 5.01-4.71 (2 dd, 4H, CH_2-6 and CH_2-7), 4.52 (m, 1H, CH-5), 4.06 (m, 1H, CH-4), 3.75-3.65 (m, 4H, CH-3, CH-2 and CH_2-1), and 3.62 (s, 3H, CH_3). $^{13}C\{^{1}H\}$ NMR (DMSO, 75.5 MHz): δ (ppm) 169.05 (C=O), 92.36 (C-7), 88.66 (C-6), 77.26 (C-5), 76.72 (C-1), 71.10 (C-3), 68.94 (C-4), 59.78 (C-2), and 52.90 (CH_3).

2,4:3,5-di-O-methylidene-D-glucitol. To a dispersion of 20 g (0.085 mol) of methyl 2,4:3,5-di-*O*-methylidene-D-gluconate in 100 mL of dry tetrahydrofuran, 6.8 g (0.179 mol) of LiAlH4 (97%) in 150 mL of dry tetrahydrofuran were added at 0 ºC under nitrogen atmosphere. The mixture was refluxed for 24 hours and then cooled to 0 ºC. H_2O (25 mL), NaOH (15% w/v, 25 mL) and H_2O (75 mL) were sequentially and slowly added and the mixture was then filtrated and concentrated to a ~20 mL oily residue from which a white solid crystallized. Yield: 60%. ^{1}H NMR (DMSO, 300 MHz): δ (ppm) 4.96-4.67 (2 dd, 4H, CH_2-6 and CH_2-7), 4.63 and 4.40 (2 t, 2H, OH), 3.74 (m, 1H, CH-5), 3.64 (m, 3H, CH_2-1 and CH-2), 3.60 (m, 1H, CH-3), 3.54 (m, 1H, CH-5), and 3.42 (m, 2H, CH_2-8). $^{13}C\{^{1}H\}$ NMR (DMSO, 75.5 MHz): δ (ppm) 93.00 (C-7), 88.52 (C-6), 79.22 (C-5), 77.23 (C-1), 71.51 (C-3), 67.80 (C-4), 60.64 (C-8), and 59.44 (C-2).

8.2.3. Synthesis of polymers

Polymerization in solution. For the synthesis of segmented polyurethanes by polymerization in solution, PCL (1 mmol) and the extender or a mixture of extenders in the chosen ratio (1,4-butanediol or/and isosorbide, 5 mmol) were charged in a round bottom flask saturated with inert gas. *N,N*-dimethylformamide (40 mL) was then added and the mixture stirred at room temperature until homogenization. 6 mmol of diisocyanate, HDI or MDI, followed by 20 ppm of dibutyltin dilaurate catalyst, were then added and the mixture was stirred for 24 h at room temperature. The reaction mixture became rapidly homogeneous and remained clear for the whole reaction period except

for PUR-(PCL-BD-HDI) that precipitated spontaneously after 2 h of reaction allowing direct recovery of the polymer. In all other cases, the reaction mixture was added dropwise into cold diethyl ether (250 mL) to precipitate the polymer. Purification was carried out by redissolution of the polymer in the minimum volume of tetrahydrofuran followed by reprecipitation into diethyl ether. All the polymers were white powders that were dried under vacuum and stored in a desiccator until needed.

Polymerization in bulk. For the synthesis of segmented polyurethanes in bulk the following one-step procedure was followed: PCL (5 mmol), the extender or combination of extenders (1,4-butanediol or/and isosorbide or/and gludioxol, total of diols 25 mmol), and Metatin catalyst (dioctyl tin mercaptide ester, 20 ppm) were mechanically stirred and heated to 130 ºC. At this temperature, 30 mmol of diisocyanate, HDI or MDI, were added. The reactants were totally miscible and the reaction was left to proceed until the viscosity increased to the point that the mechanical stirring became severely hindered. At this point, the reaction mass was placed in a heated chamber at 120 ºC and for 3 h. PUR made from 1,4-butanediol and isosorbide were perfectly white whereas those produced from gludioxol developed a slightly yellow color.

PUR-(PCL-BD-HDI): ^{1}H NMR (DMSO, 300 MHz): δ (ppm) 6.54 (bs, 2H, N-H), 3.96 (m, 4H, H-1(BD); and m, 2H, PCL), 2.91 (m, 4H, H-a), 2.22 (m, 2H, PCL), 1.52 (m, 4H, H-2(BD); and 4H, PCL), 1.29 (m, 4H, H-b; and 2H, PCL), and 1.20 (m, 4H, H-c). ^{13}C{^{1}H} NMR (DMSO, 75.5 MHz): δ (ppm) 173.24 (C=O PCL), 156.92 (C=O urethane), 64.14 (C-1(BD)), 63.95 (PCL), 40.04 (C-a), 34.17 (PCL), 29.06 (C-b), 28.51 (PCL), 26.60 (C-c), 26.17 (C-2(BD)), 25.61 (PCL), and 24.74 (PCL).

PUR-(PCL-Is-HDI): ^{1}H NMR (DMSO, 300 MHz): δ (ppm) 6.99 (bs, 2H, N-H), 4.92 (m, 1H, H-2(Is)), 4.82 (m, 1H, H-5(Is)), 4.61 (m, 1H, H-4(Is)), 4.34 (m, 1H, H-3(Is)), 3.94 (m, 2H, PCL), 3.85-3.76 (m, 4H, H-1(Is) and H-6(Is)), 2.92 (m, 4H, H-a), 2.23 (m, 2H, PCL), 1.51 (m, 4H, PCL), 1.28 (m, 4H, H-b; and 2H, PCL), and 1.21 (m, 4H, H-c). ^{13}C{^{1}H} NMR (DMSO, 75.5 MHz): δ (ppm) 173.44 (C=O PCL), 156.10 (C=O urethane), 86.54 (C-2(Is)), 81.50 (C-5(Is)), 78.56 (C-4(Is)), 74.23 (C-3(Is)), 73.70 (C-1(Is)), 70.76 (C-6(Is)), 64.05 (PCL), 41.13 (C-a), 34.25 (PCL), 30.04 (C-b), 28.62 (PCL), 26.69 (C-c), 25.73 (PCL), and 24.87 (PCL).

PUR-(PCL-Gx-HDI): ^{1}H NMR (DMSO, 300 MHz): δ (ppm) 6.94 (bs, 2H, N-H), 4.97-4.66 (2 dd, 4H, H-6(Gx) and H-7(Gx)), 3.94 (m, 2H, PCL), 3.98-3.53 (m, 8H, H-1,2,3,4,5,8(Gx)), 2.89 (m, 4H, H-a), 2.22 (m, 2H, PCL), 1.47 (m, 4H, PCL), 1.25 (m, 4H, H-b; and 2H, PCL), and 1.18 (m, 4H, H-c). ^{13}C{^{1}H} NMR (DMSO, 75.5 MHz): δ (ppm) 173.33 (C=O PCL), 156.30 (C=O urethane), 92.74 and 88.47 (C-6,7 (Gx)), 75.79, 74.63, 71.76, 67.41, 58.75, and 57.15 (C-1,2,3,4,5,8 (Gx)), 64.03 (PCL), 41.07 (C-a), 34.07 (PCL), 30.09 (C-b), 28.41 (PCL), 26.60 (C-c), 25.51 (PCL), and 24.64 (PCL).

PUR-(PCL-BD-MDI): ^{1}H NMR (DMSO, 300 MHz): δ (ppm) 9.11 (bs, 2H, N-H), 7.31-7.00 (dd, 8H, ar), 4.06 (m, 4H, H-1(BD)), 3.97 (m, 2H, PCL), 3.75 (bs, 2H, Ph-CH_2-Ph from MDI), 2.22 (m, 2H, PCL), 1.67 (m, 4H, H-2(BD)), 1.53 (m, 4H, PCL), and 1.30 (m, 2H, PCL). ^{13}C{^{1}H} NMR (DMSO, 75.5 MHz): δ (ppm) 173.29 (C=O PCL), 154.43 (C=O urethane), 137.70, 137.86, 129.44, 119.53 (ar), 64.48 (C-1(BD)), 64.19 (PCL), 40.92 (Ph-CH_2-Ph from MDI), 34.20 (PCL), 29.56 (PCL), 26.09 (C-2(BD)), 25.65 (PCL), and 24.79 (PCL).

PUR-(PCL-Is-MDI): ^{1}H NMR (DMSO, 300 MHz): δ (ppm) 9.37 (bs, 2H, N-H), 7.31-7.05 (dd, 8H, ar), 5.10 (m, 1H, H-2(Is)), 5.05 (m, 1H, H-5(Is)), 4.75 (m, 1H, H-4(Is)), 4.45 (m, 1H, H-3(Is)), 3.97 (m, 2H, PCL), 3.88–3.67 (m, 6 H, H-1(Is) and H-6(Is)), 3.77 (bs, 2H, Ph-CH_2-Ph from MDI), 2.23 (m, 2H, PCL), 1.53 (m, 4H, PCL), and 1.30 (m, 2H, PCL). ^{13}C{^{1}H} NMR (DMSO, 75.5 MHz): δ (ppm) 173.24 (C=O PCL), 153.55 (C=O urethane), 137.61, 136.38, 129.62, 119.57 (ar), 86.35 (C-2(Is)), 81.43 (C-5(Is)), 79.18 (C-4(Is)), 74.66 (C-3(Is)), 73.22 (C-1(Is)), 70.15 (C-6(Is)), 64.19 (PCL), 40.90 (Ph-CH_2-Ph from MDI), 34.06 (PCL), 28.52 (PCL), 25.65 (PCL), and 24.83 (PCL).

PUR-(PCL-Gx-MDI): ^{1}H NMR (DMSO, 300 MHz): δ (ppm) 9.42 (bs, 2H, N-H), 7.33-7.05 (dd, 8H, ar), 5.01-4.71 (2 dd, 4H, H-6(Gx) and H-7(Gx)), 4.03-3.55 (m, 8H, H-1,2,3,4,5,8(Gx)), 3.97 (m, 2H, PCL), 3.79 (s, 2H, Ph-CH_2-Ph from MDI), 2.25 (m, 2H, PCL), 1.54 (m, 4H, PCL), and 1.30 (m, 2H, PCL). ^{13}C{^{1}H} NMR (DMSO, 75.5 MHz): δ (ppm) 173.13 (C=O PCL), 153.90 (C=O urethane), 137.71, 136.07, 129.29, 119.39 (ar), 92.74 and 88.47 (C-6,7 (Gx)), 75.79, 74.63, 71.76, 67.41, 58.75, and 57.15 (C-1,2,3,4,5,8 (Gx)), 64.03 (PCL), 40.86 (Ph-CH_2-Ph from MDI), 34.07 (PCL), 28.41 (PCL), 25.51 (PCL), and 24.64 (PCL).

8.2.4. Hydrolytic degradation assays

For hydrolytic degradation studies, films of selected polyurethanes with a thickness of ~300 μm were prepared by hot-press molding. The films were cut into 10-mm diameter, 20 to 30-mg weight disks, which were dried in vacuum at 30 °C to constant weight. The degradation study was performed by placing the disks into vials and adding 10 mL of buffered solutions at the selected pH. Parallel experiments were carried out with samples immersed in sodium phosphate buffer (pH 7.4), sodium carbonate buffer (pH 10) and citric acid buffer (pH 2) at temperatures of 37 and 60 °C. Vials were sealed to avoid partial evaporation of the fluids in the heated chamber. After immersion for the scheduled period of time, the samples were rinsed thoroughly with water and dried to constant weight. Sample weighing, GPC measurements and NMR spectroscopy were used to follow the evolution of the hydrodegradation process.

8.3. Results and discussion

8.3.1. Polyurethane synthesis

The segmented polyurethanes were prepared in parallel by polymerization in solution (*s*PUR) and polymerization in bulk (*b*PUR) using both HDI and MDI as diisocyanates and PCL as soft segment. Isosorbide and gludioxol were the cyclic chain extenders used to replace 1,4-butanediol, either totally or partially. The chemical structures of all the segmented PUR studied in this work are depicted in Scheme 8.3. The constitution and composition of all the synthesized PUR was assessed by ^{1}H and $^{13}C\{^{1}H\}$ NMR; signal data and assignments are given in full detail in the Experimental Section. Data and results pertaining to polymerization in solution are given in Table 8.1.

PUR containing Gx extender could not be synthesized by this method due to the insolubility of gludioxol in DMF. Yields of isosorbide containing *s*PUR were around 80% and the polymers were found to be enriched in the diols used as extenders compared to the composition used for the feed. These results indicate some loss of PCL along the preparation procedure, most probably by failing in the precipitation step because either it remained unreacted or it was located in a PCL-enriched PUR fraction of higher solubility in diethyl ether. The molecular weights of these *s*PUR are around 20,000 $g \cdot mol^{-1}$ with polydispersities about 2 and intrinsic viscosities near 0.5 $g \cdot dL^{-1}$. All they display a largely restricted solubility that was not significantly affected by composition. It can be concluded

Table 8.1. Polymerization results and some properties of poly(ester-urethane)s prepared by polymerization in solution.

*s*PUR	Reaction					Molecular size[e]			Solubility[f]					
	PCL:Ext[a]	Solvent	Yield (%)	PCL:Ext[b]	Hard[c] (%)	$[\eta]$ ($dL \cdot g^{-1}$)	M_n ($g \cdot mol^{-1}$)	M_w/M_n	H_2O	DMSO	$CHCl_3$	THF	EtOH	AcOH
PCL-BD-HDI	(1:5)	DMF	79[d]	(1:7)	36.3	0.50	23,200	2.1	-	+	+	+	-	-
PCL-Is-HDI	(1:5)	DMF	80	(1:7)	41.0	0.46	21,500	2.1	-	+	+	+	-	-
PCL-BD-MDI	(1:5)	DMF	77	(1:7)	42.3	0.55	20,900	2.1	-	+	+/-	+	-	-
PCL-Is-MDI	(1:5)	DMF	81	(1:7)	46.0	0.50	19,700	2.1	-	+	+/-	+	-	-

[a] PCL:BD or PCL:Is molar ratio in the feed.
[b] PCL:BD or PCL:Is molar ratio in the resulting polyurethane determined by ^{1}H NMR.
[c] Content in *hard segment* in the *s*PUR.
[d] Precipitated after 2 hours of reaction.
[e] Intrinsic viscosity measured in DCA and average molecular weights determined by GPC in HFIP against PMMA standards.
[f] Solubility at 20 ± 5 ºC at sample concentration of 1 $g \cdot L^{-1}$: + soluble; +/- partially soluble; - insoluble.

therefore that substitution of 1,4-butanediol by isosorbide in the polymerization of these poly(ester-urethane)s does not modify substantially the synthesis results.

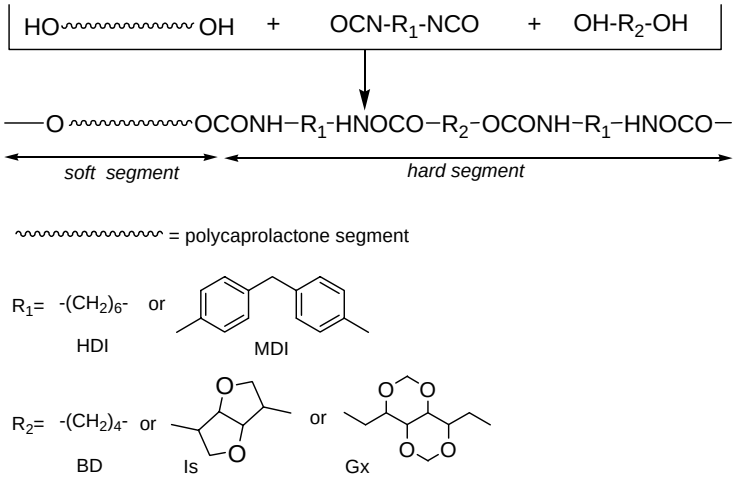

Scheme 8.3. Chemical structures of segmented poly(ester-urethane)s.

The polymerization in bulk for the synthesis of the segmented polyurethanes was performed at 130 ºC with a molar ratio of PCL to extender of 1 to 5 and using Metatin as catalyst. The initially transparent reaction mixture turned into milky white as the reaction advanced so it had to be stopped when the viscosity of the mixture was so high that mechanical stirring became severely hindered. At this point the temperature was reduced to 120 ºC and the reaction left to proceed for 3 h further. The appearance of the resulting *b*PUR was dependent on both the extender and the diisocyanate that were used for the synthesis; all the aromatic *b*PUR without exception were opaque whereas aliphatic *b*PUR made from 1,4-butanediol and/or isosorbide were translucent.

The data and results obtained in the polymerization carried out in bulk are given in Table 8.2. At difference with what happens in the polymerization in solution, the PCL to extender ratio used in the feed was almost exactly maintained in the resulting polymer (which was proven by NMR to be completely exempted from free PCL). The molecular sizes of both aliphatic and aromatic *b*PUR obtained in bulk were noticeably higher than those obtained in solution and their polydispersities oscillated between 1.8 and 2.2.

Table 8.2. Results and some properties of segmented poly(ester-urethane)s obtained by polymerization in bulk.

*b*PUR	Reaction					Molecular size[d]			Solubility[e]				A
	PCL:Ext[a]	(BD:I or Gx)	Yield (%)	PCL:Ext[b]	Hard[c] (%)	$[\eta]$ ($dL \cdot g^{-1}$)	M_n ($g \cdot mol^{-1}$)	M_w/M_n	H_2O EtOH AcOH	DMSO	$CHCl_3$	THF	
PCL-BD-HDI	(1:5)	(1:0)	100	(1:5)	29.0	1.23	56,200	2.2	-	+	+	+	t
PCL-2BD/Is-HDI	(1:5)	(2:1)	100	(1:5)	30.4	0.97	41,000	1.8	-	+	+	+	t
PCL-1BD/Is-HDI	(1:5)	(1:2)	100	(1:5)	31.8	0.88	38,000	2.0	-	+	+	+	t
PCL-Is-HDI	(1:5)	(0:1)	100	(1:5)	33.1	0.75	36,700	2.1	-	+	+	+	t
PCL-2BD/1Gx-HDI	(1:5)	(2:1)	100	(1:5)	31.9	0.93	37,600	2.0	-	+	+/-	+/-	t
PCL-1BD/2Gx-HDI	(1:5)	(1:2)	100	(1:5)	34.6	0.78	32,200	1.9	-	+	+/-	+/-	
PCL-Gx-HDI	(1:5)	(0:1)	100	(1:5)	37.1	0.69	29,000	1.9	-	+	+/-	+/-	
PCL-BD-MDI	(1:5)	(1:0)	100	(1:5)	34.4	1.18	46,200	2.2	-	+	-	+	
PCL-2BD/1Is-MDI	(1:5)	(2:1)	100	(1:5)	35.6	1.06	37,800	1.8	-	+	-	+	
PCL-1BD/2Is-MDI	(1:5)	(1:2)	100	(1:5)	36.7	0.99	36,000	1.9	-	+	-	+	
PCL-Is-MDI	(1:5)	(0:1)	100	(1:5)	37.9	0.97	33,100	2.0	-	+	-	+	
PCL-2BD/1Gx-MDI	(1:5)	(2:1)	100	(1:5)	36.9	1.04	34,100	2.1	-	+	-	+/-	
PCL-1BD/2Gx-MDI	(1:5)	(1:2)	100	(1:5)	39.1	0.91	31,900	2.0	-	+	-	+/-	
PCL-Gx-MDI	(1:5)	(0:1)	100	(1:5)	41.2	0.83	31,700	2.0	-	+	-	+/-	

[a] Molar relation of (PCL:total of *extenders* used) in reaction solution.

With regard to the kind of extender used, 1,4-butanediol provided the highest molecular weights whereas *b*PUR made from gludioxol had the lowest values; accordingly, *b*PUR containing Is or Gx units in addition to BD showed intermediate molecular weights. The intrinsic viscosity values of *b*PUR as a function of the content of the polyurethane in diols derived from the cyclic extenders are plotted in Figure 8.1.

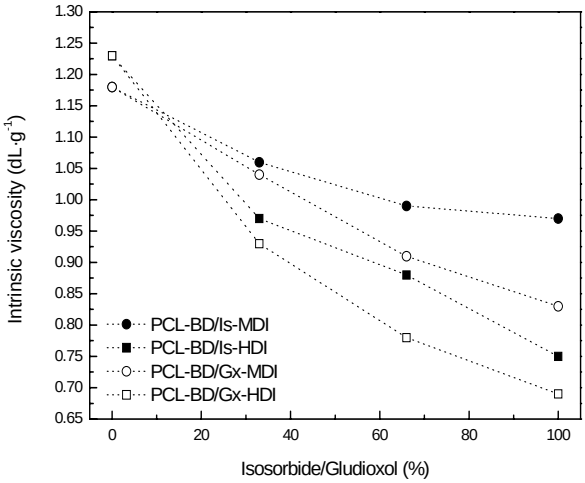

Figure 8.1. Intrinsic viscosity of *b*PUR as a function of the extender composition.

For both isosorbide and gludioxol, [η] was found to decrease with the degree of replacement of 1,4-butanediol, such decreasing being slightly less pronounced for the case of isosorbide. A first interpretation would be related to the lower reactivity of the glucitol derived diols compared to 1,4-butanediol due to the sterical hindrance caused by the relative bulky cyclic structure. Nevertheless the detrimental effect on the polyaddition reaction exerted by small amounts of residual water, which is extremely difficult to remove completely, cannot be fully excluded. This would also explain the even lower viscosity values attained for *b*PUR made from gludioxol; the results obtained with this diol are inconsistent since a higher reactivity in the addition to the isocyanate group should be expected for primary hydroxyl groups.

As far as solubility is concerned, the replacement of 1,4-butanediol by isosorbide did not change significantly the solubility of *b*PUR, *i.e.* the aromatic series is soluble in DMSO and THF and the aliphatic series is in addition soluble in $CHCl_3$. Conversely, all the

*b*PUR containing gludioxol displayed a much more restricted solubility being DMSO the only solvent known for these polymers.

8.3.2. Structure and compared thermal and mechanical properties

All the segmented PUR obtained either in solution or in bulk were semicrystalline regardless their composition; their DSC data are compared in Table 8.3. A common feature to all of them without exception is the occurrence of an endothermic peak within the 40-60 ºC range, which is interpreted as arising from the melting of the crystalline domains made of PCL soft segments. All PUR made from 1,4-butanediol or/and isosorbide displayed also melting of the hard segment at temperatures above 140 ºC regardless the method used for synthesis. Conversely, PUR containing Gx units displayed hard segment melting for the whole aromatic series but not for the aliphatic series except for the polymer with a Gx to BD units ratio of 2:1. For the study of the crystallizability of the individual segments in segmented poly(ester-urethane)s, samples were heated to maximum temperatures of 100 ºC and 200-250 ºC for the soft and hard segment, respectively. A selection of representative DSC traces registered for both *s*PUR and *b*PUR are depicted in Figures 8.2 and 8.3. In these figures polymerization methods and compositional effects on melting and crystallization behaviour associated to both soft and hard segments are compared.

A close comparison between PUR with the same composition but differing in the method of synthesis, in solution or in bulk, leads to the following conclusions:

1) PUR obtained in solution display higher T_g than PUR obtained in bulk, which is most likely due to the greater contents in extender resulting in the former method.

2) Melting and enthalpies values found for both soft and hard segments are very similar for the two series of PUR.

3) Crystallization of the hard segment upon cooling from the melt takes place in PUR obtained in bulk but it is not observed in those obtained in solution except for the case of the PUR made entirely of 1,4-butanediol, *i.e*. PUR-(PCL-BD-HDI). Such differences may be attributed again to the differences in extender content between the two series or/and in its distribution along the polymer chain.

Table 8.3. Compared thermal properties of poly(ester-urethane)s.

	Soft Segment							***Hard Segment***								
	1st Heating			Cooling		2nd Heating		1st Heating		Cooling		2nd Heating		12 h annealing		
	T_g^c (ºC)	T_m (ºC)	ΔH_m (J·g^{-1})	T_c (ºC)	ΔH_c (J·g^{-1})	T_m (ºC)	ΔH_m (J·g^{-1})	T_m (ºC)	ΔH_m (J·g^{-1})	T_c (ºC)	ΔH_c (J·g^{-1})	T_m (ºC)	ΔH_m (J·g^{-1})	t (ºC)	T_m (ºC)	ΔH_m (J·g^{-1})
PCL	-63	58	85	33	72	50	72	-	-	-	-	-	-	-	-	-
***s*PUR**																
PCL-BD-HDI	-54	54	37	21,24	23	47,51	28	152,165	25	130,145	26	162	26	155	174	18
PCL-Is-HDI	-49	51	17	-	-	43	16	151,172,191	6	-	-	-	-	170	215	6
PCL-BD-MDI	-26	52,57	3	-	-	54	2	176,204	7	-	-	-	-	190	220	6
PCL-Is-MDI	-4	46	8	-	-	44	2	226	4	-	-	-	-	170	242	4
***b*PUR**																
PCL-BD-HDI	-60	47	2	-	-	46	2	159,165	25	112	22	156,168	22	160	179	25
PCL-2BD/1Is-HDI	-59	45	2	-	-	43	2	140	14	42	4	142	7	130	157	10
PCL-1BD/2Is-HDI	-59	43	2	-	-	41	2	133,147	5	79	3	146	3	130	161	4
PCL-Is-HDI	-57	45	7	-	-	40	3	188	3	140	3	193	2	180	234	15
PCL-2BD/1Gx-HDI	-50	42,51	4	-	-	49	4	145	1	-	-	-	-	135	148	2
PCL-1BD/2Gx-HDI	-43	50	4	-	-	48	3	-	-	-	-	-	-	-	-	-
PCL-G-HDI	-38	44	4	-	-	43	3	-	-	-	-	-	-	-	-	-
PCL-BD-MDI	-36	54	2			53	2	188,204	12	137	13	196,216, 230	12	190	224	25
PCL-2BD/1Is-MDI	-35	51	2	-	-	49	2	190,203	9	72	3	162	6	195	229	8

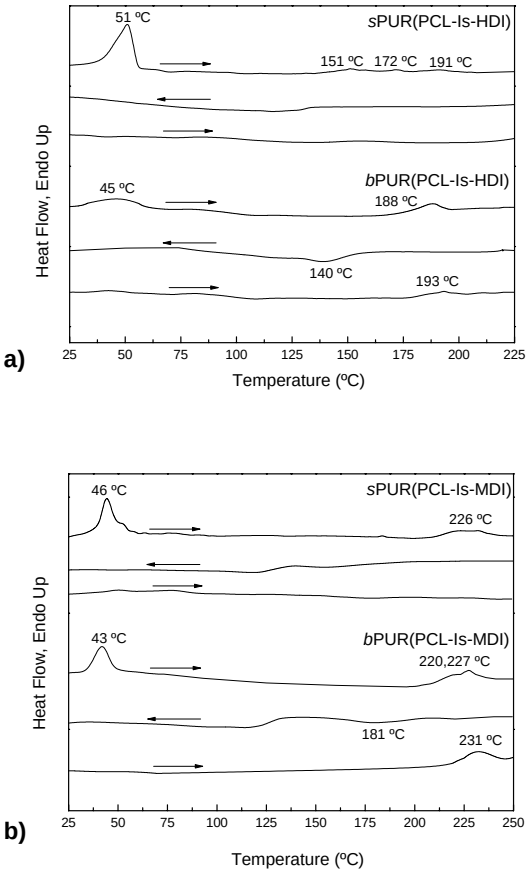

Figure 8.2. Comparative DSC traces of *s*PUR and *b*PUR containing Is units, **a)** aliphatic, and **b)** aromatic; (a) first heating, (b) cooling, and (c) second heating.

Comparison among the PUR obtained in bulk allows evaluating the effect of the composition on thermal properties and leads to the following conclusions:

1) The replacement of BD units by either Is or Gx units gives rise to an increase in T_g that is more pronounced in the latter case. As usual, the aromatic PUR displays higher T_g than the aliphatic ones; in fact T_g values are found to be within the -40 to -60 ºC and 0 to -40 ºC ranges for the two respective series.

2) All *b*PUR display melting of the PCL soft segment at temperatures between 40 and 50 ºC with very low enthalpy values (among 2 and 7 $J \cdot g^{-1}$).

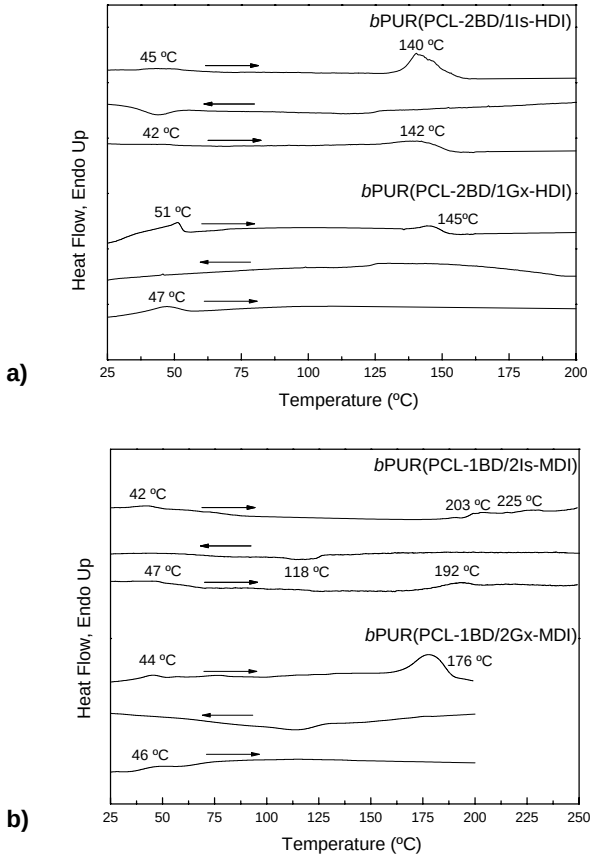

Figure 8.3. Comparative DSC traces of *b*PUR **a)** aliphatic, and **b)** aromatic; (a) first heating, (b) cooling, and (c) second heating.

3) As it could be reasonably anticipated, the crystallizability of the hard segment is highly depending on its chemical constitution; whereas all PUR made from BD and/or Is display hard segment melting, only aromatic PUR made from gludioxol show melting in the high temperature region.

4) Aromatic *b*PUR display higher hard segment T_m than aliphatic ones; highest T_m values are observed for PUR with hard segments entirely made of isosorbide whereas *b*PUR

containing Gx units display the lowest ones. Melting enthalpies decrease with the degree of replacement of BD by either Is or Gx revealing that the presence of cyclic extenders repress crystallinity.

5) Only hard segments made of 1,4-butanediol or/and isosorbide are able to crystallize from the melt.

Annealing is the thermal treatment usually applied to polymers to increase the size of crystallites defectively grown in an incomplete crystallization process. Provided that annealing conditions are optimized, the efficiency of such treatment depends on the capability of chains to form large crystallites. The heating DSC traces showing the influence of composition of the annealing treatment on the hard segment melting peak for aliphatic and aromatic *b*PUR made of 1,4-butanediol and isosorbide are displayed in Figures 8.4a and 8.4b, respectively. A noteworthy shift towards higher temperatures is observed in all cases, but the effect is even greater for *b*PUR containing Is units. In Figure 8.4c, the response of PUR containing Gx to the annealing treatment is compared to that given by PUR containing Is units; DSC traces show that upon annealing, the hard segment melting peak displayed by PUR-(PCL-2BD/1Is-HDI) shifted from 140 ºC to 157 ºC and became much sharper indicating the high sensitivity of this PUR to the thermal treatment. On the contrary, the result obtained upon annealing of PUR-(PCL-2BD/1Gx-HDI) was much poorer, the peak shifted only 3 ºC upwards without significant sharpening. The results of all the annealing treatments applied in this work are listed in Table 8.3 with indication of the conditions used in every case.

The thermal stability of segmented PUR under inert atmosphere was evaluated by TGA. The TGA of some representative PUR are compared in Figure 8.5 and the decomposition parameters measured on such traces are given in Table 8.4. Thermal decomposition takes place in one or two steps within the 280-420 ºC range followed by a final step at temperatures around 450 ºC. The residue left after heating at 600 ºC is less than 2% in the case of aliphatic PUR and between 4 and 8% in the case of aromatic ones. It is noteworthy that aromatic PUR display decomposition temperatures in the low temperature region which are inferior to those displayed by aliphatic PUR whereas no differences between the two series are appreciated in the high temperature step.

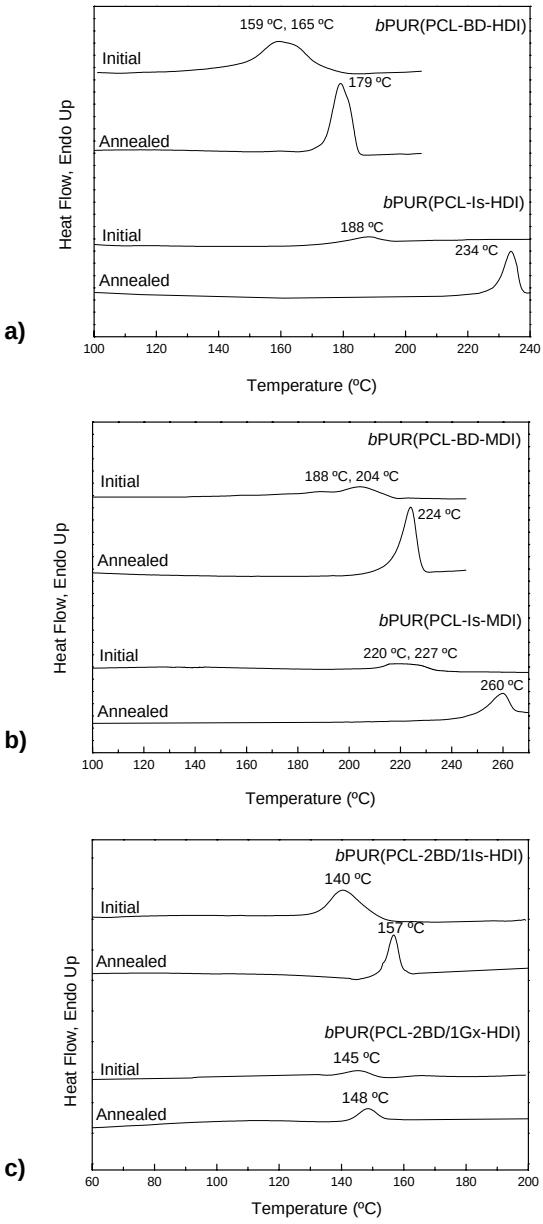

Figure 8.4. Comparative DSC traces of *b*PUR subjected to annealing treatment, **a)** replacement of BD by Is in aliphatic *b*PUR. **b)** Replacement of BD by Is in aromatic *b*PUR. **c)** Replacement of Is by Gx in aliphatic *b*PUR.

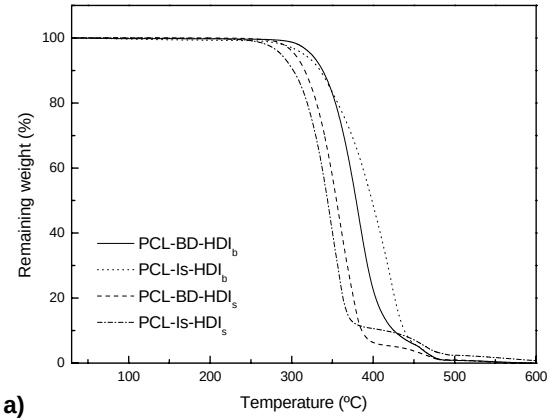
Remaining weight (%)
Temperature (ºC)
PCL-BD-HDI$_b$
PCL-Is-HDI$_b$
PCL-BD-HDI$_s$
PCL-Is-HDI$_s$

a)

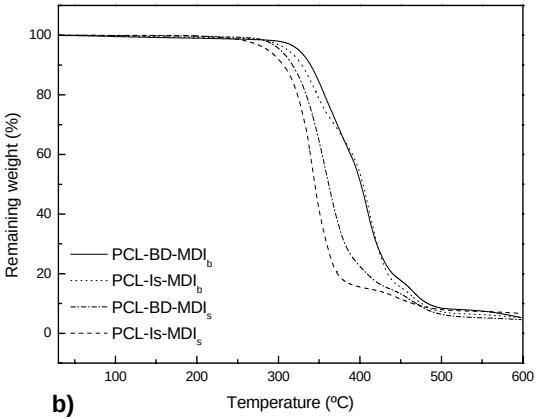
Remaining weight (%)
Temperature (ºC)
PCL-BD-MDI$_b$
PCL-Is-MDI$_b$
PCL-BD-MDI$_s$
PCL-Is-MDI$_s$

b)

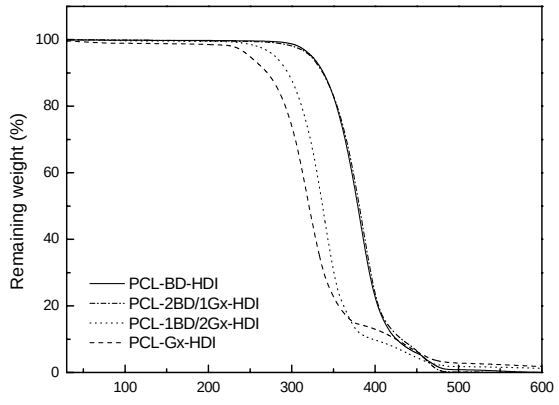
Remaining weight (%)
PCL-BD-HDI
PCL-2BD/1Gx-HDI
PCL-1BD/2Gx-HDI
PCL-Gx-HDI

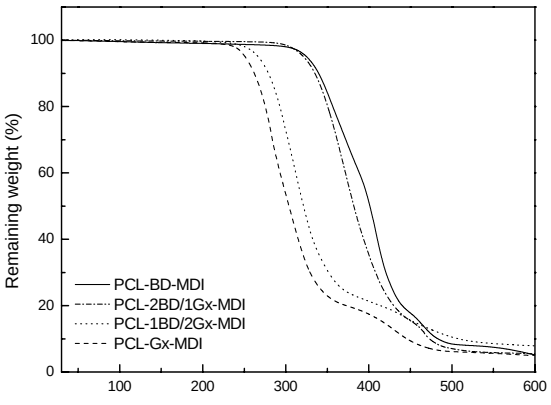
Remaining weight (%)
PCL-BD-MDI
PCL-2BD/1Gx-MDI
PCL-1BD/2Gx-MDI
PCL-Gx-MDI

Moreover, degradation takes place for *s*PUR at temperatures lower than for *b*PUR for both aliphatic and aromatic series. Replacement of 1,4-butanediol by isosorbide was found to produce a light decrease in the thermal stability reflected as a slight decay in both onset and maximum rate decomposition temperatures. Nevertheless, it is the replacement of BD by Gx units what gives place to a notable decrease in the thermal stability; such decrease is found to be more accentuated as the content in Gx units is made greater.

Table 8.4. Compared TGA results of poly(ester-urethane)s.

PUR	Inert atmosphere		
	$^{o}T_{d}$ (ºC)	$^{max}T_{d}$ (ºC)	*W* (%)
PCL	356	379, **420**	0
***s*PUR**			
PCL-BD-HDI	315	**362**, 460	0
PCL-Is-HDI	300	**352**, 463	0
PCL-BD-MDI	314	**358**, 465	5
PCL-Is-MDI	304	**346**, 467	7
***b*PUR**			
PCL-BD-HDI	334	**381**, 463	0
PCL-2BD/1Is-HDI	336	**384**, 465	0
PCL-1BD/2Is-HDI	334	**390**, 466	0
PCL-Is-HDI	310	355, **417**, 466	0
PCL-2BD/1Gx-HDI	338	**386**, 459	0
PCL-1BD/2Gx-HDI	302	**337**, 443	1
PCL-Gx-HDI	267	**319**, 442	2
PCL-BD-MDI	329	367, **408**, 466	5
PCL-2BD/1Is-MDI	329	**379**, **410**, 466	4
PCL-1BD/2Is-MDI	330	**379**, **415**, 467	5
PCL-Is-MDI	316	346, **413**, 466	5
PCL-2BD/1Gx-MDI	331	**369**, 467	6
PCL-1BD/2Gx-MDI	275	**313**, 471	8
PCL-Gx-MDI	258	**282**, **306**, 432	5

[a] Onset decomposition temperature ($^{o}T_{d}$), maximum rate decomposition temperatures ($^{max}T_{d}$) with main steps indicated in bold, and remaining weight (*W*).

Mechanical properties of segmented *b*PUR made from isosorbide were evaluated by stress-strain assays and compared to those obtained for *b*PUR made from 1,4-butanediol. Representative stress-strain plots are compared in Figure 8.6 and data are given in Table 8.5 indicating that significant changes follow substitution of BD by Is. PUR containing Is units display elastic modulus and stress-to-break increments of around 15-20% whereas the strain-to-break parameter is reduced in 3-15%; such changes are obviously due to the changes in chain stiffness introduced by the incorporation of rigid Is cyclic units. As expected, similar differences were observed when aliphatic and aromatic series are compared due in such case to the rigidity provided by MDI units.

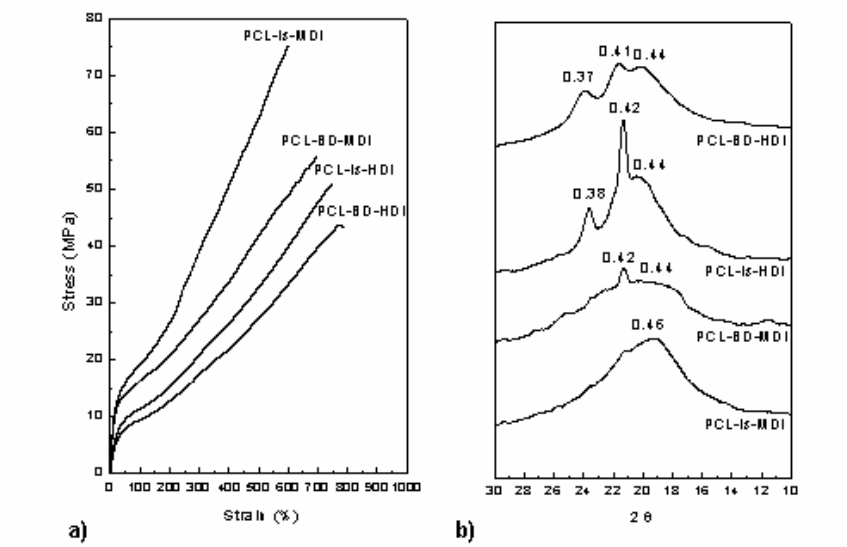

Figure 8.6. Stress-strain plot **(a)** and WAXS profiles **(b)** of *b*PUR.

A preliminary approach to the analysis of the crystalline structure of the PUR made of isosorbide was made by powder X-ray diffraction analysis. All the samples were subjected to annealing under the conditions indicated in Table 8.3 before recording diffraction data. In Figure 8.6b, the WAXS profiles of PUR-(PCL-Is-HDI) and PUR-(PCL-Is-MDI) are compared to the their homologues PUR with the hard segment entirely made of 1,4-butanediol. The most outstanding interplanar spacings measured in these profiles are compared in Table 8.5. The characteristic spacings of linear polyurethanes which are known to appear at approximately 0.44, 0.41 and 0.37 nm,[17] corresponds to the main peaks seen on the profiles of the two aliphatic PUR-(PCL-BD-HDI) and PUR-(PCL-Is-

HDI) indicating that such scattering must arise from the hard segment crystalline domains. It is worthy to note the coincidence in spacing found between the two profiles in spite that all flexible BD units have been totally replaced by cyclic rigid Is units. On the other hand, the two aromatic PUR-(PCL-BD-MDI) and PUR-(PCL-Is-MDI) present similar scattering although in this case as poorly resolved broad peaks.

Table 8.5. Mechanical properties and some structural data of bulk poly(ester-urethane)s synthesized in bulk.

*b*PUR	Stress-strain data			X-ray diffraction[a]
	E (MPa)	σ_{break} (MPa)	ε_{break} (%)	d_{hkl} (nm)
PCL-BD-HDI	43.6	44	774	0.44s 0.41s 0.37s
PCL-Is-HDI	52.3	51	750	0.44s 0.42s 0.38s
PCL-BD-MDI	113.5	56	700	0.44s 0.42s
PCL-Is-MDI	130.6	75	610	0.46s

[a]Visually estimated intensities denoted as: s, strong; m, medium; w, weak.

8.3.3. Hydrolytic degradability

The hydrolytic degradation experiments were restricted to the aliphatic poly(ester-urethane)s PUR-(PCL-BD-HDI), PUR-(PCL-Is-HDI) and PUR-(PCL-Gx-HDI) synthesized in bulk since the aim of this study was to evaluate the effect of replacing BD by the cyclic glucitols on hydrolysis rate. Assays were performed in parallel at pH 2, 7.4 and 10 and temperatures of 37 ºC and 60 ºC and the evolution of the degradation process was followed along a period of 40 days by weighting and GPC running of the residual samples at regular incubation intervals. The changes taking place in the weight and average molecular weight of the three studied PUR as a function of incubation time at 60 ºC are comparatively plotted in Figures 8.7a and 8.7b; a numerical account of degradation results for all the experiments that have been carried out is given in full detail in Table 8.6.

None of the assayed polyurethanes showed appreciable loss of weight after 40 days of incubation under any of the assayed conditions. Conversely, a noticeable decrease in the molecular weight of the three polymers was observed at 60 ºC whichever was the pH of the incubating medium; nevertheless, higher degradation rates were observed at pH 2

and 10 than at pH 7.4, which is by no means an unexpected result. The fact that such decay in molecular weight was not accompanied by any weight loss of the sample is taken as indicative that the degraded fragments remained insoluble in the aqueous medium. Regarding the extender composition, degradation was found to be faster for PUR containing Gx units than for those made of BD, the polymers made from isosorbide showing intermediate degradation rates. These results evidenced the positive although moderate influence of glucitol units on the hydrodegradability of these segmented PUR.

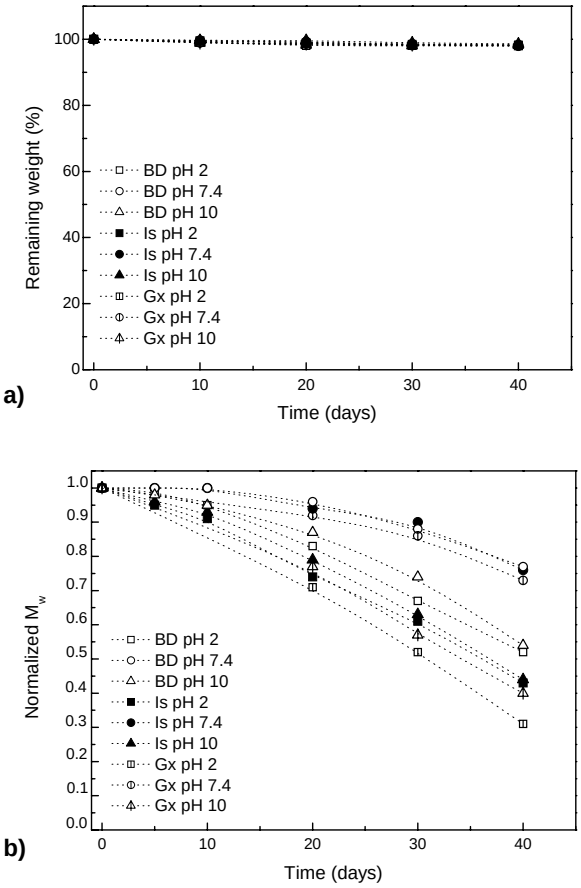

Figure 8.7. Changes in weight **(a)** and molecular weight **(b)** of aliphatic *b*PUR-(PCL-X-HDI) (X= BD or Is or Gx) at 60 ºC.

However, parallel experiments carried out on polyurethanes entirely made of Is-HDI hard segment showed total absent of degradation under similar incubation conditions (results not included). It seems therefore that degradation must take place by hydrolysis of the polyester segment rather than of the hard segment; the enhancement of hydrolysis observed for glucitol derived PUR could be interpreted therefore as a consequence of the higher hydrophilicity that the presence of such units confers to the polymer. On the other hand, the ^{1}H NMR spectrum of degraded PUR-(PCL-Gx-HDI) after incubation for 40 days at 60 ºC did not show signal arising from free hydroxyl group; it was inferred therefore that the acetal group was unperturbed along the degradation process, which is a result fully consistent with previous observations made on other acetalized polyurethanes recently reported by us.[18]

Table 8.6. Hydrolytic degradation of aliphatic poly(ester-urethane)s synthesized in bulk.

		*b*PUR-(PCL-BD-HDI)					
		pH 2		pH 7.4		pH 10	
Days		37 ºC	60 ºC	37 ºC	60 ºC	37 ºC	60 ºC
0	*W* (%)	100	100	100	100	100	100
	M_w (g·mol^{-1})	123,600	123,600	123,600	123,600	123,600	123,600
20	*W* (%)	99.8	98.2	99.8	99.3	99.7	98.0
	M_w (g·mol^{-1})	123,400	102,300	123,600	118,800	123,400	107,400
40	*W* (%)	99.2	98.2	99.2	97.9	99.1	98.0
	M_w (g·mol^{-1})	123,200	64,200	123,400	95,300	123,400	67,300
		*b*PUR-(PCL-Is-HDI)					
0	*W* (%)	100	100	100	100	100	100
	M_w (g·mol^{-1})	77,100	77,100	77,100	77,100	77,100	77,100
20	*W* (%)	99.8	99.6	99.8	99.1	99.8	98.8
	M_w (g·mol^{-1})	77,100	56,900	77,100	72,700	77,100	61,100
40	*W* (%)	98.8	98.6	99.5	98.1	99.0	98.0
	M_w (g·mol^{-1})	76,400	33,000	76,800	58,600	76,400	34,200
		*b*PUR-(PCL-Gx-HDI)					
0	*W* (%)	100	100	100	100	100	100
	M_w (g·mol^{-1})	55,100	55,100	55,100	55,100	55,100	55,100
20	*W* (%)	99.7	98.6	99.6	98.5	99.7	98.5
	M_w (g·mol^{-1})	54,500	39,100	55,100	50,700	54,900	42,400
40	*W* (%)	98.8	98.3	99.4	98.3	98.4	98.2
	M_w (g·mol^{-1})	54,900	17,000	54,200	40,200	54,400	22,000

8.4. Conclusions

The main conclusion derived from the present study can be summarized as follows:

a) Segmented poly(ester-urethane)s made of PCL soft segment and containing cyclic glucitol derived units (Is or Gx) in the hard segment could be prepared by polymerization in solution and in bulk with similar synthesis results attained in the two cases.

b) The presence of Is or Gx units did not repress the crystallinity of the PUR although the crystallizability of the hard segment became appreciably hindered; on the other side, the crystal structure did not change significantly.

c) The replacement of BD units by Is or Gx units increased the T_g of the polymer, the increment being larger for the latter. T_m also increased for a complete replacement of the BD units but decreased for intermediate substitution degrees.

d) The hydrolytic degradation of the PUR was enhanced by the presence in the chain of Is or Gx units, the effect being more noticeable for the latter. Degradation took place however by hydrolysis of the polyester soft segment without apparent breaking of the polyurethane hard segment.

8.5. References

1. Oertel, G. *Polyurethane Handbook*, Hanser Publishers, Munich **1994**.

2. Król, P. *Prog Mater Sci* **2007**, 52, 915.

3. Matsumura, S.; Soeda, Y.; Toshima, K. *Appl Microbiol Biotechnol* **2006**, 70, 12.

4. Vermette, P.; Griesser, H.J.; Laroche, G.; Guidoin, R. *Biomedical applications of polyurethanes*, Eurekah-com Publishers, Georgetown **2001**.

5. Thiem, J.; Bachmann, F. *Trend Polym Sci* **1994**, 2, 425.

6. Okada, M. *Prog Polym Sci* **2002**, 27, 87.

7. a) Bachmann, F.; Reimer, J.; Ruppenstein, M.; Thiem, J. *Macromol Rapid Commun* **1998**, 19, 21. b) Bachmann, F.; Reimer, J.; Ruppenstein, M.; Thiem, J. *J Macromol Chem Phys* **2001**, 202, 3410.

8. García-Martín, M.G.; Pérez, R.R.; Hernández, E.B.; Alla, A.; Muñoz-Guerra, S.; Galbis, J.A. *Macromolecules* **2004**, 37, 5550.

9. Yamanaka, C.; Hashimoto, K. *Polym Sci Part A: Polym Chem* **2002**, 40, 4158.

10. Yokoe, M.; Aoi, K.; Okada, M. *J Polym Sci Part A: Polym Chem* **2005**, 43, 3909.

11. Yokoe, M.; Okada, M.; Aoi, K. *J Polym Sci Part A: Polym Chem* **2003**, 41, 2312.

12. Ogata, N.; Hosoda, Y. *J. Polym Sci Part C: Polym Lett* **1976**, 14, 409.

13. Rodríguez-Galán, A.; Bou, J.J.; Muñoz-Guerra, S. *J Polym Sci: Polym Chem Ed* 1**992**, 30, 713.

14. Iribarren, J.I.; Mtz de Ilarduya, A.M.; Alemán, C.; Oraison J.M.; Rodríguez-Galán, A.; Muñoz-Guerra, S. *Polymer* **2000**, 41, 4869**.**

15. Prompers, G.; Keul, H.; Höcker, H. *Green Chem* **2006**, 8, 467.

16. Mehltretter, C. L.; Mellies, R. L.; Rist, C. E.; Hilbert, G. E. *J Am Chem Soc* **1947**, 69, 2130.

17. Saito, Y.; Nansai, S.; Kinoshita, S. *Polym J* **1972**, 3, 113**.**

18. Marín, R.; Muñoz-Guerra, S. *J Polym Sci Part A: Polym Chem* **2008**, 46, 799.

CHAPTER 9

POLYMER STEREOCOMPLEXES

Summary: *Polymer stereocomplexation or stereocomplex formation is the specific interaction that takes place between the two components of an enantiomeric pair of polymers resulting in a structurally well defined system that displays properties different from the separated pure components. The first example of stereocomplexation for enantiomeric polymers, i.e. between R- and S-configurated (or L- and D-configurated) polymer chains, was reported by Pauling and Corey for the polypeptide poly(benzyl glutamate) in 1953. In the last years, stereocomplexes were also reported from other polymer families. In this introductory chapter, the most representative stereocomplexes described in the scientific literature, their structure, properties and applications, mainly as matrices for drug controlled release, are described.*

9.1. Introduction

A polymer stereocomplex is defined as a stereoselective interaction between two complementing stereoregular polymers, which interlock and form a new composite, displaying altered physical property in comparison to the parent polymers. The complementing polymer molecules can be a pair of isotactic or syndiotactic, not necessarily optically active polymers, or two opposite enantiomeric, optically active polymer chains with identical chemical compositions, or similar but not identical chemical structure. A third group consists of heterostereocomplexes formed by polymers from different polymer families (like polyesters and polyamides) having opposite stereoregular configuration. Complexes of two opposite enantiomers are mostly referred to as homo-stereocomplexes.

Probably one of the earliest reports on the phenomenon of altered physical properties when mixing D- and L- polypeptides is by Pauling and Corey who described in 1953 the "antiparallel chain rippled sheet" formed by a mixture of D- and L- polypeptides in a new structure consisting of D-chains alternating with L-chains.[1] Consecutive articles dealt with various measurements of these mix-compounds, in particular poly(γ-benzyl L- and D-glutamate).[2,3]

Syndiotactic and isotactic PMMA, were the first pair of polymers reported to form a so-called stereocomplex. Since the discovery of this stereocomplex in 1958 by Fox *et al*.,[4] numerous studies were performed on the characterization and structure analysis of this and other related acrylic polymer stereocomplexes. Almost simultaneously stereocomplexes from other polymer families were also reported. Most of them consisted of a pair of complementary enantiomeric polymers.

9.2. Characterization of stereocomplexes

Stereocomplexes generally show a different physiochemical behaviour compared to their parent polymers. Most complexes are insoluble in those solvents that dissolve the parent polymers and display an upward shift in melting temperature.[5,6]

Differences between the stereocomplexes and its components are usually observed in the nuclear magnetic resonance (NMR), X-ray or IR spectra. The physical methods used

for the characterization and visualization of the stereocomplexes can roughly be divided into four groups: spectroscopic techniques (SAXS, WAXS, fluorescence, NMR, FTIR), thermodynamic techniques (DSC, turbidity, sedimentation), mechanical studies (tensile strength, osmometry, viscosimetry, rheology, chromatography), and imaging techniques (SEM, AFM).

9.3. Polymeric stereocomplexes

9.3.1. Polylactones/polyesters

Homo-stereocomplexes are found among those polyesters with at least one chiral center in the backbone of the repeating unit. The obtained isotacticity is a function of the enantiomeric excess of used monomers.[7] Stereocomplexes of this group of polymers are obtained between D- and L-isotactic polymers. The best-known polymeric system in this group is that composed of poly(lactic acid)s, which will be presented in section 9.4.

Blends of isotactic poly(α-methyl-α-ethyl-β-propiolactone)s (PMEPL) of opposite configurations and high optical purities lead to the formation of a stereocomplex. The complex was shown to melt at 40 ºC above the melting temperature of the corresponding parent polymers and characterized by a different X-ray diffraction pattern. The stereocomplex exhibited much larger spherulites than their corresponding polymers. However, the melting point of the complex and the size of the spherulites decreased with the decrease of tacticity of one of the polymer chains. The stereocomplex was always preferentially formed over the crystallization of the isotactic polymers, even in the non-equimolar blends, over a wide range of concentrations.[8]

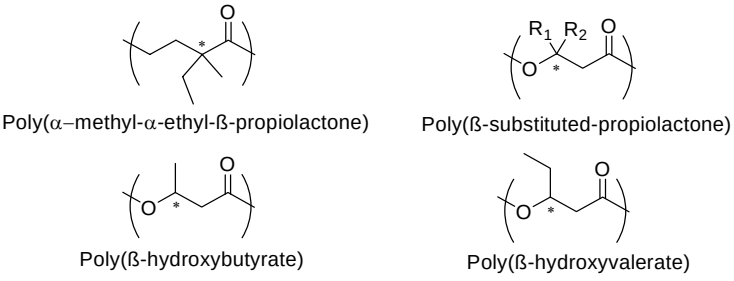

Scheme 9.1. Chemical structures of polyesters.

Figure 9.1 shows the DSC melting curves of the polymer PMEPL and some of the mixtures of *R* and *S*. Several blends exhibit a melting temperature above those of the corresponding parent polymers. For example, 50% blends of PMEPL-97R/99S, PMEPL-97R/75S, and PMEPL-97R/55S melt at 196, 180, and 172 ºC, respectively, which are 32, 16, and 8 ºC above the melting temperature of the PMEPL-97R polymer.

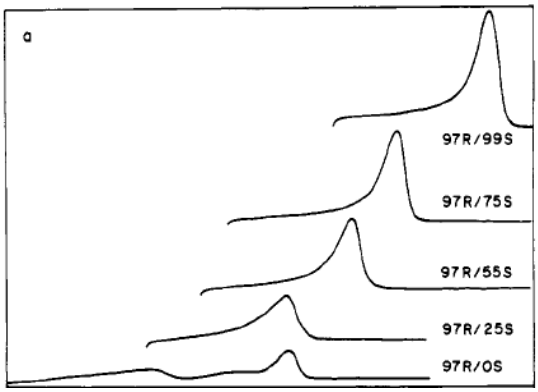

Figure 9.1. DSC curves of PMEPL blend samples registered at 20 ºC·min^{-1}(blends containing 50% PMEPL-97R and PMEPL-*n*S with different enantiomeric content (*n*) of *S*).[8]

Stereocomplexes were also obtained from isotactic chains of β-substituted poly (β-propiolactones) bearing dichloroethyl or dichloropropyl substituents which were synthesized from racemic mixtures of monomers. Melting temperatures of these complexes were found to be about 60 and 80 ºC higher than the corresponding parent polymers, respectively.[9]

9.3.2. Polypeptides and polyamides

Complexes of poly(γ-benzyl L- and D-glutamate) were described in 1961 by Tsuboi *et al*. noticing differences in the IR spectra of a dicholoroethane solution of an equimolar mixture of the two components, compared to the solutions of the isotactic or the racemic polymer.[3] The benzyl side-chain interactions between helices of the two enantiomers in the stereocomplex were studied by X-ray diffraction and IR spectroscopy. A model of the stereocomplex was proposed in which the enantiomeric polymer helices intertwined

forming a double helix with about 7.2 monomers per turn in a hexagonal or tetragonal packing.[2,10] Thermal behaviour studies of these stereocomplexes were performed by Baba and Kagemoto,[11] who reported a dissociation temperature of 100 ºC.

The only non-polypeptidic polyamide reported to form stereocomplexes is the optically active polyamide made from 2,3-di-*O*-methyl D- and L-tartaric acids and 1,6-hexamethylenediamine. On the basis of X-ray, transmission electron microscopy, ^{13}C CP-MAS NMR, and computational modelling, the crystal structure of the equimolar mixture of poly(hexamethylene-di-*O*-methyl-D- and L-tartaramide)s could be satisfactorily represented by a monoclinic unit cell containing two enantiomeric chains related by a glide plane. Energy calculations corroborated the ability of D- and L-tartaric units to cocrystallize without significant distortion of the geometry of the crystal lattice. The melting point of the D- and L-polymer mixture was determined to be 250 ºC, significantly higher than the melting temperature of its components which is around 232 ºC.[12]

Poly(γ -benzyl glutamate)

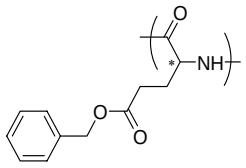

Poly(hexamethylene-di-*O*-methyl tartaramide)

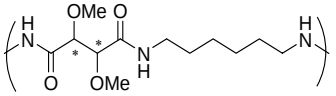

Scheme 9.2. Chemical structures of polypeptides and polyamides.

The finding of poly(tartaramide)s stereocomplex was considered to be of particular relevance because of the high density of stereocenters present in the polymer chain and the repercussion that it may have on the design of crystalline polyamides from multichiral monomers.

9.3.3. Polyketones

Jiang and Sen reported about a novel catalyst[13] enabling enantioselective synthesis of a series of α-olefin-carbon monoxide co-polymers, such as *R*- and *S*-poly(propylene

carbon monoxide). Stereocomplexes were obtained from a chloroform-hexafluoroisopropanol-methanol solution mixture, showing a higher melting temperature than the parent enantiomers. Also combinations of closely related polymers with opposite chirality, *i.e.* poly((+)-propylene-carbon monoxide) with poly((-)-1-butene-carbon monoxide) were found to form a stereocomplex with an elevated melting temperature.

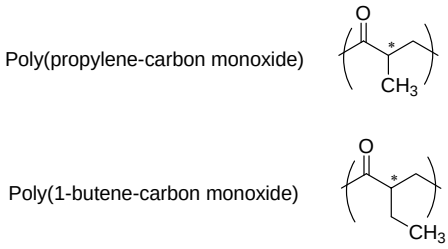

Scheme 9.3. Chemical structures of polyketones.

9.3.4. Polyethers and polysulfides

Pure *R* and *S* poly(epichlorohydrine) (PRECH and PSECH) enantiomers have been shown to form stereocomplex. Throughout the papers published on homo-stereocomplexes of D- and L-poly(epichlorohydrine), it was compared to the poly(epichlorohydrine) stereoblock-copolymer.[14,15] The spherulite radial growth rates of the 50:50 blend of the enantiomeric polymers were found to be depressed in relation to those of either of the optically pure components. A further marked reduction in growth rates was recorded for the stereoblock polymer. The optically active polymers developed regularly banded spherulites, while an equimolar blend of both enantiomers and the stereoblock copolymer formed non-banded spherulites (Figure 9.2).

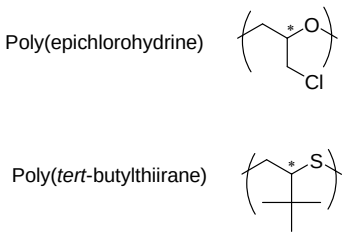

Scheme 9.4. Chemical structures of polyethers and polysulfides.

On the other side, Matsubayashi *et al.*[16] used a stereoselective mechanism in the polymerization of racemic monomer to prepare poly(*tert*-butylthiirane) composed essentially of a statistical mixture of *R* and *S* isotactic polymer chains.[17] The racemic mixture was more stable toward melting than the optically active *R* enantiomeric polymer, with a 40 ºC difference in the melting temperature. It was concluded from X-ray diffraction studies that the optically active enantiomer crystallized in a trigonal crystal lattice composed of three right-handed 3_1 helices with statistical up and down packing, while the racemic polymer mixture co-crystallized in a monoclinic crystal lattice.[16]

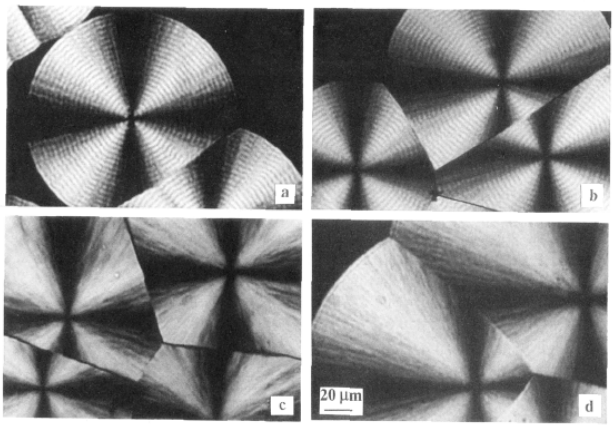

Figure 9.2. Polarized light photomicrographs of spherulites of optically active P*R*ECH **(a)**, P*S*ECH **(b)**, the stereoblok *i*-P*RS*ECH **(c)**, and the 50:50 blend of the polyenantiomeric pair **(d)**; crystallized at 80 ºC.[14]

9.3.5. Poly(methyl methacrylate)

PMMA homo-stereocomplexes were first described by Fox *et al*., who suggested the formation of a stereoblock-copolymer on the basis of X-ray diffraction data.[4] This was generally accepted for a few years until Liquori *et al.* launched the novel idea of a "polymer unit", a so-called stereocomplex, consisting of a 2:1 complex of syndiotactic and isotactic homopolymers.[18]

These stereocomplexes were characterized by a range of analytical methods summarized in a comprehensive review on aggregation of PMMA published by

Spevacek and Schneider.[19] Many observations on PMMA stereocomplex formation were based on viscosimetry and the solvent nature was found to affect complex formation.

The stereocomplexation of PMMA was also studied by size-exclusion chromatography and dynamic light scattering, yielding “viscosity” size distributions of polymer complexes (weight and intensity defined as a function of molecular/particle weight).[20]

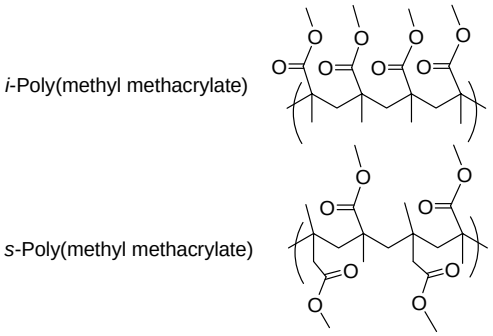

Scheme 9.5. Isotactic and syndiotactic PMMA.

The stereocomplex was actually obtained by mixing dilute solutions of the isotactic and syndiotactic polymers in dimethylformamide or acetonitrile. Upon mixing concentrated equimolar solutions of the two stereoregular PMMA polymers a gel was obtained consisting of a network in which small crystalline regions are assumed to play the role of cross-link points.[21] The occurrence of multifunctional branch points, due to the association of syndiotactic and isotactic sequences, were elucidated in more detail by Mrkvickova *et al.*[20] The viscous solution enabled fiber spinning from which an X-ray diffraction pattern differing from either of the parent polymers was obtained.[18] The rheological behaviour of these concentrated solutions was also investigated; it was discovered that the flow stream of stereocomplex gel proceeded with decompositions of strong intermolecular bonds.

The earliest schematic presentation of the PMMA stereocomplex was proposed by Liquori *et al.*[18] in which the groves of neighbouring helical stereoregular isotactic polymer chains are joined by interlocking syndiotactic polymer chains (Figure 9.3). Further investigations by Bosscher *et al.*[22] led to the conclusion that the PMMA homo-stereocomplex consists of a double stranded helix in which a helix of *i*-PMMA of small

radius is surrounded by a helix with larger radius of *s*-PMMA. The double-stranded helix was first proposed to be composed of a helix of an isotactic chain with a small radius (30/4 helical conformations), which is surrounded by a syndiotactic chain with a large radius (60/4 helical conformations) (Figure 9.3). Later, Schomaker and Challa proposed a revised helix model with 9/1 helical symmetry.[23]

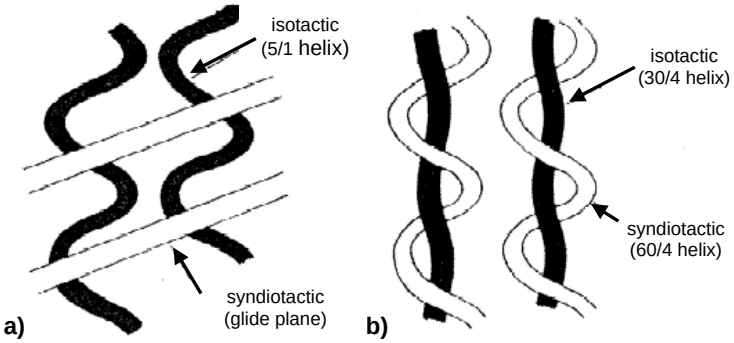

Figure 9.3. Schematic representation of chain assembly in the crystalline stereocomplex of PMMA.[19] Model proposed by Liquori *et al*. **(a)**,[18] and model proposed by *Bosscher et al.* **(b)**.[22]

Three models have been proposed for the interaction in the double helix of PMMA: (a) ester group interaction of both isotactic and syndiotactic chains, (b) ester group of isotactic chains with α-methyl group of syndiotactic chains, and (c) stereocomplex formation due to a favourable steric fit. The Quasielastic Neutron Scattering (QUENS) evidenced that the *i*-PMMA methyl ester group was involved in such interaction.[24]

9.4. Biodegradable PLA stereocomplexes

Poly(lactic acid) (PLA) and its copolymers have been widely used in various medical applications, including absorbable sutures, temporary implants and drug carriers.[25-27] Comprehensive reviews about PLA homo- and co-polymers synthesis as well as material design of PLA systems were published by Spinu *et al.*[6] and Stridsberg *et al.*[28]

Since the first report published in 1987 most of the research conducted on the synthesis, physical and chemical characteristics of the PLA homostereocomplex has been conducted by the research group of Ikada and co-workers.[29-40] Several procedures for complex formation as well as some of its applications were patented by Dupont.[41] The

PLA stereocomplex consists of poly(D-lactic acid) and poly(L-lactic acid) in a 1:1 ratio. Main characteristics of the PLA homo-stereocomplex are its higher melting temperature (about 50 ºC above that of PLA) and its insolubility in the common PLA solvents.[6]

PLA homo-stereocomplex formation from a solution of the two enantiomorphs in chloroform was observed to proceed at room temperature at a very low rate. Complexation was noticed as the formation of a precipitate after about 30 days. For high-molecular-weight PLA, the complexation reaction took even longer, up to one year. As the ratio of L-PLA and D-PLA approached to 1:1 the complex was formed more rapidly and more completely.[35] Precipitation of a mixture of D-PLA and L-PLA from a dichloromethane, chloroform or dioxane solution upon pooring into a non-solvent like methanol or ether also yielded the stereocomplex.

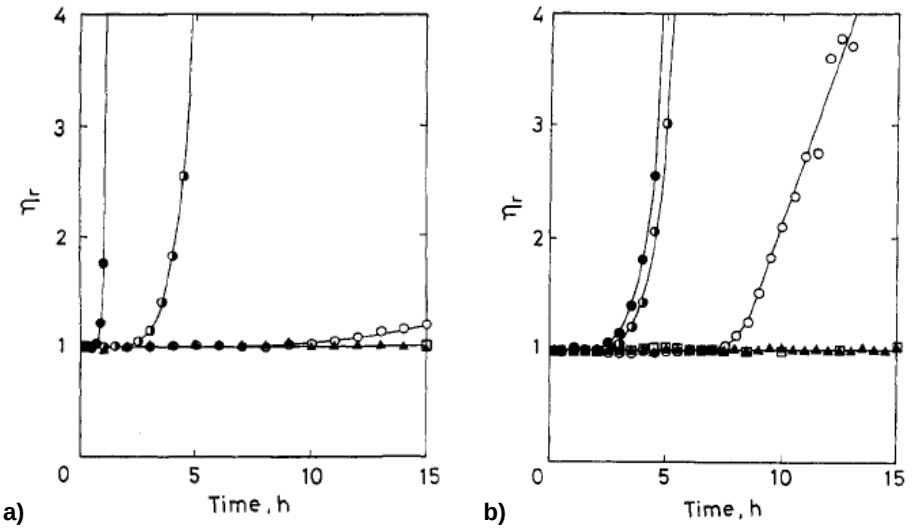

Figure 9.4. a) Relative viscosity of solutions of D- and L-PLA 1:1 mixture (X_D=0.5, 25 ºC) as a function of standing time at different concentrations: ■: 7.5 g·dL^{-1}, ▲: 10.0 g·dL^{-1}, ○: 12.5 g·dL^{-1}, ◑: 15.0 g·dL^{-1}, and ●: 17.5 g·dL^{-1}. **b)** Relative viscosity of solution mixtures of D- and L-PLA as a function of standing time at different X_D (15.0 g·dL^{-1}, 25 ºC): ●: 0.5, ◑: 0.6, ○: 0.7, ▲: 0.8, □: 1.[35]

Figure 9.4a shows the viscosity of solutions of an equimolar mixture of D-PLA and L-PLA in chloroform at different polymer concentrations and at 25 ºC as a function of standing time, the initial viscosity being set to unity. An appreciable viscosity rise is observed at polymer concentrations higher than 12.5 g·dL^{-1}. Figure 9.4b shows the relative viscosity

of solutions of mixtures of D-PLA and L-PLA at different D/L ratios (X_D). For solutions with X_D values of 0.5, 0.6, and 0.7, a viscosity rise is observed after short induction periods followed by gelation.

Formation of homo-stereocomplexes from the molten state was studied using DSC and polarizing microscopy; it occurred predominantly upon annealing the polymer mixtures provided that the molecular weight of both D-PLA and L-PLA was below 6 kDa and for D/L ratios from 4:6 to 6:4. In contrast, homo-crystallization of D-PLA and L-PLA prevailed for D/L ratios out of such range or when the molecular weight of any of the two components was higher than 100 kDa. The critical molecular weight for stereocomplex formation was lower in stereocomplexation by crystallization from the melt (6 kDa) than by casting from solution (40 kDa).

The structure of L-PLA was reported to consist of left handed helical chains with 3.3 monomers per turn (10_3-helix), whereas D-PLA consisted of a 10_7 helices.[42] Okihara *et al.* found that PLA-stereocomplex crystallized in triangular lamellar crystals, and reported about the occurrence of lattice disorders in the crystalline structure. The crystal structure was determined to be composed of a triclinic unit cell with left-handed 3_1 helices (β-conformation) of one enantiomeric polymer packed with right-handed helices of the other.[43,44] Figure 9.5a shows the lamellar stereocomplex crystals showing the uncommon triangular shape. Conversely, the single-component crystals of L-PLA display the familiar lozenge shape (Figure 9.5b). Apparently, the L-PLA and D-PLA chains pack differently in their pure enantiomeric crystals than in the stereocomplex, with the subsequent displaying of different morphologies.

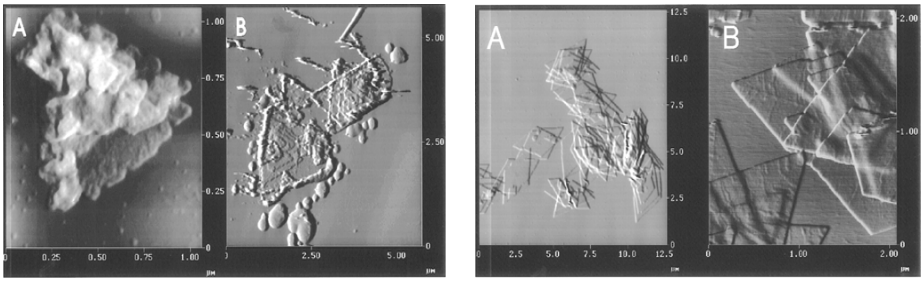

a) **b)**

Figure 9.5. AFM images of single crystals of PLA-stereocomplex **(a)**, and L-PLA **(b)**.[44]

The hydrolytic degradation of PLA, both enantiomerically pure or as sterecomplex, proceeds in two phases: (1) hydrolysis of the amorphous regions, and (2) degradation of the crystalline segments. The degradation is influenced by various factors: configuration, molecular weight and its distribution, sample texture and shape, and environmental conditions. Two types of erosions were reported to occur: surface erosion for melt-crystallized L-PLA, incubated in dilute alkaline solution (pH 12), and bulk erosion for both the PLA-stereocomplex and the L-PLA polymer incubated at pH 7.4. Hydrolysis of the PLA stereocomplex clearly showed a lower degradation rate compared to isotactic D- and L-PLA.[40] Comparative degradation of PLA and its stereocomplex is showed in Figure 9.6.

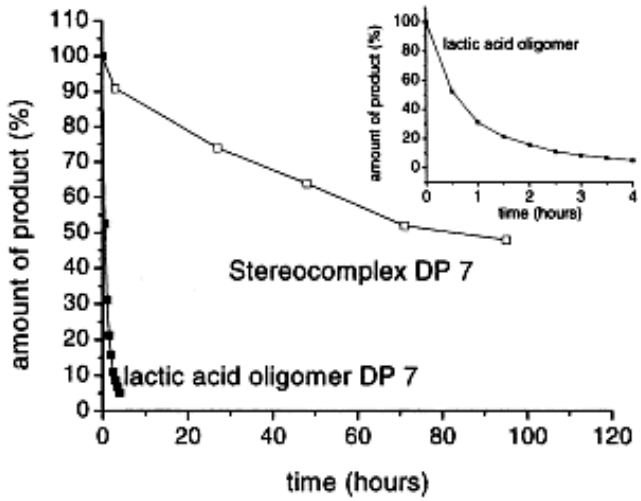

Figure 9.6. Degradation profiles of lactic acid oligomers, and their blend (stereocomplex) of L- and D-forms at pH 7 and 37 ºC.[45]

9.5. Poly(hexamethylene-di-*O*-methyl-tartaramide)s stereocomplex. Previous studies

The repeating unit of poly(alkylene-di-*O*-methyl tartaramide)s (P*n*DMLT where *n* stands for the number of carbons contained in the alkylene segment) contains two vicinal asymmetric backbone carbons in *threo* configuration (Scheme 9.6). Since L-tartaric acid has C2 symmetry, no configurational disorder due to orientation effects is expected to occur in the growing polytartaramide chain during polycondensation. Accordingly,

stereoregular polymers with a *threo*-diisotactic microstructure are obtained provided that no racemization takes place in the polymerization reaction.

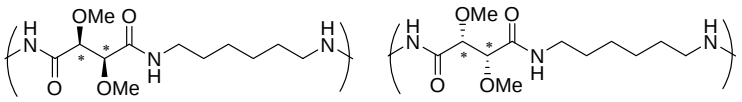

Scheme 9.6. Chemical structures of polytartaramides.

P*n*DMT are highly crystalline polymers, which is by no means a property usually found among substituted polyamides.[46] Some years ago, Iribarren *et al.*[12,47] investigated the crystal structure of pure enatiomeric polyamides P6DMT(D) and P6DMT(L), and their equimolar mixture P6DMT(D+L) by combining X-ray diffraction, electron microscopy, ^{13}C CP-MAS NMR, and computational modelling methods.

The three systems were shown to be highly crystalline; the melting point of the equimolar mixture was 250 °C, considerably higher than the melting temperature of the diisotactic homopolymers which is 232 °C. A comparative diffraction analysis was performed on powders, fibers, and single crystals for the three systems. Data collected from the different types of diagrams were almost coincident in showing that the geometry and parameters of the lattice are very similar for the three cases. However, the presence of an additional reflection in the diagrams arising from P6DMT(D+L) together with some slight variations in the intensity of the scattering profile were significant features distinguishing the mixed system from P6DMT(D) and P6DMT(L) (Figure 9.7).

Such differences were interpreted to be due to the higher crystal symmetry associated to the optically compensated systems. On the other hand, AM1 energy calculations for the polyamide chain showed that the conformation preferred by the polytartaramide is the same for both P6DMLT(D) and P6DMLT(D+L). In such arrangement, the tartaric acid moiety is in *gauche* conformation and the amide group is rotated out of the plane of the polymethylene segment, which is in a fully extended *all-trans* conformation. NMR results were in agreement with the conclusions drawn from the conformational analysis; they corroborated the structural differences between the optically pure polymers and the optically compensated system earlier evidenced by diffraction experiments.

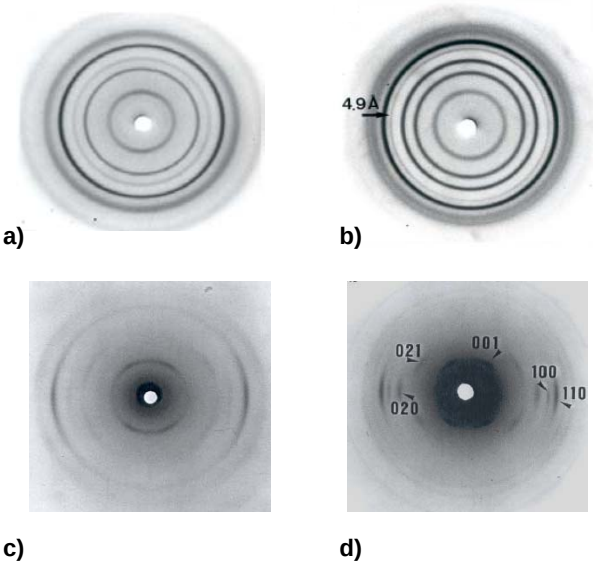

Figure 9.7. X-ray diffraction patterns of crystal sediments of P6DMT(L) **(a)**, and P6DMT(D+L) **(b)**; and fiber X-ray diagrams of P6DMT(L) **(c)**, and P6DMT(D+L) **(d)**. The (100) reflection spacing (0.49 nm) is only seen in P6DMT(D+L).

A triclinic unit cell in the space group *P1* containing one chain was put forward for P6DMT(L). The dimensions of the unit cell are a = 0.50 nm, b = 0.68 nm, c= 1.32 nm, α = 61.5°, β = 90.0°, and γ = 111.6°. Computational modelling showed that the structure may be described as a stack of hydrogen-bonded sheets staggered in a regular manner with features reminiscent of both the β-pleated sheet form of polypeptides and the triclinic α-form of nylon 66. Modelling simulation methods allowed to build the crystal structure of P6DMT(D+L) as a monoclinic lattice in the space group *P*1b1 containing two chains which are related by a glide plane parallel to the *b* axis of the crystal (Figure 9.8). It should be remarked that the essentials of the structures, *i.e.* the scheme in which hydrogen bonds are arranged and chain conformation are common for both lattices. These results prove that the isomorphic replacement between D- and L-tartaric units in poly(hexamethylene di-*O*-methyltartaramide)s is feasible without altering substantially the side-by-side packing of the chains.

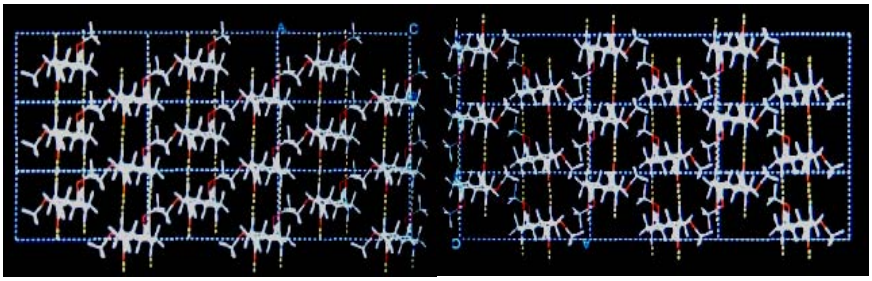

a) **b)**

Figure 9.8. Projection down the *c* axis of the simulated crystal structure for P6DMT(L) **(a)**, and P6DMT(D+L) **(b)**.

9.6. Applications and perspectives of stereocomplexes

The phenomenon of stereocomplex formation has been described for different classes of polymers, including polyesters, polyamides, polyketones, polyethers and polysulfides;[48] but only sporadic examples of stereocomplexes used for drug controlled release, tissue engineering or other biomedical purposes have been reported so far.[49]

In most reports on drug controlled release from sterecomplexes, the polymer-matrix was based on enantiomeric PLA. Related to PLA-stereocomplexes, but forming a phenomenon on their own, are the heterostereoselective complexes obtained from D-PLA and L-configured peptides. Spontaneously formed particles made from such heterocomplex with uniform size and a porous texture have been shown to deliver their peptide content in a first-order controlled release over a period of 1-3 months. This phenomenon may be generalized to complexes between any pairs of polymers and biological macromolecules with opposite chirality. Therefore this discovery opens up many future perspectives both in stereoselective polymers and biomacromolecules and, more specifically, in possible occurrences of these complexes among biopolymers in living organisms. Moreover, the field of stereocomplexes in general and of stereoselective peptide-polymer complexes in particular, has many potentials as a model system for studying polymer interactions as well as other applications in the biomedical sciences.

9.7. References

1. Pauling, L.; Corey, R.B. *Proc Natl Acad Sci Wash* **1953**, 39, 253.

2. Mitsui, Y.; Iitaka, Y.; Tsuboi, M. *J Mol Biol* **1967**, 24, 15.

3. Tsuboi, M.; Wada, A. *J Mol Biol* **1961**, 3, 480.

4. Fox, T.G.; Garrett, B.S.; Goode, W.E.; Gratch, S.; Kincaid, J.F.; Spell, A.; Stroupe, J.D. *J Am Chem Soc* **1958**, 80, 1768.

5. Grenier, D.; Prud'homme, R.E. *J Polymer Sci Polym Phys* **1984**, 22, 577.

6. Spinu, M.; Jackson, C.; Keating, M.Y.; Gardner, K.H. *J Macromol Sci-Pure Appl Chem* **1996**, A33, 1497.

7. Albertsson, A.-C.; Varma, I.K. *Adv Polym Sci* **2001**, 157, 1.

8. Lavallee, C.; Prud'homme, R.E. *Macromolecules* **1989**, 22, 2438.

9. Voyer, R.; Prud'Homme, R.E. *Eur Polym J* **1989**, 25, 365.

10. Squire, J.M.; Elliott, A. *J Mol Biol* **1972**, 65, 291.

11. Baba, Y.; Kagemoto, A. *Macromolecules* **1977**, 10, 458.

12. Iribarren, I.; Aleman, C.; Regano, C.; de Ilarduya, A.M.; Bou, J.J.; Muñoz-Guerra, S. *Macromolecules* **1996**, 29, 8413.

13. Jiang, Z.; Sen, A. *J Am Chem Soc* **1995**, 117, 4455.

14. Singfield, K.L.; Brown, G.R. *Macromolecules* **1995**, 28, 1290.

15. Singfield, K.L.; Brown, G.R. *J Mater Sci* **1999**, 34, 1323.

16. Matsubayashi, H.; Chatani, Y.; Tadokoro, H.; Dumas, P.; Spassky, N.; Sigwalt, P. *Macromolecules* **1977**, 10, 996.

17. Dumas, P.; Spassky, N.; Sigwalt, P. *Makromol Chem* **1972**, 156, 55.

18. Liquori, A.M.; Anzuino, G.; Coiro, V. M.; D'Alagni, M.; de Santis, P.; Savino, M. *Nature* **1965**, 206, 358.

19. Spevacek, J.; Schneider, B. *Adv Coll Int Sci* **1987**, 27, 81.

20. Mrkvickova, L.; Porsch, B.; Sundelof, L.O. *Macromolecules* **1999**, 32, 1189.

21. Grohens, Y.; Castelein, G.; Carriere, P.; Spevacek, J.; Schultz, J. *Langmuir* **2001**, 17, 86.

22. Bosscher, F.; Ten Brinke, G.; Challa, G. *Macromolecules* **1982**, 15, 1442.

23. Schomaker, E.; Challa, G. *Macromolecules* **1989**, 22, 3337.

24. Pillay, R.; Arrighi, V.; Kagunya, W.; Higgins, J.S. *Macromol Symp* **2001**, 166, 269.

25. Von Schroeder, H.P.; Kwan, M.; Amiel, D.; Coutts, R.D. *J Biomed Mater Res* **1991**, 25, 329.

26. Okada, H. *Adv Drug Deliv Rev* **1997**, 28, 43.

27. Kissel, T.; Brich, Z.; Bantle, S.; Lancrajan, I.; Nimmerfall, F.; Vit, P. *J Control Release* **1991**, 16, 27.

28. Stridsberg, K.M.; Ryner, M.; Albertsson, A.-C. *Adv Polym Sci* **2001**, 157, 41.

29. Ikada, Y.; Jamshidi, K.; Tsuji, H.; Hyon, S.-H. *Macromolecules* **1987**, 20, 904.

30. Tsuji, H.; Horii, F.; Nakagawa, M.; Ikada, Y.; Odani, H.; Kitamaru, R. *Macromolecules* **1992**, 25, 4114.

31. Tsuji, H.; Ikada, Y. *Polymer* **1999**, 40, 6699.

32. Tsuji, H.; Hyon, S.H.; Ikada, Y. *Macromolecules* **1992**, 25, 2940.

33. Tsuji, H.; Hyon, S.H.; Ikada, Y. *Macromolecules* **1991**, 24, 5651.

34. Tsuji, H.; Hyon, S.H.; Ikada, Y. *Macromolecules* **1991**, 24, 5657.

35. Tsuji, H.; Horii, F.; Hyon, S.H.; Ikada, Y. *Macromolecules* **1991**, 24, 2719.

36. Tsuji, H.; Ikada, Y. *Macromolecules* **1992**, 25, 5719.

37. Tsuji, H.; Ikada, Y. *Macromolecules* **1993**, 26, 6918.

38. Tsuji, H.; Ikada, Y. *J Appl Polym Sci* **1994**, 53, 1061.

39. Tsuji, H.; Ikada, Y.; Hyon, S.H., Kimura, Y.; Kitao, T. *J Appl Polym Sci* **1994**, 51, 337.

40. Tsuji, H. *Polymer* **2000**, 41, 3621.

41. Spinu, M. *Manufacture of Polylactide Stereocomplexes*, Du Pont de Nemours & Co., US Patent 5,317,064, **1994**.

42. De Santis, P.; Kovacs, A.J. *Biopolymers* **1968**, 6, 299.

43. Okihara, T.; Tsuji, M.; Kawaguchi, A.; Katayama, K.; Tsuji, H.; Hyon, S.H.; Ikada, Y. *J Macromol Sci-Phys* **1991**, B30, 119.

44. Brizzolara, D.; Cantow, H.J.; Diederichs, K.; Keller, E.; Domb, A.J. *Macromolecules* **1996**, 29, 191.

45. De Jong, S.J.; Van Eerdenbrugh, B.; Ban Nostrum, C.F.; Kettenes-Van de Bosch, J.J.; Hennink, W.E. *J Control Release* **2001**, 71, 261.

46. Bou, J.J.; Rodríguez-galán, A.; Muñoz-Guerra, S. *Macromolecules* **1993**, 26, 5664.

47. Iribarren, I.; Aleman, C.; Bou, J.J.; Muñoz-Guerra, S. *Macromolecules* **1996**, 29, 4397.

48. Slager, J.; Domb, A.J. *Adv Drug Deliv Rev* **2003**, 55, 549.

49. Slager, J.; Domb, A.J. *Biomaterials* **2002**, 23, 4389.

CHAPTER 10

STEREOCOMPLEX FORMATION FROM ENANTIOMERIC POLYAMIDES DERIVED FROM TARTARIC ACID *

Purpose and specific aims: *The target of this work was the study of the preparation method and crystallizability of the stereocomplex from two enantiomeric polytartaramides. DSC, X-ray diffraction, and polarizing optical microscopy were used for this purpose. Additionally, the possible stereocomplex formation in other closely related polytartaramides was a explored.*

Summary: *The formation of stereocomplexes from the pair of enantiomorphs of the chiral polyamide poly(hexamethylene di-O-methyl tartaramide) was investigated for a variety of experimental conditions. DSC and X-ray diffraction data evidenced that efficiency in enantiomeric coupling is highly sensitive to the procedure used for preparing the complex. A comparative isothermal crystallization study revealed that the stereocomplex crystallized from the melt at lower rate than the enantiomerically pure components. The radial growth of individual spherulites was also delayed in the crystallization of the complex. No evidence of stereocoupling was detected for other poly(alkylene di-O-methyl tartaramide)s with the alkylene unit length different from six. It was concluded that molecular interlocking of hydrogen-bonds in the enantiomeric pair is highly selective in this family of polymers.*

* Publication derived from this work: Marín, R.; Alla, A.; Muñoz-Guerra, S. *Macromol Chem Rap Comm* **2006**, 27, 1955.

10.1. Introduction

Polymer stereocomplexes result from the stereoselective interaction between two complementing stereoregular polymers. The force of complexation may come from electrostatic interactions, hydrogen-bonding formation, or stereospecific Van der Waals interactions. Interlocking of the chains gives rise to a supramolecular composite differing in crystal structure and physical properties from the parent polymers. Stereocomplexes made of biocompatible polymers are looked with particular interest because of their potential as matrices for controlled drug delivery systems, tissue engineering or other biomedical purposes.[1] A particular class of stereocomplexes is that constituted by pairs of opposite enantiomeric polymers, which have been referred in the literature as homo-stereocomplexes.[1,2] Historical examples of complexes made of polymeric enantiomeric pairs are D- and L-poly(γ-benzylglutamate)s,[3,4] *R* and *S* poly(α-methyl-α-ethyl-propiolactone)s[5,6] and D- and L-poly(lactic acid)s.[7,8] However, formation of homo-stereocomplexes is by no means always possible and there are a good number of cases in which the two opposite enantiomeric chains fail to interlock and prefer to crystallize in separate crystalline domains. Well known examples of systems displaying such behaviour are poly(β-alkanoate)s[9] and polyethers.[10,11]

Some years ago, Iribarren *et al.* reported on the homo-stereocomplex made of enantiomeric D and L poly(hexamethylene di-*O*-methyltartaramide)s (P6DMT), a pair of stereoregular polyamides of AA-BB type prepared from 1,6-hexamethylenediamine and di-*O*-methyl D- and L-tartaric acids.[12]

On the basis of X-ray diffraction, DSC and CP-MAS NMR data, the existence of an equimolar stereocomplex melting approximately 20 ºC above the separate components was ascertained. The crystal structure of the stereocomplex was described by a monoclinic lattice with a unit cell containing two enantiomeric chains related by a glide plane. Computational analysis assessed the ability of the D- and L-tartaric units to cocrystallize in an energetically favoured crystal structure without severe distortion of the lattice geometry. To our knowledge, this is the only case reported so far on the formation of homo-stereocomplexes made of non-polypeptidic chiral polyamides.

In this chapter, the influence of the preparation method on the formation of the P6DMT(D+L) stereocomplex is firstly evaluated. Secondly, the crystallization behaviour

of the complex is thoroughly examined and compared to that displayed by the enantiomerically pure components. Finally, the stereocomplex formation from enantiomeric pairs of other closely related poly(tartaramide)s (P*n*DMT with *n* = 5 and 8) is explored.

10.2. Experimental Section

Poly(tartaramide)s P*n*DMT studied in this work were synthesized by polycondensation in solution of the corresponding α,ω-diamines and pentachlorophenyl di-*O*-methyl D- and L-tartrates according to previous report.[13] A scheme of the chemical synthetic route leading to these polyamides is depicted in Scheme 10.1.

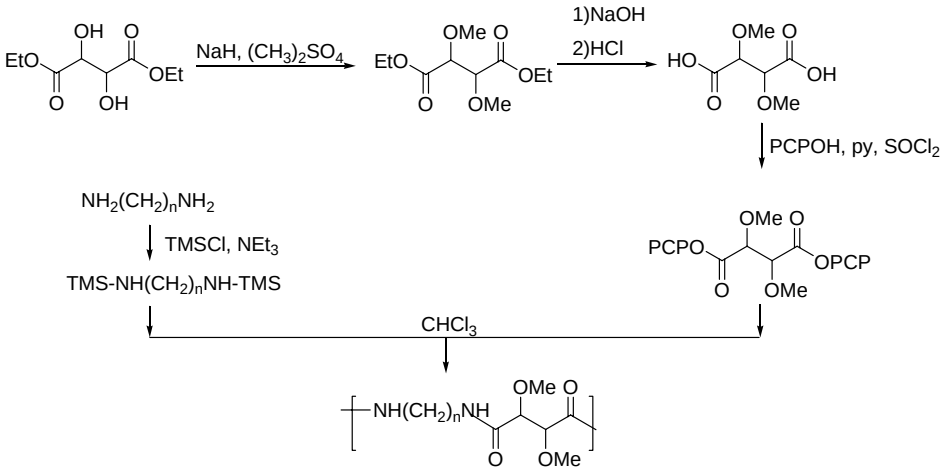

Scheme 10.1. Synthetic route to polyamides P*n*DMT.

The crude polyamides resulting from synthesis were purified by reprecipitation from chloroform with diethyl ether addition and subsequently fractionated, if needed, in order to obtain comparable molecular weights and polydispersities for all the samples. The nomenclature, intrinsic viscosity, and molecular weight data of P*n*DMT are given in Table 10.1. Calorimetric measurements were performed with a Perkin-Elmer Pyris DSC instrument calibrated with indium. Sample weights of about 2-5 mg were used in a temperature range from -20 up to 300 ºC at heating and cooling rates of 10 ºC·min^{-1} under a nitrogen atmosphere. Optical microscopy was carried out on an Olympus BX51

polarizing microscope equipped with a digital camera system and a Linkam THM5600 hot stage. X-ray diffraction was performed with a Statton-modified Wharus camera using CuK_α radiation of wavelength 0.1541 nm, and the patterns were recorded on flat photographic films.

Table 10.1. Characteristics of the enantiomeric polyamide pairs studied in this work.

Polyamide	polymethylene segment		$[\eta]^a$ (dL·g^{-1})	$M_w{}^b$ (g·mol^{-1})	$M_n{}^b$ (g·mol^{-1})	PD^b
P5DMT	-$(CH_2)_5$-	D	1.1	79,500	37,000	2.1
		L	0.9	75,000	38,100	2.0
P6DMT	-$(CH_2)_6$-	D	1.0	76,400	36,800	2.1
		L	1.0	78,500	37,400	2.1
P8DMT	-$(CH_2)_8$-	D	0.7	48,000	25,300	1.9
		L	0.7	52,000	27,400	1.9

[a] Intrinsic viscosity determined in dichloroacetic acid at 25 ± 0,1 ºC.
[b] Weight and number-average molecular weights and polidispersity determined by GPC.

10.3. Results and discussion

10.3.1. Preparation of the stereocomplex

Preparation of the P6DMT(D+L) stereocomplex has been previously described by coprecipitation from solution of an equimolar mixture of the two enantiomers P6DMT(D) and P6DMT(L), induced either by adding a non-solvent or by lowering the temperature.[12] The stereocomplex was identified by an increase in the melting point of approximately 20 ºC and an increase of about 20% in the melting enthalpy with respect to the values measured for the separated components.

X-ray diffraction patterns of the stereocomplex showed an additional reflection at 0.48 nm associated to the 100 plane of the doubled the unit cell, which is also used for characterization. The polyamides investigated at that occasion had M_w/M_n ≈20,000/10,000. As it is shown in Tables 10.2 and 10.3, similar results have been obtained in the present work for a P6DMTs pair having a nearly fourfold larger molecular size. Such results prove the reproducibility of the stereocoupling phenomenon in the P*n*DMT system for high molecular weight samples. This is worthy of mention since a

dependence of complex formation on molecular size has been reported for the case of poly(lactic acid).[14]

In order to evaluate the influence of the preparation method on the enantiomeric coupling, the formation of the stereocomplex in cast films, and in samples solidified from the melt at different cooling rates were investigated. Results obtained from this study are compared in Table 10.2.

Table 10.2. Compared DSC behaviour of enantiomerically pure P6DMTs and the equimolar mixture of the two enantiomorphs.[a]

	T_c (ºC)	ΔH_c (J·g^{-1})	T_m (ºC)	ΔH_m (J·g^{-1})
powder from synthesis[b]				
P6DMT(D)	-	-	232	52
P6DMT(L)	-	-	233	54
P6DMT(D+L)	-	-	253	65
cast film[c]				
P6DMT(D)	122	14	231	38
P6DMT(L)	127	20	231	34
P6DMT(D+L)	-	-	251	56
from the melt				
P6DMT(D)[d]	137	26	230	48
P6DMT(L)[d]	137	23	230	41
P6DMT (D+L)[d]	127	22	243	48
P6DMT(D)[e]	-	-	207	23
P6DMT(L)[e]	-	-	200	25
P6DMT(D+L)[e]	-	-	229	34

[a] Cold crystallization and melting temperature and enthalpy at heating.
[b] Prepared by precipitation with diethyl ether from chloroform solution.
[c] Film cast from $CHCl_3$ at room temperature.
[d] Quenched from the melt at a rate of 100 ºC·min^{-1}.
[e] Crystallized from the melt at 10 ºC·min^{-1}.

Complex formation by casting was examined using $CHCl_3$, formic acid and trifluoroethanol (TFE) solvents. Solutions of the separate components yielded amorphous films for the three solvents in spite that evaporation was left to proceed at extremely low rate. Such films crystallized sharply upon heating (cold crystallization) within the 120-140 ºC temperature range to melt subsequently at 232-233 ºC. Results

obtained for the equimolar mixture P6DMT(D+L) were clearly different. Amorphous films displaying a thermal behaviour similar to that observed for the individual components were obtained by casting in either formic acid or TFE whereas a highly crystalline film melting 20 ºC above the melting temperature of both P6MDT(D) or P6DMT(L) and involving a significantly larger enthalpy was obtained upon casting in $CHCl_3$. The characteristic reflection of 0.48 nm confirming the existence of the complex was present with medium intensity in the X-ray diffraction patterns of this film. These DSC and X-ray diffraction evidences were much slighter or even inexistent in films cast from formic acid or TFE indicating that the complex was difficulty formed in these solvents.

Table 10.3. Compared powder X-ray diffraction spacings for enantiomerically pure P6DMTs and the equimolar mixture of the two enantiomorphs.

Polyamide	d_{hkl}[a] (nm)						
A)[b]	001	011	020		101	0-11	12-1
B)[b]	001	021	010	100	110	0-21	11-1
P6DMT(D)	1.13s	0.65s	0.55m	-	0.46s	0.43df	0.39df
P6DMT(L)	1.12s	0.64s	0.55m	-	0.46s	0.42df	0.39df
P6DMT(D+L):							
Powder	1.08s	0.68s	0.57s	0.49m	0.45s	0.41m	0.39m
Cast film	1.09s	0.69w	0.58w	0.49m	0.45s	0.41m	0.39m
From melt	1.09s	0.68s	0.57s	0.48w	0.45s	0.40df	0.39df

[a] Visually estimated intensities denoted as: s, strong; m, medium; w, weak; df, diffuse.
[b] Indexing on the basis of triclinic or monoclinic unit cells of parameters: A) P6DMT (D and L), a = 0.500 nm, b = 0.684 nm, c =1.320 nm, α = 61.5 °, β = 90 ° and γ = 111.6 º; B) P6DMT(D+L), a = 0.495 nm, b = 1.370 nm, c = 1.293 nm, α = 58 °, and β= γ = 90 °.

Solidification from the melt afforded results highly depending on the previous thermal history of the samples and crystallization conditions. Samples prepared by quenching (extremely rapid cooling) exhibited a thermal behaviour very similar to that observed for films cast in TFE or formic acid showing weak evidences of complex formation. Upon cooling at moderate rate (10 ºC·min^{-1}) from a temperature of 265 ºC, P6DMT(D+L) crystallized in a material showing increase in both melting temperature and enthalpy as expected for the stereocomplex.

On the contrary, crystallization of the P6DMT(D+L) mixture at the same cooling rate but from a temperature of 275 ºC rendered a material that did not show significant melting differences with the enantiomeric components. Nevertheless, X-ray diffraction patterns

containing the 0.48 nm reflection characteristic of the complex were obtained from these two crystallized P6DMT(D+L) samples. Differences in crystallite size should be invoked therefore to explain the differences in DSC melting observed between them. The conclusion that may be drawn from these observations is that formation of P6DMT(D+L) stereocomplex from the opposite enantiomeric pair P6DMT(L) and P6DMT(D) is highly sensitive to preparation conditions. Apparently, stereocoupling is favoured by the presence of non-disrupting hydrogen bond solvents, as it is the case of $CHCl_3$, and by the presence of pre-existent nuclei previously formed by coupling in solution or in the liquid molten state.

10.3.2. Crystallization kinetics

The kinetics of the isothermal crystallization from the melt was comparatively examined for P6DMT(D), P6DMT(L) and the equimolar mixture P6DMT(D+L). Crystallization rate in the bulk was followed by DSC and quantified using the Avrami's approach.[15] The evolution of the crystallinity with time and the corresponding Avrami's plots for crystallization at 190 ºC are showed in Figure 10.1.

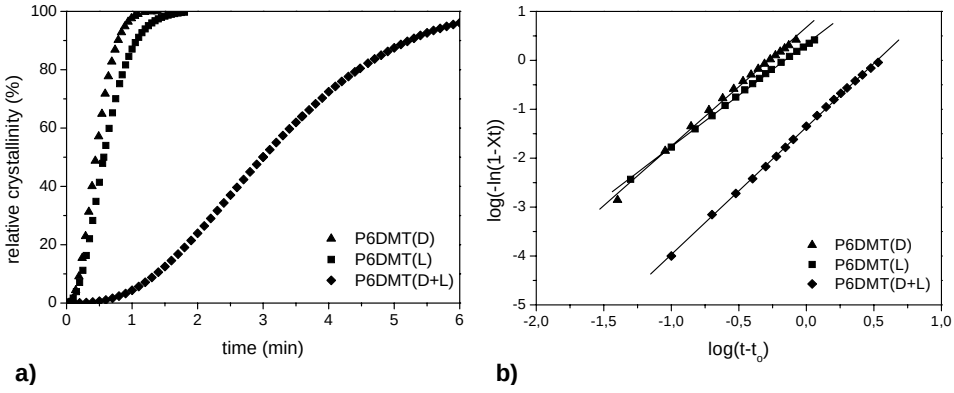

Figure 10.1. Compared plots of isothermal crystallization of enantiomorphs and the stereocomplex at 190 ºC. Crystallinity evolution with time **(a)**, and Avrami's plot **(b)**.

Crystallization of the mixed sample is seen to take place at lower rate than the enantiomerically pure samples indicating that a longer time is needed by the enantiomorphic pair to attain the molecular packing in the crystal. In the three cases,

nearly straight lines are obtained in the Avrami double-logarithmic plots. The kinetics parameters *n* and *K* resulting from the analysis of data are compared in Table 10.4 for the three studied samples. Similar values of *n* were obtained for the three samples indicating that a common crystallization mechanism is likely operating in all cases.

Optical microscopy revealed that crystallization of the two enantiomorphs as well as of the enantiomeric mixture was heterogeneously nucleated and evolved displaying a banded spherulitic texture (Figure 10.2). The growth of individual spherulites in the isothermal crystallization of molten thin films was followed by polarizing optical microscopy. The radial growth was estimated at different crystallization temperatures and compared for the enantiomorphs and the stereocomplex. Results are plotted in Figure 10.3 and numerical data for crystallization at 190 ºC are included in Table 10.4 to compare with kinetics data obtained for crystallization in the bulk.

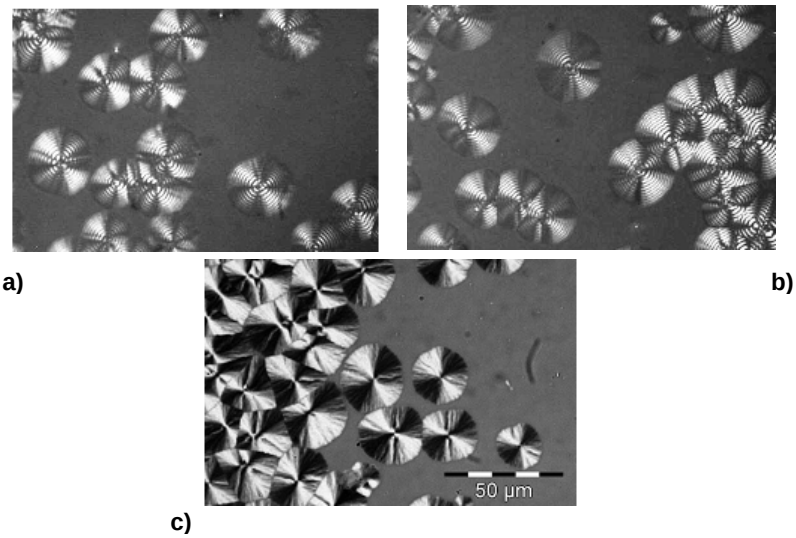

Figure 10.2. Polarizing optical micrographs of P6DMT(D) **(a)**, P6DMT(L) **(b)**, and P6DMT(D+L) **(c)**. Crystallization happened at 200 ºC from a molten thin film heated at 265-275 ºC, as indicated in Table 10.4. Same scale bar for all micrographs.

Apparently, spherulitic growing in the crystallization of the complex is slower than in the crystallization of the separate components. This observation is consistent with the occurrence of enantiomeric cocrystallization and allows excluding segregation as the cause of the delayed rate observed in the crystallization in the bulk. In the polylactide

system, higher crystallization rates were found for the stereocomplex than for the optically pure components,[16] which is opposite to our observations with P6DMT(D+L). Although the optical compensation within the racemic crystallites is achieved by a similar packing arrangement in both systems.[12,17] the polyamide crystal structure is greatly determined by the presence of strong intermolecular hydrogen-bonding between amide groups. Chain selection and topological accommodation required for proper setting of hydrogen-bonds are thought to be the cause of the crystallization delay observed for the P6DMT(D+L).

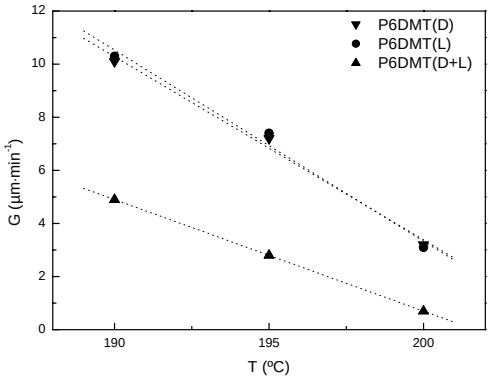

Figure 10.3. Spherulitic radial growth of enantiomorphs and the stereocomplex as a function of temperature.

10.3.3. P*n*DMT with *n* other than 6

On the premise that stereocomplex occurrence in P6DMT(D+L) relies on the coupling of the complementary tartaric moieties, its existence for other enantiomeric P*n*DMT pairs with *n* close to 6 should be reasonably expected. With this idea in mind, stereocomplex formation was explored for the poly(tartaramide) enantiomeric pairs P5DMT(D+L) and P8DMT(D+L). The different preparation procedures used in the study of P6DMT were applied for these systems and the resulting products analyzed by DSC and X-ray diffraction. DSC results obtained in the case of films cast from $CHCl_3$ are giving in Table 10.5. Differences observed in the crystallization behaviour between P5DMT and P8DMT are in agreement with what should be expected from the different molecular flexibility of these two systems. Thus significantly stiffer P5DMT chains did not crystallize at cooling

from the melt but they displayed cold crystallization upon heating. Nevertheless, what is relevant to these investigations is that no significant differences were found in the melting behaviour between the separate components and their equimolar mixtures for none of the two explored systems. X-ray diffraction patterns did not show either any difference in spacings or intensities between components and their mixtures.

Table 10.5. Compared thermal behaviour for P*n*DMT(D+L) mixtures and the enantiomerically pure enantiomers.

	T_c[a] (ºC)	ΔH_c[a] (J·g^{-1})	T_m (ºC)	ΔH_m (J·g^{-1})
P5DMT(D)	156	14	200	23
P5DMT(L)	138	14	200	22
P5DMT(D+L)	-	-	195[b]	33
P8DMT(D)	-	-	208[b]	35
P8DMT(L)	-	-	207	32
P8DMT(D+L)	-	-	213	37

[a] Crystallization temperature and enthalpy at heating.
[b] Additional melting peaks at 162 ºC and 188 ºC for P5 and P8, respectively.

The absence of indications of stereocomplex formation is a highly striking result that evidences the extremely high specificity of the P6DMT(D+L) coupling to form a stable sterical arrangement. The complex scheme of inter- and intramolecular hydrogen-bonding involving both amide and methoxy side groups may be the key of this behaviour.[18]

10.4. Conclusions

Main conclusions drawn from this piece of work are the followings: a) The enantiomeric mixture of P6DMDT and P6DMLT with M_w of ~80,000 g·mol^{-1} was proven to form stereocomplex similar to that previously described for much lower molecular weight samples; and stereocomplex formation was found to be highly sensitive to preparation conditions. b) Crystallization from the melt was delayed, both in the bulk and at the spherulitic level, when stereocomplex formation was involved in the process. c) No evidence of stereocomplex formation was observed for P5DMT or P8DMT indicating the high structural specificity required by these systems to attain stable stereo-pair coupling.

10.5. References

1. Slager, J.; Domb, A.J. *Adv Drug Deliv Rev* **2003**, 55, 549.

2. Tsuji, H. *Macromol Biosc* **2005**, 5, 569.

3. Baba, Y.; Kagemoto, A. *Macromolecules* **1977**, 10, 458.

4. Mitsui, Y.; Iitaka, Y.; Tsuboi, M. *J Mol Biol* **1977**, 24, 15.

5. Grenier, D.; Prud'homme, R.E. *J Polymer Sci Polym Phys* **1984**, 577.

6. Lavallee, Y.C.; Prud'homme, R.E. *Macromolecules* **1989**, 22, 2438.

7. Ikada, Y.; Jamshidi, K.; Tsuji, H.; Hyon, S.-H. *Macromolecules* **1987**, 20, 904.

8. Okihara, T.; Tsuji, M.; Kawaguchi, A.; Katayama, K.; Tsuji, H.; Hyon, S.-H.; Ikada, Y. *J Macromol Sci-Phys* **1991**, B30, 119.

9. Yokouchi, M.; Chatani, Y.; Tadokoro, H.; Teranishi, K.; Tani, H. *Polym J* **1973**, 14, 267.

10. Yokouchi, M.; Chatani, Y.; Tadokoro, H.; Tani, H. *Polym J* **1974**, 6, 248.

11. Sakakihara, H.; Takahashi, Y.; Tadokoro, H.; Oguni, N. *Macromolecules* **1993**, 26, 2139.

12. Iribarren, I.; Alemán, C.; Regaño, C.; Martínez de Ilarduya, A.; Bou, J.J.; Muñoz-Guerra, S. *Macromolecules* **1996**, 29, 8413.

13. Bou, J.J.; Rodríguez-Galán, A.; Muñoz-Guerra, S. *Macromolecules* **1993**, 26, 5664.

14. Tsuji, H.; Ikada, Y. *Macromolecules* **1993**, 25, 6918.

15. Avrami, M. *J Chem Phys* **1939**, 7, 1103.

16. Tsuji, H.; Tezuka, Y. *Biomacromolecules* **2004**, 5, 1181.

17. Brizzolara, D.; Cantow, H.-J.; Diederichs, K.; Keller, E.; Domb, A.J. *Macromolecules* **1996**, 29, 191.

18. Sarasua, J.R.; Rodríguez, N.L.; Arraiza, A.L.; Meaurio, E. *Macromolecules* **2005**, 38, 8362.

CHAPTER 11

SPECTROSCOPIC EVIDENCE FOR STEREOCOMPLEX FORMATION BY ENANTIOMERIC POLYAMIDES FROM TARTARIC ACID *

Purpose and specific aims: *In the previous chapter the formation of the polytartaramide stereocomplex was proved and studied in detail. Because of the extreme sensitivity of the stereocomplex to preparation conditions, the target of this work was the obtention of further evidences of the formation of the stereocomplex by viscosimetry and spectroscopic techniques such as NMR and FTIR.*

Summary: *Stereocomplex formation between the stereoisomeric optically active polyamides derived from tartaric acid and 1,6-hexamethylenediamine was investigated by spectroscopic methods. Upon standing for a few days, a steadily increase in viscosity ending in apparently visible gelification took place in the chloroform solution of the stoichiometric mixture of the enantiomeric pair. Broadening of the ^{1}H NMR peaks with time revealed a progressive decrease in chain mobility of the mixed polyamides. The diffusion coefficients of the polyamides measured by DOSY were found to decrease to 33% of the initial values upon aging. DSC provided evidences on the presence of the stereocomplex in the solid generated upon evaporation of the gel but not in that prepared from the fresh mixed solution. Detailed FTIR analysis confirmed DSC observations and afforded evidences on the occurrence of specific intermolecular interactions involving both methylene main chain and methoxy side groups in the stereocomplex.*

* Publication derived from this work: Marin, R.; Martinez de Ilarduya, A.; Romero, P.; Sarasua, J.R.; Meaurio, E.; Zuza, E.; Muñoz-Guerra, S. *Macromolecules* **2008**, 41, 3734.

11.1. Introduction

A polymer stereocomplex is formed by stereoselective coupling between two complementing stereoregular polymers. The stereocomplex characterizes by displaying altered physical properties respect to its parent polymers. Since the discovery of the first stereocomplex formed by the *syn*- and *is*-PMMA in 1958,[1] a fair number of stereocomplexes, most of them consisting of pairs of complementary enantiomeric polymers, has been reported.[2] A comprehensive overview of the stereocomplexation phenomenon in both polymers and biopolymers has been recently reported by Domb.[3]

Until today the use of stereocomplexes for biomedical applications has been sporadic. However, a recent series of works on the use of polylactic-based stereocomplexes has evidenced the interest of these systems for controlled release and stabilization of peptide and protein drugs.[4] Stereocomplexes are looked with particular interest because of their potential as matrices for controlled drug delivery systems, tissue engineering, or other biomedical purposes.

Previous chapter has evidenced the extreme sensitivity of P6DMT(D+L) stereocomplex formation to preparation conditions and has shown that crystallization from the melt of the stereocomplex is delayed compared to the parent polyamides.[5] Furthermore, no stereocomplex formation was observed for other homologous polyamides P5DMT or P8DMT made from 1,5-pentanediamine and 1,8-octanediamine, indicating the extremely high structural specificity required by these polyamides to attain stable stereo-pair coupling.

To the best of our knowledge, P6DMT(D+L) is the only case reported so far on the formation of stereocomplexes made of non-polypeptidic chiral polyamides. The interest of this system is therefore exceptional since it is demonstrative of the occurrence of stereocomplexation in synthetic polycondensates other than polyesters. The focus of this section has been set on the formation of the P6DMT(D+L) stereocomplex in solution, and on the influence of history of the solution on the occurrence of the stereocomplex in the solid state. NMR and FTIR spectroscopies have been the techniques of choice to carry out this study.

11.2. Experimental section

P6DMT studied in this work were synthesized by polycondensation in solution of the corresponding α,ω-diamines and pentachlorophenyl di-*O*-methyl D- and L-tartrates according to previous report.[6] The crude polyamides resulting from synthesis were purified by reprecipitation from chloroform with diethyl ether addition and subsequently fractionated, if needed, in order to obtain comparable molecular weights and polydispersities for all the samples. The chemical structures of P6DMT are depicted in Scheme 11.1. Nomenclature, molecular weight, and surface, optical and thermal properties of enantiomeric polyamides and the stereocomplex are given in Table 11.1.

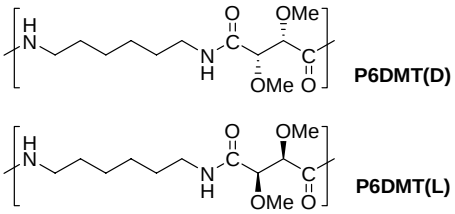

Scheme 11.1. Chemical structures of polyamides studied in this work.

Calorimetric measurements were performed with a Perkin-Elmer Pyris DSC instrument calibrated with indium. Sample weights of about 2-5 mg were used in a temperature range from -20 up to 300 ºC at heating and cooling rates of 10 ºC·min^{-1} under a nitrogen atmosphere. Contact angles between water and solid surfaces were measured by means of an OCA 15+ contact angle measuring system supported by a SCA20 software (Dataphysics, Germany). Angle values were registered at room temperature after 30 seconds of dropping the water onto the polymer surface and at least 10 measurements were made. The ^{1}H NMR analysis of peak broadening of polyamides solutions was performed on a Bruker AMX-300 equipment at 300.13 MHz from samples dissolved in deuterated chloroform at 298.1 K. Spectra were acquired with a pulse width p1 of 2.8 µs (30 º), a relaxation delay of 2 s, 32 k data points and 128 scans. 50 mg of P6DMT(L) or P6DMT(D+L) mixture were dissolved in 1 mL of $CDCl_3$ and NMR spectra from these samples were recorded at different intervals of time. ^{1}H NMR diffusion measurements were performed on a 400 MHz Bruker Avance Spectrometer using a bipolar pulse longitudinal eddy current delay (BPLED)[7] pulse sequence. The pulse sequence included a 5 ms delay to allow residual eddy currents to decay. Diffusion time (Δ) was set to 350

or 400 ms. The pulsed gradients were incremented from 2 to 95% of the maximum strength in sixteen spaced steps with a duration (δ/2) of 3 to 4 ms. Data were acquired in $CDCl_3$ with sample rotation and the temperature was controlled at 298 K to minimizing convection effects.[8] Transmission infrared spectra of polytartaramide films were recorded on a Nicolet AVATAR 370 Fourier transform infrared spectrophotometer (FTIR). The P6DMT(L) FTIR sample was prepared by casting from a chloroform solution (1% w/v) on a KBr pellet. The P6DMT(D+L) sample was prepared by sandwiching between a KBr pellet and a teflon plate a small amount of the gel-like stereocomplex formed after a week in the bottom of a 1% w/v chloroform solution. In both samples residual solvent was removed in a vacuum oven at 60 º C for 48 hours before spectral recording.

Table 11.1. Characteristics of the enantiomerically pure polyamides and the equimolar mixture of the two enantiomorphs.

Polyamide	$[\eta]^a$ ($dL \cdot g^{-1}$)	$M_w/M_n{}^b$ ($g \cdot mol^{-1}$)	Contact Angle (º)	$[\alpha]^c$ (º)	$T_m{}^d$ (ºC)	$\Delta H_m{}^d$ ($J \cdot g^{-1}$)
P6DMT(D)	1.0	76,400/36,800	59.5	-92.5	232/232	52/38
P6DMT(L)	1.0	78,500/37,400	60.0	+90.4	233/231	54/34
P6DMT(D+L)	-	77,950/37,100	52.5	+2.0	253/251	65/56

[a] Intrinsic viscosity determined in dichloroacetic acid at 25 ± 0,1 ºC.
[b] Weight and number-average molecular weights measured by GPC.
[c] Specific optical rotation measured in chloroform.
[d] Melting temperature and enthalpy measured by DSC for the precipitated material and for the film casted from chloroform.

11.3. Results and discussion

11.3.1. Formation of the stereocomplex

The P6DMT(D+L) stereocomplex in powder form may be readily prepared by precipitation with diethyl ether from a chloroform solution containing equal amounts of the two enantiomers. On the other hand, the formation of a film of the stereocomplex by casting is a process whose efficiency is strongly affected by process conditions, specifically by solution history and evaporation rate. Figure 11.1a shows the evolution of the intrinsic viscosity of the chloroform solution of P6DMT(L) and the stoichiometric mixture of P6DMT(D) and P6DMT(L) at increasing standing times at room temperature. Whereas the solution of single P6DMT(L) remained unchanged, the viscosity of the

mixed solution increased to reach infinite value after two days of aging. Visual changes taking place in these solutions with time are shown in Figure 11.1b; whereas the appearance of the P6DMT(L) solution did not change, the P6DMT(D+L) solution was turn into a transparent gel after 24 h to end in a white precipitated after 48 h of aging. This visually comparative experiment revealed the time dependent sol-gel transformation taking place in the mixed enantiomeric solution concomitant to the formation of the stereocomplex. A similar observation has been reported for a triblock copolymer containing segments of D and L-polylactic acid, which interlock in aqueous solution to form a temperature-dependent stereocomplex.[9]

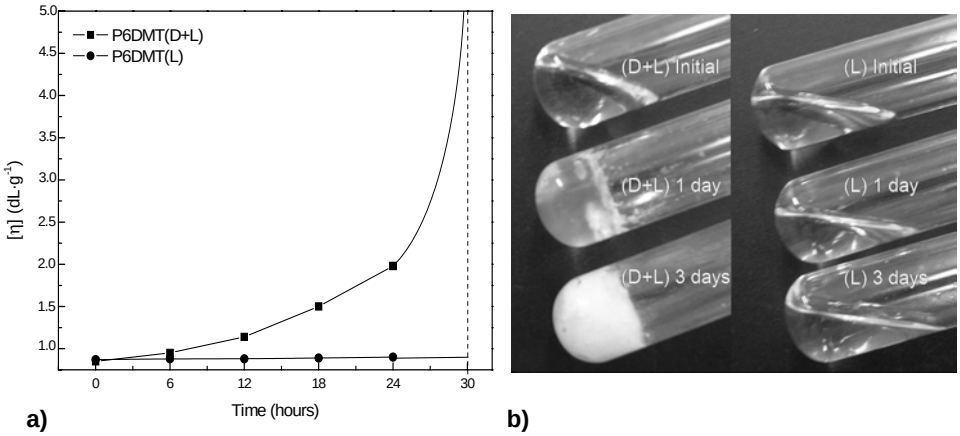

Figure 11.1. Evolution of the intrinsic viscosity of P6DMT(D+L) and P6DMT(L) chloroform solutions **(a)**, and photographs of these solutions aged for the labelled time periods **(b)**.

11.3.2. ^{1}H NMR diffusion studies

The stereocomplexation process happening in solution was followed by ^{1}H NMR. The unidimensional spectra recorded at increasing times from dilute chloroform solutions of P6DMT(L) and P6DMT(D+L) are shown in Figure 11.2. Significant differences concerning the signals profile are observed between the two sets of spectra. Whereas no changes could be perceived in the spectra of the solution of the pure enantiomer, a noticeable peak broadening was observed in the spectra of the mixture. This observation is a clear indication of an increasing restriction in the molecular mobility of the polyamides chains, which should be interpreted as due to the stereoselective coupling taking place between the two enantiomorphs. Since the broadening effect affects to all

the peaks contained in the spectra it can be inferred that both main chain and side chain groups must be involved in the interlocking mechanism leading to the formation of the stereocomplex.

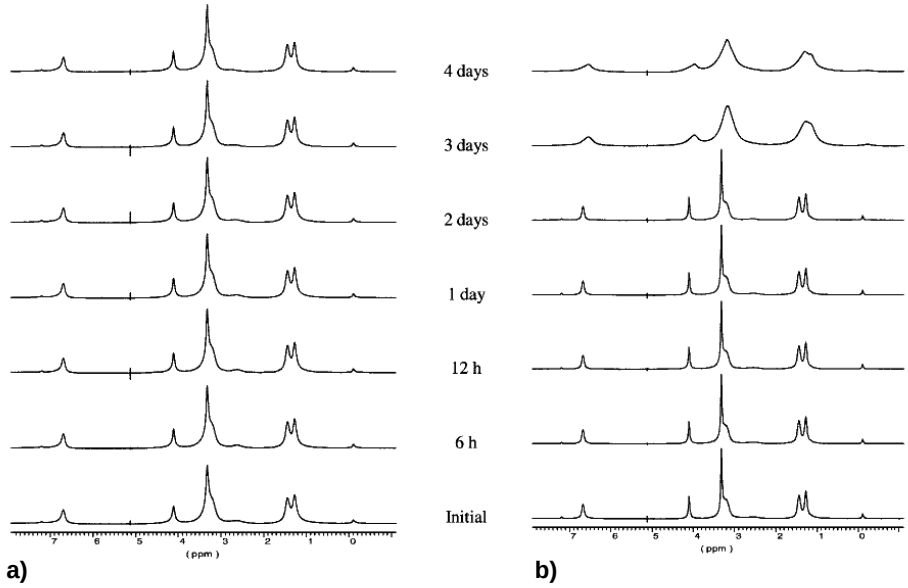

Figure 11.2. Evolution of the ^{1}H NMR spectra of P6DMT(L) **(a)** and P6DMT(D+L) **(b)** chloroform solutions with time at the indicated intervals.

Additional evidence on the stereoselective interaction taking place in the enantiomeric pair in chloroform solution was provided by bidimensional ^{1}H RMN diffusion ordered spectroscopy (DOSY).[10] By this technique the diffusion coefficients of each enantiomorph were estimated when separately dissolved and when dissolved together in stoichiometric amounts. The DOSY spectra of P6DMT(D), P6DMT(L) and P6DMT(D+L) are displayed in Figure 11.3.

As expected, peak broadening in the spectra of the mixture compared to the spectra of the pure enantiomorphs was apparent. In order to have a quantitative insight into the change in molecular mobility taking place in the solute upon mixing the two enantiomers, the diffusion coefficients *D* were calculated taken TMS as internal reference.[11] *D* values resulting from such analysis were $3.57 \cdot 10^{-11}$ and $3.67 \cdot 10^{-11}$ $m^2 \cdot s^{-1}$ for P6DMT(D) and P6DMT(L), respectively, and $2.22 \cdot 10^{-11}$ $m^2 \cdot s^{-1}$ for the P6DMT(D+L) mixture. The diffusion

coefficient of TMS in the solution containing the single enantiomorphs was $1.80 \cdot 10^{-9}$ $m^2 \cdot s^{-1}$, and $1.68 \cdot 10^{-9}$ $m^2 \cdot s^{-1}$ in the solution containing the (D+L) mixture. The diffusion coefficient ratios to TMS were therefore $D^D/D^{TMS} = 202$, $D^L/D^{TMS} = 196$, and $D^{D+L}/D^{TMS} = 130$, corresponding to a decrement close to 33% for the mixture. Diffusivity is affected by both molecular size and shape as well as by intermolecular interactions operating in solution. The equation of Stokes-Einstein relates the diffusion coefficient with the hydrodynamic radius. For small molecules it is known that a doubling in the molecular weight results in a decrease in *D* of 26% or 18% for spherical and elongated molecules, respectively. Unfortunately, this relationship is not so clear in polymeric samples.[12]

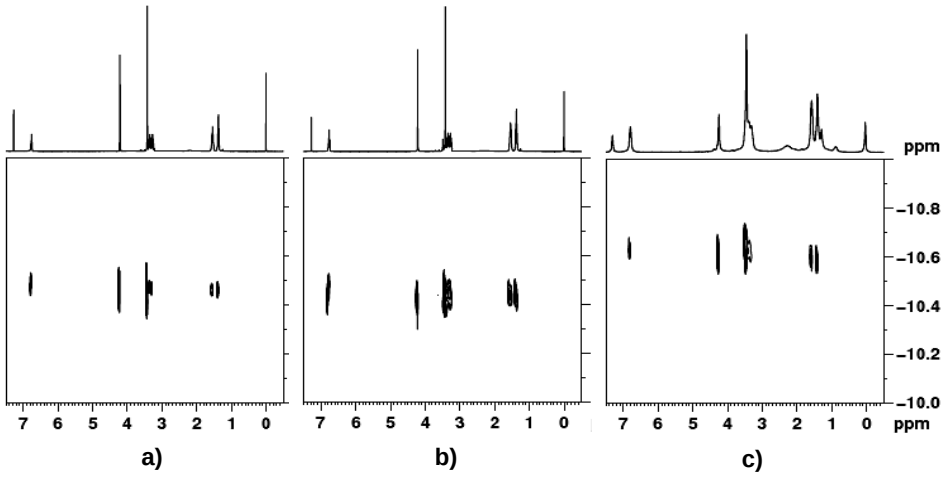

Figure 11.3. DOSY spectra of P6DMT(D) **(a)**, P6DMT(L) **(b)**, and the P6DMT(D+L) mixture **(c)**.

In PSGE experiments, the signal intensity of a given resonance experiment decays following the Stejskal-Tanner equation (eq.1) as:

$$I = I_o \exp(-\gamma^2 g^2 \delta^2 (\Delta - \delta/3) D) \quad \text{(eq. 1)}$$

where *I* and I_o are the signal intensities in the presence and absence of the pulsed-field gradients respectively, γ is the gyromagnetic ratio ($rad \cdot s \cdot G^{-1}$), *g* is the strength of the diffusion gradients ($G \cdot m^{-1}$), *D* is the diffusion coefficient of the observed spins ($m^2 \cdot s^{-1}$), δ is the length of the diffusion gradients (s), and Δ is the time separation between the leading edges of the two diffusion pulsed gradients (s).

Figure 11.4 shows a semi-logarithmic of the NMR signal attenuations versus $\gamma^2g^2\delta^2(\Delta-\delta/3)$ (Stejskal-Tanner plot) for the determination of *D*. For data processing, the DOSY software package included in XWINNMR 3.5 was used and the data were also processed by a non linear least-squares fitting method with Origin 6.0 software.

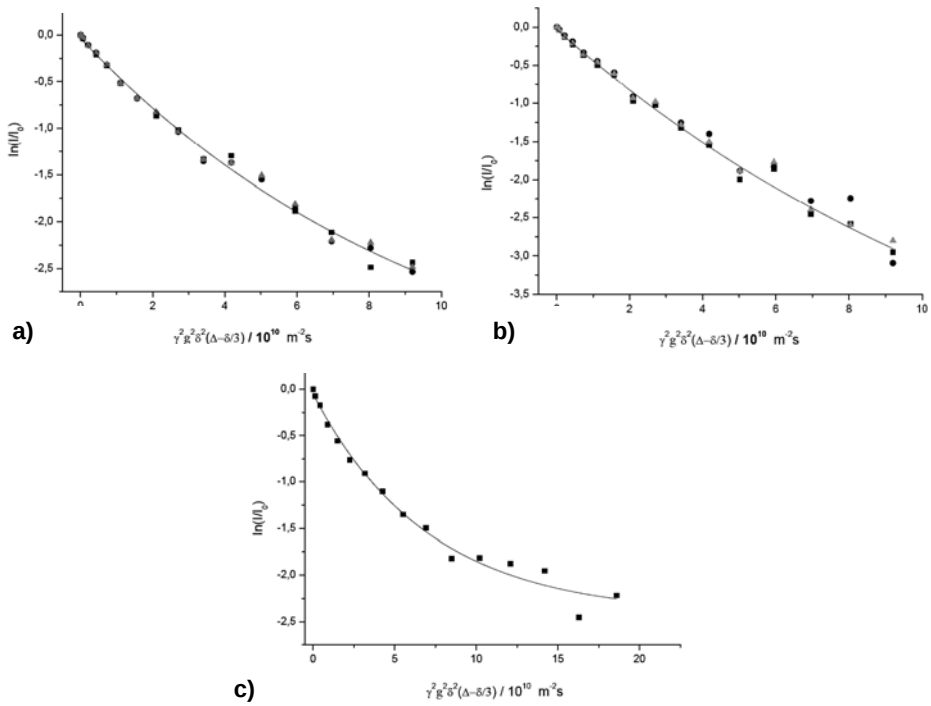

Figure 11.4. Stejskal-Tanner plot of signal attenuation for P6DMT(D) **(a)**, P6DMT(L) **(b)**, and P6DMT(D+L) **(c)**.

In order to asses how the solution history may determine the presence of the complex in the solid left after evaporation, this was analyzed by DSC. As it is seen in Figure 11.5, melting of the solid coming from the gelified mixture of P6DMT(D) and P6DMT(L) in chloroform took place 20 ºC above the melting temperature of the film coming from the single P6DMT(L) solution. According to previous works[5] such increment in the melting temperature is taken as demonstrative of the presence of stereocomplex. On the contrary, the film prepared from the fresh solution of the enantiomeric mixture did not show any increment in the melting temperature indicating that the stereocomplex was not formed in this case. These results indicated that the presence of stereocomplex in

the solid prepared by evaporation requires previous stereocoupling between the two enantiomorphs in the mother solution.

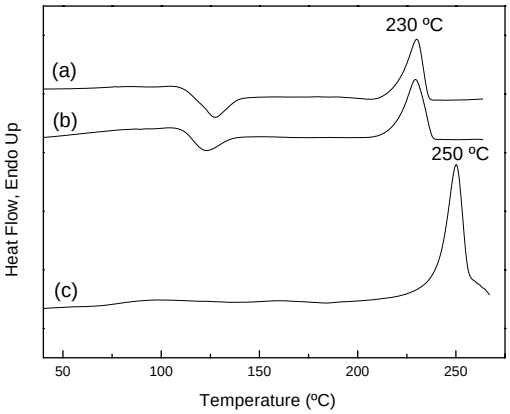

Figure 11.5. DSC traces of films from chloroform solution of P6DMT(L) **(a)**, fresh P6DMT(D+L) mixture **(b)** and gelified P6DMT(D+L) mixture **(c)**.

11.3.3. FTIR analysis

Additional evidence on the occurrence of the stereocomplex in the mixed film was afforded by FTIR analysis, which also provided valuable information on the nature of the intermolecular interactions that govern the stereocomplex formation. Samples for this study were prepared by solvent evaporation of the chloroform solution and subsequently subjected to heating at 160 ºC for one hour in order to promote crystallization of those being initially amorphous. According to DSC results, significant differences in the spectra of the P6DMT(L) sample were observed after heating whereas no changes were detected in the case of the P6DMT(D+L) sample.

The most characteristic spectral regions of P6DMT polytartaramides are shown in Figure 11.6 where traces of the P6DMT(L) sample before and after the heating treatment and of the heated P6DMT(D+L) sample are closely compared. A broad profile indicative of amorphous state is displayed by the amide I band (Figure 11.6a) in the spectrum of non-heating treated P6DMT(L). The second derivative curve of this band revealed the presence of two components at 1678 and 1656 cm^{-1} attributable to free and hydrogen-bond associated carbonyl groups, respectively. After the heating treatment, this band

appears narrower and shifted slightly to lower wavenumbers. Such changes reflected the contribution of a third component located at 1654 cm^{-1} which arises from hydrogen bonded carbonyl groups located in the crystalline domains.

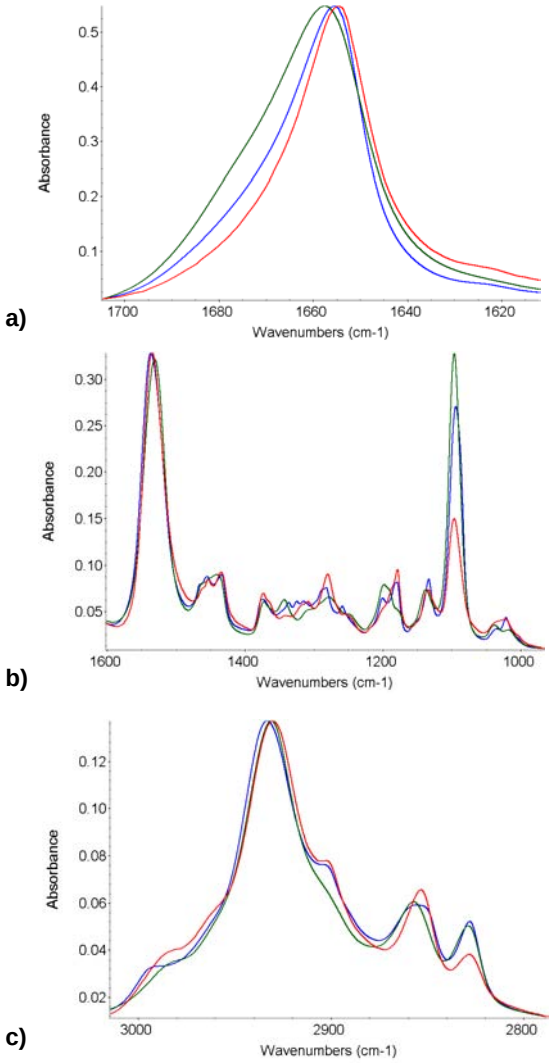

Figure 11.6. Room temperature IR spectra of P6DMT(L) (green traces), P6DMT(L) crystallized at 160º C (blue traces), and P6DMT(D+L) (red traces). **(a)** Amide I region, **(b)** 100-1600^{-1} region, and **(c)** C-H stretching region.

The amide I band of P6DMT(D+L) displayed identical features as for crystallized P6DMT(L) suggesting a similar hydrogen bonding strength in the two systems. These results were in full agreement with the DSC observation described above and depicted in Figure 11.5, which revealed that the film made of single L-enantiomer was amorphous and crystallized upon heating whereas the material obtained from the gelified P6DMT(D+L) mixture was initially crystalline. Similar results were obtained in the analysis of the N-H stretching band.

In the finger print region of these spectra, the band at 1096 cm^{-1} (Figure 11.6b) of these polytartaramides corresponding to the C-O-C asymmetric stretching is prominent. The most noticeable change affecting this band is the decrease of intensity observed in the case of the stereocomplex spectrum. Such a decrease is related to the lower transition moment displayed by this group in the crystalline structure of the stereocomplex compared to P6DMT(L). This leads to conclude that the OCH_3 side groups must display different orientation in the crystal structure of P6DMT(L) and P6DMT(D+L).[13]

The C-H stretching region also showed interesting results that help to explain the reason for stereocomplex formation. The bands at 2830 and 2855 cm^{-1} are assigned to the symmetric C-H stretching of the OCH_3 side groups and main chain CH_2 whereas the broad profile at about 2930 cm^{-1} can be assigned to the asymmetric CH_2 stretching. As can be seen in Figure 11.6c, the location of the $v_s(CH_3)$ stretching band is essentially the same for the three samples, in spite that this group is pending from the stereocenter present in the polyamide main chain. This constant location suggests a similar chemical environment for this side group for the three samples.

Conversely, significant changes are observed for the $v_s(CH_2)$. In the amorphous P6DMT(L) sample it is located at about 2857 cm^{-1} whereas in the crystallized P6DMT(L) sample it appears as a broad peak centered at about 2855 cm^{-1} suggesting the presence of two overlapped peaks of similar intensity. In the stereocomplex, the band shows again a relatively narrow profile, and is shifted 4 cm^{-1} to lower wavenumbers. The $v_{as}(CH_2)$ band also shows significant spectral shifts with similar features. These results strongly suggest the occurrence of different lateral contacts between methylene chains in P6DMT(L) and P6DMT(D+L) that could account in part for the stability of the stereocomplex.

The occurrence of different contacts between methylene groups is fully compatible with the crystal structure of P6DMT(L) and P6DMT(D+L) where hydrogen bonds are located in planes parallel to the chain direction, while methylene contacts take place in the transverse direction.[13] Whereas the packing of the OCH_3 side groups in the stereocomplex does not modify interchain distances in the hydrogen bonded planes, it affects contacts in the transverse direction, where methylene-methylene interaction occurs. The favoured contact between methylene groups in the stereocomplex would be due therefore to the lower steric shielding produced by the OCH_3 side groups in the optically compensated structure. This point will be investigated in a near future work with the aid of molecular modelling.

11.4. Conclusions

The main conclusion deriving from this study is that stereocomplex formation of the stereoisomeric P6DMT polyamide pair took place in solution upon aging. The stereocomplex formation entailed gelification of the mixed solution which could be visually observed. The molecular restriction caused by interlocking of the complementary enantiomeric chains was clearly manifested in the ^1H NMR spectra as a considerable peak broadening and it could be evaluated by measuring the diffusion coefficient of the polyamide by DOSY. Evaporation to dryness of the gelified solution occurred with retention of the stereocomplex structure, as it was revealed by both DSC and infrared data. The detailed infrared analysis indicated different interchain contact between methylene units for the homopolymer and the stereocomplex.

11.5. References

1. Fox, T.G.; Garrett, B.S.; Goode, W.E.; Gratch, S.; Kincaid, J.F. *J Am Chem Soc* **1958**, 80, 1768.

2. a) Baba, Y.; Kagemoto, A. *Macromolecules* **1977**, 10, 458. b) Grenier, D.; Prud'homme, R.E. *J Polymer Sci Polym Phys* **1984**, 22, 577. c) Ikada, Y.; Jamshidi, K.; Tsuji, H.; Hyon, S.-J. *Macromolecules* **1987**, 20, 904. d) Voyer, R.; Prud'homme, R.E. *Eur Polym J* **1989**, 25, 365. e) Lavallee, C.; Prud'homme, R.E. *Macromolecules* **1989**, 22, 2438. f) Ignatova, M.; Manolova, N.; Rashkov, I.; Sepulchre, M.; Spassky, N. *Macromol Chem Phys* **1995**, 196, 2695. g) Lim, D.W.; Park, T.G. *J Appl Polym Sci* **2000**, 75, 1615. h) Martínez de Ilarduya, A.; Ittobane, N.; Bermúdez, M.; Alla, A.; El Idrissi, M.; Muñoz-Guerra, S. *Biomacromolecules*

2002, 3, 1078. i) Slivniak, R.; Langer, R.; Domb, A.J. *Macromolecules* **2005**, 38, 5634.

3. Domb, A.J. *Adv Drug Deliv Rev* **2003**, 55, 549.

4. a) Slager, J.; Domb, A.J. *Biomaterials* **2002**, 23, 4389. b) Slager J.; Domb, A.J. *Biomacromolecules* **2003**, 4, 1316. c) Slager, J.; Domb, A.J. Eur *J Pharm Biopharm* **2004**, 58, 461. d) Bishara A.; Domb A.J. *J Control Release* **2005**, 107, 474.

5. Marín, R.; Alla, A.; Muñoz-Guerra, S. *Macromol Chem Rap Comm* **2006**, 27, 1955.

6. Bou, J.J.; Rodríguez-Galán, A.; Muñoz-Guerra, S. *Macromolecules* **1993**, 26, 5664.

7. Wu, D.; Chen, A.; Johnson, C.S. *J Magn Reson* **1995**, 115, 260.

8. Esturau, N.; Sánchez-Ferrando, F.; Gavin, J.A.; Roumestand, C.; Delsuc, M.A. *J Magn Reson* **2000**, 142, 323.

9. Fujiwara, T.; Mukose, T.; Yamaoka, T.; Yamane, H.; Sakurai, S.; Kimura, Y. *Macromol Biosci* **2001**, 1, 204.

10. Morris, K.F.; Johnson, C.S. *J Am Chem Soc* **1992**, 114, 3139.

11. Cabrita, E.J.; Berger, S.M. *Magn Reson Chem* **2001**, 39, S142.

12. a) Zhao, T.; Beckham, H.W.; Ricks, H.L.; Bunz, U.H.F. *Polymer* **2005**, 46, 4839. b) Plumer, R.; Hill, D.J.T.; Whittaker, A.K. *Macromolecules* **2006**, 39, 3878.

13. Iribarren, I.; Alemán, C.; Regaño, C.; Martínez de Ilarduya, A.; Bou, J.J.; Muñoz-Guerra, S. *Macromolecules* **1996**, 29, 8413.

CHAPTER 12

EXPLORATION OF STEREOCOMPLEX FORMATION IN CHIRAL CARBOHYDRATE-BASED POLIMERS

Purpose and specific aims: *The aim of this work was to explore the stereocomplex formation in other polycondensates containing units derived from carbohydrates such as threitol, tartaric acid, or arabinaric acid. Enantiomeric pairs of polyamides, poly(ester-amide)s, and polyurethanes were investigated.*

Summary: *On the premise that stereocomplex formation in P6DMT(D+L) relies on the coupling of the complementary tartaric moieties, its occurrence for other enantiomeric pairs of polymers derived from tartaric acid could be expected. With this idea in mind, stereocomplex formation was explored for poly(ester-amide)s and polyurethanes derived from tartaric acid and threitol, respectively. Also other polyamides with n=6 but from arabinaric acid were studied. The preparation procedure used in the study of P6DMT was applied for these systems and the resulting products were analyzed by DSC and X-ray diffraction. No significant differences were found in melting behaviour between the separate components and their equimolar mixtures in any of for the explored systems. X-ray diffraction patterns did not show either any difference in spacings or intensities between components and their mixtures indicative of stereocomplex formation.*

12.1. Introduction

Chapters 10 and 11 have been focused on the study of the stereocomplex made of the enantiomeric pair of polyamides made from tartaric acid and 1,6-hexamethylenediamine. However, the phenomenon of stereocomplex formation should be expected to be of general occurrence and other stereocomplexes should be found therefore in other systems containing carbohydrate-derived polychiral units. In this section, pairs of enantiomeric polymers derived from tartaric acid or arabinaric acid were explored in order to disclose new non-described stereocomplexes. The systems studied are depicted in Scheme 12.1 and named as:

a) *i*-PEAT6, isoregic poly(ester-amide)s from 2,3-di-*O*-methyl tartaric acid and 6-aminohexanol,
b) *s*-PEAT6, sindioregic poly(ester-amide)s from 2,3-di-*O*-methyl tartaric acid and 6-aminohexanol,
c) PA6Ar, polyamides from 2,3,4-tri-*O*-methyl-arabinaric acid and 1,6-hexamethylenediamine,
d) PUR(ThMe-HDI), polyurethanes from 2,3-di-*O*-methoxy-threitol and 1,6-hexamethylene diisocyanate,
e) PUR(ThOH-HDI), polyurethanes from threitol and 1,6-hexamethylene diisocyanate,
f) PUR(TarEt-HDI) polyurethanes from tartaric diethyl ester, and 1,6-hexamethylene diisocyanate.

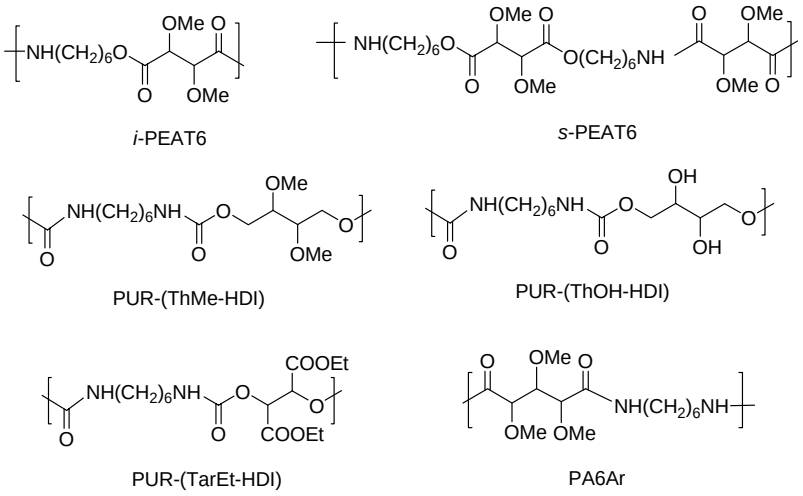

Scheme 12.1. Different systems studied.

12.2. Experimental section. Polymer synthesis

Polymers studied in this work were synthesized by polycondensation in solution of the corresponding monomers according to previous reports.[1-5] Schemes of the chemical synthetic routes leading to these polymers are depicted in Schemes 12.2-12.7. The main characteristics of the polymers studied in this work are listed in Table 12.1.

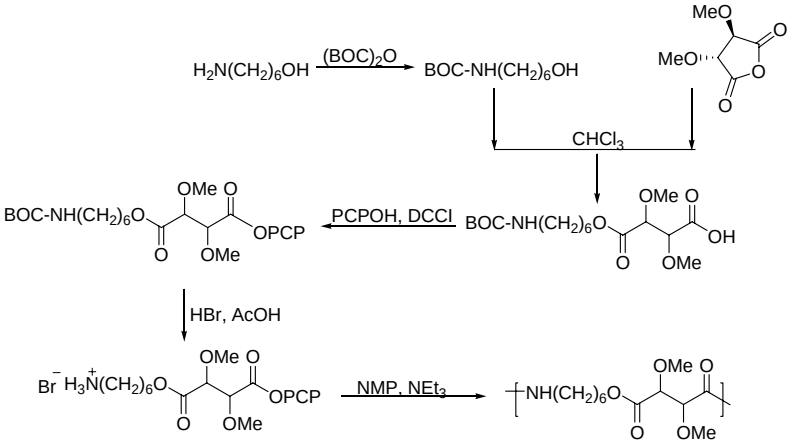

Scheme 12.2. Synthesis of D and L *i*-PEAT6.[1]

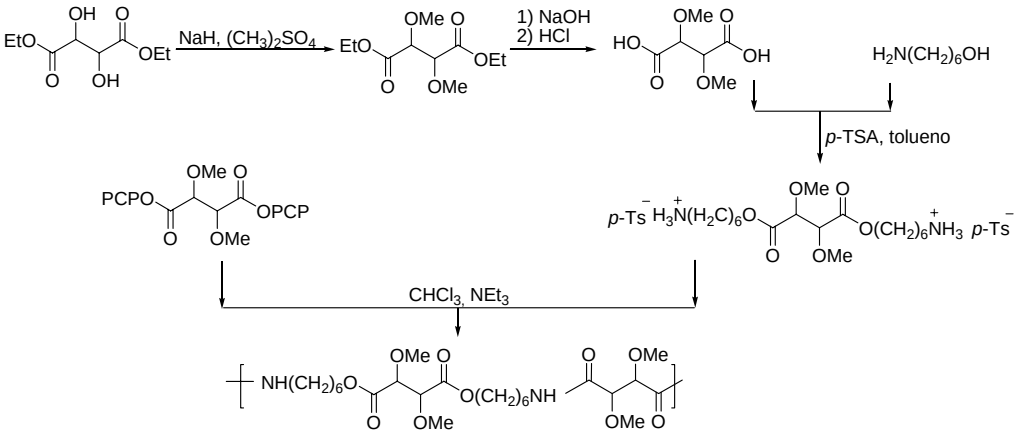

Scheme 12.6. Synthesis of D and L *s*-PEAT6.[1]

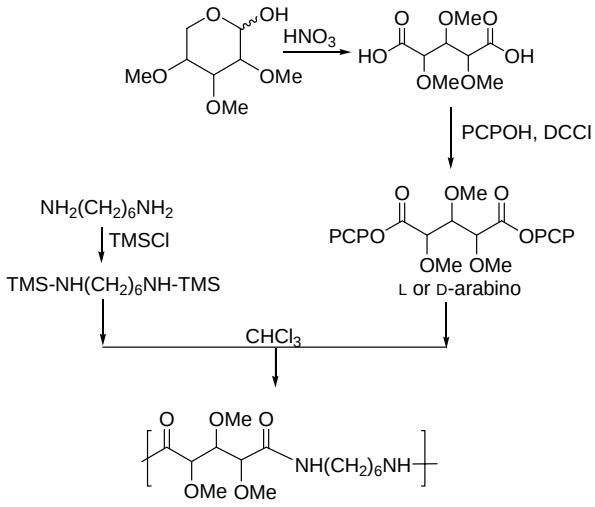

Scheme 12.7. Synthesis of D and LPA6Ar.[2]

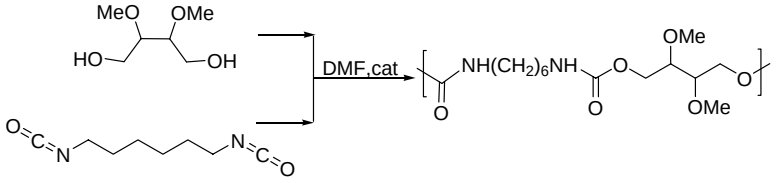

Scheme 12.3. Synthesis of D and L PUR-(ThMe-HDI).[3]

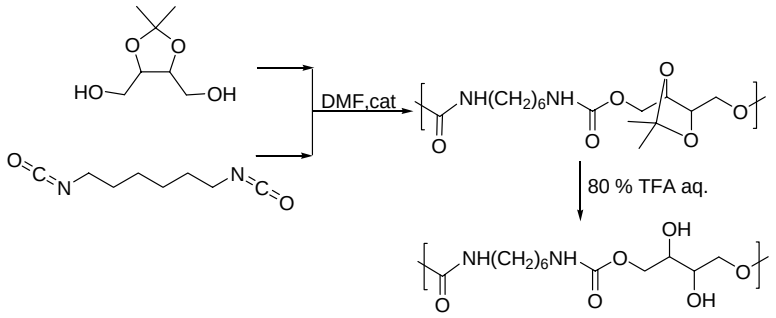

Scheme 12.4. Synthesis of D and L PUR-(ThOH-HDI).[4]

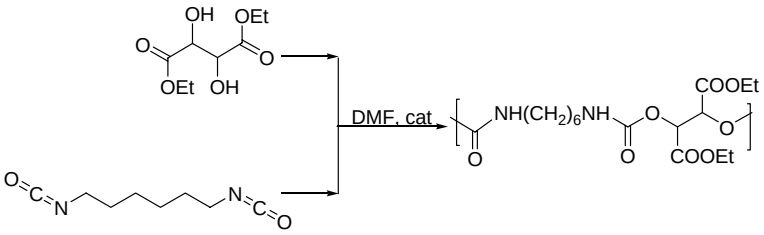

Scheme 12.5. Synthesis of D and L PUR-(TarEt-HDI).[5]

Table 12.1. Characteristics of the enantiomeric pairs studied.[a]

Polymer		$[\eta]$ (dL·g^{-1})	M_w (g·mol^{-1})	M_n (g·mol^{-1})	PD
i-PEAT6	D	0.22	6,000	3,100	1.9
	L	0.23	5,800	2,900	1.9
s-PEAT6	D	0.43	20,000	12,000	1.7
	L	0.40	18,700	11,200	1.7
PUR-(TarEt-HDI)	D	0.66	58,200	26,200	2.2
	L	0.68	60,400	28,500	2.1
PUR-(ThMe-HDI)	D	0.68	56,400	23,700	2.3
	L	0.71	58,000	25,200	2.3
PUR-(ThOH-HDI)	D	0.75	52,200	27,500	1.9
	L	0.70	49,500	26,000	1.9
PA6Ar	D	nd	39,900	22,500	1.8
	L	nd	40,200	26,900	1.5

[a] Intrinsic viscosity measured in DCA and molecular weights determined by GPC in HFIP (PMMA standards). nd: not determined.

The crude polymers resulting from synthesis were purified by reprecipitation from chloroform with diethyl ether, dried under vacuum and stored in desiccator until needed. The stereocomplex preparation was attempted as previously described for P6DMLT, *i.e.* coprecipitation from a solution in chloroform of an equimolar mixture of the two enantiomers by addition of diethyl ether as non-solvent. The precipitation was performed after 7 days of standing the chloroform solution of the enantiomeric pair mixture at room temperature under stirring. Precipitates were recovered by centrifugation and dried under

vacuum. PUR-(ThOH-HDI)(D+L) was exceptional in being obtained from a DMSO solution because of the insolubility in chloroform of the parent polymers.

Viscosities were measured in dichloroacetic acid at 25.0 ± 0.1 °C using an Ubbelohde microviscometer. ^{1}H and $^{13}C\{^{1}H\}$ NMR spectra were recorded on a Bruker AMX-300 spectrometer operating at 300.1 and 75.5 MHz for ^{1}H and $^{13}C\{^{1}H\}$, respectively, and using TMS as internal reference. Sample concentrations of about 1-5% (w/v) were used for these analyses. The spectra were acquired with 64 scans and 1000-10,000 scans, and relaxation delays of 1 and 2 s for ^{1}H and $^{13}C\{^{1}H\}$, respectively. Gel permeation chromatograms were acquired at 35 ºC with a Waters equipment provided with a refraction-index detector. The samples were chromatographed using 0.05 M sodium trifluoroacetate-hexafluoroisopropanol (NaTFA-HFIP) as eluent on a polystyrene-divinylbenzene packed linear column at a flow rate of 0.5 $mL \cdot min^{-1}$. Chromatograms were calibrated against poly(methyl methacrylate) (PMMA) monodisperse standards. Calorimetric measurements were performed with a Perkin-Elmer Pyris DSC instrument calibrated with indium. Sample weights of about 2-5 mg were used in a temperature range from -20 up to 300 ºC at heating and cooling rates of 10 $ºC \cdot min^{-1}$ under a nitrogen atmosphere. X-ray diffraction was performed with in a Statton-modified Wharus camera using CuK_{α} radiation of wavelength 0.1541 nm, and the patterns were recorded on flat photographic films.

12.3. Results and discussion

All the enantiomeric pairs of polymers were analyzed by ^{1}H NMR, viscosimetry, GPC, DSC and X-ray diffraction. Intrinsic viscosity, and molecular weight data are given in Table 12.1. The precipitated mixtures were analyzed by DSC and X-ray diffraction and data compared with those obtained from their parent polymers. Results obtained are showed in Tables 12.2 and 12.3.

No significant differences were found in the melting behaviour between the separate components and their equimolar mixtures for any of the explored systems. Figure 12.1 shows the DSC traces of the mixtures of enantiomers in comparison to the pure enantiomeric polymers. X-ray diffraction patterns did not show either any difference in spacings or intensities between the components and their mixtures.

Table 12.2. Compared thermal behaviour and X-ray diffraction of polyamides.[a]

Polymer	DSC[b]			X-ray diffraction
	T_g (ºC)	T_m (ºC)	ΔH_m (J·g^{-1})	d_{hkl}[c] (nm)
i-PEAT6 (D)	24	143	28	1.00s 0.87s 0.71s 0.59m 0.49df 0.39df 0.35df
i-PEAT6 (L)	26	142	27	1.00s 0.87s 0.71s 0.60m 0.48df 0.39df 0.35df
i-PEAT6 (D+L)	26	137	31	1.00s 0.87s 0.71s 0.60m 0.48df 0.39df 0.35df
s-PEAT6 (D)	26	131	45	1.00df 0.72w 0.66s 0.54w 0.47s 0.42w 0.36w
s-PEAT6 (L)	23	128	45	1.00df 0.73w 0.66s 0.53w 0.47s 0.42w 0.36w
s-PEAT6 (D+L)	25	128	32	1.00df 0.73w 0.66s 0.53w 0.47s 0.42w 0.36w
PA6Ar (D)	97	224	39	1.07w 0.84s 0.67w 0.56w 0.47s 0.45w 0.37df
PA6Ar (L)	95	223	42	1.07w 0.84s 0.67m 0.55w 0.47s 0.44w 0.37w
PA6Ar (D+L)	95	220	39	1.07w 0.84s 0.67w 0.55w 0.47s 0.37df

[a] Mixtures (D+L) obtained from $CHCl_3$.
[b] Melting observed during first heating of the samples.
[c] Visually estimated intensities denoted as: s, strong; m, medium; w, weak; df, diffuse.

Table 12.3. Compared thermal behaviour and X-ray diffraction of polyurethanes.[a]

Polymer	DSC[b]			X-ray diffraction
	T_g (ºC)	T_m (ºC)	ΔH_m (J·g^{-1})	d_{hkl}[c] (nm)
PUR-(ThMe-HDI) (D)	30	--	--	--
PUR-(ThMe-HDI) (L)	31	--	--	--
PUR-(ThMe-HDI) (D+L)	31	--	--	--
PUR-(ThOH-HDI) (D)	38	180	50	2.89w 1.76s 0.46s 0.42s 0.39s
PUR-(ThOH-HDI) (L)	41	179	54	2.89w 1.76s 0.46s 0.42s 0.39s
PUR-(ThOH-HDI) (D+L)	40	172	55	2.89w 1.76s 0.46s 0.42s 0.39s
PUR-(ThOH-HDI) (D)[d]	--	180	52	--
PUR-(ThOH-HDI) (L)[d]	--	179	53	--
PUR-(ThOH-HDI) (D+L)[d]	---	172	51	--
PUR-(TarEt-HDI) (D)	61	118	26	1.19s 0.89s 0.76m 0.48s 0.45s 0.42s 0.38s 0.36m
PUR-(TarEt-HDI) (L)	62	117	26	1.19s 0.90s 0.77s 0.48s 0.46s 0.42s 0.38df 0.36df
PUR-(TarEt-HDI) (D+L)	62	115	27	1.19s 0.89s 0.76m 0.48m 0.46s 0.42s 0.38s 0.36m

[a] Mixtures (D+L) obtained from $CHCl_3$ solution except for PUR-(ThOH-HDI)(D+L) which was obtained from DMSO solution, and precipitated in diethyl ether.
[b] Melting observed during first heating of the samples.
[c] Visually estimated intensities denoted as: s, strong; m, medium; w, weak; df, diffuse.
[d] Thermal data for films obtained by fast evaporation of 20% (w/w) polyurethane solutions in HFIP.

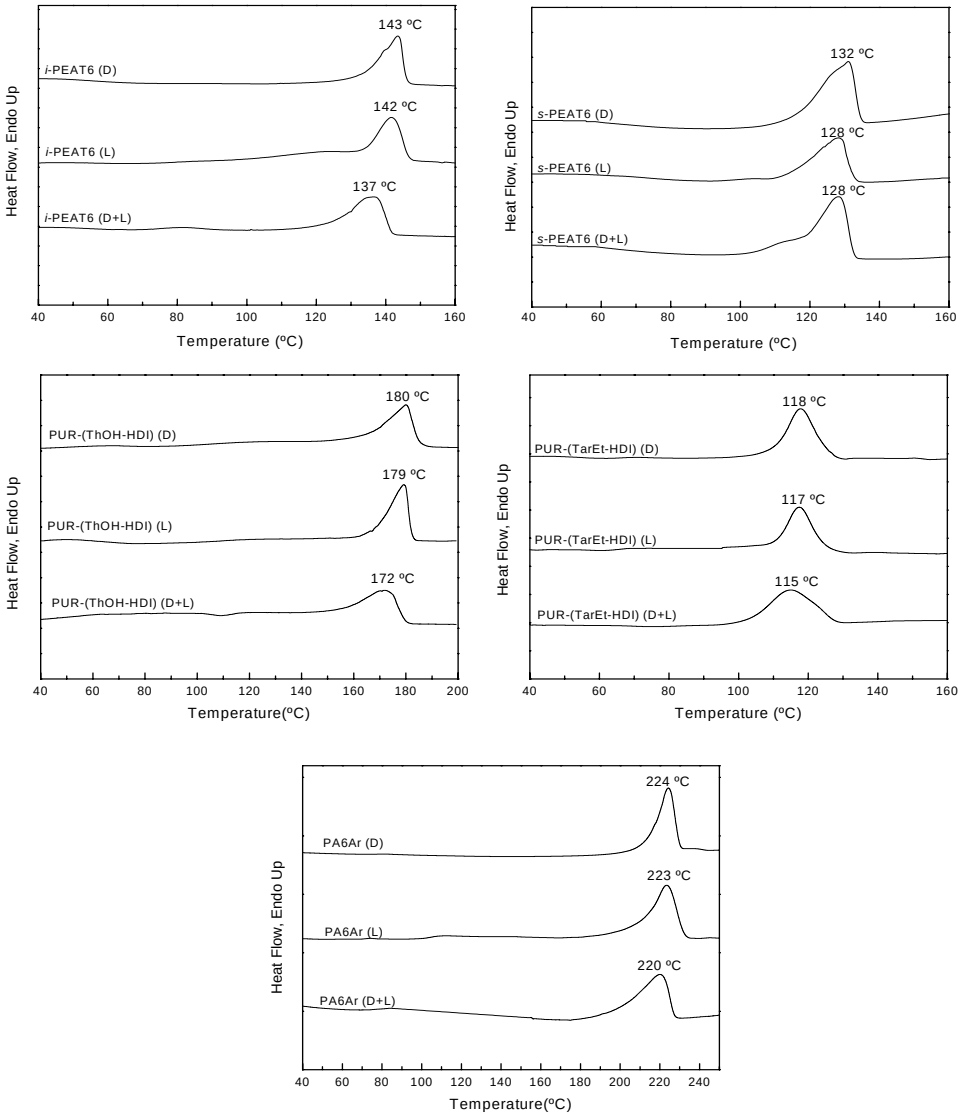

Figure 12.1. DSC traces of the explored systems.

12.4. Conclusions

Different pairs of enantiomeric polycondensation polymers derived from threitol, tartaric acid and arabinaric acid were tested with the aim to explore possible stereocomplex formation in other polymers than P6DMT. However, no evidence of stereocomplex

formation was observed for any of the systems, which was a highly striking result. It seems that an extremely high structural specificity is required by these systems to attain stable stereo-pair coupling.

12.5. References

1. Villuendas, I.; Iribarren, J.I.; Munoz-Guerra, S. *Macromolecules* **1999**, 32, 8015.

2. Bueno, M.; Zamora, F.; Molina, I.; Orgueira, H.A.; Varela, O.; Galbis, J.A. *J Polym Sci PartA: Poly m Chem* **1997**, 35, 3645.

3. De Paz, M.V.; Marín, R.; Zamora, F.; Hakkou, K.; Alla, A.; Galbis, J.A.; Muñoz-Guerra, S. *J Polym Sci Part A: Polym Chem* **2007**, 45, 4109.

4. Marín, R.; Muñoz-Guerra, S. *J Polym Sc Part A: Polym Chem* **2008**, 46, 7996.

5. Marín, R.; Martínez de Ilarduya, A.; Muñoz-Guerra, S. *J Polym Sci Part A: Polym Chem* (accepted **2008**).

GENERAL CONCLUSIONS

1. Alditols coming from reduction of aldoses or aldaric acids with all the secondary hydroxyl groups adequately protected were used to obtain linear polyurethanes by reaction with diisocyanates. Polyurethanes made of methylated, benzylated and acetalized L-threitol, L-arabinitol and xylitol, and either aliphatic or aromatic diisocyanates, were prepared in high yields and with satisfactory molecular weights by polymerization in solution under mild conditions. The presence of the side groups in the polyurethane chain repressed polymer crystallization and increased hydrophilicity, thermal stability and glass transition temperatures in comparison to the unsubstituted PUR.

2. Polyurethanes bearing free hydroxyl side groups could be prepared by hydrogenation under pressure of the fully benzylated L-threitol-derived polyurethane. Partially debenzylated products containing 20, 40 and 70% of hydroxyl side groups were obtained. Hydrogenolysis degree decreased glass transition temperatures and thermal stability but increased hydrophilicity and hydrodegradability.

3. The treatment of the isopropylidene-acetal derivatives with TFA led to the corresponding fully free-hydroxyl threitol derived PUR. The deprotection reaction was found to be complete and to take place without apparent breaking of the main backbone. The hydroxylated PUR made from HDI was semycristalline with highly interesting thermal properties and stable up to 250 ºC. X-Ray diffraction suggested that hydroxylated PUR adopt the same crystalline structure as unsubstituted PUR with only slight variations arising from the expansive effect of the side hydroxyl groups on chain packing.

4. The carbohydrate-based polyurethanes with protected hydroxyl side groups were difficult to degrade. Significant hydrolysis was only attainable at basic pH and high temperatures. On the contrary, partially deprotected PUR showed enhanced hydrodegradability. The 70% deprotected PUR being significantly degraded at 37 ºC under basic conditions. The aliphatic PUR bearing all the hydroxyl side groups in the free state was the polyurethane showing greatest hydrodegradability, being almost completely degraded at 37 ºC and pH 10.

5. Optically active alkyl (Me, Et and ^{i}Pr) and benzyl tartrates were successfully used for the synthesis of linear polyurethanes by reaction with aliphatic and aromatic diisocyanates. Aliphatic tartrate-derived PUR were semicrystalline polymers with melting temperatures in the 100-150 ºC range and glass transition temperatures increasing with the size of the alkyl side group. WAXS data suggested that all aliphatic tartrate-derived PUR may adopt a crystal structure made of helical chains with hydrogen bonds intramolecularly set without precedent in this class of polymers.

6. The tartrate derived PUR displayed enhanced susceptibility to hydrolysis compared to their PUR analogues without substituents. They were significantly hydrolyzed at 80 ºC and hydrolysis rate increased with pH and temperature and was found to be dependent also on the size of the alkyl side group. Degradation proceeded firstly by hydrolysis of the carboxylate side group and subsequent breaking of the polyurethane backbone.

7. Hydrogenation of benzyl tartrate-derived polyurethanes allowed preparing polyurethanes bearing free carboxylic side groups. Hydrogenolysis degrees of 20 and 40% were achieved under severe reaction conditions. PUR bearing free carboxylic groups were amorphous and displayed higher glass transition temperatures and lower thermal stability than their benzylated PUR precursors. Free carboxylic groups were proved to be extremely effective in enhancing the hydrodegradability; the carboxylic bearing PUR significantly degraded under physiological conditions whereas the fully esterified polymer remained unaffected even at pH 10.

8. Polyurethane homopolymers and copolymers containing isosorbide units were synthesized by polymerization in solution. Copolymers with 1,4-butanediol were enriched in 1,4-butanediol units with predominance of isosorbide end groups. The insertion of the rigid isosorbide ring hampered molecular mobility of the polymer chain increasing glass transition temperature, and increasing slightly the hydrolysis rate.

9. Two different carbohydrate-based cyclic diols, 1,4:3,6-dianhydrosorbitol (isosorbide) and 2,4:3,5-di-*O*-methylidene-D-glucitol (gludioxol) and aliphatic and aromatic diisocyanates were used to synthesize segmented poly(ester-urethane)s with polycaprolactone of 3,000 $g \cdot mol^{-1}$ as *soft segment*. Polymerization in the bulk produced PUR with higher molecular weights and more controllable composition than polymerization in solution. Replacement of 1,4-butanediol by cyclic diols as *chain extender* increased glass transition temperatures but repressed the crystallization of *hard segment* domains. The thermal stability was improved by the use of isosorbide but deteriorated when gludioxol was the replacing diol. Hydrolytic degradation proceeded by hydrolysis of the ester groups of the *soft segment* according to a pattern similar to that observed in the hydrolysis of polyurethanes made from 1,4-butanediol.

10. The enantiomeric mixture of P6DMDT and P6DMLT with M_w = 80,000 $g \cdot mol^{-1}$ was proven to form a stereocomplex similar to that previously described for much lower molecular weight samples. The formation of the complex was observed to take place in solution upon aging and showing high sensibility to preparation conditions. The molecular restriction caused by interlocking of the complementary enantiomeric chains was clearly manifested in the ^1H NMR spectra as a peak broadening and was roughly quantified by the decrease in diffusion coefficient measured by DOSY. The infrared analysis indicated a different interchain contact between methylene units in the homopolymers and the stereocomplex. Crystallization from the melt both in the bulk and at the spherulitic level was delayed when the stereocomplex structure was present.

11. Possible stereocomplex formation was investigated in a series of related enantiomeric pairs of polyamides, poly(ester-amide)s and polyurethanes containing *threo* and *arabino* configurational polyhydroxylated moieties. No evidence of

stereocomplex formation was observed by DSC or WAXS for any of the systems studied indicating the high structural specificity required by them to attain stable stereo-pair coupling.